DEPOSITIONAL AND TECTONIC HISTORY OF THE GUERRERO TERRANE, SIERRA MADRE DE SUR; WITH EMPHASIS ON SEDIMENTARY SUCCESSIONS OF THE TELOLOAPAN AREA, SOUTHWESTERN MEXICO

MARTIN GUERRERO-SUASTEGUI

Depositional and tectonic history of the Guerrero Terrane, Sierra Madre de Sur; with emphasis on sedimentary successions of the Teloloapan area, Southwestern Mexico

By

Martin Guerrero-Suastegui

A thesis submitted to the
School of Graduate Studies
in partial fulfillment of the
requirements for the degree of
Ph. D

Department of Earth Sciences

Memorial University of Newfoundland

December, 2004

St. John's Newfoundland

Abstract

The Pacific margin of Mexico is formed by Upper Jurassic–Lower Cretaceous arc-related successions of the Guerrero Terrane. The Guerrero Terrane in southwestern Mexico is divided into three subterranes: from west to east: the Zihuatanejo–Huetamo subterrane, Arcelia – Palmar Chico subterrane, and Teloloapan subterrane.

This thesis research targets the Teloloapan subterrane and is aimed at establishing its stratigraphy, sedimentology, petrography and geochemistry as the basis for an improved understanding of its tectonic history. The Teloloapan subterrane contains a thick Lower Cretaceous age sequence of volcanic, volcaniclastic, and carbonate rocks (the arc-related succession), which is covered by Upper Cretaceous mostly deep-water siliciclastic rocks (the sedimentary cover successions). All rocks are strongly deformed.

The arc-related succession contains three formations (Villa Ayala, Acapetlahuaya and Teloloapan formations) showing concordant and transitional boundaries. Facies analysis of the Villa Ayala and Acapetlahuaya formations (Berriasian–Late Aptian) records the construction of volcanic build-ups and their destruction by gravity-current processes that formed slope-apron deposits. Carbonate rocks of the Teloloapan Formation developed on top of extinct volcanoes and formed an Aptian–Albian carbonate platform.

The Miahuatepec and Mezcala formations constitute the sedimentary cover succession. The Mezcala Formation is comprised of interbedded sandstone and shale with minor thin-bedded limestone and calcareous breccias. The Miahuatepec Formation is a thick sequence of interbedded sandstone and shale with minor thin-bedded limestone.

Facies analysis shows both units were deposited by low- to high- concentration turbidity currents on the middle to lower parts of submarine fans.

Volcaniclastic and epiclastic sandstones from the arc-related succession are rich in volcanic lithic grains derived from contemporaneous volcanic source. They have an undissected to transitional arc provenance (terminology of W. R. Dickinson). Geochemical data indicate a mafic to felsic volcanic source with a calc-alkaline affinity. REE patterns are similar to those of evolved intraoceanic arcs.

Sandstones from the Mezcala Formation show quartzolithic and carbonate-rich petrofacies, while the sandstones of the Miahuatepec Formation are mainly quartzolithic. Both formations were derived by erosion of volcanic sources and have a transitional to dissected arc provenance. The Mezcala Formation also has a coeval formations contribution from the erosion of platform carbonates of the Teloloapan Formation. Geochemistry of the Miahuatepec Formation supports a calc-alkaline volcanic source with REE patterns similar to those of evolved intraoceanic arcs.

The tectonic history of southwestern Mexico seems to be characterized by intraoceanic arcs (Late Jurassic–Early Cretaceous), followed by cessation of volcanism and development of an island-arc carbonate platform (Albian–Cenomanian) in the Teloloapan area. Contemporaneously, a jump in subduction forms the volcanic rocks of the Arcelia – Palmar Chico subterrane. The Guerrero Terrane was accreted to the "cratonic" Mixteca Terrane during the Late Cretaceous.

DEDICATION

This thesis is dedicated to:

My dearest Mother:

Antonia Suastegui Ortiz

My three supporters and continuous source of motivation and love:

Paula

Oscar Sandino

José Francisco

ACKNOWLEDGEMENTS

I would like to thank Consejo de Ciencia y Tecnología (CONACYT) and the Secretaria de Educación Pública (SEP) for financial support to do this work through a scholarship from 1997–2000 and 2004, respectively. Special thanks go to Dr. Richard N. Hiscott, a great advisor and friend, for his advice throughout this project.

I would like to thank to my friends and colleagues of the Unidad Académica de Ciencias de la Tierra (UAG). I especially thank Joel Ramírez Espinosa, Oscar Talavera Mendoza and Ma. Fernanda Campa Uranga for their long discussions about the geological problems of the Guerrero Terrane in southwestern Mexico, as well as José Luis García Díaz, José Luis Farfán Panamá, Luis Antonio Flores de Dios González, Israel Castrejon Gonzalez, and Rita G. Angulo Villanueva for their constant support and friendship. Ernesto YamZul, Fredy, Juan Manuel, and Erick Diego provided invaluable help in the field and drawing of some figures.

My gratitude to my supervisor committee: Dr. Richar N. Hiscott, Dr. Arthur King, and George Jenner and examiners Dr. Elena Centeno-García, Dr. Rudi Meyer, and Dr. Iain Sinclair for their valuable comments that help to clarify and improve the final version of this thesis.

I would also like to extend my gratitude to all the staff at the department of Earth Sciences and MUN, particularly Dr. Sherif Awadallah for his friendship.

Special thank to David and María Foley, and Paula Flynn for their constant support and friendship. Finally, I want to especially thank to all the members of my family in Acapulco and Iguala.

TABLE OF CONTENTS

CHAPTER 3. SEDIMENTARY COVER SUCCESSIONS: STRATIGRAPHY AND FACIES

CHAPTER 5. PETROGRAPHY, GEOCHEMISTRY AND PROVENANCE

CHAPTER 6. TECTONIC EVOLUTION OF THE TELOLOAPAN SUBTERRANE AND IMPLICATIONS FOR ORIGIN OF THE GUERRERO TERRANE

CHAPTER 7. CONCLUSIONS

List of Figures

List of Tables

List of Appendices

CHAPTER 1. INTRODUCTION

1.1. STATEMENT OF THE PROBLEM

Western Mexico is the southward extension of the Cordilleran system of western North America, and originated by accretion of oceanic terranes during Late Mesozoic to Early Cenozoic time (Campa and Coney, 1983). Low-grade metamorphosed volcanic and volcaniclastic Mesozoic rocks known as the Guerrero Terrane are exposed along the Pacific margin of Mexico (Figure 1). This terrane represents the active margin during Late Jurassic to Early Cretaceous time (Campa and Coney, 1983). Because of its intriguing origin, age, wide distribution, and lithological diversity, several authors have studied the Guerrero Terrane since the middle 1970s.

In contrast to the western side of Mexico, a contemporary passive margin developed by Jurassic extensional and strike-slip tectonics related to the opening of the Gulf of Mexico along the eastern side of Mexico. This contrasting tectonic setting initiated the growth of carbonate platforms followed by pelagic carbonate and siliciclastic deposits during Late Cretaceous time.

The Guerrero Terrane originally was considered as a huge mosaic of volcanic and volcanosedimentary rocks (Campa and Coney, 1983). Recently, however, it was subdivided into three north-south-trending, parallel subterranes (Ramírez et al., 1991; Centeno et al., 1993), based on lithology, structural geology and geochemical characteristics, and separated by regional tectonic discontinuities: (a) the Teloloapan

subterrane; (b) the Arcelia – Palmar Chico subterrane; and (c) the Zihuatanejo-Huetamo subterrane (Figure 2). The Teloloapan subterrane is the main focus of this thesis.

The Teloloapan subterrane is located on the eastern side of the Guerrero Terrane (Figure 2). In this area, three lithostratigraphic assemblages, separated by west-dipping thrust faults, are exposed. These assemblages are, from east to west (Figure 3): (1) the Guerrero-Morelos platform, which is considered to be a passive-margin succession formed of Albian–Cenomanian carbonates to Upper Cretaceous clastic sedimentary rocks (Fries, 1960); (2) the Teloloapan subterrane consisting of Lower Cretaceous volcanic and volcaniclastic rocks and arc-related limestones covered by Upper Cretaceous siliciclastic rocks (Campa et al., 1974; Guerrero et al., 1990; Talavera, 1993); and (3) the Arcelia – Palmar Chico subterrane consisting of Albian–Cenomanian Cretaceous tholeiitic island-arc volcanic and plutonic rocks, capped by radiolarian tuffaceous chert associated with black shales (Dávila and Guerrero, 1990; Delgado et al., 1990; Ramírez et al., 1991; Talavera, 1993).

Early studies suggested that the Guerrero Terrane represented an allochthonous magmatic arc which formed during either eastward subduction (Campa and Ramírez, 1979; Campa and Coney, 1983) or westward subduction (Coney, 1983). These hypotheses were broadly based on regional stratigraphy and structural data. However, the affinities, paleogeographic position, and age of the magmatic-arc sequences were unknown or poorly constrained. Subsequently, tectonic interpretations have become more complicated as new structural, stratigraphic and geochemical information have been

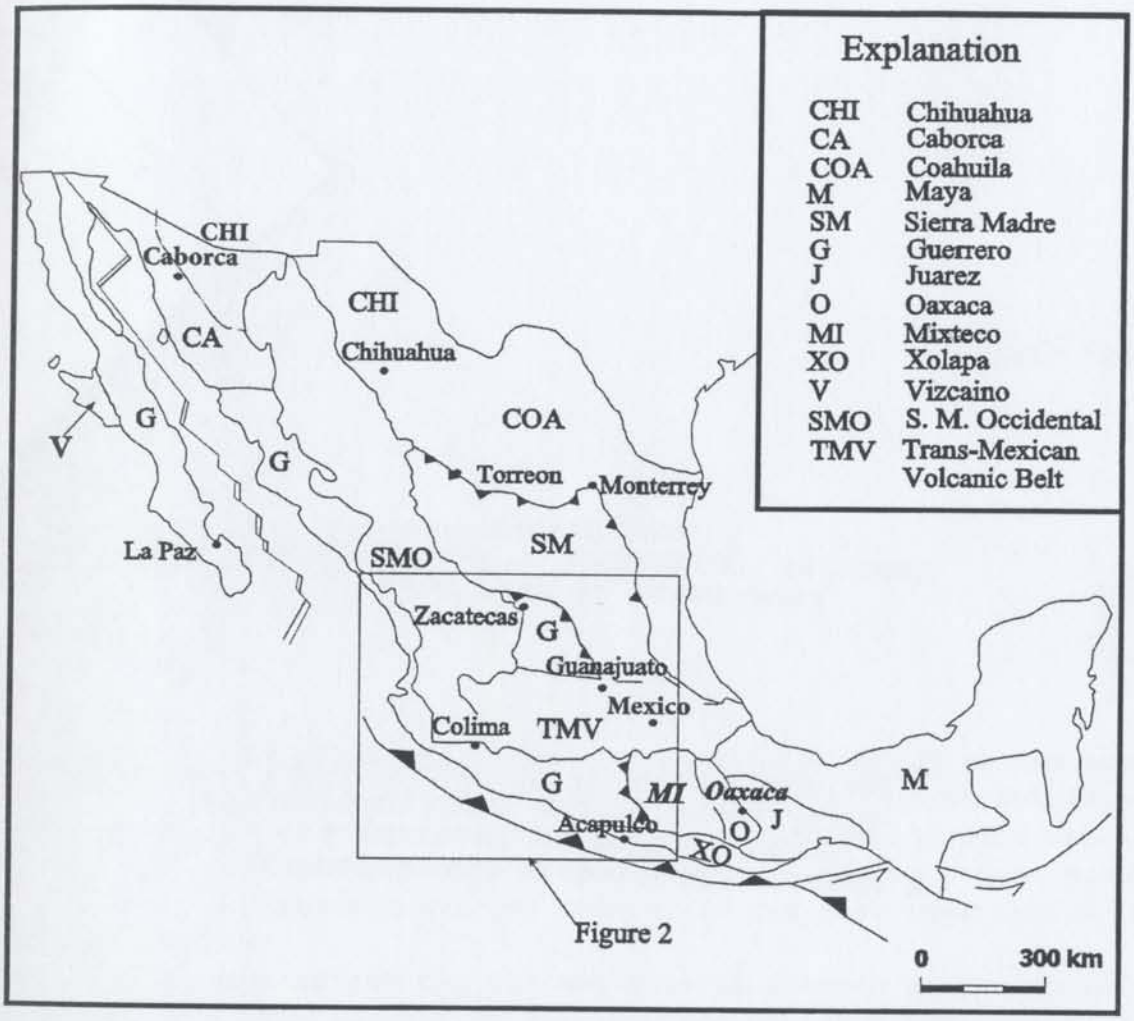

Figure1. Tectonostratigraphic terranes of Mexico (From Campa and Coney, 1983).

Names of major urban centers are mixed upper and lower cases.

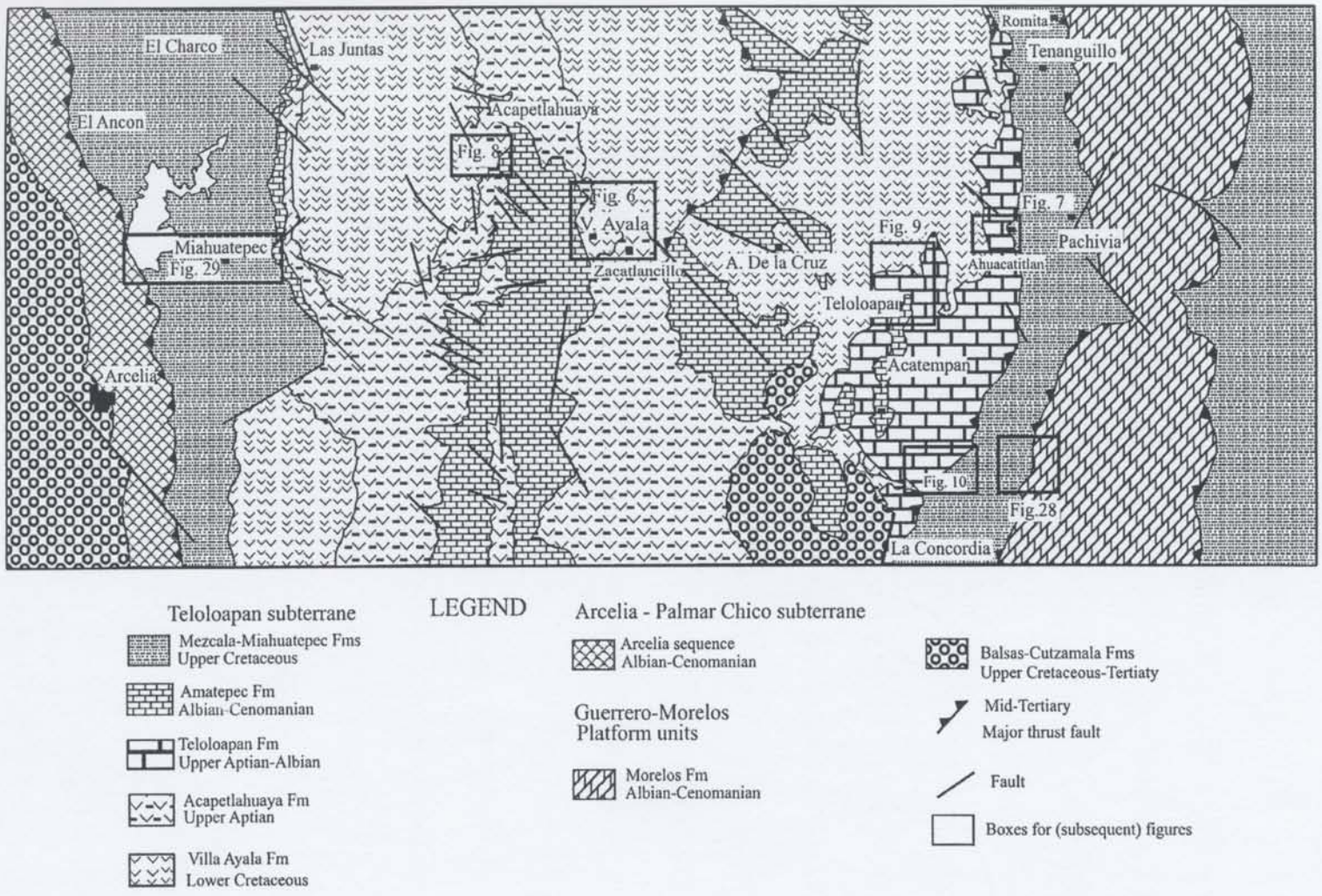

Figure 3. Geological map of the Teloloapan subterrane in the Teloloapan-Arcelia area (from Ramírez et al., 1990). Names of towns and villages are provided on the map for location.

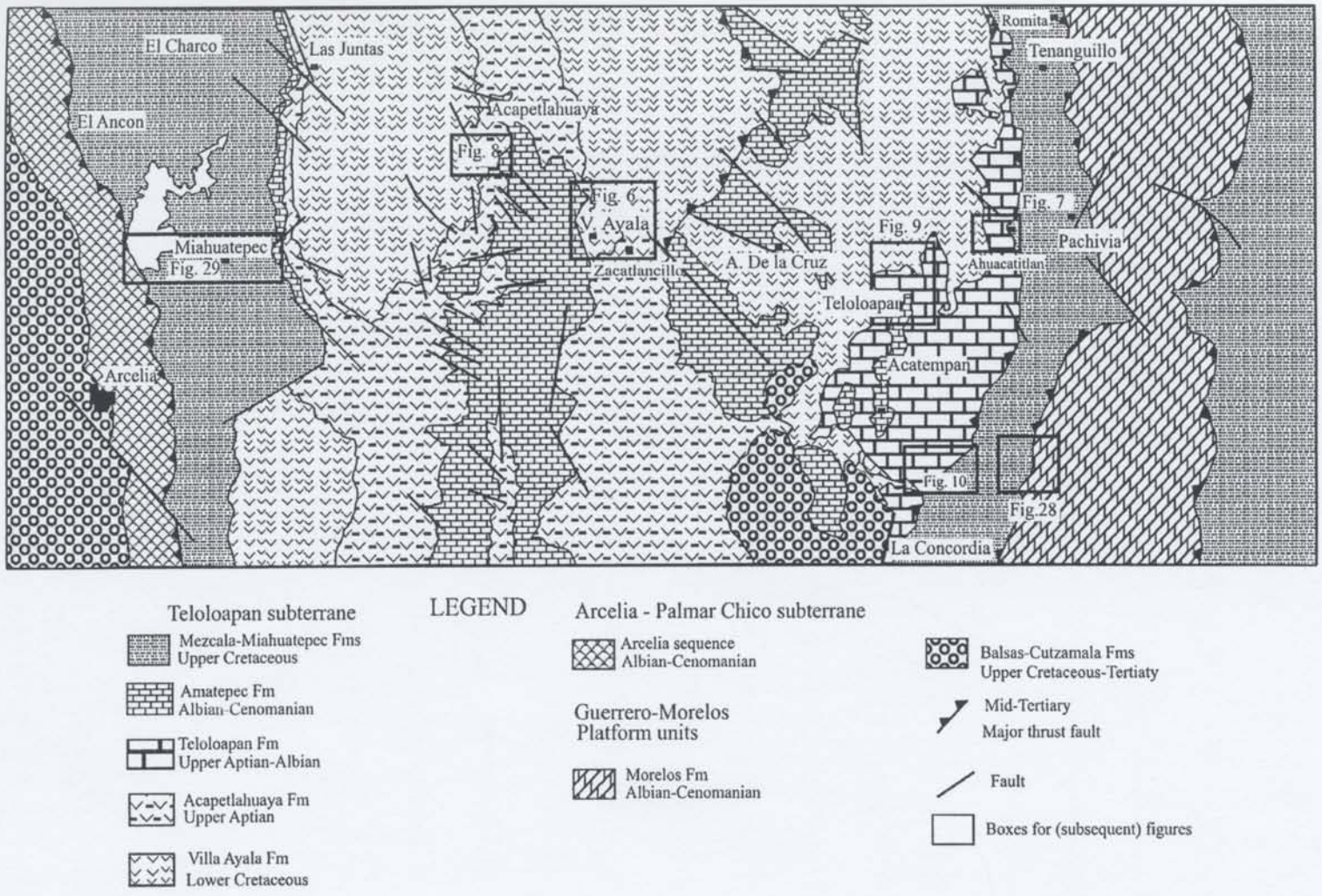

Figure 3. Geological map of the Teloloapan subterrane in the Teloloapan-Arcelia area (from Ramírez et al., 1990). Names of towns and villages are provided on the map for location.

gathered, and are the basis for two main models. The first model recognizes an island arc built on a transitional crust (partly oceanic and partly continental) of Late Jurassic to Early Cretaceous age (Elías and Sánchez, 1992; Tardy et al., 1992; 1994; Dickinson and Lawton, 2001). The second model hypothesizes several allochthonous arcs associated with backarc basins of different ages, mainly Early Cretaceous (Ramírez et al., 1991; Talavera, 1993; Centeno et al., 1993).

The uncertain tectonic framework is in part related to the poorly understood stratigraphy of the volcanic and volcaniclastic rocks of the Guerrero Terrane and its sedimentary cover successions, resulting in different proposed ages and terminologies for the sequences (see Figure 4, and Campa et al., 1974; De Cserna and Fries, 1981; De Cserna, 1983; Guerrero et al., 1990; Elías and Sánchez, 1992; Cabral, 1995). The deformation and folding in the rocks can lead to misinterpretation of the stratigraphy because of structural repetition. Finally, few or no detailed sedimentological and provenance studies have been done in the different parts of the Guerrero Terrane. This lack of reliable stratigraphic and depositional data has prevented both a correct interpretation of the arc-related basin(s), and a rigorous evaluation of the different tectonic models proposed for the Guerrero Terrane and its sedimentary cover successions.

This study has five objectives designed to significantly advance the knowledge of the Guerrrero Terrane:

1. To provide stratigraphic control for the volcanosedimentary and the sedimentary cover successions of the Teloloapan area (Teloloapan subterrane) based on field relationships;

2. To compile previous data and new identifications of both macrofossils and microfossils to provide better age control on the depositional facies and petrological evolution of the basin;
3. To conduct a depositional and compositional study of the volcaniclastic (arc) units and sedimentary cover (post-arc) rocks through analysis of the vertical distribution and character of lithofacies;
4. To provide a regional context for the depositional and compositional analysis by comparing the study area with neighboring "suspect" assemblages: the Arcelia – Palmar Chico and the Zihuatanejo-Huetamo subterranes; and
5. To integrate the stratigraphic, sedimentologic, petrologic and geochemical data to evaluate and explain the tectonic evolution of the Guerrero Terrane in southwestern Mexico.

1.2. PREVIOUS WORK

The first geological studies of the volcanic and volcaniclastic rocks in the region interpreted these as a "eugeosynclinal" sequence (Fries, 1960; De Cserna, 1965). In later studies, employing plate tectonic theory, Campa and Ramírez (1979) interpreted the area as a magmatic arc sequence. Finally, Campa and Coney (1983), using the terrane concept, divided the arc sequences and defined the Guerrero Terrane.

The Guerrero Terrane was interpreted as a complex allochthonous terrane that extends along the western margin of Mexico (Campa and Coney, 1983). In terms of paleogeography, the Teloloapan area was defined to be an island-arc sequence, the

Huetamo area was considered a marginal-sea basin, and the Zihuatanejo region was interpreted as a subduction complex (Campa and Ramírez, 1979; Campa and Coney, 1983). In this thesis they are termed Teloloapan and Zihuatanejo-Huetamo subterranes, respectively. Recently, studies based on regional stratigraphical, structural, petrological, and geochemical data (mainly in volcanic rocks) have proposed different and controversial tectonic models for the Guerrero Terrane, mentioned in § 1.1 and considered at length in chapter 5 (Ramírez et al., 1991; Elías and Sánchez, 1992; Tardy et al., 1992, 1994; Talavera, 1993; Centeno et al., 1993; Dickinson and Lawton, 2001).

Regional studies have established, in a general way, the stratigraphy and basin evolution of the Teloloapan subterrane (see Figure 4, and Fries, 1960; Ontiveros, 1973; Campa et al., 1974; De Cserna et al., 1978; Guerrero et al., 1990; Elías and Sánchez, 1992; Sánchez, 1993; Cabral, 1995). Paleontological and radiometric data have suggested quite different ages for the sequence: Precambrian to Triassic (Fries, 1960, De Cserna et al., 1978); Triassic to Early Cretaceous (Elías and Sánchez, 1992; Sánchez, 1993); Late Jurassic to Early Cretaceous (Campa et al., 1974 and 1980; Campa and Ramírez, 1979); and Early Cretaceous (Guerrero et al., 1990; Campa and Iriondo, 2003).

Despite extensive geological studies carried out in the Guerrero Terrane, the sedimentology, sedimentary petrography, provenance, and sedimentary geochemistry have been little studied. Available documentation on these topics is reviewed below.

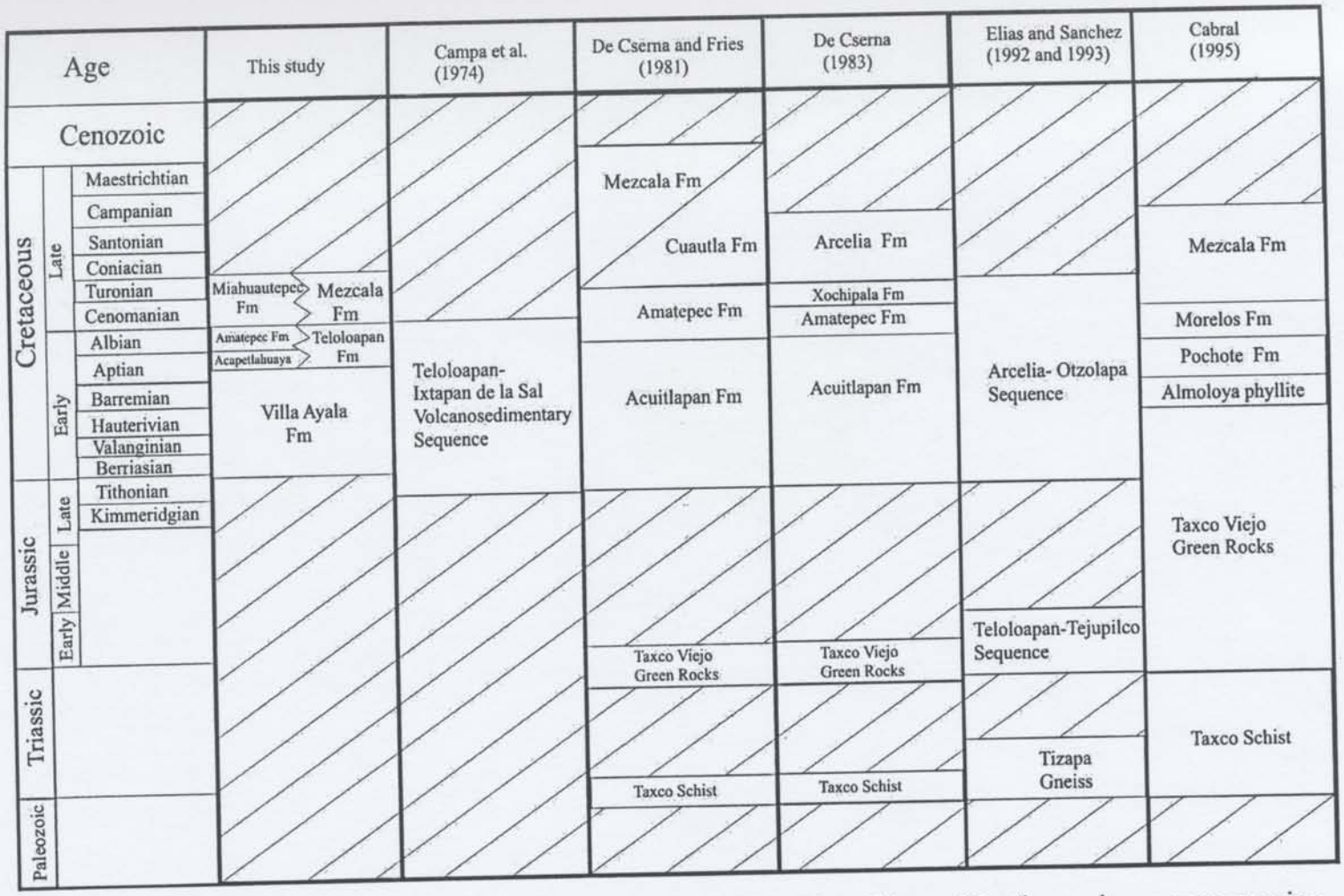

Figure 4. Stratigraphic schems for the Teloloapan area. Diagonal rules = hiatus. The figure shows a progression of terminology/interpretation for the study area, except column 4 that is the currently accepted chart for the Tejupilco area.

Based on regional lithofacies analysis in Michoacan and Guerrero states, De Cserna et al. (1978) proposed an Albian through Turonian basin evolution for the area during the Early Cretaceous; while volcanic activity was hypothesized to have occurred only in Late Cretaceous time.

Johnson et al. (1991), in the Huetamo region of the Zihuatanejo-Huetamo subterrane (Figure 2), assigned turbidites and debris-flow deposits to a deep-sea environment. However, their main contribution was the application of LandSat images as a new technique to elucidate the stratigraphy. Subsequently, Guerrero (1997) proposed a sedimentological model, in the same Huetamo area, of deep- to shallow-water deposition based on lithofacies analysis. He also divided the sandstones and volcaniclastic rocks of the Huetamo area into several compositional suites and suggested a petrofacies evolution for the region.

Petrographic studies of siliciclastic rocks of the Guerrero Terrane have been conducted by Rodríguez (1994) in the Teloloapan subterrane; and Centeno (1994) and Guerrero (1997) in the Zihuatanejo-Huetamo subterrane.

Several geochemical studies of the volcanic rocks of the Guerrero Terrane have been conducted to define the magmatic signatures of the different areas; for example, a calc-alkaline affinity for the Teloloapan subterrane (Talavera, 1993), tholeiitic affinity for the Arcelia – Palmar Chico subterrane (Ortiz and Lapierre, 1991; Talavera, 1993), and tholeiitic, calc-alkaline, and shoshonitic affinities for the Zihuatanejo–Huetamo subterrane (Talavera, 1993; Centeno, 1994; Freydier et al., 1996, 1997).

1.3. DISTRIBUTION, GEOLOGICAL SETTING, AND STRUCTURAL GEOLOGY OF THE TELOLOAPAN SUBTERRANE

The Teloloapan subterrane (Figures 2 and 3) is exposed in the easternmost part of the Guerrero Terrane, close to of the adjacent Mixteca Terrane (Campa and Coney, 1983) which is the postulated passive margin represented by the Albian–Cenomanian Morelos-Guerrero Platform. The Teloloapan subterrane is characterized structurally by a complex thrust-fault system that verges eastward. Its rocks are deformed and metamorphosed to low-grade, prehnite-pumpellyite and greenschist facies (Campa et al., 1974; Talavera, 1993). The volcanic and volcaniclastic rocks in the Teloloapan subterrane are basaltic to andesitic pillowed and massive lava flows, volcanic breccias, and coarse- to fine-grained volcaniclastic rocks deposited in a marine depositional environment. Compositions are calc-alkaline with geochemical and isotopic characteristics that suggest formation in an intra-oceanic, but evolved island arc (Talavera, 1993). The volcanic and volcaniclastic sequence (the Villa Ayala Formation, Figure 4) changes upward transitionally either to a thick limestone package in the east (The Teloloapan Formation) that contains carbonate platform to slope deposits, or to distal tuff deposits in the west (the Acapetlahuaya Formation), overlain transitionally by an Albian–Cenomanian thin-bedded limestone sequence, termed the Amatepec Formation (not studied in this thesis).

Two siliciclastic units cover the carbonates in the east and west of the study area (Figures 3 and 4). Fine-grained siliciclastic rocks of the Mezcala Formation complete the Upper Cretaceous stratigraphic column where they overlie the Teloloapan Formation along the eastern edge of the Teloloapan subterrane. The Mezcala Formation is made up

of interbedded shale and sandstone, with scattered calcareous debris-flow deposits and thin-bedded limestone deposits as well as siliceous rocks, all deposited in a deep-water setting (Fries, 1960; De Cserna et al., 1978; Ontiveros, 1973; Ramírez et al., 1990). To the west, highly altered and deformed coarse- to fine-grained and thick- to thin-bedded sandstone of the Miahuatepec Formation is exposed above the Amatepec Formation where the Teloloapan subterrane is in structural contact with the Arcelia – Palmar Chico subterrane (Figure 3).

The Teloloapan subterrane was strongly deformed during the Laramide orogeny. There is a complex pattern of east-vergent isoclinal folds associated with penetrative foliation. Thrust faults define the western and eastern boundaries of the Teloloapan subterrane (Campa et al., 1974; Ramírez et al., 1991; Talavera, 1993; Salinas, 1994).

The Teloloapan subterrane shows at least two phases of deformation, and some authors (Elías, 1989; Tolson, 1993) have specified three phases of deformation in the Tejupilco region, north of the study area. The first deformation produced large recumbent folds showing an axial-planar cleavage and bedding-cleavage relationships indicating overturning to the east. The second deformation is characterized by schistosity surface and crenulation schistosity, with general strike of N70°–100°, displaying a well-defined mineral lineation and stretching of clasts and pillow lavas. Fine-grained tuffs and sandstones of the Acapetlahuaya, Mezcala, and Miahuatepec formations, as well as the thin-bedded carbonates of the Amatepec Formation, show a well-developed parallel cleavage, which intersects the bedding planes, as well as fold axial planes that can be used to establish whether units are upright or inverted. The same units are highly

deformed in their finest grained portions in a ductile way, producing small-scale folds showing a wide range of features, such as asymmetric, isoclinal, curvilinear folds, pressure solution, and tectonic stylolites. Intense penetrative deformation in the Teloloapan subterrane has been defined as "broken formation" textures in the Teloloapan area (Cabral, 1995). In thin oriented sections, cut parallel to L1 and perpendicular to S1 in dark micrites or pelites, conspicuous asymmetrical structures include sigmoidal phyllosilicates and quartz or calcite pressure shadows flanking pyrite cubes. The asymmetry of these features supports the eastern sense of tectonic transport (Salinas, 1994).

1.4. DISSERTATION FORMAT

Results of this Ph.D. research are presented in five chapters (chapters 2–6), followed by a chapter summarizing the conclusions (chapter 7). Each chapter finishes with a discussion and comparison with neighboring areas, in order to obtain a regional view of the problem.

Chapter two (**Arc-related successions: stratigraphy and facies**) describes the stratigraphy and facies of the arc-related succession. The chapter gives detailed lithostratigraphic and petrologic descriptions. The main contributions of this chapter are the confirmation of an Early Cretaceous age for the arc-related sucession, and documentation of the facies evolution of the arc sequence.

Chapter three (**Sedimentary Cover Successions: stratigraphy and facies**) documents the stratigraphy and facies in the Upper Cretaceous formations that comprise the post-arc sedimentary cover successions.

Chapter four (**Environmental interpretation and basin development**) interprets the lithofacies present in both the arc-related sequence and the sedimentary cover succession. A depositional history and paleoenvironmental interpretation is proposed for each formation of the Teloloapan subterrane.

Chapter five (**petrography, geochemistry and provenance**) describes the sandstone and volcaniclastic petrography and provenance of the arc-related and sedimentary cover successions. The petrographic results are used to document the similarities and differences between the clastic and volcaniclastic rocks, as well as the sedimentary cover sequences, while the provenance analysis constrains the analysis of the tectonic evolution. Finally, the chapter describes the geochemistry of the volcaniclastic rocks of both the arc-related and the sedimentary cover successions, and makes inferences as to the tectonic affinity of the volcanic source rocks.

The stratigraphic, sedimentological, petrographic, and sedimentary geochemical data are used in chapter six (**Tectonic evolution of the Teloloapan subterrane and implications for origin of the Guerrero Terrane**) to interpret provenance and to develop a tectonic model for the Teloloapan subterrane. Furthermore, regional and local information from neighboring areas is utilized to constrain this tectonic model. Thus, chapter six integrates all the data, summarizes the geological evolution of the Teloloapan

subterrane, and extends this model to the southwestern part of the Guerrero Terrane and its role in the evolution of the Pacific margin of Mexico.

Finally, chapter seven (**Conclusions**) provides an overview of the major contributions of the research.

1.5. COLLABORATION

The field work, section measurement, and sample collection for petrography, geochemistry, macro- and microfossil analysis are entirely the work of the author of this thesis. Subsequently, paleontological specialists from different Mexican institutions identified the fossils. Radiolarian specimens were prepared and classified by M. Sci. Victor Dávila-Alcocer (Instituto de Geología, Universidad Nacional Autónoma de México). Dr. Elizabeth Lara (Instituto Mexicano del Petróleo) classified the calcareous nannoplankton (coccoliths). Ms. Sci. Victoria González-Casildo (Paleontology Department, Instituto Politécnico Nacional) identified the planktonic foraminifera and calcispherulid microfossils. Ms. Sci. María Eugenia Gómez-Luna (Instituto Mexicano del Petróleo) classified the ammonites. Finally, Dr. Blanca E. Buitrón-Sánchez (Instituto de Geología, Universidad Nacional Autónoma de México) identified the nerineids and rudists. All other analyses were completed by the author or by the research technicians in the geochemical laboratories of Memorial University of Newfoundland.

CHAPTER 2. ARC-RELATED SUCCESSIONS: STRATIGRAPHY AND FACIES

2.1. INTRODUCTION, CLASSIFICATION AND TERMINOLOGY

The study area, approximately 1000 km^2, is chiefly covered by two 1:50,000 - scale topographic maps: the Teloloapan and Arcelia maps of the Mexican cartographic office (INEGI). Two distinctive geologic elements delimit the study area: the westernmost limit is the thrust fault that brings the Arcelia – Palmar Chico subterrane over the Teloloapan subterrane; the easternmost limit is the Morelos-Guerrero Platform, considered as the passive margin of the Mixteco Terrane.

The study area is located in the northern part of the state of Guerrero, and is part of the Guerrero Terrane (Campa and Coney, 1983). The rocks in the area strike north - south and are bounded by regional and local faults (Figure 3). The lithological diversity in the region is high, including Lower Cretaceous volcanic, volcaniclastic, and calcareous rocks with low-grade metamorphism in the lowermost units (the arc-related succession, termed here the Villa Ayala, Acapetlahuaya, and Teloloapan formations), to Upper Cretaceous, unmetamorphosed, fine-grained siliciclastic rocks interbedded with thin-bedded limestone and scattered siliceous levels (the sedimentary cover succession, termed here the Mezcala and Miahuatepec formations).

Deformation and low-grade metamorphism of the arc-related rocks are the main obstacles to establishing a stratigraphic framework. Deformation causes stratigraphic repetition and low-grade metamorphism produces strong alteration that partially obscures the welding effect in pyroclastic rocks and some of the original sedimentary structures in

volcaniclastic rocks. Despite these problems, the relationships among units are in some areas clear and help to explain the stratigraphic evolution of the sequences. For brevity, the prefix "meta" to signify low-grade metamorphism in the rocks is dropped and terms such as "metavolcanic" and "metasedimentary" are not used in the thesis.

Formal structural study was not conducted; however, structural studies of other authors (Salinas, 1994; Cabral, 1995; see § 1.3) and the author's own structural observations were used to elucidate the stratigraphy in the field and to avoid duplicate measurement of unit thicknesses. Way-up criteria (e.g., graded bedding and sole markings among others) were used to recognize the base and top of the sequences.

The North America Stratigraphic Code (1984) was followed to revise the stratigraphic nomenclature in the area. Recommendations include: (1) redefinition and elevation of the Villa Ayala and Acapetlahuaya formations, to formal status; and (2) separation of an arc-related carbonate platform from passive-margin rocks of the Morelos Formation, and redefinition of the Teloloapan Formation to include the arc-related carbonate unit. The second recommendation places the carbonate-platform rocks in the Guerrero Terrane (the Morelos Formation) in the Mixteco Terrane.

None of the units studied here have been subjected to a detailed paleontological study in the thesis area, but new samples collected for this thesis demonstrate an Early Cretaceous age for the arc-related succession. This is supported by biostratigraphic and radiometric ages reported by other authors. The Early Cretaceous age proposed here for the arc-related succession is the youngest age ever proposed for this sequence (Figures 4 and 5).

The arc-related succession in the thesis area includes both primary volcanic and volcaniclastic rocks. Nevertheless, facies analysis was conducted mainly on the latter. Talavera (1993) characterized the primary volcanic rocks and they will be described only briefly to document their relationships with the volcaniclastic rocks.

Most of the volcaniclastic rocks in the Villa Ayala and Acapetlahuaya formations were deposited by subaqueous gravity flows in deep-water environments. The facies classification and interpretations applied to these rocks are based on the deep-water facies scheme of Pickering et al. (1989). Similarly, pyroclastic rocks are described and interpreted using criteria provided by a number of authors (e.g., Busby-Spera, 1987; 1988; Cas and Wright; 1987, 1991; Kokelaar and Busby, 1992).

Classifications of bed thickness and grain size for the volcaniclastic rocks are those proposed by Ingram (1954) and Chough and Sohn (1990), respectively (Table 1). Tuffs are subdivided into fine- and coarse-grained varieties as proposed by Fisher and Schmincke (1984). Facies are described based on lithology, textures, sedimentary structures, biological features, bedding thickness, and bed contacts. As proposed by Cas and Wright (1987, 1991), descriptive facies terminology is used for the volcaniclastic rocks. Finally, an alphabetic and numeric code is used following Pickering et al. (1989) for all the facies.

The term "volcaniclastic" is used as a wide non-genetic term that includes autoclastic and epiclastic rocks directly erupted or derived from the erosion of contemporaneous or redeposited volcanic material. Units derived by weathering and/or

erosion of penecontemporaneous or older volcanic rocks are described as epiclastic rocks (Fisher and Schmincke, 1984; Lajoie and Stix, 1992).

The term "pyroclastic flow" is here restricted to deposits with some evidence of emplacement by volcanic eruptions. Welding textures, presence of fiamme, euhedral phenocrysts, highly angular volcanic lithic fragments, abundance of broken crystals, and a monolithic composition of the volcanic rock fragments are used to indicate a pyroclastic rather than an epiclastic origin (cf. White and Busby-Spera, 1987). Cas and Wright (1987) stated that a detailed description and paleoenvironmental interpretation of the bounding facies is essential in determining the possibility of subqueous welding in pyroclastic flow deposits. Fisher and Schmincke (1984) noted that subaqueous pyroclastic flow deposits resemble turbidites and thus may remobilized pyroclastic debris originally deposited by fallout or other processes on flanks of active volcanoes. However, Fisher and Smith (1991) argued that accumulations of pyroclastic particles that are carried to their final site of deposition by transporting agents (e.g. turbidity currents) are not epiclastic because are not formed by weathering.

The terminology in this thesis conforms to the viewpoint of Fisher and Schmincke (1984) and Fisher and Smith (1991) that epiclastic deposits must be derived by weathering and/or erosion. Units formed principally of pyroclasts, with a monolithic composition and no evidence of prior weathering, are therefore described using the terminology for pyroclastic rocks. For example, as advocated by Orton (1996), "tuff" is used in this thesis for lithified units of ash-sized volcanic particles (texturally equivalent to sandstones). As a result, "tuff" indicates the near-exclusive pyroclastic composition

and/or origin of the particles, rather than the mode of their final emplacement, which might include settling through the water column with or without bottom-current redistribution, or lateral redistribution by turbitidy currents without contamination by older detritus. During the surficial redistribution of such materials, or even during settling of ash through the water column, contemporaneous microfossils may be incorporated. After accumulation, benthic organism like mollusks or benthic foraminifera may be burrow into the pyroclastic deposits, forming a mixed biogenic-pyroclastic sediments. "Ash turbidites" is used when pyroclastic origin is not completely sure.

Lithologic description of carbonate rocks of the Teloloapan Formation is based on the classification scheme of Embry and Klovan (1971). This classification, based on Dunham (1962), emphasizes the depositional textures of the carbonates rocks. The carbonate facies are characterized by their lithology, bed thickness, contacts, textural features, and organic material such as macrofossils and microfossils present in each facies. This field information was complemented with petrographic descriptions of more than 100 thin sections.

This chapter also contrasts the new ages and stratigraphic terminology with older concepts, and discusses controversies related to the proposed existence of pre-Mesozoic basement in the area, as suggested by other authors (Figure 4). The stratigraphic relationships of the arc-related succession are described in detail in order to obtain a better understanding of the sedimentary evolution of the area.

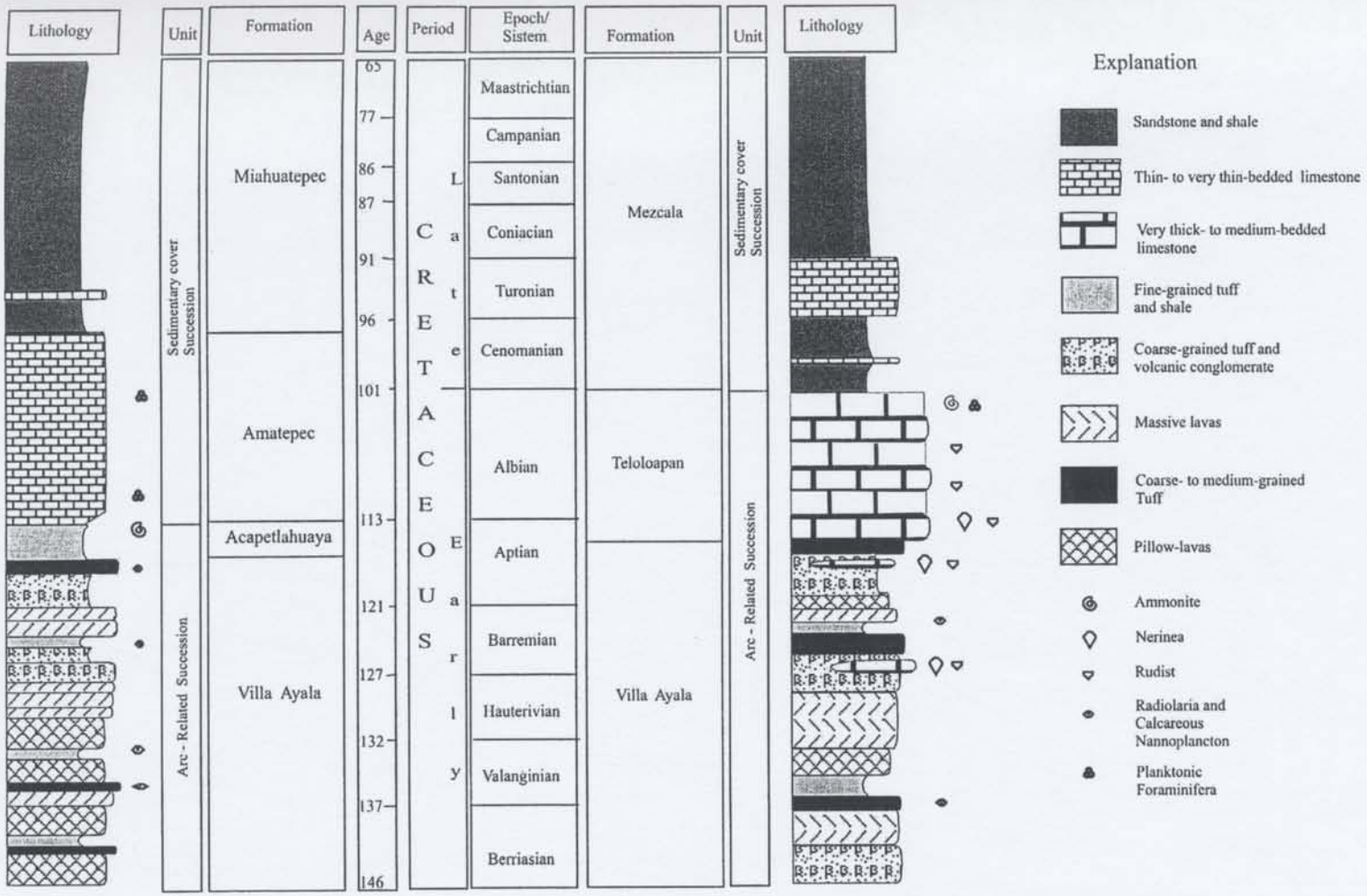

Figure 5. Composite stratigraphic columns of the Teloloapan subterrane. Left and right columns represent the western and eastern stratigraphy, respectively. Time scale from Gradstein et al. (1995). Note that relatively thickness are not accurately rendered

Table 1. Classifications of bed thickness and grain size

A.	Bed thickness*	Thickness (cm)
	Very thin beds	1–3
	Thin beds	3–10
	Medium beds	10–30
	Thick beds	30–100
	Very thick beds	>100
B.	Grain size+	Diameter (mm)
	Silt	<0.0625
	Very fine sand	0.0625–0.125
	Fine sand	0.125–0.25
	Medium sand	0.25–0.50
	Coarse sand	0.50–1
	Very coarse sand	1–2
	Granule	2–4
	Pebble	4–64
	Cobble	64–256
	Boulders	>256
C.	Grain size++	Diameter (mm)
	Fine-grained ash	<0.0625
	Medium-grained ash	0.063–0.5
	Coarse-grained ash	0.5–1
	Very coarse-grained ash	1–2
	Fine-grained lapilli	2–4
	Medium grained lapilli	4–16
	Coarse-grained lapilli	16–64
	Fine-grained blocks	64–256
	Coarse-grained blocks	>256

* Ingram (1954); + Wentworth (1922); ++ Chough and Sohn (1990)

2.2. LITHOSTRATIGRAPHIC STUDIES OF THE TELOLOAPAN SUBTERRANE

Despite the many geological studies conducted in the Teloloapan area, only a few have dealt, superficially, with the stratigraphy of the region (Campa et al., 1974; De Cserna, 1983; Ramírez et al., 1990; Cabral, 1995). Nevertheless, there are many regional studies that include hypothetical stratigraphic tables despite the controversial age of various units. The stratigraphic controversies in the Teloloapan area are mainly related to the age of, and possible basement to, the volcanosedimentary sequence, as well as to the significance of the carbonate platform rocks.

The Teloloapan subterrane does not have a formal stratigraphy. Because of the structural complexity, metamorphism, and dearth of well preserved fossils, these rocks have been assigned to the Precambrian, Paleozoic and/or Triassic (Fries, 1960; De Cserna, 1983); Triassic to Upper Jurassic (Elías and Sánchez, 1992; Sánchez, 1993); Upper Jurassic to Lower Cretaceous (Campa et al., 1974 and 1980); and Lower Cretaceous (Guerrero et al., 1990; Ramírez et al., 1990; Campa and Iriondo, 2003).

Fries (1960) originally defined the volcanosedimentary sequence cropping out in the Taxco-Taxco El Viejo area, 35 km northeast of the study area (see Figure 1), as "Esquisto Taxco" and "Roca Verde Taxco Viejo". He assigned a Paleozoic age to the former and a Triassic age to the latter based on lithological correlation with similar rocks from the Zacatecas region in central Mexico. However, Fries did not correlate this sequence with the Teloloapan subterrane, although other authors subsequently have

(Ontiveros, 1973; De Cserna et al., 1978; De Cserna and Fries, 1981; De Cserna, 1983; Elías and Sánchez, 1992; Cabral, 1995).

In a regional study, Ontiveros (1973) studied the stratigraphy of the Taxco-Teloloapan area and concluded that the volcanosedimentary rocks cropping out in the Teloloapan region belong to the "Esquisto Taxco" and the "Roca Verde Taxco Viejo", postulating a Late Jurassic or Early Cretaceous age for the former and a pre–Cretaceous age for the latter. Both ages were argued solely on the basis of lithology, and possible unconformities with overlapping units.

Subsequently, Campa et al. (1974) defined the Teloloapan volcanosedimentary rocks as the "Secuencia Volcanosedimentaria de Teloloapan-Ixtapan de la Sal", and postulated a Late Jurassic to Early Cretaceous age based on scattered ammonites and microfauna. They divided the sequence into two units termed metavolcanic and metasedimentary rocks. In later articles, Campa and coauthors (Campa and Ramírez, 1979; Campa et al., 1980) reiterated their support for a Late Jurassic to Early Cretaceous age, rather than a Paleozoic-Triassic age.

Recently, Guerrero et al. (1990) and Ramírez et al. (1990) proposed an Early Cretaceous age for the Teloloapan arc-related successions based on Aptian fauna found in the uppermost levels of the volcaniclastic sequence and concordant stratigraphic contacts throughout all units. Furthermore, informal names and lithological divisions were proposed for the arc-related succession. The same Early Cretaceous age has been advocated in internal reports of PEMEX, the Mexican national oil company (Gonzalez, 1991).

Elías and Sánchez (1992) proposed that the volcanosedimentary sequence cropping out in the Tejupilco area, north of the thesis area (their Teloloapan-Tejupilco Sequence, see Figures 2 and 4) might represent an arc assemblage older than the rest of the Guerrero Terrane. However, this unit has been considered as part of the Late Jurassic to Early Cretaceous arc assemblage by other authors (Campa and Ramírez, 1979; Ramírez et al., 1991; García and Talavera, 1994).

Gneissic rocks cropping out in the Tejupilco region have been interpreted as the basement of the Teloloapan volcaniclastic sequence (Parga, 1981; Elías, 1981; Elías and Sánchez, 1992). Pursuing this idea, Ortega (1981) studied the metamorphic belts of southern Mexico and included the rocks of the Teloloapan subterrane in the "Tierra Caliente Complex". He also included all the volcanosedimentary rocks cropping out from Zihuatanejo to Taxco as part of this complex and assigned it a Late Paleozoic to Cretaceous age based on previous publications. Ortega (1981) assumed a granitic basement for the complex.

Campa et al. (1980) divided the volcanosedimentary rocks of the Sierra Madre del Sur into different assemblages and included the sedimentary and volcanosedimentary rocks of the Teloloapan subterrane in the "Teloloapan–Ixtapan assemblage". Later, Campa and Coney (1983) assigned all these sequences to the Guerrero Terrane, and interpreted a Late Jurassic to Early Cretaceous age for the arc sequences along the Pacific margin of Mexico. No basement rocks were recognized for these sequences.

Supporters and non-supporters of the hypothesis that basement rocks are preserved have provided evidence for their points of view. Elías and Sánchez (1992)

reported a preliminary late Permian Rb–Sr age for a granitoid rock and suggested a peraluminous affinity for the rock based on petrographic studies. However, they concluded that the contact with the volcanosedimentary rocks is tectonic. Recently, Elías and Ortega (1997) reported high-grade metamorphic xenoliths in Oligocene rhyodacitic rocks, suggesting the existence of pre-Mesozoic basement, probably Precambrian, beneath the Guerrero Terrane. On the other hand, Ramírez (1984) concluded based on intrusive field relationships that the gneissic rock in the Tejupilco region is an Upper Cretaceous age intrusion. Based on mapping, stratigraphic, structural, and petrographic data, García and Talavera (1994) proposed that this orthogneiss might represent a syntectonic intrusion because the intrusive contact is itself not deformed.

Another long-standing problem concerns the middle Cretaceous carbonate rocks cropping out in the Teloloapan and Huetamo regions. Two interpretations have been put forward for these Albian–Cenomanian carbonate platforms. One group has postulated that the carbonates are related to the middle Cretaceous (Albian–Cenomanian) Tethyan transgression into the Gulf of Mexico (Fries, 1960; Ontiveros, 1973; De Cserna et al., 1978; Johnson et al., 1991). In this scenario, carbonate rocks represent part of a postulated passive margin that existed during this time. However, in southern Mexico, long distances generally separate outcrops of carbonates so that continuity with the Tethyan passive margins cannot be proven. Nevertheless, researchers in this first group have interpreted the lack of carbonate rocks between the Teloloapan and Huetamo areas either as the result of non-deposition or as a lateral facies change into an intervening deep-water setting (De Cserna et al., 1978; Johnson et al, 1991).

Another group has reported an older age (Aptian–Albian) for the carbonate rocks in the Teloloapan and Huetamo areas. They have postulated that these rocks are more related to an island-arc setting than to a passive margin (Guerrero et al., 1990, 1991; Ramírez et al., 1990, 1991). This postulated arc-related carbonate bank has been named the Teloloapan platform. A close association with the arc is based on gradational contact between the carbonate and volcanosedimentary sequences. The view that these carbonates are related to an arc terrane is also supported by Cabral (1995), although he interpreted a disconformity between the carbonate and volcaniclastic rocks.

Because of a lack of detailed stratigraphic and paleontological studies in the arc-related and associated sequences, neither a formal stratigraphic terminology nor a precise age for the sequences has been established. This thesis aims to erect a coherent stratigraphic framework and age model based on previous geological studies and the new paleontological data obtained during the study.

2.3. LOWER CRETACEOUS LITHOSTRATIGRAPHY: THE ARC-RELATED SUCCESSION

Stratigraphic repetitions and inversions are common because of the high level of deformation. Therefore, the full stratigraphic thickness is difficult to determine. Nevertheless, a coherent volcanic and volcaniclastic succession has been recognized based on way-up criteria and structural features.

The succession consists of a thick sequence of volcanic and volcaniclastic rocks. The best outcrops are distributed in the east–central part of the field area (Figure 3).

Three formations, here defined as Villa Ayala, Acapetlahuaya, and Teloloapan, comprise the arc-related succession. This section contains the basic stratigraphic descriptions. Facies descriptions and field photograps are provided in § 2.6.

2.3.1. The Villa Ayala Formation

a. History and name

Ontiveros (1973) correlated the volcaniclastic rocks of the Teloloapan area with the "Roca Verde Taxco Viejo", described in the Taxco region by Fries (1960) as foliated and low-grade metamorphosed andesitic tuff, breccias and lavas. Ontiveros (1973) described the unit as tuff and yellow siltstone interbedded with lavas and calcareous breccias, all slightly metamorphosed.

Based on stratigraphic and petrographic characteristics, Campa et al. (1974) formally divided the volcaniclastic rocks into two lithostratigraphic units: (1) a volcanic unit, including tuffs, agglomerates, and lavas; and (2) a metasedimentary unit, containing phyllites, sandstones, quartzites and foliated limestones. They defined these rocks as the "Secuencia Volcano-Sedimentaria de Teloloapan-Ixtapan de la Sal" and assigned a Late Jurassic (Tithonian) to Early Cretaceous (Neocomian) age.

Guerrero et al. (1990) informally redefined the arc-related succession as the Villa Ayala and Acapetlahuaya formations and attributed a Hauterivian to late Aptian age to the sequence. They described the Villa Ayala Formation as lavas, coarse- to fine-grained epiclastic and pyroclastic rocks, including breccias, volcanic conglomerate, tuff, and sandstone.

Cabral (1995) assigned the volcanic and volcaniclastic rocks of the Teloloapan region to the "Taxco Schist" and "Roca Verde Taxco Viejo". He proposed a pre-Aptian age for the sequence because of its deformation and metamorphism.

The name Villa Ayala comes from the occurrence of the formation at the town of Villa Ayala in the Teloloapan municipality, located on Federal Road 51 (Figures 3 and 6). In this area, the Villa Ayala Formation is well exposed and the lithology is representative of the unit.

b. Type section and thickness

The proposed type section is located between Villa Ayala and Ranchos Nuevos (Appendix 1, Figures 3 and 6), where the lowest and middle parts of the formation crop out. Although the area is affected by normal faulting and folding good exposures are available along Federal Road 51 and north of the area (Figure 3).

The complete formation is not exposed at the type section. An approximately 1000 m thickness is exposed. The lower contact is not exposed and the thick sequence of pillow lavas in the town of Villa Ayala is recognized as the lowest level and arbitrary base of the unit (Figure 6B and 6C). The upper contact with the Acapetlahuaya Formation is observed north and south of the type area (Figure 6A). In the eastern part of the study area, the Acapetlahuaya Formation is absent and the Villa Ayala Formation is overlain by the Teloloapan Formation. A reference section for the upper contact with the Teloloapan Formation is proposed at the town of Ahuacatitlan (Appendix 2, Figures 3 and 7). In addition good outcrops of the middle portion of the Villa Ayala Formation are present in and north of the Alpixafia-Teloloapan area (Figure 3).

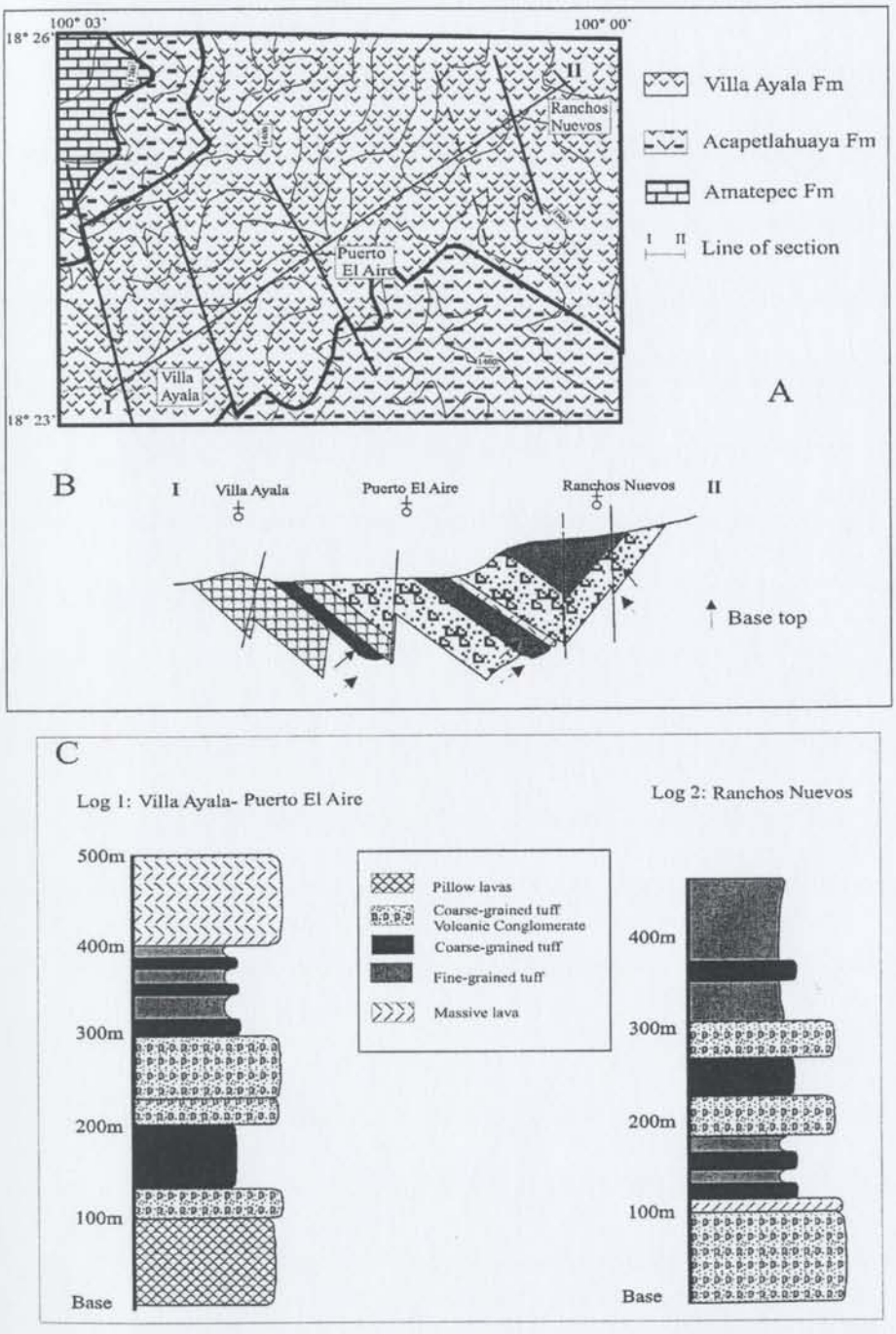

Figure 6. Villa Ayala Formation: (A) type area, (B) schematic structural section along I–II, and (C) logged section through the lower and middle portions of the unit.

The true thickness of the Villa Ayala Formation is unknown because of the structural complexity in the area, even at the type section. The formation varies in thickness from 1000 m at the type section to 100 m at the reference section. It is ~500 m thick on Arroyo Zacatlancillo and along the Alpixafia to Teloloapan road (see Figure 3). It was not possible to measure more than small sections in detail (see facies description, § 2.6. in this chapter), but the complete thickness might be more than 2 km, as has been suggested by other authors (Campa et al., 1974; Talavera, 1993; Cabral, 1995). Nevertheless, it is not clear whether the variable thicknesses reported are the result of deformation or whether these are original depositional differences.

c. Lithology

Detailed description of the facies is on § 2.6.1. Volcanic rocks predominate at the base of the Villa Ayala Formation, while in the middle and upper portions of this unit the volcanics are interbedded with pyroclastic and epiclastic rocks such as radiolarian chert, coarse- to fine-grained tuff and tuffaceous sandstones, as well as debris-flow deposits (Figures 6C and 7C).

At the type section, the Villa Ayala Formation is mainly volcanic rocks that are dark green to light green, porphyritic pillow lavas and hyaloclastites with the composition of basalt and basaltic-andesite. This succession is followed by almost 40m of interbedded fine- to medium-grained tuff. The succession shows abundant sedimentary structures such as normal grading, planar and ripple lamination.

Along the type section between Villa Ayala and Puerto el Aire towns, there is a succession of masive lavas, pyroclastic rocks, conglomerates and volcanic breccias.

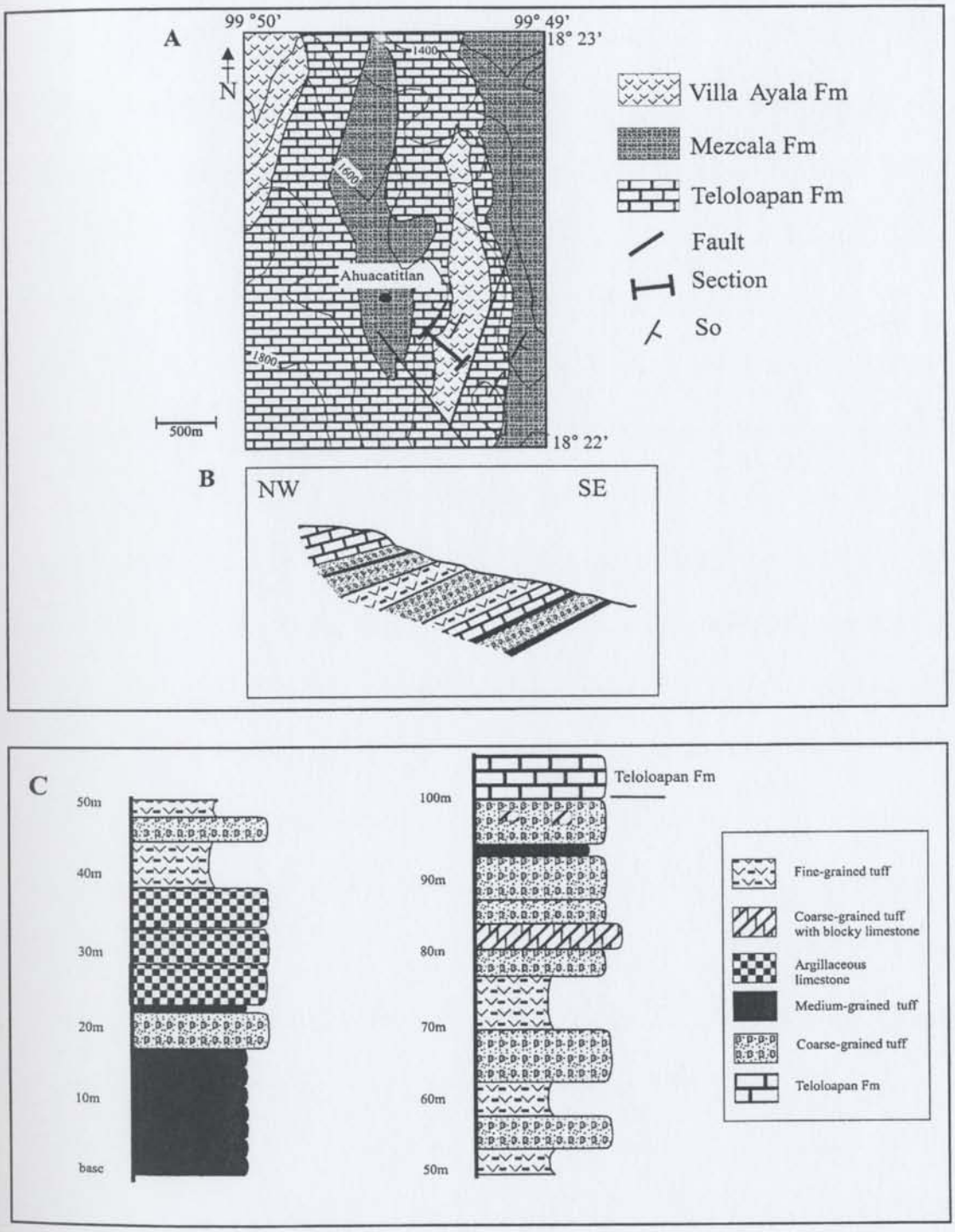

Figure 7. Villa Ayala Formation: (A) reference area, (B) schematic structural section, and (C) reference section representing the upper portion of the unit in the Acapetlahuaya area.

Only the lower level contains pillow lavas, while masive lava flows are interbedded with the younger pyroclastic rocks, volcanic conglomerates and breccias. Pyroclastic rocks contain angular to subangular volcanic fragments. The intense weathering in this region obscures the primary depositional features of the rocks. However, in the Alpixafia area, there are matrix-rich and matrix-poor, masive to graded beds of volcanic conglomerate and breccias interbedded with tuffs.

Above the poorly exposed volcanic conglomerate and breccias, there is a thick succession (~60 m) of thin- to medium-bedded tuff interstratified with thin-bedded and fine- to very fine-grained tuff exposed in the town of Puerto el Aire (Figure 6). Petrographically, both the tuffs have lithic fragments (basalt and andesite), devitrified glass, pyroxenes, amphiboles, and feldspars, in a fine tuffaceous, locally glassy or devitrified matrix. Radiolarians are also abundant. A crude cyclicity is observed in this interval with coarse-grained tuffs at the base of each cycle followed by fine- to very fine-grained tuff beds showing Bouma sequences. The main characteristic of this level is the intense alteration by kaolinitization that is easily recognized by the black and light-yellow color of the rocks.

Finally, in the Ranchos Nuevos area (Figure 6), there is a repetitive succession of lava flows, volcanic conglomerates, and breccias similar to those previously described. Only the uppermost level, in the town of Ranchos Nuevos, shows volcanic epiclastic conglomerates with polygenetic clasts of basalt, basaltic-andesite, and tuff. The same level displays lateral and vertical grain-size variation and rip-up clasts, as well as poorly developed reverse grading.

The upper level of the Villa Ayala Formation is variable. In the central area, in contact with the Acapetlahuaya Formation, it is a monotonous succession of thin-bedded and fine- to medium-grained tuff that is more than 100 m thick. Where overlain by the Teloloapan Formation in the east, the Villa Ayala Formation shows channelized coarse-grained epiclastic sandstone and epiclastic volcanic conglomerate interbedded with lavas, and fine-grained epiclastic sandstones containing abundant debris of mollusks and corals. Abundant fossils of nerineids and corals are also typical of this level. The best exposures are located in the town of Ahuacatitlan and on the road between Teloloapan and Ahuacatitlan towns (Figures 3 and 7).

d. Boundaries and distribution

The lower contact is not observed in the study area. In the central and western areas the Villa Ayala Formation is overlain by the Acapetlahuaya Formation with a concordant and transitional contact in different areas (Figures 3 and 6). The contact is characterized by volcanic conglomerates and breccias interbedded with thin- to medium-bedded tuffs, all belonging to the Villa Ayala Formation followed by a monotonous fine-grained tuff without coarse pyroclastic beds, typical of the Acapetlahuaya Formation. The best exposure of this contact is northwest of Acapetlahuaya and south of the town of Villa Ayala in the central area. To the west, the town of Juntas de Zicatecoyan is the best place to observe the contact.

The Villa Ayala Formation is overlain in the east of the thesis area by the Teloloapan Formation (Figures 5 and 7). This contact is observed at the Ahuacatitlan locality and west of Teloloapan along the road to Ahuacatitlan, where it is concordant

and gradational (Figure 7C). The contact is characterized by lava flows interbedded with medium-bedded and coarse-grained tuff and epiclastic sandstones containing an abundant fauna of nerineids and corals, all belonging to the Villa Ayala Formation. The coarse-grained tuff level changes upward to thin- to medium-bedded and medium-grained epiclastic sandstone that is interstratified with medium-bedded bioclastic limestone with abundant nerineids, belonging to the Teloloapan Formation.

The Villa Ayala Formation is well exposed in the west in the Tenanguillo area, as well as along Federal Road 51 from Teloloapan to Alpixafia (Figure 3). There are also good outcrops in the central part of the thesis area, along and northward from Federal Road 51 between the Cerro El Chivo and Villa Ayala localities.

e. Fauna, flora and age

Radiometric and paleontologic data reported by other authors, and fossils collected for this thesis indicate that the age of the Villa Ayala Formation ranges from Berriasian to Aptian.

Radiometric ages from the thesis area have been ascribed to post-depositional metamorphic events. These ages range from Albian to Turonian (Talavera, 1993; Salinas, 1994; Cabral, 1995). The older radiometric dates of the Teloloapan subterrane have been reported south of the study area (Campo Morado and Apaxtla areas). Gonzalez (1991) reported an Early Cretaceous K-Ar age (133±4 Ma, late Valanginian) in the Apaxtla area. Mortensen et al. (2003) obtained a latest Jurassic–earliest Cretaceous (145.9-137.4 Ma) U-Pb zircon age in the Campo Morado area. Urrutia and Linares (1981) reported 108±5 Ma (Early Albian) and 125±5 Ma (Late Barremian) whole rock K-Ar dates for volcanic

rocks from Ixtapan de la Sal area, north of the study area. The Albian–Turonian ages reported by Cabral (1995) and, perhaps, the Albian age of Urrutia and Linares (1981) could date metamorphism.

The age of the Villa Ayala Formation has been unclear due to a lack of age diagnostic macrofossils and microfossils. During fieldwork, 30 samples were collected and processed for radiolarian fauna. Unfortunately, only recrystallized and badly preserved radiolarians (external spheres and recrystallized shapes) were obtained. A second processing was done using six of the best samples. However, the same results were obtained. Next, 20 samples were collected from fine- and medium-grained tuffs for extraction of calcareous nannoplankton (coccoliths). Six samples contained scarce poorly preserved coccoliths but they could be tentatively assigned to the Hauterivian–Aptian (Elizabeth Lara 1999, written communication and Appendix 3).

Salinas (1994) reported Valanginian–Aptian radiolarians from the Luvianos locality, north of the study area (Appendix 3 lists the species). Although Salinas (1994) considered the area to be part of the Arcelia – Palmar Chico subterrane (see Figure 2 and 3), the lithology, stratigraphic distribution of the units, and petrography better match characteristics of the Teloloapan subterrane. The radiolarian ages are, in particular, consistent with the Early Cretaceous age obtained using calcareous nannoplankton (coccoliths) and radiometric data.

The lowermost and middle portions of the Villa Ayala Formation contain poorly preserved and scarce microfauna; in contrast, the uppermost level of the unit, in the Acatempan-Ahuacatitlan area, contains abundant nerineid fauna. These included

Nerinella dayi (Blanckenhorn), *Cossmannnea (Eunerinea) titania*, *Plesioptyxis fleuriani* (d' Orbigny), and *Cossmanea* (*Eunerinea*) *hicoriensis* (Cragin), an Aptian assemblage (Buitrón, 1999; written communication). These nerineid fauna have been exclusively reported in Aptian rocks from central Mexico (Buitrón and Barcelo, 1988; Garibay et al., 1996).

The Early Cretaceous age for the formation is well constrained by previous paleontologic and radiometric studies, as well as by the fauna, flora, and stratigraphic relationships reported here. The precise age of the formation is particularly important as a constraint on tectonic and regional correlations among the arc sequences in southwestern Mexico. Previous tectonic interpretations assume Late Jurassic to Early Cretaceous ages for all the sequences. However, the age control for the Villa Ayala Formation restricts the Teloloapan subterrane exclusively to the Early Cretaceous (Berriasian–Aptian).

2.3.2. The Acapetlahuaya Formation

a. History and name

Few researchers have considered rocks assigned to the Acapetlahuaya Formation as an independent unit. These rocks have instead been included as a part of a larger volcanosedimentary unit by different authors. Campa et al. (1974) assigned these rocks to the metasedimentary unit "Secuencia volcanosedimentaria de Teloloapan-Ixtapan la Sal", describing them as light brown to gray-green micaceous phyllites. De Cserna (1983) included similar rocks in the Acuitlapan Formation (Figure 4), described as a sequence of shales, graywackes, and sandstones with gray-green color due to tuffaceous material.

Ramírez et al. (1990) informally recognized a unit of interbedded finely laminated shale and siltstone. Finally, Cabral (1995) reported similar rocks in his "Taxco Schist Formation" (Figure 4). He described the sequence as fine-grained micaceous and/or chloritic pelitic schists and considered it to be basement to volcanic arcs in the area (see § 2.5).

The name Acapetlahuaya comes from the town of Acapetlahuaya where the lower and upper contacts are well exposed. The unit, although deformed and partially covered, is completely exposed around the town.

b. Type section and thickness

The section measured northwest of the Acapetlahuaya locality, along the rural road from Huayatengo to Acapetlahuaya, is designated as the type section for the Acapetlahuaya Formation (Appendix 4, Figures 3 and 8). The section includes the lower and upper contacts with the Villa Ayala and Amatepec formations, respectively.

At the type section, the formation is a minimum of 434 m thick. In this area, only small portions were measured in detail because of the deformation and discontinuous outcrops (Figure 8B), so the estimated thickness should be viewed with caution. In the western portion of the study area, in the Almoloya and Juntas de Zicatecoyan areas (Figure 3), a thickness of 100 m was calculated. Other authors have reported almost the same thickness for this unit. De Cserna (1982) calculated 350–400 m in the northwestern part of the thesis area for the same unit that he termed the Acuitlapan Formation, while Cabral (1995) estimated 800 m for the unit that he named the "Taxco Schist Formation".

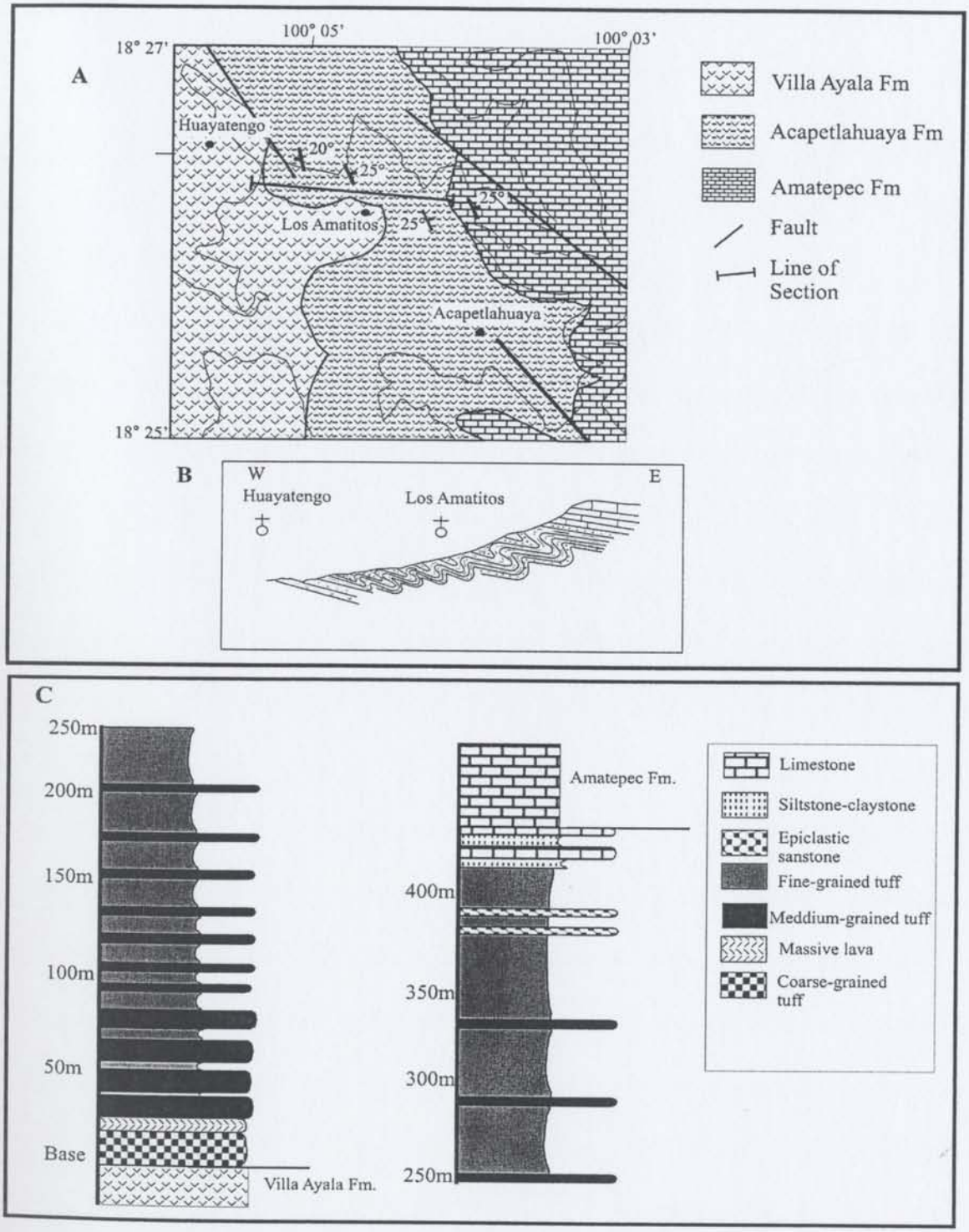

Figure 8. Acapetlahuaya Formation: (A) type area, (B) schematic structural section, and (C) composite log.

c. Lithology

The Acapetlahuaya Formation in the study area is characterized by a monotonous sequence of light green to yellow medium- to fine-grained tuff that changes upward to very fine-grained tuff interstratified with siltstone and claystone (Figure 8c). Petrographic analysis confirms a pyroclastic origin for these rocks.

Thick-bedded (60–80 cm) and medium-grained tuffs are characteristic of the base of the sequence. Graded beds and parallel lamination are the predominant sedimentary structures. At this level, thin-bedded and very fine-grained tuff is sporadically present in beds less than 5–8 cm thick. Only one lava flow is present at this level (Figure 9C). Above, in the middle part of the formation, the meddium-grained tuff and fine-grained tuff beds occur in a 1:1 ratio. The uppermost part of the middle portion of the formation contains mainly fine-grained tuff beds; medium-grained tuffs are scarce or sporadic (ratio is 2:1 to 3:1).

The upper portion of the unit is characterized by millimeter-thick laminae of tuff interrupted sporadically by thin to medium beds of fine-grained epiclastic sandstone. No petrographic study was done to confirm the pyroclastic composition because of the very fine grain size and the intense deformation at this level, so the so-called tuff might be epiclastic siltstone or claystone. However, the epiclastic nature of the sandstone was confirmed in thin section. Finally, a transitional zone (10–20 m) is observed with the overlying Amatepec Formation. This transitional zone is included in the Acapetlahuaya Formation (Figure 8C) and consists of very thin-bedded limestone associated with siltstone and claystone, changing upward to thin-bedded limestone with scarce siltstone.

d. Boundaries and distribution

The lower boundary with the Villa Ayala Formation is gradational and was described above. The upper boundary is also gradational with thin-bedded limestones of the Amatepec Formation. This contact can be observed around the town of Acapetlahuaya (Figures 3 and 8). In the west of the thesis area, the contact is also well exposed around Almoloya and Las Juntas de Zicatecoyan.

The Acapetlahuaya Formation is mainly distributed in the central part of the thesis area in a north- to south-trending belt (Figure 3). A similar north–south trend is observed in the west where the unit is well exposed in the Almoloya to Las Juntas de Zicatecoyan areas. The Acapetlahuaya Formation is not exposed in the eastern part of the thesis area. Fine-grained tuff in this area is assigned to the Villa Ayala Formation.

e. Fauna, flora, and age

Although extensive sampling was done throughout the unit for radiolarians and calcareous nannoplankton (coccoliths), no microfossils were obtained, perhaps due to the intense deformation and low-grade metamorphism observed in these fine-grained volcaniclastic rocks.

Others authors have reported ammonites in rocks similar to the Acapetlahuaya Formation. Burckhard (1930), in the Campo Morado area, reported an ammonite classified as *Dufrenoya* aff. *Turcata* (Sow) and assigned a late Aptian age. Campa et al. (1974, 1980) found several types of ammonites in one locality in the region, the El Pochote locality. They reported *Dufrenoya* sp., *Parahoplites* sp., and *Hamites* sp., which give a late Aptian age. The same fauna was reported south of the area, at the Campo

Morado locality. Finally, Lorinczi and Miranda (1978) reported an Aptian age based on an ammonite classified as *Acanthoplites* sp.

The late Aptian age reported by several authors is consistent with a concordant stratigraphic relationship between the fine-grained tuff deposits of the Acapetlahuaya Formation and the volcanic-volcaniclastic rocks of the Villa Ayala Formation. All available data support a late Aptian age for the Acapetlahuaya Formation.

2.3.3. The Teloloapan Formation

a. History and name.

Different studies have considered limestones in the Teloloapan region as the western edge of the Guerrero-Morelos platform, so that the Teloloapan Formation of this thesis is usually assigned to the Morelos Formation (Fries, 1960; Ontiveros, 1972; De Cserna et al., 1978; Johnson et al., 1991). The Morelos Formation was formally defined by Fries (1960) as a masive to thick-bedded limestone and dolostone of Albian–Cenomanian age with abundant miliolids and rudists. The failure to differentiate the Teloloapan Formation from the more extensive Morelos Formation stems from their close proximity in the field (Figure 3) and their similar facies. However, it will be demonstrated here that the Teloloapan Formation is part of the arc-related succession, and therefore should not be part of the Morelos Formation, which is found in a different tectonic terrane.

Ontiveros (1973) described abundant masive beds of rudist boundstone and interpreted these as a reef facies in the Teloloapan area. Campa et al. (1974) included the

Teloloapan Formation in the metasedimentary part of the "Secuencia volcanosedimentaria de Teloloapan-Ixtapan de la Sal" and described it as a thick-bedded and foliated limestone with mudstone and breccia textures. Ramírez et al. (1990) informally termed the limestone the Teloloapan Formation. They described the unit as a masive to medium-bedded limestone with textures varying from mudstone to boundstone, and showing a close relationship with volcaniclastic rocks. They also proposed an Aptian–Albian age for the unit. Finally, Cabral (1995) assigned these same rocks to the Morelos Formation; nevertheless, he concluded that the lithology observed in his study area does not correspond exactly to original descriptions of the Morelos Formation.

The name Teloloapan Formation is proposed for the upper Aptian to Albian calcareous rocks that show vertical gradational passage from underlying volcaniclastic rocks belonging to the Villa Ayala Formation. This distinguishes these calcareous rocks from the Albian–Cenomanian Morelos Formation, exposed east of the thesis area in the Chilacachapa structure (Figure 3). The type Morelos Formation neither contains volcanic influence nor is underlain by volcanic rocks. The name Teloloapan is derived from the town of the same name in the area (Figure 3).

b. Type section and thickness

Limestones of the Teloloapan Formation exhibit considerable textural variation and the complete formation is not contained in one section. The section measured northeast of the town of Teloloapan, in the west flank of an anticline (Appendix 5, Figures 3 and 9), is here proposed as the type section and type area for the unit. Although the upper contact is not exposed here because of a fault, the lower contact and almost all

the unit crops out in the section. A reference section (Appendix 6, Figure 10) is proposed west of the town of La Concordia where the uppermost levels of the formation and the lower contact with the Mezcala Formation are exposed.

Because the Teloloapan Formation is not completely exposed, an accurate thickness cannot be measured. However, at the type section, the unit is 485 m thick without its top exposed. At the reference section, 80 m was measured below the Mezcala Formation. The thickness of the Teloloapan Formation is variable in the region and in some areas it might be thinner or thicker than indicated above.

c. Lithology

The lower portion of the Teloloapan Formation is exposed in the Ahuacatitlan and Teloloapan areas where it is interbedded with volcaniclastic rocks belonging to the Villa Ayala Formation. At the type section, this part is composed of medium-bedded packstone to wackestone, sometimes partially or completely recrystallized and dolomitized, with algal mats, burrows, and abundant fossils of nerineids, corals, benthic foraminifera, and rudists (Figure 9C). In the Ahuacatitlan area, the lower part of the Teloloapan Formation is instead masive to thick-bedded packstone to grainstone with abundant intraclasts (bioclasts and lithoclasts) with a coarse-grained texture but also interstratified with volcanosedimentary rocks. This lower part of the formation changes gradationally upward to the middle part of the unit.

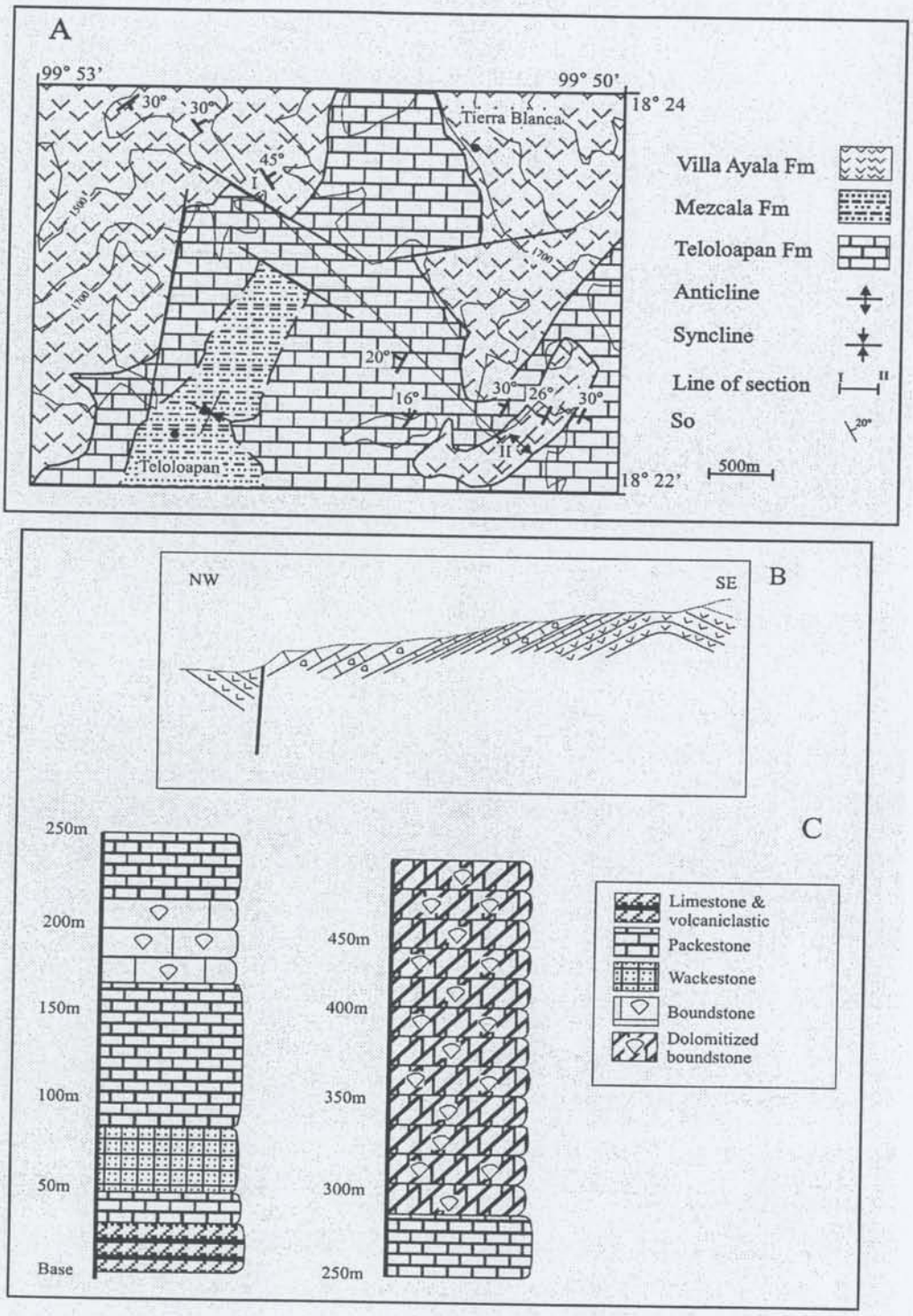

Figure 9. Teloloapan Formation: (A) type area, (B) schematic structural section; and (C) log representing the lower and middle portions of the unit.

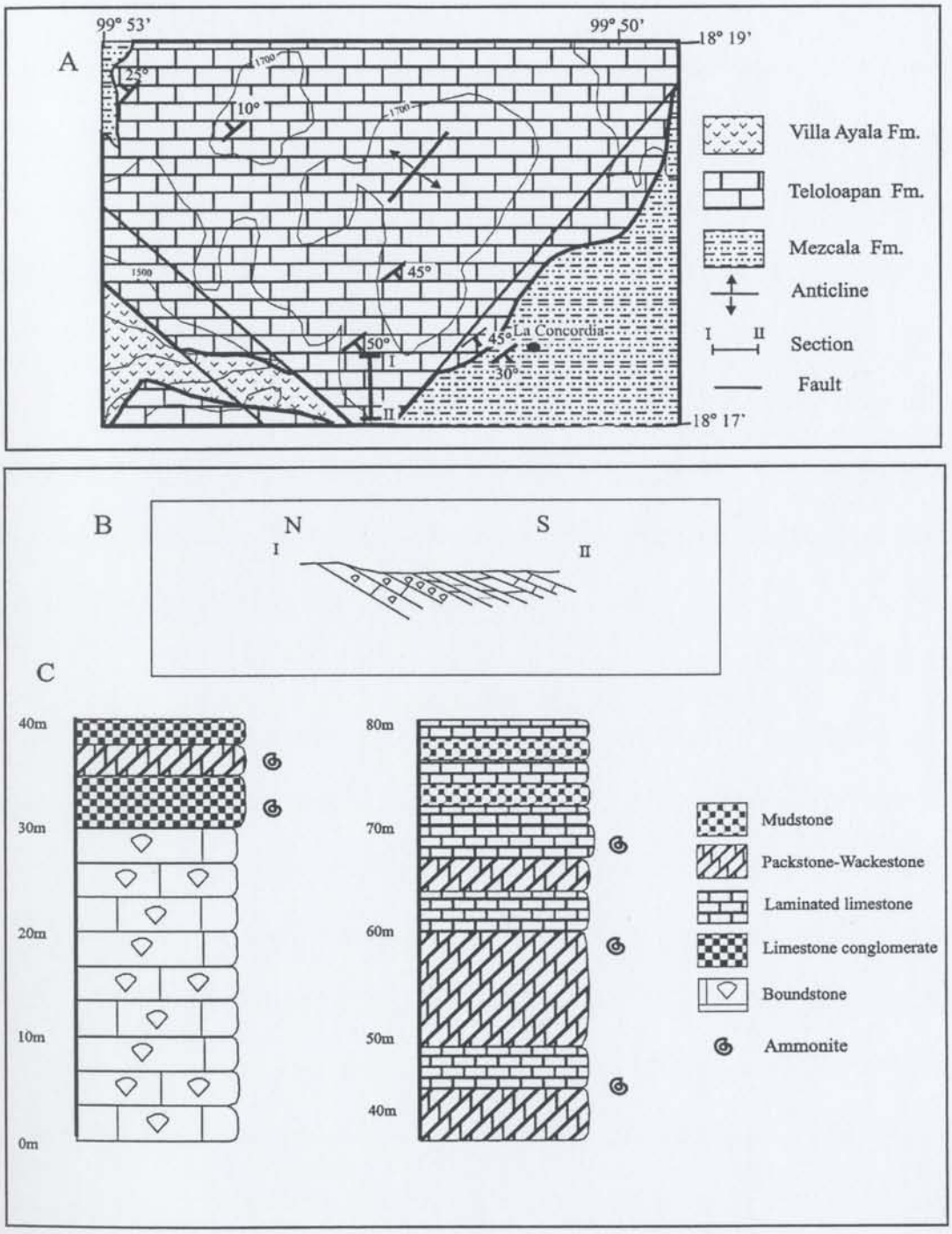

Figure 10. Teloloapan Formation: (A) reference area, (B) schematic structural section; and (C) reference log representing the upper portion of the unit.

The middle part of the formation is composed of masive boundstone and floatstone–rudstone and medium- to thick-bedded packstone–grainstone, partially or completely recrystallized and dolomitized (Figure 9C). This level contains abundant rudists (caprinids, radiolitids, and monopleurids) and nerineids as the predominant fauna. Some parts exhibit crude cyclicity and channeled beds where a crude gradation is observed. Also, in the Acatempan area, the middle part is characterized by masive and thick-bedded packstone to wackestone textures with abundant debris-flow deposits rich in intraclasts and bioclasts. The intraclasts are slightly to completely recrystallized and deformed; they also were plastically deformed during deposition. Reworked bioclasts of corals and rudists are also present at this level.

Finally, the upper portion of the Teloloapan Formation is characterized by thin- to medium-bedded and channeled conglomeratic levels composed of cobbles to boulders of limestone, rich in bioclasts and lithoclasts; some ammonites and reworked rudists are observed in these beds (Figure 10C). This level is overlain by medium-bedded highly fossiliferous packstone and wackestone with an abundant fauna of ammonites and planktonic microfossils (foraminifera, radiolarians, and calcispherulids) associated with scarce belemnites. Hummocky cross-bedding, as well as cross- and planar-laminations characterize this level. The top of the sequence is composed of thin-bedded and laminated mudstone and packstone with exclusively planktonic microfossils.

d. Boundaries and distribution

At the type section, the base of the Teloloapan Formation is gradational with volcaniclastic rocks of the Villa Ayala Formation. The contact between the two units is

defined as the last bed of light green tuffaceous rock of the Villa Ayala Formation. A 10–15 m transitional zone consists of thin-bedded tuff and epiclastic sandstone interbedded with thin-bedded limestones (Figure 9) containing abundant nerineids. The transitional zone is considered as the uppermost level of the Villa Ayala Formation. Above, thin- to medium-bedded, richly fossiliferous claystone and limestone with no tuffaceous levels define the base of the Teloloapan Formation.

The basal unit in the Ahuacatitlan area is different. In this area, the volcaniclastic rocks of the Villa Ayala Formation are characterized by thick-bedded and coarse-grained epiclastic rocks alternating with levels of thin- to medium-bedded bioclastic limestone beds with abundant coral fragments – these are considered as the transitional zone. The base of the Teloloapan Formation is placed at the first medium-bedded limestone with abundant lithoclasts and bioclasts and with no interbedded epiclastic rocks. Above lie thick-bedded and coarse-grained packstone to grainstone beds.

The base of the Teloloapan Formation was traditionally interpreted as a disconformity with the volcaniclastic rocks (Ontiveros, 1973; De Cserna et al, 1978; Cabral, 1995; their Morelos Formation). The preceding data show that the contact is transitional and gradational.

The upper contact with fine-grained siliciclastic rocks of the Mezcala Formation is concordant and well exposed everywhere along the eastern end of the carbonate platform from the towns of Concordia in the south to Romita in the north (Figure 3). Although faulting affects this contact in some areas, the faults do not always follow the contact. The contact is characterized by medium-bedded and laminated packstone with

abundant ammonites and hummocky cross-bedding, overlain by finely laminated wackestone with abundant planktonic microfauna. The base of the overlying unit, the Mezcala Formation, is placed at the first appearance of thin interbeds of fine-grained sandstone, without carbonate interbeds.

e. Fauna and age

The Teloloapan Formation contains well-preserved and abundant fauna that commonly give a good age resolution from the base to the top of the unit. Ages range from late Aptian to late Albian. See Appendix 7 for the complete list of macro and microfossils found in the Teloloapan Formation.

Nerineids found at the base of the Teloloapan Formation are classified as *Nerinea* (*Plesioptygmatis*) *tomasensis* (Allison), *Nerinella dayi* (Blackernhorn), *Plesioptyxis prefleuriani* (Delpey), and *Cossmanea* (*Eunerinea*) *hicoriensis* (Cragin) [Buitrón-Sánchez, 1999, written communication]. Although some of these nerineids have been reported in Aptian–Albian sequences, *Plesioptyxix prefleuriani* (Delpey) and *Cossmanea (Eunerinea) hicoriensis* (Cragin) are only known from Aptian rocks in southern Mexico (Buitrón and Rivera, 1985; Buitrón and Barceló, 1988; Garibay et al., 1996).

Ramírez et al. (1990) reported *Calpionella alpina* and *Microcalamoides diversus* in these rocks. The same fauna were collected during the course of the thesis research in the Ahuacatitlan area near the contact with volcaniclastic rocks of the Villa Ayala Formation. These fauna indicate a late Aptian–early Albian age (Casildo, written communication, 2000).

The presence of *Nerinea* (*Plesioptygmatis*) *tomasensis* (Allison) and *Adiozoptyxis coquandiana* (d'Orbigni) associated with *Coalcomana ramosa*, *Caprinuliodea* sp., and *Toucasia* sp. in the middle portion of the unit give an Albian age. Considering that ammonites and planktonic fauna in the upper member give a late Albian age (see Appendix 7), this part of the Teloloapan Formation is interpreted as late or middle Albian.

The upper member contains an abundant fauna of ammonites, planktonic foraminifera, and calcispherulids that give a secure late Albian age (see Appendix 7; Guerrero et al., 1993 and González, 1999, written com.).

2.4. DISCUSSION OF THE STRATIGRAPHIC CONTROL

The age control for the arc-related succession is limited. However, the fauna and stratigraphic relationships reported here, as well as radiometric data published by other authors, support an Early Cretaceous age for the arc-related succession. The stratigraphic nomenclature for the Teloloapan area and neighboring areas, mainly Tejupilco and Taxco Viejo areas (De Cserna and Fries, 1981; Elías and Sánchez, 1992; Campa and Iriondo, 2003) is shown in Figures 4 and 11.

Radiometric data for volcanic rocks of the Teloloapan subterrane have been ambiguous and imprecise because of the deformation and metamorphism of these rocks. This has allowed misinterpretation of the age of the arc-related sequences in southern Mexico (e.g., De Cserna and Fries, 1981; Elías and Sánchez, 1992; Cabral, 1995). Despite this fact, some radiometric data support an Early Cretaceous age for the arc-

related sequence (Urrutia and Linares, 1981; González, 1991; Mortensen et al., 2003; Campa and Iriondo, 2003).

The Taxco and Tejupilco areas (Figure 2) are small thrust-bounded belts of isolated outcrops showing high structural complexity. De Cserna et al. (1974) reported, in the Taxco area, a Precambrian age (1020±110 Ma, Pb-alpha method) for the Esquisto Taxco (Figures 1 and 4). Campa and Ramírez (1979) discussed this age and they concluded, based on the clastic nature and petrography of the sequence, that zircons dated by De Cserna et al. (1974) were detrital and that the Precambrian age represents the source rock rather than the depositional age of the sequence. Recently, Campa and Iriondo (2003) reported 130±2.6 and 131±0.85 Ma ages using TIMS U-Pb zircon geochronology in the same area.

Elías and Sánchez (1992) and Sánchez (1993) have published Jurassic and Triassic ages for the Tejupilco area (Figures 4 and 11). These ages were obtained using Pb isotopes in a masive sulfide deposit that is syngenetic and concordant with volcaniclastic rocks (cf. Sánchez, 1993). Sánchez (1993) stated that a simple one-stage model yielded ages of 156.3 Ma (late Oxfordian), 128.7 Ma (Barremian), and 103.4 Ma (Albian). However, he also revealed that the Oxfordian age is incorrect and has been recalculated to 114.1 Ma (late Aptian).

Cretaceous ages have been reported for the Teloloapan-Ixtapan de la Sal sequence (cf. Campa et al., 1974; Figure 4) but these have been interpreted as anomalous ages produced by metamorphism (Urrutia and Linares, 1981; Urrutia and Valencio, 1986; Elías and Sánchez, 1992). The Cretaceous radiometric ages can be divided into two

categories: (a) Albian–Turonian ages and (b) Berriasian–Barremian ages (see fauna and age description in § 2.2.1).

It could be postulated that the Albian–Turonian ages are related to metamorphism or thermal events in the area while the Berriasian–Barremian ages could be the depositional/eruptive ages of the sequence. It is interesting that only "anomalous" ages (Albian–Turonian) have been reported to the study area while Berriasian–Barremian ages have been reported north and south of the study area (Apaxtla, Campo Morado, and Ixtapan de la Sal localities). The interpretation that Berriasian–Barremian ages could represent the original rock age is well supported by paleontological data, previously published and newly reported in this thesis.

Early Cretaceous fossil ages for the Teloloapan sequence are few but consistent. The Late Jurassic to Early Cretaceous age of the arc-related sequence postulated by Campa et al. (1974) in the Teloloapan-Ixtapan de la Sal area is therefore narrowed to an Early Cretaceous age in the Teloloapan subterrane. The ages of the Villa Ayala and Acapetlahuaya formations (the arc-related succession) are considered to span the Early Cretaceous (Berriasian–Aptian). The carbonate rocks of the Teloloapan Formation have a well-documented age from late Aptian to Albian.

The chronological significance of the paleontological data for the Teloloapan subterrane is as follows (see Appendices 3 and 7 for specific fauna for each sequence):

a) Calcareous nannoplankton (coccoliths) collected for this thesis research indicate a Hauterivian–Aptian age for the Villa Ayala Formation.

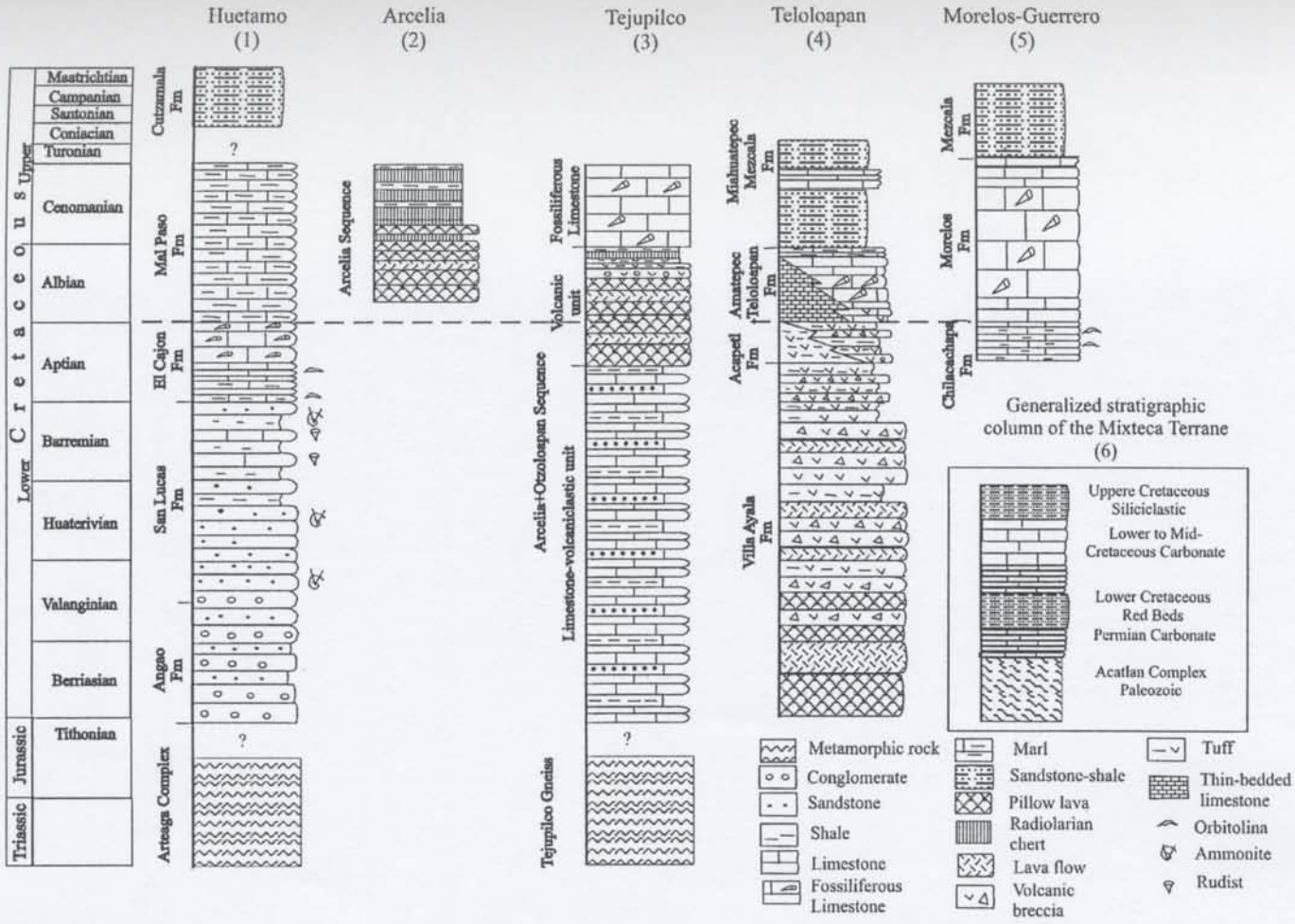

Figure 11. Generalized regional correlation diagram of Upper Jurassic–Cretaceous rocks between the study area and neighboring areas. Column 5 represents only Aptian–Maastrichtean sequences of the Mixteca Terrane, whereas column 6 is an overview of the entire succession of the Mixteca Terrane. Figure 2 shows localities of each column.

b) Radiolarian fauna reported north of the study area by Salinas (1994) define a Valanginian–Aptian age. According to Salinas' (1994) lithologic description, it is assumed that this radiolarian association was collected from the Villa Ayala Formation.

c) The late Aptian age reported by several authors (Burkhard, 1930; Campa et al., 1974; 1980; Lorinczi and Miranda, 1978) based on ammonites is here assigned to the Acapetlahuaya Formation.

d) Nerineid fauna collected for this study in the uppermost levels of the Villa Ayala Formation give a late Aptian age.

e) Abundant macrofossils (nerineids, rudists, and ammonites) and microfossils (planktonic foraminifera and calcispherulids) collected in the Teloloapan Formation document a late Aptian to late Albian age for the unit.

Based on radiometric data, paleontological data, and the stratigraphic relationships among the sequences, the entire Early Cretaceous (Berriasian–Albian) is recorded by the arc-related succession. No Jurassic or older rocks are known to the author.

2.5. THE BASEMENT CONTROVERSY IN THE TELOLOAPAN SUBTERRANE

Some authors (Salinas, 1994; Cabral, 1995) have suggested that phyllitic rocks belonging to the Villa Ayala and Acapetlahuaya formations, exposed north of the Acapetlahuaya area, are the basement rocks of the arc sequence. This area was visited, in particular the Cruz del Sur Formation of Salinas (1994), in the Juntas de Zicatecoyan area. This formation is a highly deformed polygenetic conglomerate with quartz, feldspar,

and volcanic fragments capped by volcanic rocks. Despite the high level of deformation, these rocks indeed appear to belong to the Villa Ayala Formation. The schist fragments mentioned by Salinas are highly deformed tuffs derived from fine-grained tuff beds of the same formation (i.e., they are intraclasts). Furthermore, this conglomeratic level is interbedded with lavas and tuff, which are petrographically similar to those studied in the Villa Ayala Formation of the thesis area. The contact between this unit and the overlying Acapetlahuaya Formation is gradational, as observed elsewhere. Hence, it is concluded that there are not basement rocks, but rather typical Villa Ayala Formation.

Cabral (1995) describes "the Taxco Schist Formation, north of the Acapetlahuaya region, as a mica schist with well developed cleavage outcropping exclusively in the lower slopes of the Sultepec river valley". Certainly, well developed cleavage and schistosity are observed in the rocks cropping out in the Sultepec river area. However, the same features can be observed in different areas where the Acapetlahuaya Formation is exposed. Petrographically, these rocks have the same composition as the fine-grained tuffs from the Acapetlahuaya Formation. Moreover, these rocks change transitionally eastward and westward to the Villa Ayala and the Amatepec formations (see Figure 3). Hence, rocks that Cabral (1995) considers as "basement" are instead assigned here to the Acapetlahuaya Formation.

It is therefore concluded that no basement rocks are exposed in the thesis area. The original controversy was caused by the different degrees of deformation between the coarse- and fine-grained tuffs. These conclusions are supported by the lithology of the rocks, and by the gradational nature of contacts with adjacent formations.

2.6. FACIES DESCRIPTIONS AND PROCESS INTERPRETATIONS OF THE ARC-RELATED SUCCESSION

2.6.1. Lithofacies of the Villa Ayala and Acapetlahuaya formations

Breccias and volcanic conglomerates are predominantly exposed in the Villa Ayala Formation, while volcaniclastic rocks such as tuff and epiclastic deposits, are found throughout the Villa Ayala and Acapetlahuaya formations (Appendix 8 contains a summary of the facies). Four distinctive lithofacies are recognized in these formations. They are: (a) volcanic flows; (b) volcanic breccias and conglomerates; (c) tuff and epiclastic deposits; and (d) hybrid sandstones and hybrid limestones. These lithofacies are subdivided into different subfacies in order to easily interpret each one.

2.6.1.1. Volcanic

2.6.1.1.1. Facies VA1: Volcanic flows

The volcanic lithofacies are restricted to the Villa Ayala Formation. They include basaltic and andesitic lavas with different textural features such as: (1) masive lava flows, (2) pillow lavas, (3) hyaloclastites, and (4) peperites.

1. Masive lava flows

Masive lava sheet flows are found throughout the formation. However, they are better exposed in the lower and middle parts of the Villa Ayala Formation where they are predominantly interbedded with volcanic breccias and conglomerate facies (Figure 12). According to Talavera (1993), basaltic and andesitic compositions represent 90% and

10%, respectively, of the volcanic rocks exposed in the area. Masive lavas exhibit variable thickness from medium beds (40 cm) to very thick beds (>20 m).

Basalts show variable textures ranging from aphyric to porphyric, whereas andesites exhibit exclusively porphyric textures. Phenocrysts in basalts include olivine, clinopyroxene, amphibole, and plagioclase. Andesite phenocrysts are predominantly clinopyroxene, amphibole, and plagioclase sometimes forming glomeroporphyritic textures. Phenocrysts in both basalts and andesites are contained in a vitric and microlitic groundmass, altered and devitrified. Talavera (1993) provides a more detailed petrographic description of the basalt and andesite.

Because no intrusive relationships were observed, the basalts and andesites are interpreted to represent direct eruptive products of arc volcanism from either vents or fractures.

2. Pillow lavas

Basaltic pillow lavas are restricted to the lower and upper parts of the Villa Ayala Formation (Figures 6 and 12). The pillow lavas are best exposed in the town of Villa Ayala and south of the Zacatlancillo area (Figure 12), at the Arroyo San Francisco. Poorly developed pillow lavas are also found in the Acatempan area, along the road from Teloloapan to Apaxtla, west of Acapetlahuaya, and north of the town of Ahuacatitlán. In the Ahuacatitlan locality, porphyritic pillow lavas have abundant amygdules filled by chlorite and celadonite.

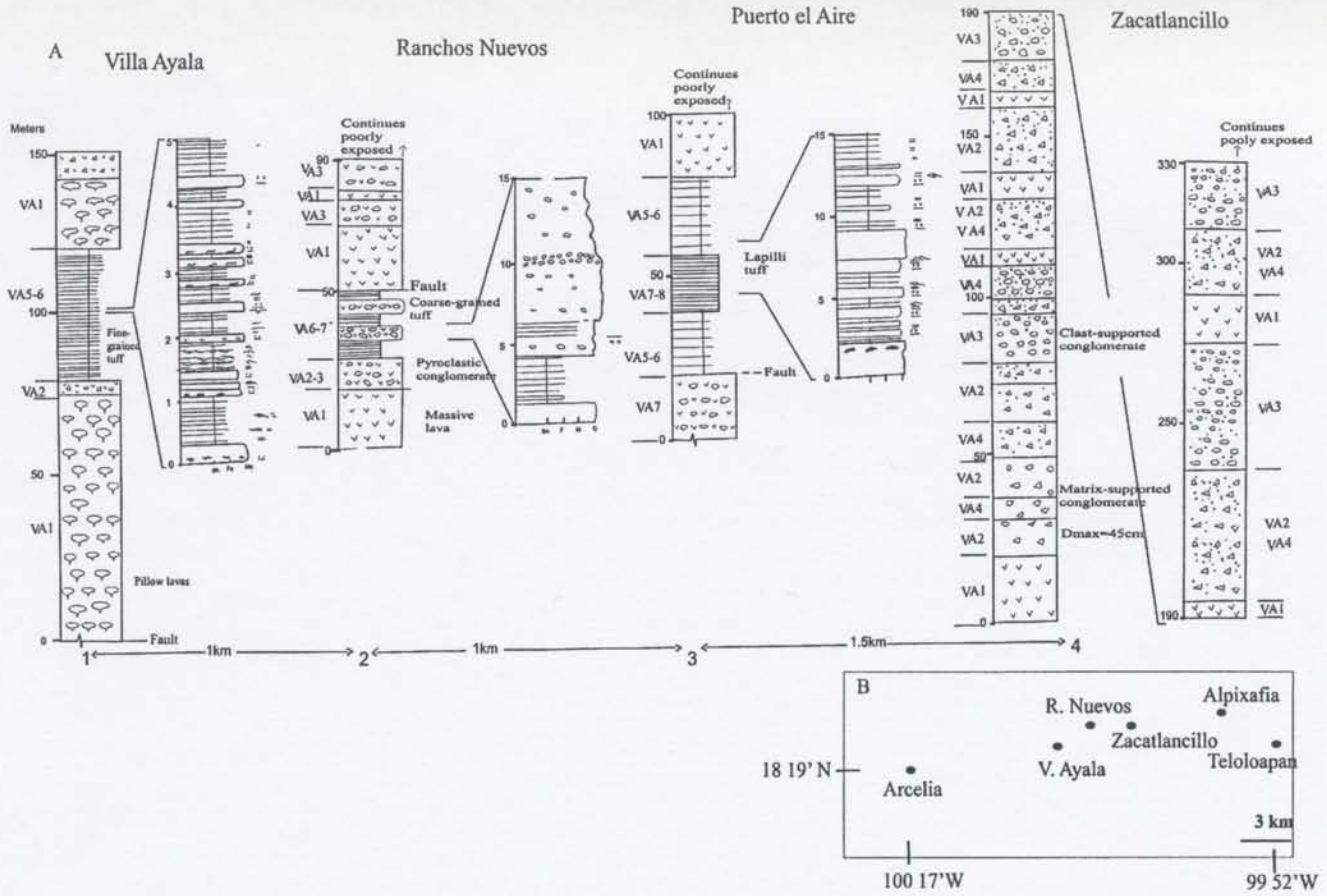

Figure 12. Lithofacies of the Villa Ayala Formation. A. Sections showing lateral variation between Villa Ayala and Zacatlancillo localities. Column 1 represents proximal vent deposits. Columns 2 and 3 show variation among primary volcanic and tuff-pyroclastic deposits; column 2 is proximal and column 3 is distal. Column 4 displays an active erosive phase in a proximal vent area. B. Location map.

The pillow lavas consist of regular and uniform accumulations of cylindrical pillow lobes (Figure 13A) with hyaloclastic matrix. No internal features were observed in the lobes. Each pillow lobe is usually ~1 m thick. However, smaller (20–30 cm) or bigger (2–3 m) pillow lobes are also found in some localities (e.g. Zacatlancillo area).

The pillow-lava units are variable in thickness. For instance, in the town of Villa Ayala they reach up to 100 m thick while in the Acapetlahuaya and Acatempan areas they are only 10–15 m thick. Pillow-lava units are usually overlain by, or intercalated with, hyaloclastites and lava sheet-flows, although fine-grained tuff beds sometimes cover pillow lavas. Talavera (1993) reported a size variation from small pillow lobes at the base of the formation to larger pillows at the top.

The presence of pillow structures in the lavas indicates that they formed in a subaqueous setting. The overlying and closely related fine-grained tuff containing radiolarians indicates a water depth of ~100 m (Bignot, 1985). The pillow lava homogeneity, thickness, and size of the pillow lobes indicate slow effusion rates and low lava viscosity, producing rare or no explosions or implosions. The upward increase in pillow size throughout the formation (Talavera, 1993) might indicate increased eruption rates.

3. Hyaloclastites

Most of the hyaloclastic rocks were produced by quench brecciation of pillow lavas and masive lava sheet-flows (Figure 13B). Hyaloclastites are mainly underlain or associated with pillow lavas and other lava flows (Figure 14). The thickness is variable from one meter to tens of meters (>10 m).

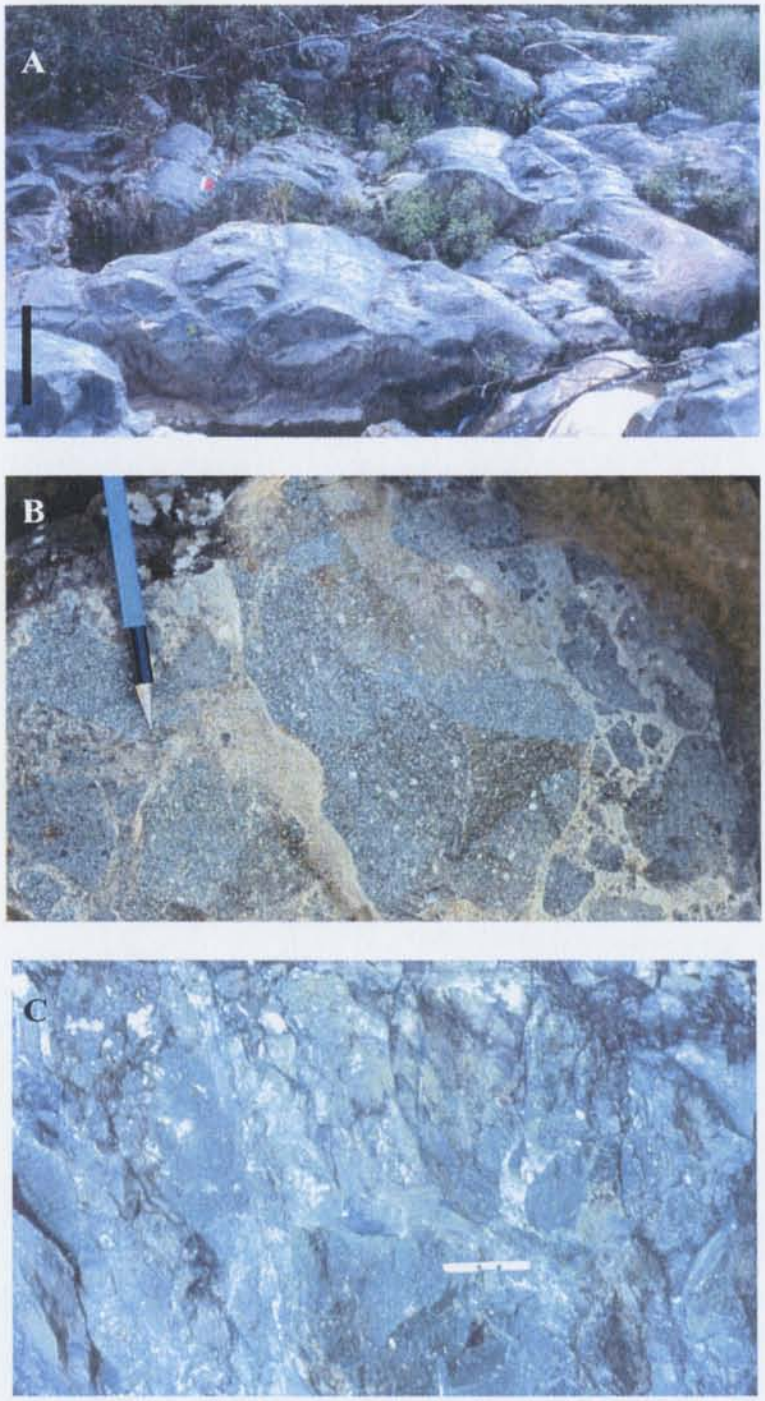

Figure 13. Representative volcanic facies: (A) pillow lavas, Villa Ayala town; (B) hyaloclastites, Villa Ayala town; and (C) peperites, Arroyo Las Bombas, Acapetlahuaya locality. Bar and pencil are 1 m and 14 cm long, respectively.

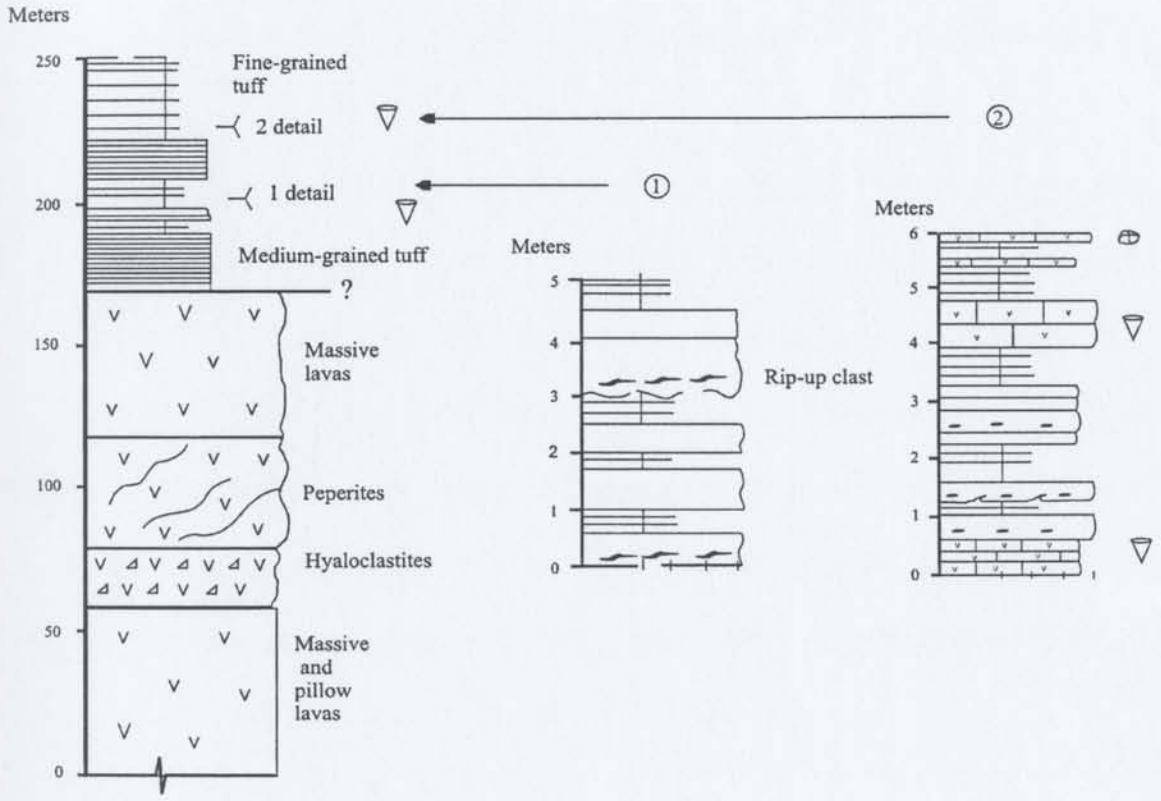

Figure 14. Acatempan section showing volcanic facies associated with tuff, epiclastic and hybrid facies. Columns 1 and 2 are detailed logs of strata of about 210 and 230 meters, respectively. See Figure 3 for location of the Acatempan area.

Partial gradation in the extent of fragmentation is sometimes observed above the contact with the pillow lavas. Hyaloclastites are differentiated from volcanic breccia because of their direct relationship with both pillow lavas and lava sheet-flows, while volcanic breccias form thick sequences, which were derived from explosive pyroclastic events.

The homogeneous basaltic composition of the hyaloclastites indicates that they formed by either quench brecciation or mechanical breakage of pillow lavas and lava sheet-flows (cf. Lajoie and Stix, 1992; Stix, 1991). The transition observed between the pillow lavas and hyaloclastites might indicate a decrease in effusion rate toward the end of each individual eruption. Furthermore, the angular fragments and brecciation of the hyaloclastites can be ascribed to cooling contraction and granulation. Similar relationships have been reported by Busby-Spera (1988) and White and Busby-Spera (1987) in a deep marine arc in Baja California, Mexico.

4. Peperites

The term peperite is used here for a mixture of magma and wet sediments (cf. White and Busby-Spera, 1987). Peperites are mainly observed in the uppermost part of the Villa Ayala Formation, exclusively in the Acatempan and Ahuacatitlan areas (Figures 3 and 13C). In the Acatempan area, the peperites form approximately 50 m of a mixed zone of lava flows associated with micritic limestone (Figures 13C and 14). The zone comprises a mixture of micritic limestone either interbedded with or intruded by basaltic lava. The contacts with the micritic limestone are highly vesicular. Original textures in the carbonates are recrystallized and alterated. Scattered contorted limestone fragments

are also observed in this zone. Furthermore, coral and shell fragments of rudists are also present. Some limestone fragments have an internal fabric of poorly defined "wispy" elements.

Peperites have been interpreted as solidified admixtures of magma and sediment that occur along the margins of intrusions and at the basal contacts of lava flows involving autobrecciation, quenching, phreatomagmatic explosions, or a combination of these processes (White and Busby-Spera, 1987; Orton, 1996). The intrusion relationship between the lava and micritic limestone supports the interpretation that the peperite zone in the study area was produced by intrusion of the lava into the sediment. However, the interbedded relationships observed in some parts of the formation also indicate that lava flowed across calcareous beds. The partial "wisp" features developed suggest that the clasts were plastically deformed, and therefore likely wet and only weakly consolidated when incorporated into the hot lava.

2.6.1.2. Volcanic breccias and conglomerates

Volcanic breccias and conglomerates are exclusively found in the Villa Ayala Formation. Three facies can be differentiated: (a) volcanic breccias, (b) clast-supported volcanic conglomerates; and (c) matrix-supported and chaotic conglomerates.

2.6.1.2.1 Facies VA2: Volcanic breccia

This facies is mainly found in the lower and middle portions of the Villa Ayala Formation and is well exposed in the Alpixafia and Zacatlancillo sections (Figures 12 and 15). Thickness of the facies is variable but generally the deposits are thick to very thick,

ranging from 4 m to more than 30 m (Figure 12). The facies is associated with lava flows facies (VA1) and conglomeratic facies (VA3–VA4). Contacts between breccia and lava flows or conglomeratic facies are sharp, although erosional contacts are also observed with the latter.

Volcanic breccias contain monogenetic basaltic fragments with variable grain size from granules (2–4mm) to blocks (64–256 mm). The clasts are usually angular to subangular in shape (Figure 16A). Furthermore, small scale and poorly developed "wisp" structures are observed at the contact between the matrix and the clasts where foliation is less intense (e.g. Zacatlancillo section in Figure 12). Clasts are contained in a fine- to medium-grained and abundant tuffaceous matrix. Petrographically, the matrix is a microcrystalline material derived from alteration of an original glassy matrix, based on the fact that shards are locally observed.

Two interpretations of the deposition of the volcanic breccias can be made.

1) Volcanic breccias that are formed by monogenetic nature of the fragments and their angular shape, as well as the homogeneous tuffaceous matrix, suggest that the volcanic breccias were a direct result of pyroclastic eruptions. This interpretation is also supported by the presence of shards and wisp structures, pseudo-fluidal features in the matrix, and the interbedded lava flows.

2) Other breccias have angular shape of the fragments, abundant tuffaceous matrix, and heterogeneous clast size suggesting a high-density debris-flow origin. This interpretation is made where breccias change upward to matrix-supported and chaotic conglomerate beds.

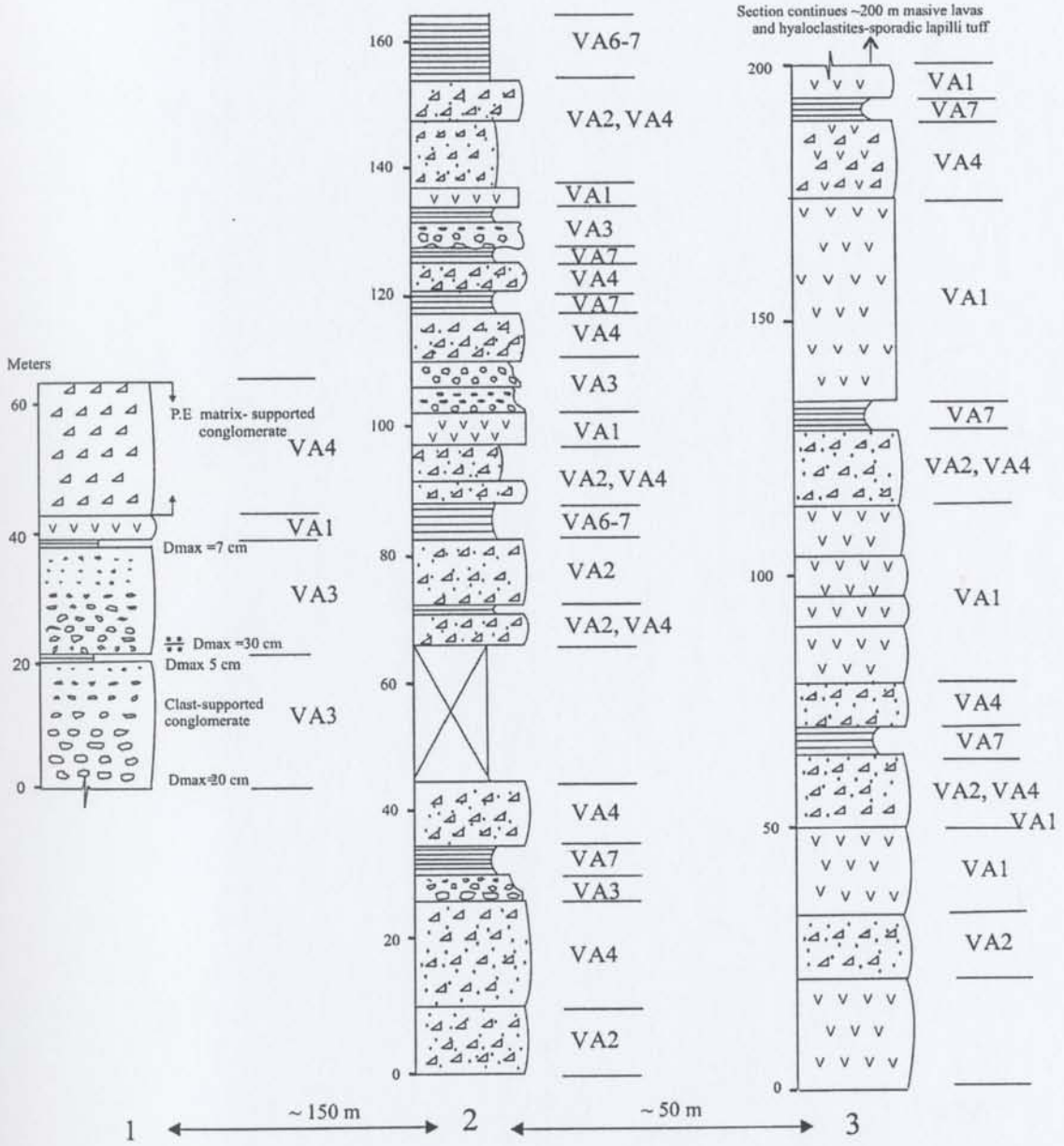

Figure 15. Alpixafia section showing volcanic breccia – conglomerate interstratified with tuff – epiclastic facies (columns 1 and 2). Column 3 shows primary volcanic and breccia – conglomerate facies. Facies names are prefixed by VA, for Villa Ayala Formation. P.E. = poor exposure. Figure 3 shows location of Alpixafia locality.

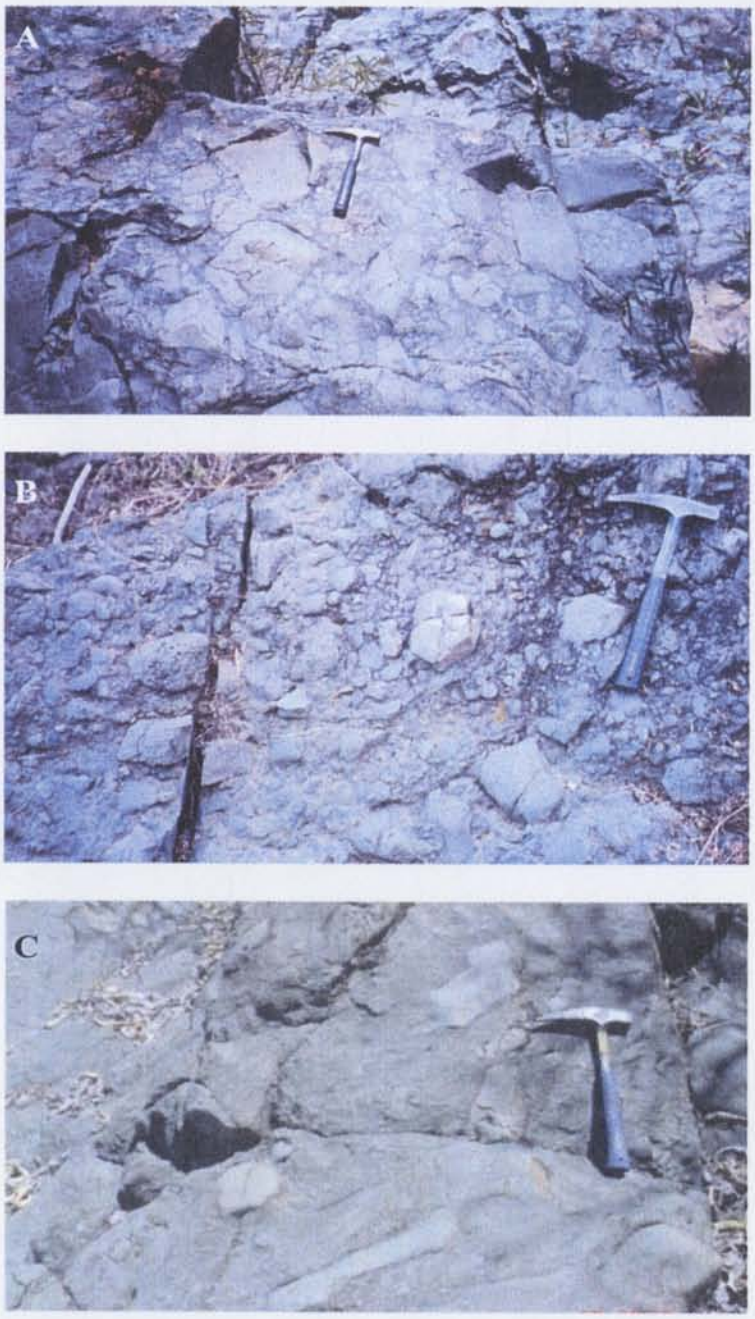

Figure 16. Representative volcanic breccias and conglomerate lithofacies: (A) volcanic breccia; (B) Clast-supported volcanic conglomerate; (C) Matrix-supported and chaotic conglomerate. All pictures from the Zacatlancillo locality. Hammer is 25 cm long. See Figure 12 for reference map of the Zacatlancillo locality.

Busby-Spera (1988) reported a similar facies in the arc apron from Baja California, Mexico, and interpreted a pyroclastic origin because of the monogenetic composition and presence of shards.

2.6.1.2.2. Facies VA3: Clast-supported volcanic conglomerate

This facies is mainly found in the middle portion of the Villa Ayala Formation and is best exposed in the Alpixafia, Rancho Viejo, and Zacatlancillo localities (Figures 12 and 15). The facies conformably overlies volcanic breccias, lava flows, and lapilli tuff facies. However, it is mainly covered by lapilli tuff and epiclastic facies in the Alpixafia area (Figure 15). The bases of conglomerate beds are irregular and locally channelized. The upper contact with lapilli tuff and epiclastic facies is gradational to sharp. The facies occurrences are generally 2–5 m thick, but in the Zacatlancillo area single units of facies VA3 are more than 30 m thick (Figure 12). The main characteristic of the facies is its clast-supported nature (Figure 16B).

The facies contains clasts of basaltic lava and fine-grained tuff, although the former are predominant. The clasts are contained in a tuffaceous matrix. Clasts are mainly subrounded to subangular in shape and range from 5 to 60 cm in size, averanging ~15 cm (Figure 16B). Beds may be normally graded throughout, or in just part of the bed. Normal grading is ubiquitous.

The grading, erosional contacts, and clast-supported nature of the clast-supported conglomerate facies resemble facies class A2.3 (normally graded gravel) of Pickering et al. (1989). The irregular shapes of the basal contacts suggest deposition in scours or

channels. The normal grading, clast support and thick bedding suggest high-density gravity flows as the mechanism of transport and deposition. Rapid deposition is suggested by the scarcity of tractional structures. Pickering et al. (1989) describe their facies A2.3 as abruptly graded beds showing the coarsest clasts in the lower parts of the beds rapidly giving way upward to fine pebbles. The same characteristics are observed in this facies. Finally, heterogeneous lithic and matrix composition associated with scouring suggest that the flows were highly erosive, possibly sampling contemporaneous pyroclastic deposits.

2.6.1.2.3. Facies VA4: Matrix-supported and chaotic conglomerate

This facies is restricted to the lower and middle parts of the Villa Ayala Formation. Good exposures of this facies are located in the Alpixafia and Zacatlancillo areas (Figures 12 and 15). The matrix-supported and chaotic beds are interbedded with volcanic breccias, clast-supported conglomerate, tuff and epiclastic sediments, and lava flows (Figure 15). The lower and upper boundaries are generally sharp but upper contacts with the clast-supported conglomerate facies VA3 are erosive. In rare cases, this facies is partially or poorly graded. The thickness is highly variable, mostly 2–20 m, although thin horizons (<1 m) are sporadically observed in some areas.

The main characteristic of this facies is its matrix-supported nature (Figure 16C). Angular to subrounded granules to blocks of lavas and lapilli tuff fragments are set in a medium-grained, abundant tuffaceous matrix showing rare shard structures. Although

disorganized and chaotic beds typify this facies, some levels in the Ranchos Nuevo locality (Figure 12) exhibit normal grading in the uppermost part of the bed.

This facies is interpreted as "epiclastic gravity-flows deposits" because of the lack of any evidence of a hot state of emplacement. However, a pyroclastic origin cannot be ruled out. Textural characteristics of the deposits, such as poor sorting, thick bedding, chaotic appearance and matrix support resemble facies A1.1 (disorganized gravel) of Pickering et al. (1989). The most likely mode of deposition would be from highly concentrated turbidity currents or debris flows. White and Busby-Spera (1987) suggest the same interpretation for similar facies in a deep-marine arc apron from Baja California, Mexico. If a pyroclastic origin were postulated for this facies, it would indicate episodic and highly explosive pyroclastic flows that might record the advanced stages of construction of the arc volcanoes.

At some localities, the tuffaceous matrix appears to show shard structures but deformation and metamorphism prevent confident identification of pyroclastic features. Therefore, distinction between a hot subaqueous pyroclastic flow and sedimentary gravity-flow is difficult. Because associated deposits are water-lain, the author follows the advice of Cas and Wright (1987, 1991) that a water-supported mass-flow mechanism is more appropriate.

2.6.1.3. Tuff and epiclastic sandstones

Seven facies are recognized as tuff and epiclastic lithofacies. Petrographic studies were used to differentiate tuff from epiclastic sandstones.

2.6.1.3.1. Facies VA5: Very thin- to thin-bedded tuff

Facies VA5 is broadly exposed in both the Villa Ayala and Acapetlahuaya formations. This facies is mainly interbedded with facies VA6 and VA7 in the Villa Ayala Formation (Figure 12) and facies VA11 in the lower and middle portions of the Acapetlahuaya Formation.

Facies VA5 consists of very thin- to thin-bedded (2–10 cm) and thinly laminated radiolarian-rich tuff (Figure 17A). Petrographically, facies VA5 shows an alternation of fine and very fine grains that are identified as ash. Radiolarians are abundant in both formations showing calcification and recrystalization. Radiolarians are also observed in hand sample as rounded white grains.

Beds of this facies form bedsets up to 20 cm thick separated by intervals <15 m thick of medium-grained tuff (Figure 12). The beds exhibit lateral continuity for more than 20 m, although in some cases they are also discontinuous. Beds generally have sharp bases. Tops are sharp, transitional and loaded by medium-grained tuff and epiclastic sandstone (Figure 17A). Sedimentary structures include parallel and current-ripple laminations that are consistently found throughout the facies.

The very thin to thin tuff beds resemble facies D2.3 (thin regular silt-mud laminae) of Pickering et al. (1989), which they interpret as the deposits of low concentration turbidity currents. No evidence of hot emplacement was observed in this facies. However, the interbedded facies VA6 and VA7 show evidence of pyroclastic emplacement, so at least part of this facies might be the finest fraction of pyroclastic flows, termed "tuff turbidites" by Cas and Wright (1987).

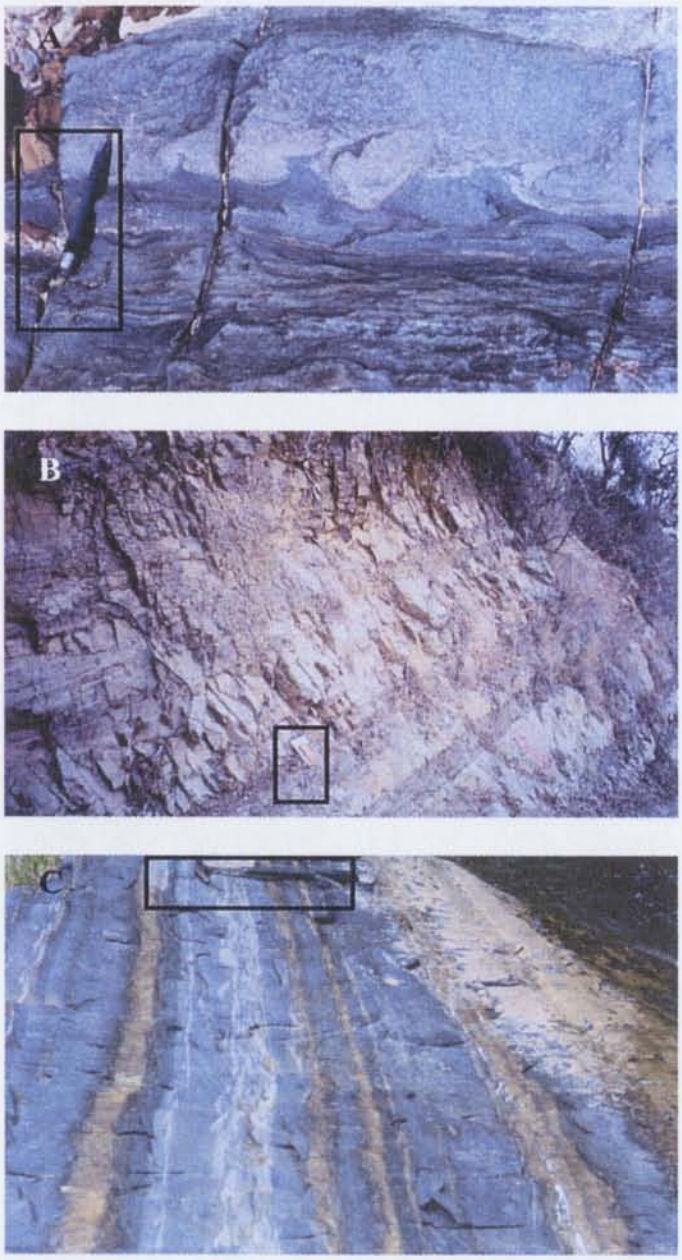

Figure 17. Representative tuff and epiclastic lithofacies: (A) Very thin- to thin-bedded tuff and medium-bedded tuff (VA6 facies) with load casts, Ranchos Nuevos locality; (B) Thick-bedded tuff (VA7 facies), Zacatlancillo locality; and (C) Thin-bedded current-rippled epiclastic sandstone (VA8 facies), Laguna Seca locality. Pen, notebook and hammer are 14 cm, 30 cm, and 25 cm long, respectively.

Facies VA5 deposits are usually associated with coarser resedimented volcaniclastic flows. However, the presence of radiolarians in this facies suggests eruption of the ash must have occurred in relatively deep water. White and Busby-Spera (1987) described deposits of "ash turbidites", similar to this facies, which were interpreted as having been generated by remobilization of ash from the shallow-water flanks of volcanoes.

2.6.1.3.2. Facies VA6: Medium-bedded tuff

Facies VA6 crops out throughout the Villa Ayala Formation and the lower part of the Acapetlahuaya Formation. It is associated with facies VA5 and VA7 in packets up to 20 m thick (Figure 12).

Facies VA6 is a medium-bedded and fine- to coarse-grained tuff exhibiting partial Bouma sequences. The most common Bouma sequence is Tbc with abundant parallel and current-ripples laminations. Rare Tabc Bouma sequences with weak normal grading are also observed (Figures 12). Petrography of this facies shows a lithic and feldspar-rich tuffaceous sandstone in a quartzofeldspathic groundmass, possibly recrystallized from original glassy ash. Relict cuspate shards and fiamme structures are also observed in this facies. Radiolarians are scattered and generally recrystallized. Load casts on the soles of beds are common in this facies, sometimes separated by well-developed flame structures (Figure 17A).

Facies VA6 resembles facies C2.2 (medium-bedded sand-mud couplets) and C2.3 (thin-bedded sand-mud couplets) of Pickering et al. (1989), interpreted as the deposits of

low-concentration turbidity currents. Relict shards and fiamme structures suggest hot emplacement. Radiolarians, although rare, support a subaqueous setting.

Different authors (White and Busby-Spera, 1987; Busby-Spera, 1988; Houghton and Landis, 1989) have described similar Bouma sequences in thin- to medium-bedded tuff or volcanic arenites. They inferred deposition from turbidity currents originating on arc flanks. These might be "tuff turbidites" formed during pyroclastic eruptions (cf. Cas and Wright, 1987).

2.6.1.3.3 Facies VA7: Thick-bedded tuff

Facies VA7 is restricted to the lower and middle parts of the Villa Ayala Formation. It is associated with facies VA5 and VA6 in the fine-grained levels (Figure 12) while in the coarse to conglomeratic parts it is interbedded with the conglomeratic facies VA3 and VA4 (Figures 12 and 15).

Facies VA7 is made up of thick-bedded tuff that ranges in grain size from coarse-grained tuff to fine-grained tuff (Figure 17B). Bed thickness ranges from 30–100 cm. Beds are normally graded with parallel lamination near the bed top (Figures 12 and 15). In the fine-grained tuff levels of the Villa Ayala Formation, this facies frequently shows sharp lower bed boundaries and occasional rip-up clasts (Figure 12). The upper boundaries of the beds are gradational with overlying medium-bedded tuff (Facies VA6). Where it is associated with volcanic conglomerates (Figure 15), facies VA7 exhibits gradational lower contacts with the conglomerates while bed tops are frequently eroded by the next conglomerate bed.

The poorly developed grading and thickness of facies VA7 resemble characteristics of facies B1.1 (thick/medium-bedded disorganized sands) of Pickering et al. (1989). However, facies VA7 lacks the fluid -escape structures described by Pickering et al. (1989) for facies B1.1. The thick-bedded tuff could be considered as the result of rapid mass deposition from highly concentrated turbidity currents, based on partial Bouma sequences (Tab) and bed thickness. Sporadic trains of rip-up clasts at the base of some beds suggest erosive flows.

2.6.1.3.4 Facies VA8: Thin-bedded rippled epiclastic sandstone

This facies is sporadically found in both the lower levels of the Acapetlahuaya Formation and the Villa Ayala Formation, especially in the Laguna Seca locality (Figure 3). It is associated with VA5 and VA6 where they are stacked, forming packages up to 20 m thick (Figures 12 and 17C). Facies VA8 comprises mainly thin beds (although medium beds are also observed) of fine-grained lithic and feldspathic, epiclastic sandstone. Beds are laterally persistent for more than 15 m in some areas, although discontinuous beds are also observed. Facies VA8 is distinguished from the others facies because of the presence of asymmetrical current ripples forming irregular lenses showing small-scale cross-stratification and parallel lamination (Figure 17C). Ripple amplitude varies from 0.5–3 cm, whereas ripple wavelength ranges from 4–18 cm. Beds display sharp bases and tops. Load casts are sporadically present.

Facies VA8 is somewhat similar to facies D2.1 (graded-stratified silt) of Pickering et al. (1989). According to these authors, this facies records grain-by-grain sedimentation

from suspension, followed by a traction phase that produces lamination. Low-concentration turbidity currents are envisaged as the primary transport mechanism. Busby-Spera (1988) described similar facies in Baja California, Mexico, and suggested deposition from silt-load turbidity currents produced by erosion of adjacent volcanoes or arc segments.

2.6.1.3.5 Facies VA9: Folded and contorted layers.

Facies VA9 is restricted to the Villa Ayala Formation. It is commonly associated with medium- to thick-bedded tuff facies (VA6 and VA7), and rarely associated with matrix-supported and chaotic conglomerates (facies VA3). The folded and contorted layers consist of beds of contorted and folded clasts. The folded clasts are 2–40 cm long (Figures 18A and 19), and have a disorganized fabric. Bed thickness ranges from 8 cm to 5 m. Clasts are mainly monogenetic, composed of fine- to medium-grained tuff set in a medium-grained tuffaceous matrix (Figure 19). However, a few examples show polygenetic composition with both tuff and basalt fragments.

Facies VA9 includes folded and contorted structures similar to those described by Pickering et al. (1989) for their facies F2.1 (coherent folded and contorted strata). Facies VA9 is interpreted to reflect slope failure either due to rapid buildup of debris- flow deposits or depositional overloading of weak sediments (Busby-Spera, 1988; Pickering et al., 1989). Deformed clasts and abundant matrix suggest a debris-flow deposit. However, formation by overloading and disruption of weak sediments is more consistent with the monogenetic clast composition in association with identical

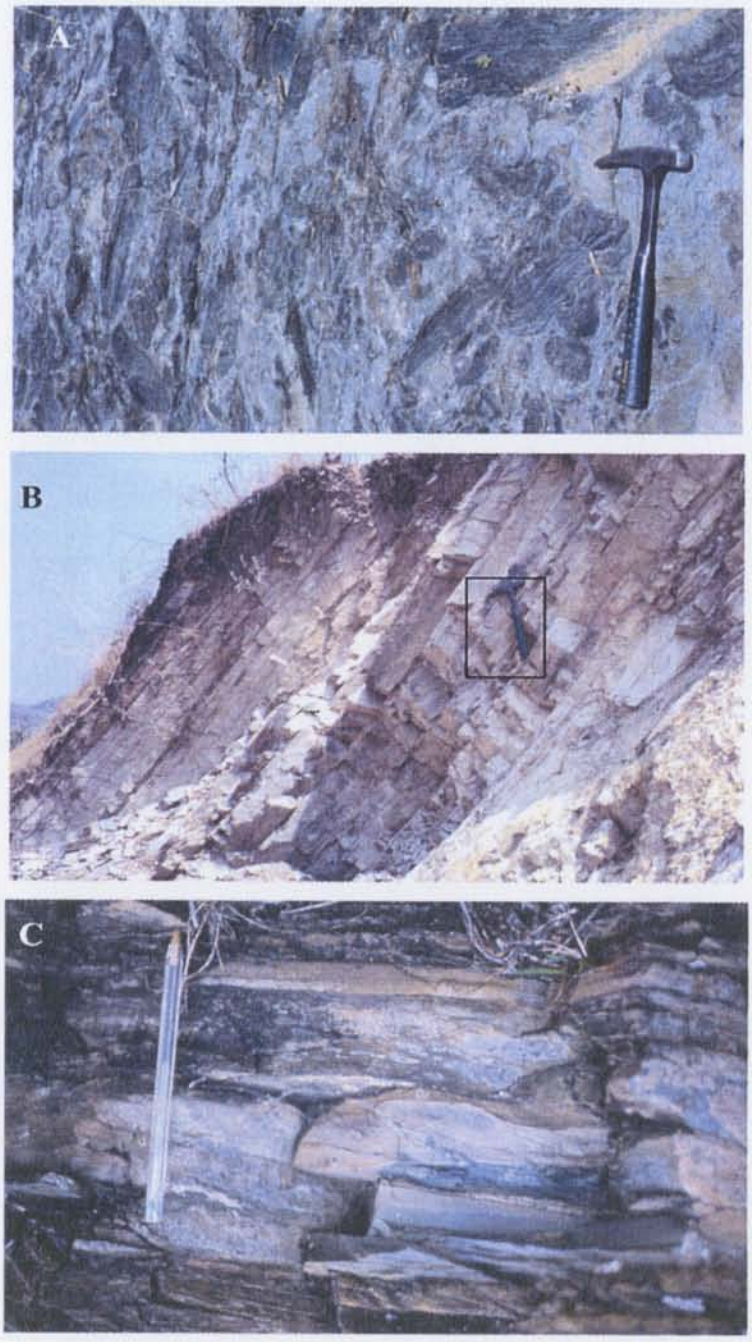

Figure 18. Representative tuff and epiclastic lithofacies: (A) Folded and contorted layers (VA9), Laguna Seca locality; (B) Thin- to medium-bedded epiclastic sandstone (VA10), south Acapetlahuaya locality; and (C) Laminated siltstone and fine-grained tuff (VA11), north Acapetlahuaya locality. Hammer and pen are 25 cm and 15 cm long, respectively.

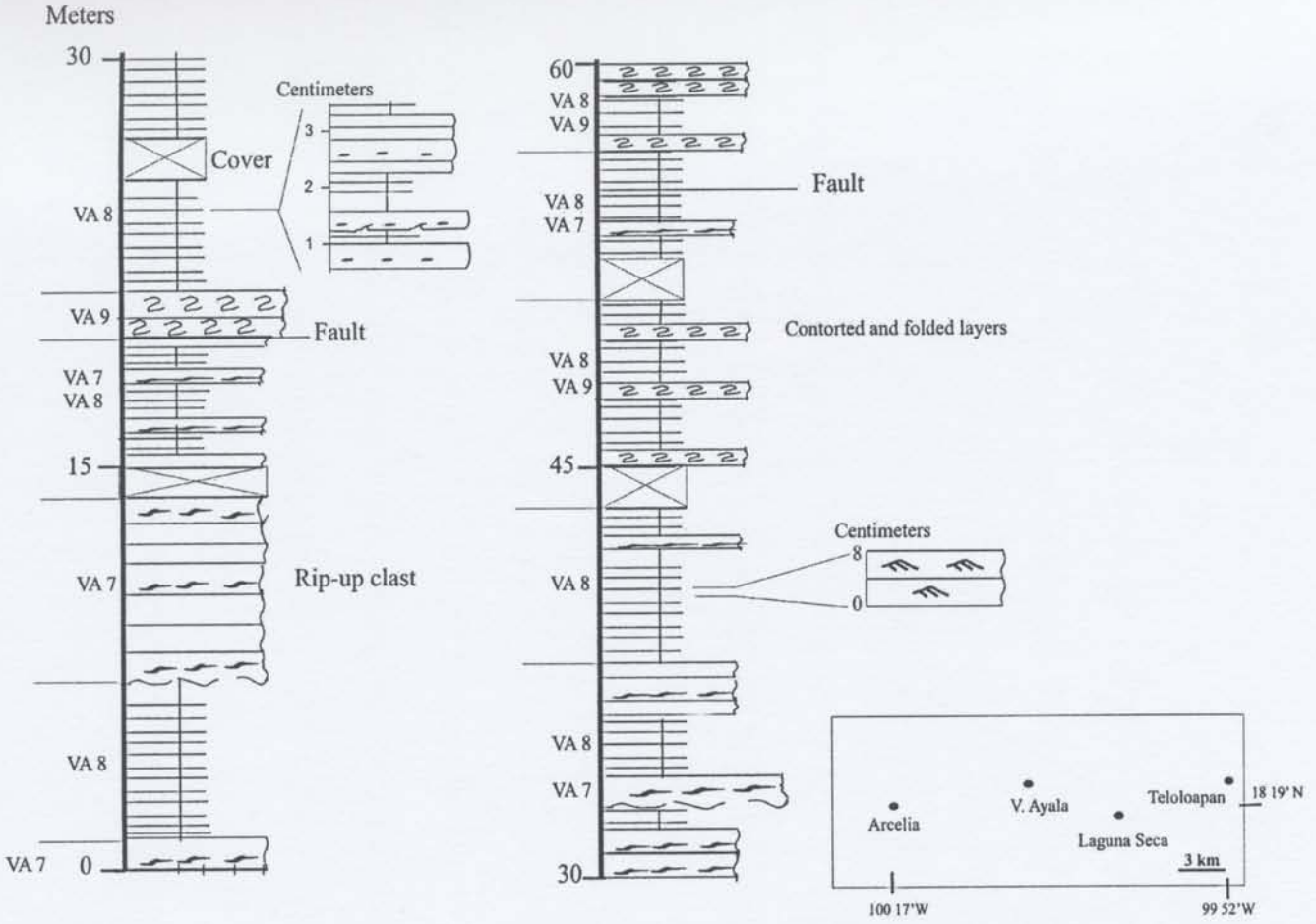

Figure 19. Laguna Seca section showing thick-bedded tuff (VA7), thin-bedded rippled epiclastic sandstone (VA8), and folded and contorted layers (VA9).

undeformed tuff matrix. In contrast, the polygenetic folded and contorted strata associated with chaotic and matrix-supported volcanic conglomerates might be debris-flow deposits.

2.6.1.3.6 Facies VA10: Thin- to medium-bedded epiclastic sandstone

Facies VA10 is restricted to the upper parts of the Villa Ayala Formation, as well as the upper levels of the Acapetlahuaya Formation. It is frequently associated with the medium-bedded tuff of the Villa Ayala Formation (Figure 19) and laminated siltstone and fine-grained tuff facies of the Acapetlahuaya Formation (Figure 20).

Facies VA10 consists of thin- to medium-beds of medium-grained sandstone showing Bouma sequences, mainly Tab and Tbce. Thin levels of rip-up clasts are observed at the base of some beds. Each bed is overlain gradationally by siltstone (Figure 18B). Amalgamation of beds in this facies is quite uncommon in the Villa Ayala Formation. However, amalgamated beds as thick as 4 m are observed in upper levels of the Acapetlahuaya Formation (Figure 18B). Sharp contacts are common at bed bases. In thin section, the VA10 facies is medium-grained, volcanic lithic-rich sandstone without evidence of ash, or glass alteration. Volcanic lithics are angular to subrounded in character while the matrix is feldespathic. Patches of calcite cement are observed in some samples.

Although this facies is similar in appearance to the thin- and medium-bedded tuff facies (VA5 and VA6) that are interpreted as the products of pyroclastic flows, facies VA10 is interpreted as epiclastic deposits.

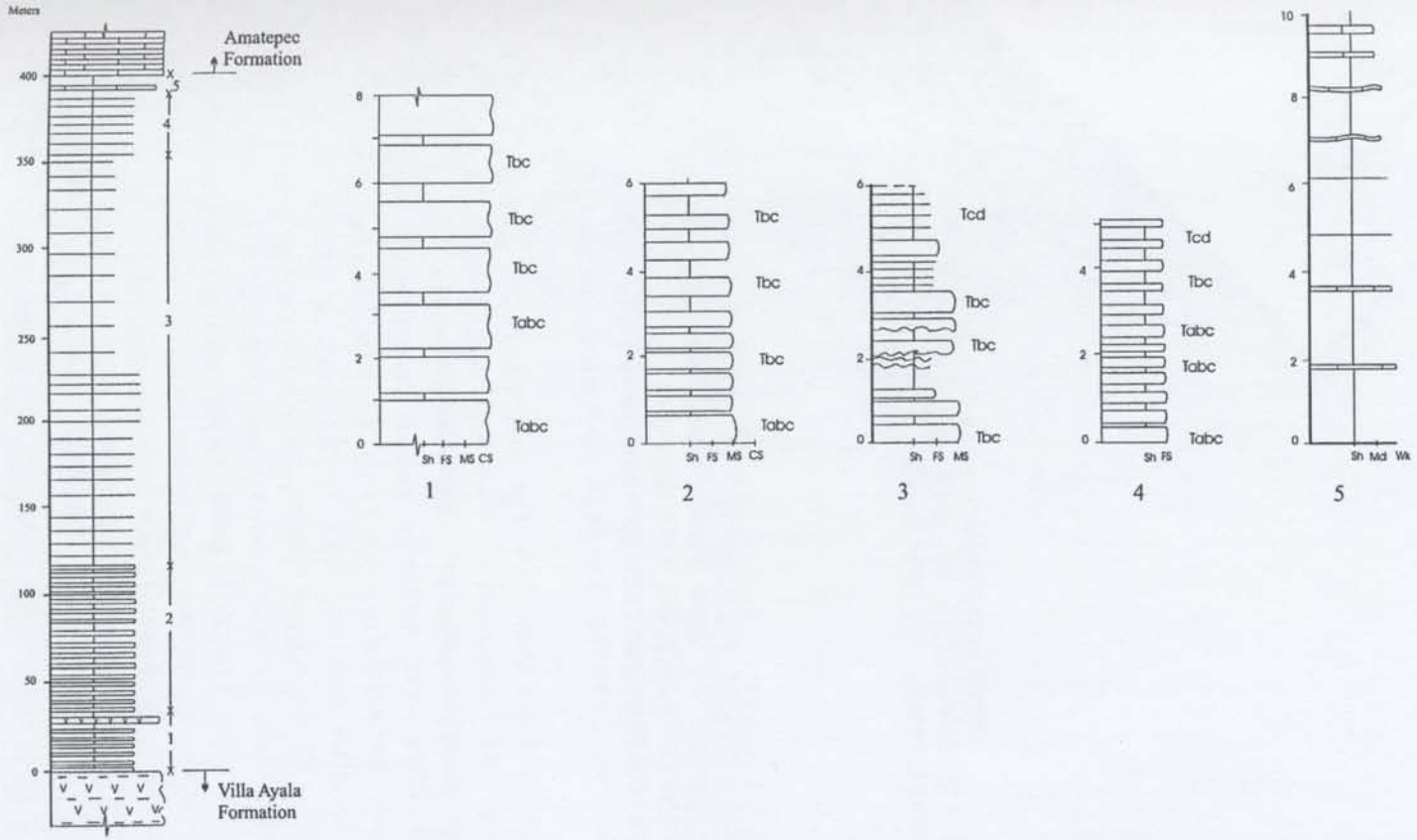

Figure 20. Schematic stratigraphic section of the Acapetlahuaya Formation showing fine-grained epiclastic, tuff, and laminated siltstone facies. Numbers 1–5 show representative detailed sections measured throughout the formation that are typical of the intervals marked (e.g. section 2 is typical of ~30–115 m in the Acapetlahuaya Formation). Sh (shale); FS (fine sand); MS (medium sand); CS (coarse sand); Md (mudstone); Wk (wackestone).

Characteristics such as bed thickness as well as the presence of Bouma sequences with a dominant b division are similar to characteristics observed in facies C2.2 (medium bedded sand-mud couplets) of Pickering et al. (1989). Facies VA10 is interpreted as having been emplaced by turbidity currents. Sand accumulated grain-by-grain from suspension, and then experienced traction transport to form lamination.

2.6.1.3.7 Facies VA11: Laminated siltstone and fine-grained tuff

Given the strong deformation and alteration in the Acapetlahuaya Formation (see Figure 8), it is difficult to distinguish very fine-grained tuff from epiclastic siltstone in the field. Petrographic analysis is needed to determine whether or not the facies is tuffaceous.

Facies VA11 is restricted to the Acapetlahuaya Formation (Figure 20). Very thin-bedded and very fine-grained tuff is usually found in the lower part of this formation, while very thin beds of laminated siltstone predominate in the middle and upper parts (Figure 18C). The facies is associated with thin-bedded tuff (facies VA5) in the lower levels and thin- to medium-bedded epiclastic sandstone (facies VA10) in the upper levels.

Facies VA11 consists of yellowish white, thinly laminated and micaceous siltstone and very fine-grained tuff (Figure 18C). Although parallel lamination is the dominant sedimentary structure, some beds instead show poorly developed normal grading and lenticular laminations. Bed bases and tops are usually sharp against thin- to medium-bedded epiclastic sandstone, although gradational contacts are sporadically present. Black calcareous beds (transitional zone with the Amatepec Formation) are interbedded with this facies in the uppermost levels of the Acapetlahuaya Formation.

Radiolarians showing elongate shapes due to deformation are common in thin sections. These fossils show recrystallization and calcification.

The laminated siltstone and fine-grained tuff facies resembles facies group D2, especially facies D2.3, of Pickering et al. (1989). Lack of organic carbon and biogenic muds distinguish VA11 from their facies E2.2. Pickering et al. (1989) interpret their facies D2.3 (thin regular silt and mud laminae) as the deposits of dilute turbidity currents alternating with a hemipelagic rain from suspension. The occurrence of tuff with radiolarians in some intervals might indicate that some beds are distal pyroclastic "tuff turbidites" (cf. Cas and Wright, 1987).

2.6.1.4 Hybrid sandstone and hybrid limestone

The term "hybrid" is used here for rocks that show mixed terrigenous and calcareous composition with fragments of both extrabasinal and intrabasinal origin (cf. Zuffa, 1980). Hybrid sandstone and limestone lithofacies are exclusively exposed in the uppermost levels of the Villa Ayala Formation in contact with limestones of the Teloloapan Formation, eastern area (Figure 3). Three facies are recognized at this level: (1) hybrid sandstone, (2) hybrid limestone, and (3) fossiliferous tuffaceous sandstone.

2.6.1.4.1 Facies VA12: Hybrid sandstone

Facies VA12 consists of medium- to thick-bedded and medium-grained sandstone with abundant calcareous lithoclasts and bioclasts (corals and mollusks) in a tuffaceous or epiclastic sand matrix. Hybrid sandstones are usually associated with epiclastic and

primary volcanic levels in the sections measured (Figure 21). The facies is recognized in different localities (Acatempan, Teloloapan, and Ahuacatitlan, see Figure 3). Facies VA12 is distinguished from fossiliferous tuffaceous sandstone (facies VA14) because fossils in VA12 are reworked and fragmented.

In the Acatempan area, at Arroyo Las Bombas (Figure 14), facies VA12 is characterized by graded beds. These graded beds have centimer-thick concentration of bioclasts, mainly mollusks and corals (Figure 22A). The bioclasts are mainly reworked mollusks with fewer corals and nerineid gastropods. The nerineids show well-preserved original shell structure. Lower and upper bed boundaries are mostly sharp and flat, but loaded bases exhibiting well-developed flame structures, as well as ball and pillow structures, are observed (Figure 14). Thickness of this facies is variable, ranging from 1.5–5 m.

In the Ahuacatitlan area, facies VA12 consists of very thick to medium-bedded, and medium- to coarse-grained tuffaceous sandstone with abundant volcanic and calcareous lithoclasts, as well as bioclast fragments. Volcanic fragments are basaltic in composition and range in size from coarse to fine sand. Calcareous lithoclasts are packstones to grainstones, and are highly recrystallized. The bioclasts are mainly reworked mollusks and scattered nerineids and corals. Channelized beds are observed in this area. Normal grading is present but poor (Figure 21).

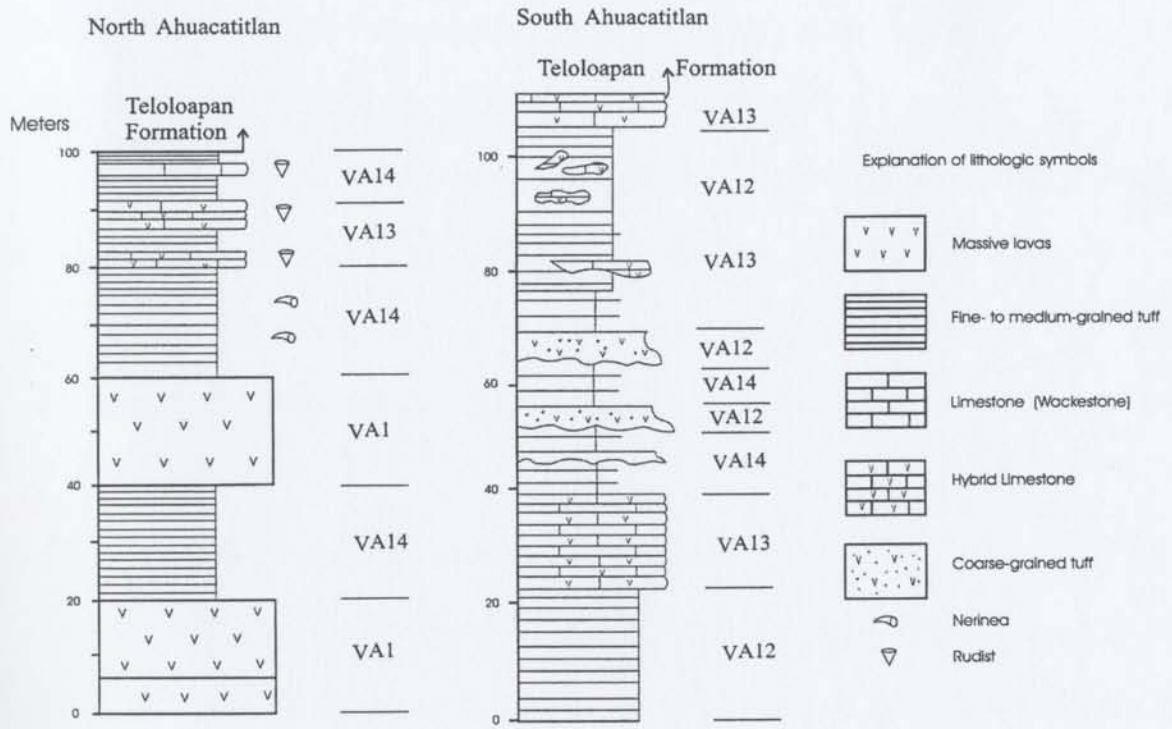

Figure 21. Ahuacatitlan area. Schematic sections showing hybrid facies interbedded with limestone facies and tuff-epiclastic facies

Petrographically, the facies shows fine- to medium-grained volcanic lithic-rich tuffaceous sandstone with minor feldspars grains, bioclasts (mollusks and corals) and pyroxene crystals.

The mixture of reworked fauna and volcanic lithic fragments suggests that the sand was derived by erosion of a shallow-water platform and volcaniclastic rocks. This facies is closely associated with lavas flows and epiclastic rocks of the Villa Ayala Formation, suggesting that accumulation was contemporaneous with volcanism.

2.6.1.4.2 Facies VA13: Hybrid limestone

Facies VA13 is well exposed in the Ahuacatitlan area (Figure 21). The term hybrid is used here to differentiate this facies from the Teloloapan carbonate facies. This hybrid limestone facies contains many volcanic fragments.

Facies VA13 is a medium- to very thick-bedded limestone with abundant bioclast fragments (corals and mollusks) and variable amounts of volcanic lithic fragments and feldspar crystals (Figure 22B). Some beds are a limestone breccia of sand to granule grain size. The volcanic lithic fraction decreases upward while limestone fragments and bioclasts increase (Figure 21), eventually changing upward to the carbonate rocks of the Teloloapan Formation. Corals are abundant in some levels and are subrounded to rounded, suggesting that they were reworked. Wackestone beds with minor siliciclastic detritus are interbedded in some portions of the facies.

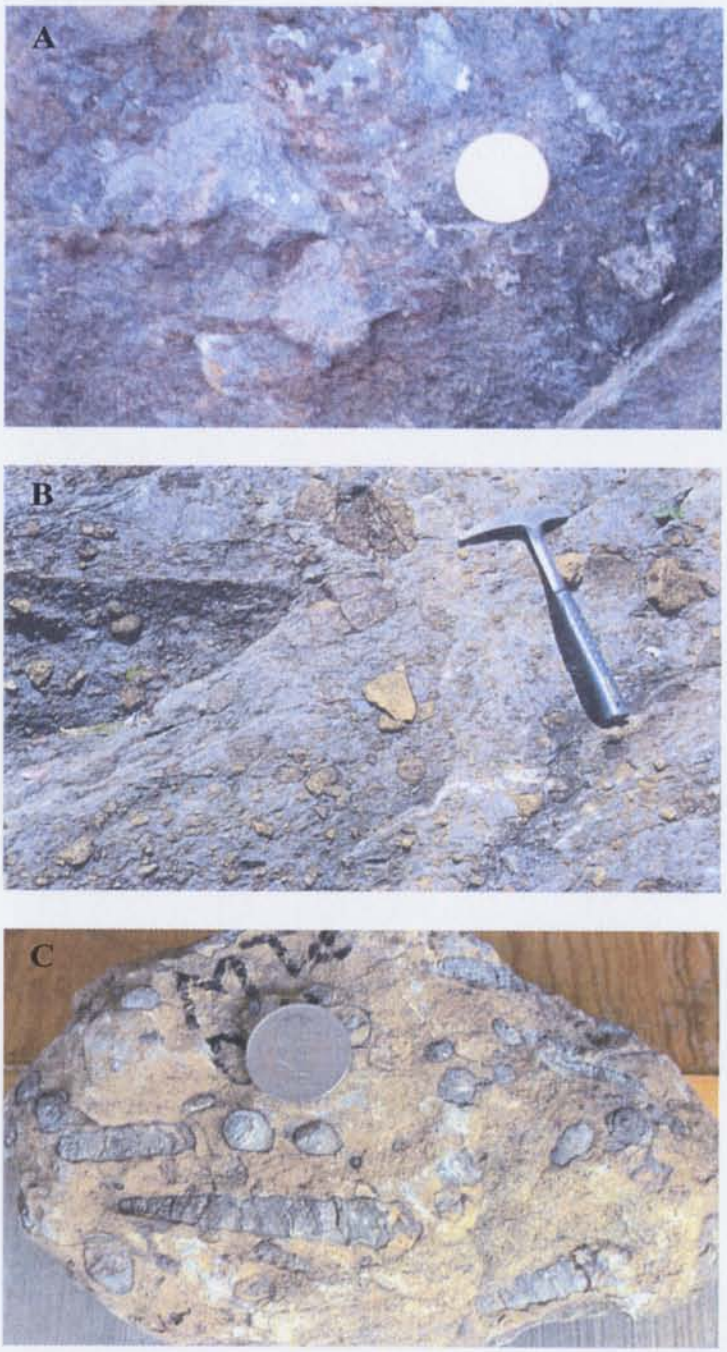

Figure 22. Hybrid sandstone and hybrid limestone lithofacies: (A) hybrid sandstone (VA12), Arroyo Las Bombas, Acatempan locality; (B) hybrid limestone (VA13), north Ahuacatitlan locality; and (C) fossiliferous tuffaceous sandstone (VA14), Teloloapan-Ahuacatitlan road. Coins are 3 cm across and hammer is 25 cm long.

This facies is interbedded with the hybrid sandstone facies, together forming units up to 30 m thick (Figure 21). Lower and upper bed boundaries are usually sharp.

Petrographically, this facies is characterized by the presence of abundant recrystallized coral and mollusk fragments that are associated with equally abundant volcanic lithic grains and crystals of feldspar. The volcanic grains are highly altered to metamorphic minerals such as chlorite and sericite.

Like the hybrid sandstone facies (VA12), this facies is also interpreted as the product of erosion of calcareous and volcanic-volcaniclastic sequences. However, the upward increase in bioclasts and the interbedding with limestones at the base of the Teloloapan formation suggest that this facies was a contemporaneous product of deposition in a shallow-water platform setting. The wackestone beds with minor clastic content were possibly deposited during a period of volcanic quiescence on a newly established carbonate platform.

2.6.1.4.3 Facies VA14: Fossiliferous tuffaceous sandstone

Facies VA14 is mainly exposed in the Ahuacatitlan and Teloloapan areas (Figures 3 and 21). The facies is mainly associated with the masive lava flows and hybrid sandstones of the Villa Ayala Formation, as well as facies TE1 of the Teloloapan Formation (see below). The main characteristic of this facies is tuffaceous sandstone with abundant *in situ* fossils of nerineid gastropods (Figure 22C). The gastropods are preserved in medium-grained tuffaceous sandstone. Petrographically, the tuffaceous sandstone consists of volcanic lithic grains and feldspar crystals. Facies VA14 includes

intervals as thick as 5 m. Individual beds range is thickness from 0.4 to 2.5 m. Most of the nerineids are silicified adults, although juvenile shells are also found. The assemblage is monospecific *Cossmanea* (*Eunerinea*) *hicoriensis* (Cragin). Juveniles show an incipient development of the chambers, while mature nerineids have well-developed chambers.

The tuffaceous sandstone composition and interstratification of this facies with masive lavas and tuffaceous sandstone facies suggest that facies VA14 is contemporaneous with the latter stages of arc volcanism and the early stage of carbonate-platform development in the area. The monospecific assemblage of nerineids, just below shallow-water limestones of the Teloloapan Formation, suggests that the nerineids were pioneers that just colonized the shallow seafloor.

2.6.2. Lithofacies of the Teloloapan Formation

Seven sections were measured through the Teloloapan Formation to characterize its depositional setting, as well as its relationship with the Villa Ayala Formation (Figure 23). The carbonate facies were defined by both field and petrographic criteria. Textural descriptions are based on Dunham's (1962) carbonate classification modified by Embry and Klovan (1971), while facies are named on the basis of predominant lithology, modified by the name(s) of the most abundant allochems (Appendix 8). Wilson's (1975) standard carbonate facies are used to interpret the depositional setting. Where portions of the Teloloapan Formation are severely altered and recrystallized, field criteria alone are used to describe the facies.

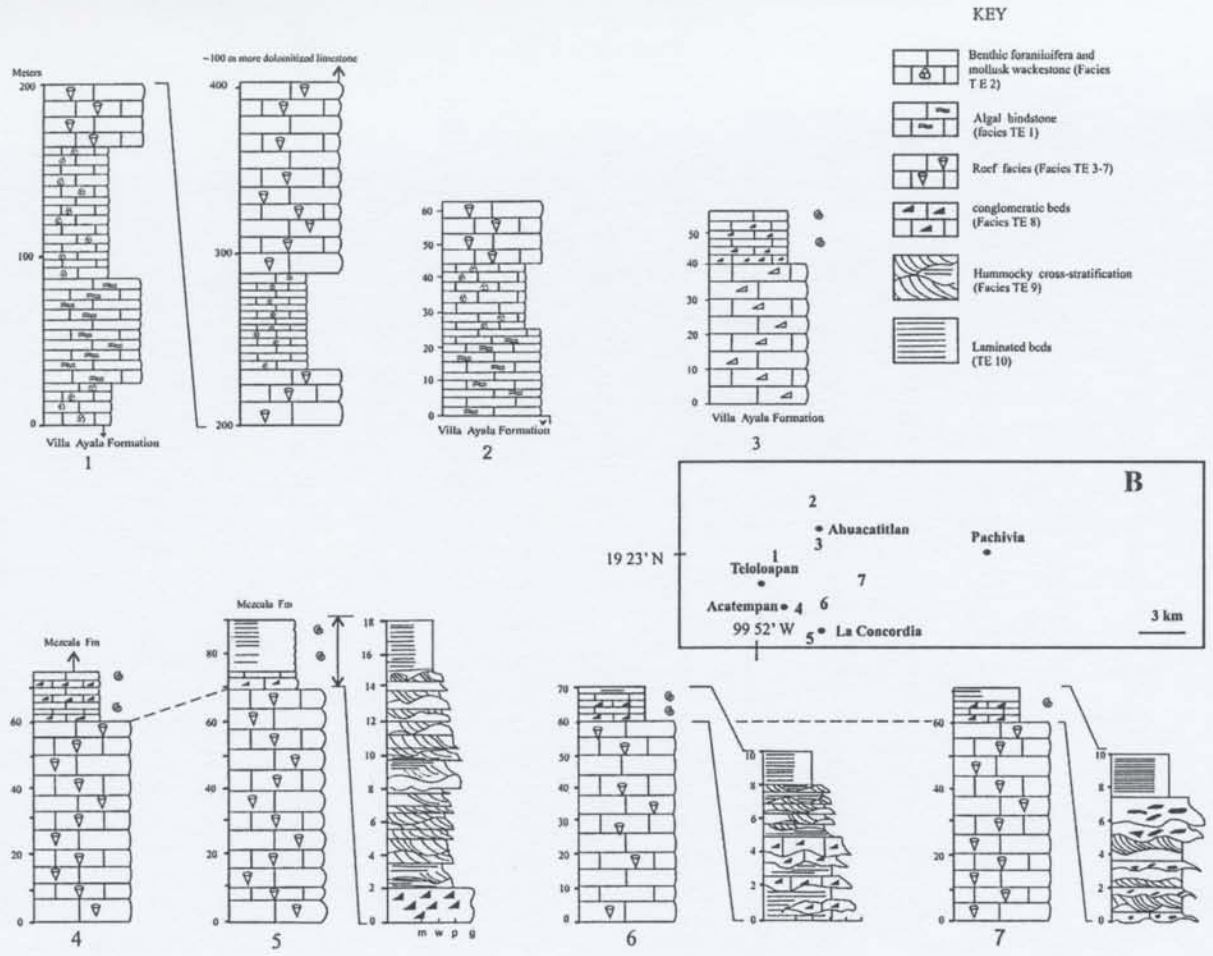

Figure 23. Columns showing limestone facies of the Teloloapan Formation. 1. Teloloapan; 2. north of Ahuacatitlan; 3. south of Ahuacatitlan; 4. east of Acatempan; 5–7 west of La Concordia. Localities are shown in B.

2.6.2.1. Facies TE1: Algal bindstone

Facies TE1 makes up ~5% of the Teloloapan Formation and it is mainly found at the base of the Teloloapan Formation. The formation base is mainly exposed in the vicinity of Teloloapan and north of Ahuacatitlan (Figure 23). Facies TE1 is a thin- to medium-bedded light to dark gray, finely laminated algal bindstone. The beds are made up of algal laminations in sets up to 30 cm thick. The algal laminations are separated by carbonate muds, showing laminar and wavy shapes (Figure 24A). In thin section, this facies contains microcrystalline millimeter-scale wavy laminae that show variation from light to dark gray. The original texture and components are generally well preserved despite the dolomitization observed in some levels that tends to obscure the original structure. Mollusk fragments are scattered. Fragments of thin-shelled rudists (*Toucacia* sp.) are locally present. Intense bioturbation is found at the bases of beds in the lowermost levels of the Teloloapan Formation.

The low diversity of fossils indicates restricted shallow-water conditions. Algal bindstone suggests deposition in a shallow-water setting (~2–10 m depth) under low energy conditions above fairweather wave base. Thin-shelled rudists (*Toucacia* sp) associated with algal laminae might represent a supratidal zone.

2.6.2.2. Facies TE2: Mollusk and benthic foraminifera wackestone

Facies TE2 is the most abundant facies in the base of the Teloloapan Formation. It forms ~60% of this level (Figure 23) and 20% of the entire formation. It is better exposed

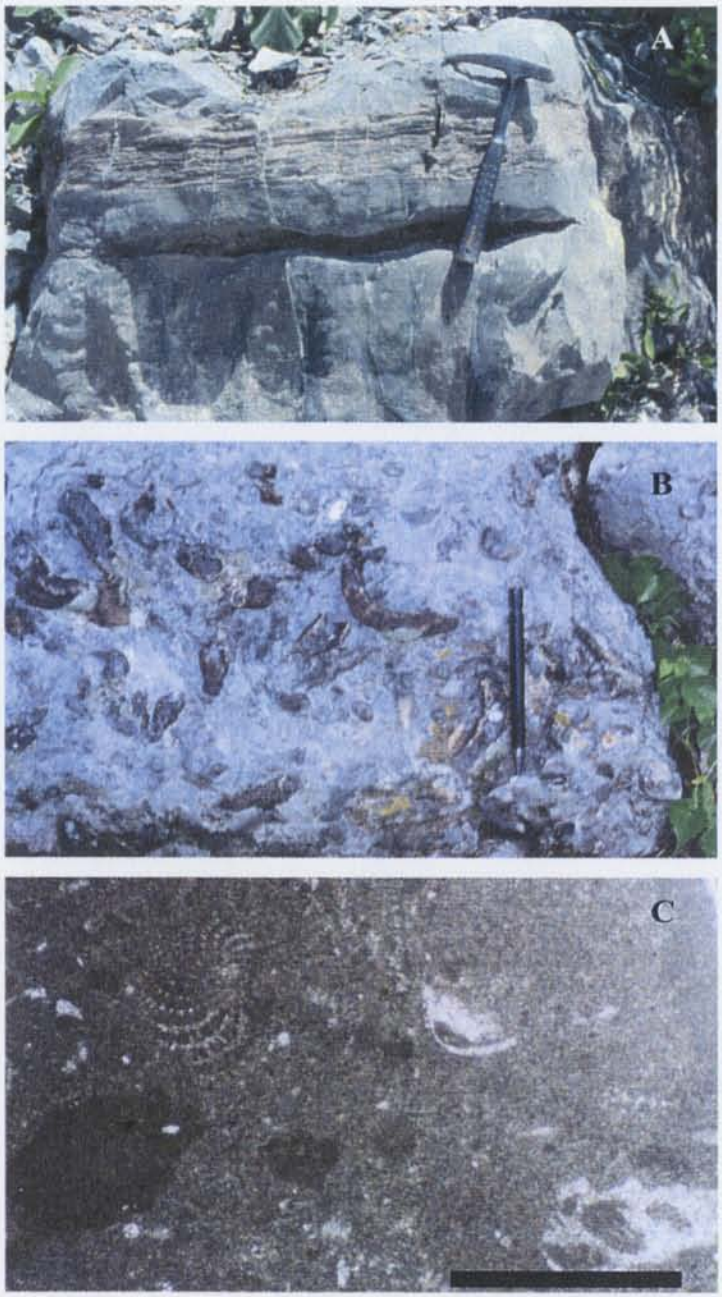

Figure 24. Representative Teloloapan Formation lithofacies: (A) Algal bindstone (TE1), Teloloapan-Ahuacatitlan road; (B) mollusk and benthic foraminifera wackestone (TE2), Teloloapan town; and (C) thin section of facies TE2, showing benthic foraminifera wackestone texture. Hammer and pencil are 25 cm and 14 cm long, respectively. Bar scale = 0.15 mm. See Figure 3 for location map.

in the Ahuacatitlan area where it is dominantly thin- to medium-bedded mollusk and benthic foraminifera wackestone, although micritic limestone textures are also observed in some levels. The rocks show a low degree of dolomitization.

An association of mollusks, benthic foraminifera, and scattered corals characterizes facies TE2. The mollusks are thin-shelled rudists (monopleurids and *Toucacia* sp., Figure 24B), which in some beds are associated with gastropods (nerineids). Where rudists are abundant and monogenetic (e.g., *Toucacia* sp.), they tend to form a concentration of coquinas. A few beds exclusively display nerineid gastropods associated with high bioturbation. The benthic foraminifera are mainly textularids, lituolids, and scattered miliolids (Figure 24C). Ostracod shells and occasional red algal fragments are also present in this facies. Branching corals are sporadically found in some beds, growing in vertical position. The allochemical particles are contained in a micritic and recrystallized matrix.

Thin-shelled rudists (monopleurids), benthic foraminifera, and micritic limestone beds are consistent with shallow-water conditions (cf. Masse and Phillips, 1988). This association might indicate the restricted conditions and protected environment of the intertidal zone or perhaps the protected part of a lagoon.

2.6.2.3. Facies TE3: Bioclast and intraclast rudstone and grainstone

Facies TE3 makes up ~20% of the Teloloapan Formation and is mainly observed in the Acatempan section and uppermost portion of the Teloloapan and Ahuacatitlan sections, although it is best exposed in the latter (Figure 23). This facies is mainly

Figure 25. Representative Teloloapan Formation lithofacies: (A) and (B) Bioclast and intraclast rudstone and grainstone (TE3), south Ahuacatitlan; (C) Rudist and nerinea framestone (TE4), Acatempan locality. Hammer and pencil are 25 cm and 14 cm long, respectively. Bar scale = 0.15 mm. See Figure 3 for localities location.

composed of thick beds of medium- to coarse-grained bioclast and intraclast rudstone and grainstone (Figure 25A). The most common bioclasts are mollusks (caprinid and monopleurid rudists) and corals. These are also highly micritized bioclasts and lithoclasts (classified as peloids). The intraclasts show variable texture from mudstone to packstone. The bioclasts and intraclasts are angular to subrounded (Figure 25B). Planktonic fauna are rare in these rocks. Dolomitization and recrystallization in this facies obscure sedimentary structures and textures. However, in some places, the facies exhibits poorly developed normal grading, cross-stratification or soft-sediment deformation structures.

The rudstone to grainstone textures indicates constant wave agitation and winnowing, perhaps between fairweather wave base and storm wave base. This interpretation is supported by the presence of contemporaneous bioclasts and intraclasts derived from facies which were originally deposited under restricted conditions, such as highly micritized thin-shelled rudists and corals mixed with planktic fossils (globigerinid foraminifera, radiolaria, and calpionelids). Soft-sediment deformation structures observed in this facies suggest sloping seabed during deposition of the facies, but not necessarily a major basin-margin slope.

2.6.2.4. Facies TE4: Rudist and nerinea framestone

Facies TE4–TE7 characterize the middle and upper portions of the Teloloapan Formation throughout the area, and they constitute almost the 40% of the formation. Good exposures of TE4 are present in the Acatempan-La Concordia area (Figure 23).

Rudist and nerinea framestone is composed of very thick- to thick-bedded strata

with a caprinid and radiolitid rudist assemblage and subordinate amounts of nerinea (Figure 25C). This level is dominated by thick-walled and very large shells of caprinid rudists (*Coalcomana ramosa* and *Caprinuloidea* (?) sp.) whose form isolated and recumbent clusters preserved in life position. Although caprinids are dominant, some beds show bioherms containing assemblages of requienids and caprinids associated with nerineids. In thin section, the rudists exhibit a coarse recrystallized shell with geopetal structures and pallial canals filled with either micritic cement or with a matrix of rounded bioclasts and intraclast wackestone. Nerinea have recrystallized and silicified shells. The nerinea shape is variable but large specimens dominate (8–15 cm long). Low faunal diversity (caprinid rudist and nerinea assemblage) and thick-walled and large shells of rudists and nerinea indicate high-energy conditions, possibly below fair-weather wave base. This interpretation is supported by the concentration of intraclasts and bioclasts suggesting episodes of high energy.

2.6.2.5. Facies TE5: Rudist floatstone with matrix of bioclast/intraclast wackestone–packstone

Facies TE5 is thick- to very thick-bedded, and is characterized by abundant whole rudist shells or large shell fragments in a matrix of bioclast/intraclast wackestone–packstone (Figure 26A and 26B). Caprinids and radiolitids are common throughout the facies but caprinids dominate in some levels (Figure 26A). Rudists occur as individuals or as upright clusters. Silicification and recrystalization of rudist shells is common. The

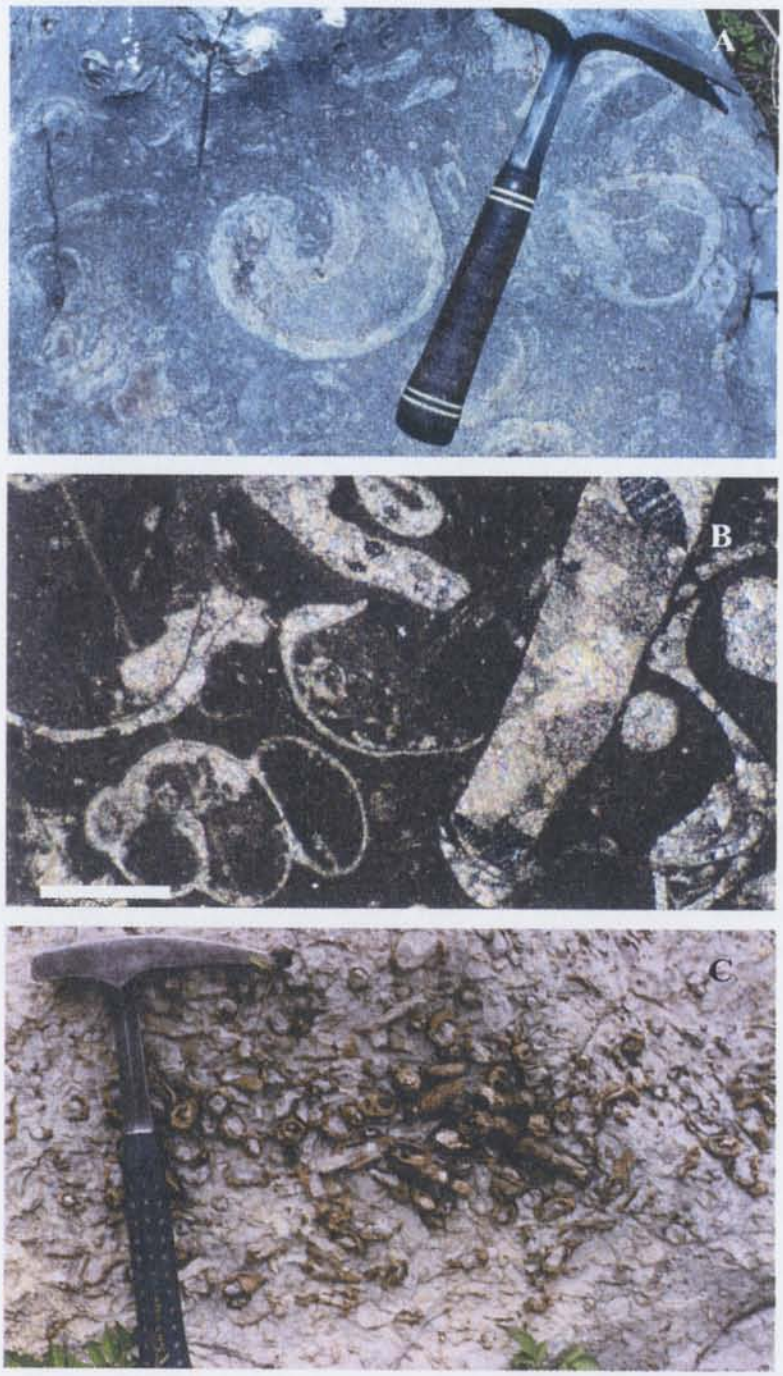

Figure 26. Representative Teloloapan Formation lithofacies: (A) and (B) Rudist floatstone with matrix of bioclast/intraclast wackestone–packstone (TE5), Acatempan locality. (C) Rudist framestone (TE6), La Concordia locality. Hammer is 25 cm long. Bar scale = 0.25 mm. See Figure 3 for localities location.

matrix contains benthic foraminifera, gastropods and scattered fragments of echinoderms (Figure 26B). The lack of corals in most of the rudist-rich beds implies that caprinid rudists preferred a higher energy environment than corals could withstand, perhaps between fairweather wave base and storm wave base (cf. Masse and Phillips, 1988). This interpretation is also supported by the presence of bioclasts (benthic foraminifera, gastropods and corals) and intraclasts (wackestone–packstone textures) which were originally deposited under restricted conditions and laterly reworked in this energetic environment.

2.6.2.6. Facies TE6: Rudist framestone

The rudist framestone facies is medium- to thick-bedded, and characterized by mostly requienid and monopleurid rudists. It is mainly associated with facies TE5 and TE7. The rudists occur as both closely packed and isolated clusters and are predominantly found in life position (Figure 26C). The rudist shells are recrystallized to either calcite or silica. Benthic foraminifera (textularids) are commonly associated with the rudist framestone, and supported by a micritic matrix or recrystallized pseudospar cement. Nerineids and corals are scattered throughout the facies.

The association of rudists and benthic foraminifera suggests shallow water with moderate to low energy in protected areas of the platform. This interpretation is also supported by micritic matrix suggesting quiet conditions, which permitted mud accumulation. The association of requienids and monopleurids has been reported in low

energy conditions during the Early Cretaceous (Wilson, 1975; Masse and Phillips, 1988; Kauffman and Johnson, 1988).

2.6.2.7. Facies TE7: Rudist and coral framestone with matrix of bioclast/intraclast packstone–grainstone

Facies TE7 is medium- to thick-bedded rudist and coral framestone with matrix of bioclast/intraclast packstone–grainstone. This facies is commonly overlain by caprinid biostromes of the rudist and nerinea framestone facies (TE4). Thick-shelled caprinids and masive, solitary corals are the main fauna in the facies. Rudists are mainly caprinids although radiolitids are also present. Corals are abundant in the facies froming branching structures and scattered solitary framework. Corals could not be identified even at the genus level because of recrystallization. The proportions of corals and rudists are highly variable through the different levels of the facies. Rudist and coral framestone contains poorly sorted bioclasts and rudist shells within a matrix of bioclast/intraclast packstone–grainstone. Both the bioclasts and intraclasts are usually rounded and occasionally sufficiently micritized to be termed peloids.

The association of caprinid rudists and corals indicates moderate to high wave energy above fairweather wave base in shallow water. The presence of corals also indicates low sedimentation rates and normal salinity conditions.

2.6.2.8. TE8: Conglomeratic beds

Facies TE8–TE10 characterize the uppermost levels of the Teloloapan Formation (showing variable thickness from 1–15 m); they constitute almost 5% of the formation. These facies crop out from the Concordia locality in the south to Tenanguillo in the north but good exposures of the facies are restricted to the Acatempan-La Concordia area (Figures 3 and 23).

Facies TE8 is mainly associated with TE3, TE5, and TE6, and is capped by hummocky cross-beds of facies TE9. This facies is made up of medium- to thick-bedded conglomeratic limestones, which contain lithoclasts ranging in size from granules to boulders (Figure 23 and 27A). The thickness of these beds is variable from 10–200 cm. Conglomeratic beds occur both as continuous and lenticular deposits, although the lenticular beds are predominant in the sections measured.

Most lithoclasts and bioclasts are most abundant where they are derived from the rudist-bearing facies below (TE3, TE5, and TE6). Casts of packstone–grainstone with abundant microfossils and juvenile ammonites are common in the facies. Large ammonites and rudists are also observed at this facies. Basal contacts of conglomerates are mainly erosional, forming channelized beds.

The usual complete sequence for a conglomerate bed (see Figure 23) begins with an erosional base, followed by lithoclasts of boulder to granule size mixed in disorganized beds. Above this level, a crude normal grading is typical of the conglomerates. No imbrication is present in the disorganized beds.

Figure 27. Teloloapan Formation lithofacies: (A) Conglomeratic beds (TE8), Ahuacatitlan locality; (B) Medium-bedded packstone–wackestone with hummocky cross-stratification rich in planktonic micofossils and amontes (TE9), La Concordia locality; and (C) Laminated wackestone–packstone with planktonic fauna (TE10), La Concordia locality. Hammer and pen are 25 cm and 14 cm long, respectively.

Bourgeois (1980) described similar conglomeratic beds in the Cape Sebastian Sandstone, southwestern Oregon. She interpreted the conglomerates as the deposits of intense waves in a beach to shoreface setting. Erosional bases, clast size, and disorganized nature are consistent with intense wave action. Intense waves possibly eroded a nearly emergent rudist-bearing facies. Boulder sizes indicate breaker-wave heights of at least 3 m (cf. Bourgeois, 1980). The poor normal grading is interpreted as an indicator of either storm deposits produced between fair-weather wave base and the breaker zone, or declining energy after the more intense waves had passed.

2.6.2.9. TE9: Medium-bedded packstone–wackestone with hummocky cross-stratification, rich in planktonic micofossils and ammonites

Facies TE9 consists of meddium-bedded packstone–wackestone rich in planktonic microfossils (globinerinids, calcispherulids, and radiolarians) and juvenile and adult forms of ammonite fauna. Bed bases are usually sharp above conglomeratic beds. Tops are mainly gradational into laminated beds. Internally, the beds are hummocky cross-stratified (Figures 23 and 27B).

Beds range from 10–30 cm thick, forming bedsets up to 1 m thick. Single hummocks are 10–30 cm thick. Two main varieties of hummocky stratification are present: (a) hummocks separated by inclined laminae, and (b) amalgamated hummocks (see Figures 23 and 27B).

The hummocks with inclined laminae show a typical arched or antiformal shape capped by inclined lamination. The inclined laminate are overlain either by more

hummocky cross-stratification or by parallel laminated beds. Occasionally, hummocks are isolated within laminated limestone. This variety of hummocky cross-stratification forms stacked deposits up to 2 m thick. Lower bed boundaries are wavy and flat while upper boundaries are arched to flat, depending on whether the hummocks die out upward.

The amalgamated hummocky cross-stratification is characterized by repeated beds with hummocky cross-stratification forming 3–5 m-thick bedsets. The characteristics of the hummocks are similar to those associated with laminated intervals. Some hummocks are small, only 3–5 cm high. Some bed bases are coarse grained with a high concentration of juvenile ammonites.

Hummocky cross-stratification is a sedimentary structure attributed to storms (Bourgeois, 1980, Dott and Bourgeois, 1982, among others), and formed on the shoreface and shelf by wave action. It is believed that the hummocky cross-stratification in the Teloloapan Formation formed near the platform margin where large storm waves could be expected.

The hummocks with laminae versus the amalgamated intervals are explained in terms of distal to proxima trends within storm deposits. Thicker and amalgamated intervals represent proximal deposition, whereas the hummocks encased in parallel lamination are interpreted as lower energy deposits (cf. Dott and Bourgeois, 1982).

Some of the beds resemble amalgamated hummocky cross-stratification of Dott and Bourgeois (1982), which they attributed to relatively frequent storms events or events so vigorous that all fairweather deposits are scoured away before deposition of the next hummocky bed.

2.6.2.10. TE10: Laminated wackestone–packstone with planktonic microffossils

Laminated wackestone-packstone (TE10) occurs between facies TE9 below and fine-grained sandstone of the Mezcala Formation above. Facies TE10 consists of thin- to medium-bedded, medium-grained, laminated wackestone–packstone with abundant planktonic fauna (globigerinids, calcispherulids, and radiolarians) and scattered ammonites. The facies is predominantly characterized by parallel lamination (Figure 27C), although inclined laminations are also present associated with hummocky cross-stratification. Planktonic microfossils are easily observed in hand-sample. Alternating intervals with mainly radiolarians, mainly globigerinids, and mainly calcispherulids make the laminae more distinct. Lower and upper bed boundaries are usually gradational.

The laminated beds resemble the upper mudstone or siltstone structural division of Dott and Bourgeois (1982). They suggest that this division can represent both waning-storm and normal fairweather sedimentation. The abundant pelagic microfossils and inclined laminae suggest that these beds resulted from accumulation toward the end of the storm, as resuspended microfossil tests rained back to the seafloor. Alternating assemblages of different fossils are ascribed to hydraulic sorting.

2.7. REGIONAL CORRELATION AND DISCUSSION

Figure 11 (p. 53) shows a regional correlation of adjacent areas with the Teloloapan subterrane. An Aptian–Albian tie line is employed because it represents the best age control in the study area and neighboring localities. This correlation incorporates

data collected during this thesis research and published stratigraphic data from other authors.

To begin, a brief but detailed stratigraphic overview and summary is provided for the arc-related succession in the Teloloapan area in order to allow the reader to evaluate the correlation with other areas. A similar format is then followed for the other areas. No facies correlation is done in this chapter because of the lack of facies description in the neighboring areas (except in the Huetamo area). However, a discussion of the sedimentological evolution of each area is presented in Chapter 4.

2.7.1. Teloloapan area

The arc-related succession in the Teloloapan area (this study; column 4 of Figure 11) consists of the Villa Ayala and Acapetlahuaya formations. The Villa Ayala Formation is composed of a thick sequence of pillowed and masive lavas interbedded with coarse-grained tuff, breccias, and volcanic conglomerate in the basal and middle parts, while the upper part of the formation is made up of fine-grained tuff and epiclastic rocks. The Acapetlahuaya Formation consists of fine-grained tuff and epiclastic sandstones interbedded with thin-bedded limestone in the uppermost portion. Fauna, flora, and radiometric ages support a Berriasian–Aptian age for the Villa Ayala and Acapetlahuaya formations and a late Aptian age for the uppermost level of the arc-related succession (see § 2.4).

Volcanic rocks are calc-alkaline basalts and andesites with geochemical and isotopic characteristics that suggest formation in an intra-oceanic, but evolved island-arc (Talavera, 1993; Talavera et al., 1995).

The arc-related succession is capped by carbonate sequences. In the Teloloapan region, the Teloloapan Formation rests conformably on the Villa Ayala Formation, while in the central part of the thesis area, the Amatepec Formation rests conformably on the Acapetlahuaya Formation (Figures 4 and 11). The Teloloapan Formation displays thin-bedded limestone containing abundant nerineids, interstratified with epiclastic sandstone at the base, succeeded by thick-bedded limestone with abundant rudists and nerineids in the middle and upper parts of the formation. Based on different kinds of fossils, the Teloloapan Formation is late Aptian to late Albian in age. The Amatepec Formation is composed of homogeneous thin-bedded black limestone containing abundant radiolaria, planktonic foraminifera, and calcispherulids of Albian–Cenomanian age (De Cserna, 1983; Ramírez et al., 1990).

Finally, along the west and east sides of the thesis area, siliciclastic formations rest on the Amatepec and Teloloapan formations, respectively. The western sequence is termed the Miahuatepec Formation, and consists of a coarse to fine-grained and thick-bedded sandstone. The eastern siliciclastic formation is named the Mezcala Formation, and is made up of homogeneous fine-grained sandstone. Both formations are highly deformed and Late Cretaceous in age. They are described in Chapter 3.

2.7.2. Tejupilco area

Elías and Sanchez (1992) reported two arc-related sequences in the Tejupilco area. The older unit (not shown in Figure 11) is termed the Teloloapan-Tejupilco Sequence. It is characterized by highly deformed phyllite, carbonaceous phyllite, and lenses of rhyolite metamorphosed to greenschist metamorphic facies. Elías and Sánchez (1992) did not find fossils in the sequence, but they established a Late Triassic–Early Jurassic age based on Pb-isotopic data. Correlation between the Teloloapan arc-related succession and this sequence is controversial because of poor stratigraphic control. Despite this fact, several authors have considered the Teloloapan arc-related succession and this sequence similar. However, they are neither lithologically nor chronologically correlated. Based on the strong metamorphism, volcanic composition, and age reported by Elías and Sánchez (1992) for their Teloloapan-Tejupilco Sequence, those rocks might be considered as an arc-related unit older than the Teloloapan arc-related succession.

Elías and Sánchez (1992) and Sánchez (1993) also reported a Late Jurassic to Early Cretaceous arc sequence termed the Arcelia-Otzoloapan Sequence (column 3 in Figure 11). This sequence consists of a thin-bedded limestone interstratified with black slates and graywackes (the limestone-volcaniclastic unit) in the lower part. It passes upward into thick pillow and masive lavas interstratified with breccias, volcanic conglomerate, and tuff (the volcanic unit). Finally, the uppermost part is characterized by masive and thick-bedded fossiliferous limestone interstratified with sporadic masive lavas in its lower part (the fossiliferous limestone unit).

The Teloloapan arc sequence could be correlated with the Arcelia-Otzoloapan Sequence with a certain level of confidence. Lithologically, the volcanic and volcaniclastic rocks from both sequences are similar. However, there are two apparent differences between the two sequences. First, pillow lavas in the Teloloapan arc-related succession (Villa Ayala Formation) are thinner than the "volcanic unit" described by Elías and Sánchez (1992) and Sánchez (1993). These volcanic rocks are restricted to the lowermost part of the sequence in the study area, while in the Tejupilco area they are found throughout the sequence. One possibility is that at least part of the pillow lava belonging to the "volcanic unit" can be correlated to rocks cropping out in the Arcelia area (see column 2 in Figure 11). The second difference is that the Teloloapan arc-related succession is the oldest unit of the region, while in the Tejupilco area the oldest rocks comprise a limestone-volcaniclastic unit.

Finally, carbonate-platform facies cap the arc-related sequences in both areas. The Teloloapan Formation (Teloloapan area, column 4 in Figure 11) and a fossiliferous limestone (Tejupilco area, column 3 in Figure 11) can be correlated with a certain level of confidence. Both carbonate units rest conformably and transitionally on the arc-related successions and show interstratification with volcaniclastics near their lower contact. The carbonate platform is apparently older in the Teloloapan area, but this apparent age discrepancy might be because of a lack of fossils in the Tejupilco area, while in the Teloloapan region fossils are abundant.

2.7.3. Arcelia area

The Arcelia arc succession is made up of two sequences (column 2 in Figure11). The lower sequence consists of basaltic pillow lavas (~2000 m thick, Talavera, 1993) and rare masive lavas intruded by ultramafic igneous bodies (Ortiz and Lapierre, 1991). The upper sequence contains radiolarian-bearing tuffaceous chert and black shale (Ortiz and Lapierre, 1992; Talavera, 1993). An Albian–Cenomanian age is well documented using paleontological and radiometric data (Dávila and Guerrero, 1990; Delgado et al., 1990; Ortiz and Lapierre, 1991; Talavera, 1993).

No correlation is apparent between the Arcelia and the Teloloapan arc sequences. Volcanic rocks in the Teloloapan arc-related succession are calc-alkaline basalts to andesites, while the Arcelia sequence is exclusively composed of tholeithic basalts. The Arcelia sequence does not contain breccias and/or volcanic conglomerates, which are widespread in the Teloloapan arc-related succession. Finally, no carbonate-platform rocks are present in the Arcelia area. The absence of carbonate rocks might be attributed to a deeper water depth. However, the Arcelia arc sequence is chronologically younger (Albian–Cenomanian) than the Teloloapan arc-related succession (Berriasian–Aptian; see Figure 11). This, along with different rock types, strongly suggests that the Arcelia and Teloloapan arcs are distinct and unrelated.

2.7.4. Huetamo area

The Huetamo sequence contains four formations (column 1, Figure 11). The lower unit (Angao Formation) is a thick succession of polygenetic conglomerates

interbedded with epiclastic sandstone and scarce tuff. This unit contains, in its lower part, scarce basaltic pillow lavas (5–10 m thick). Basalts are calc-alkaline and shoshonitic while volcanic fragments in the conglomerates are tholeiitic and medium- to high-K calc-alkaline typical of intra-oceanic settings (Talavera, 1993; Mendoza and Suastegui, 2000). The age for the Angao Formation is Berriasian–Valanginian (Guerrero, 1997). This formation changes transitionally upward to a monotonous sequence of medium- to fine-grained epiclastic sandstone, scarce tuff, and shale with abundant ammonites, nerineids, and plants (San Lucas Formation). A late Valanginian to early Aptian age is well documented (Pantoja, 1959; Campa, 1977; Pantoja, 1990; Gómez et al., 1994). The San Lucas Formation is capped by a thick interval of thin- to thick-bedded limestone interstratified with epiclastic sandstone of the El Cajon Formation containing abundant rudists, nerineids, and orbitolinids (Pantoja, 1990; Guerrero, 1997). The age of this formation is Aptian. Finally, a monotonous Albian–Cenomanian thin-bedded argillaceous limestone caps the sequence (The Mal Paso Formation; Pantoja, 1959).

Several authors (Pantoja, 1959; De Cserna et al., 1978; Johnson et al., 1991; Sánchez, 1993) have attempted to correlate the Huetamo and Teloloapan sequences. However, correlation of these areas poses several problems.

First, the Huetamo sequence does not show metamorphism, while the Teloloapan sequence is at prehnite–pumpellyite to greenschist grade. Second, deformation in the Huetamo area consists of broad anticlines and synclines, while the Teloloapan sequence is highly deformed and folded. Third, in the Teloloapan sequence, the Lower Cretaceous formations are characterized by abundant volcanics and coarse- to fine-grained

volcaniclastic rocks, while epiclastic sandstone and scarce tuff predominate in the Huetamo area. Fourth, carbonate-platform rocks of the Teloloapan and Huetamo sequences (see Figure 11, columns 1 an 4) show different lithologic and paleontologic features. The carbonates rest conformably and transitionally on siliciclastic of the Huetamo area and volcaniclastic rocks of the Teloloapan sequences, respectively. However, carbonate rocks are older (Barremian) and built biostromal structures in the Huetamo area; they are interbedded with sandstone at the uppermost levels of the San Lucas Formation (Figure 11, column 1). Abundant orbitolinids are present at the lower contact of the carbonate platform in the Huetamo area, while nerineids are abundant in the Teloloapan region and orbitolinids are absent. Rudist limestones are present in both areas. However, they are older in the Huetamo sequence. Finally, Albian–Cenomanian argillaceous limestones and Cenomanian–Turonian fine-grained siliciclastics cover the Huetamo and Teloloapan sequences, respectively.

The long list of stratigraphic and age differences suggest that the Huetamo and Teloloapan sequences are distinct tectonostratigraphic elements in the Guerrero Terrane.

2.7.5. Morelos–Guerrero Platform.

Another controversy in the region is related to the carbonate-platform sequences. Some authors have considered them to all be related to a passive margin of the Gulf of Mexico and a Cretaceous transgressive Tethyan event widely known from that area. Other authors have linked carbonate-platform sequences in the Teloloapan subterrane to the arc sequences (see § 2.2).

The Morelos Formation, belonging to the Morelos-Guerrero platform, has been described as Albian–Cenomanian, masive- to medium-bedded rudist limestone and dolostone deposited in restricted-platform and reef settings. The lithological description of the Teloloapan Formation in this chapter is very similar to that of the Morelos Formation. Stratigraphic data show that the Pacific-margin carbonate sequences rest conformably and transitionally on arc-related sequences (Zihuatanejo, Huetamo, Teloloapan, and Tejupilco areas, see columns 1, 3,and 4 in Figure 11). However, detailed chronostratigraphy (Figure 11) shows that the transition is of variable age. For instance, in the Huetamo area it is early Aptian, while this transition is late Aptian in the Teloloapan area, and early Albian in the Zihuatanejo and Tejupilco regions. Fauna are also variable from region to region. However, more paleontologic studies are required to document the full range of this variation. In contrast, the central Mexican carbonate platforms (represented by the Morelos-Guerrero platform in the study area) do not show interbedding with volcanic or volcaniclastic rocks, and they are exclusively Albian–Cenomanian in age.

A preliminary hypothesis is that the Morelos-Guerrero platform formed far away from the arc-related platforms, and that they were brough together at a latter time by convergence and terrane accretion. This hypothesis and the evolution of the carbonate platform of southern Mexico will be discussed more fully in chapters 4 and 7.

2.8. SUMMARY

Three formations form the arc-related succession ranging in age from Berriasian to Albian. The lowermost unit is the Villa Ayala Formation (Berriasian–Late Aptian), which is composed of volcanic and coarse- to fine-grained volcaniclastic rocks. Followed by very fine- to fine-grained sandstone, tuff and shale of the Acapetlahuaya Formation (Late Aptian) in the central part of the thesis area. The Teloloapan Formation (Late Aptian–Albian) covers the Villa Ayala Formation in the eastern part of the thesis area, and comprises medium- to thick-bedded limestone.

A Berriasian–Albian age is well documented for the arc-related succession based on new paleontologic data and the relationship among the formations. Furthermore, the Early Cretaceous age here documented is the youngest age ever proposed for the volcanic, volcaniclastic and sedimentary rocks of the Teloloapan subterrane.

Based on the stratigraphy developed in this thesis, fourteen lithofacies are recognized in the Villa Ayala and Acapetlahuaya formations. These are grouped into primary volcanic facies, volcanic breccias and conglomerates, tuff and epiclastic deposits, and hybrid sandstone and hybrid limestone facies. Limestones of the Teloloapan Formation are divided in ten lithofacies. Furthermore, the sedimentologic processes responsible for each lithofacies are assessed.

Finally, a regional lithostratigraphic correlation was attempted with the neighboring sequences to the north (Tejupilco area), west (Arcelia and Huetamo) and east (the Morelos-Guerrero Platform) areas. The Teloloapan area (subterrane) might correlate

with the uppermost parts of the succession in the Tejupilco area, but no lithostratigraphic correlation is evident with the other areas.

CHAPTER 3. SEDIMENTARY COVER SUCCESSIONS: STRATIGRAPHY AND FACIES

3.1. INTRODUCTION AND TERMINOLOGY

Two Upper Cretaceous highly deformed siliciclastic sequences crop out in the thesis area (Figure 3, p. 5). The eastern sequence is predominantly fine- to medium-grained sandstone interbedded with calcareous debris-flows deposits and chert beds. This siliciclastic sequence is named the Mezcala Formation. The western siliciclastic sequence is similarly deformed but it is dominantly medium- to coarse-grained sandstone in texture. It is named the Miahuatepec Formation.

This chapter presents the stratigraphy of the Upper Cretaceous siliciclastic successions (Figures 3 and 4). The stratigraphic relationships of the sedimentary cover successions are described in detail in this chapter in order to obtain a better understanding of the sedimentary evolution of the area Guerrero Terrane. Like Chapter 2, the North American Stratigraphic Code (1984) was followed to revise the stratigraphic nomenclature in the area. Recommendations include the redefinition of the western Upper Cretaceous siliciclastic sequence, the Miahuatepec Formation, and assignment of a Cenomanian–Turonian age to the Mezcala Formation, the eastern siliciclastic sequence.

Structural complexity in both sequences prevents correlation between facies because of a lack of lateral and vertical continuity of strata. Way-up criteria (e.g., graded bedding and sole markings among others) were used to recognize the base and top of the sequences. Facies analysis was therefore done using the methodology proposed for

similarly deformed rocks by Underwood (1984) in studies of the Franciscan mélange belt, California; and modified by Leverenz (2000) in the Mesozoic Torlesse accretionary complex, New Zealand. Facies description and interpretation followed Pickering et al. (1989). Bed-thickness and categories are those of Ingram (1954, see Table 1).

Three regional sections were measured in the Mezcala Formation. A further sixty outcrops were examined in order to measure detailed sections that range from 1–80 m thick; however, the typical exposed section thickness is 1–30 m. In the Miahuatepec Formation, two regional sections were measured and thirty-four other sections ranging from 2–20 m thick were used to document the facies. In addition, sketches where made at lookout points to characterize both formations in intensely deformed areas.

Both formations have been interpreted to be related to accretionary processes in southern Mexico. The Miahuapetec Formation has been interpreted as a product of the collision between the Teloloapan and Arcelia – Palmar Chico subterranes, and the Mezcala Formation has been given a similar interpretation related to collision between the Guerrero and the Mixteca terranes (Campa and Coney, 1981; Ramírez et al., 1991; Talavera, 1993). Therefore, an additional aim of the facies analysis is to develop sedimentological criteria, which might aid in (1) the recognition of principal pre-accretionary depositional environments (chapter 4), and (2) the development of a tectonic model for this part of the Guerrero Terrane (chapter 6).

A regional stratigraphic and facies correlation is attempted with the neighboring Upper Cretaceous siliciclastic sequences of the Zihuatanejo-Huetamo subterrane, Arcelia – Palmar Chico subterrane, and the Mixteca Terrane. This correlation is done to establish

affinities and differences concerning the evolution of Upper Cretaceous siliciclastic sequences in southwestern Mexico.

3.2. UPPER CRETACEOUS LITHOSTRATIGRAPHY: THE SEDIMENTARY COVER SUCCESSIONS

3.2.1. The Mezcala Formation

The Mezcala Formation is monotonous fine- to medium-grained sandstone interbedded with siltstone, claystone, carbonate debris-flows, and thin-bedded black carbonaceous rocks. It is exposed in the eastern part of the thesis area, along the Pachivia valley (Figure 3).

a. History and name

Upper Cretaceous siliciclastic sequences in southern Mexico have traditionally been assigned to the Mezcala Formation. Lately, it has been suggested that some Upper Cretaceous siliciclastic rocks in Guerrero State do not conform to the original description (González, 1991). Fries (1960) formally proposed the name Mezcala Formation for sandstone interbedded with calcareous siltstone and claystone, and rare lenses of clastic limestone, and containing an abundant fauna of ammonites, pelecypods, and planktonic foraminifera. Fries (1960) also proposed a section type at the town of Mezcala, located in central Guerrero State, south of the study area.

Ontiveros (1973) assigned the siltstone and thin-bedded sandstone interbedded with thin-bedded calcareous sandstone and lens of shaly mudstone in the Pachivia valley

to the Mezcala Formation. He separated the fine-grained siliciclastic rocks of the Mezcala Formation from thin-bedded black mudstones and wackestones–packstones with planktonic fossils that he assigned to the Agua Nueva Formation.

González (1991) informally divided the Mezcala Formation into "shallow" and "deep" members. The "deep" member is exactly as originally defined by Fries (1960), but the "shallow" member is defined as bioclastic mudstone to wackestone, changing upward to litharenite and red siltstone displaying cross-bedding. It also changes laterally to grainstone with abundant quartz and limestone fragments.

The rocks in the Pachivia Valley of the eastern part of the thesis area correspond better to the original description of the Mezcala Formation provided by Fries (1960).

b. Thickness

The Mezcala Formation in its type area (not shown here) is characterized by sandstone beds interbedded with siltstone and scarce lenses of bioclastic limestone (Fries, 1960). Despite strong deformation, good outcrops in the San Martin Pachivia, El Calvario, and Apatzingan localities clearly show the relationship among the different lithologies of the formation.

An accurate thickness cannot be measured through the Mezcala Formation because of its structural complexity. However, some authors have previously estimated the thickness at different localities. Fries (1960) reported 1220 m at the type section in the Mezcala area. Campa and Ramírez (1979) estimated 500 m in the Taxco region, northeast of the thesis area. González (1991) calculated more than 1300 m for the "shallow" member in the Temalac-Atlapa area. In the study area, Ontiveros (1973) measured 150 m

of limestone and 450 m of siliciclastic rocks for a total of 600 m. Finally, Cabral (1995) estimated a minimum thickness of 2000 m in the Pachivia valley. A section measured by the author between El Calvario and La Concordia gives 700 m for the Mezcala Formation (Figure 28C).

c. Lithology

The Mezcala Formation is highly deformed and it is difficult to identify and characterize a complete vertical sequence. The regional section measured in the El Calvario–La Concordia area is used here to describe the Mezcala Formation (Figure 28). In this area, basaltic dikes intrude the Mezcala Formation. The lower level of the formation (0–250 m in column, Figure 28C) is predominantly made up of thin-bedded and fine-grained sandstone interstratified with thick intervals of siltstone. Sandstone/shale ratio is 1:1 at the base (0–25 m in column, Figure 28C) and ~1:4 at the top (420–680 m in column, Figure 28C). Sandstone beds show normal grading and planar lamination. Thin to medium beds of coarse-grained black packstone to wackestone with abundant lithoclasts are intercalated in this interval. They show scoured bases and pitch out laterally.

The fine-grained sandstone interstratified with siltstone (0–250 m in column, Figure 28C) changes upward to a monotonous, thin-bedded and laminated black mudstone and wackestone with nodules and lenses of chert, containing abundant microfossils (radiolarians and planktonic foraminifera are observed in hand-samples). This level changes gradationally upward to a sequence similar to that of the lower level (0–250 m in column, Figure 28C), but with beds of massive carbonate breccia containing

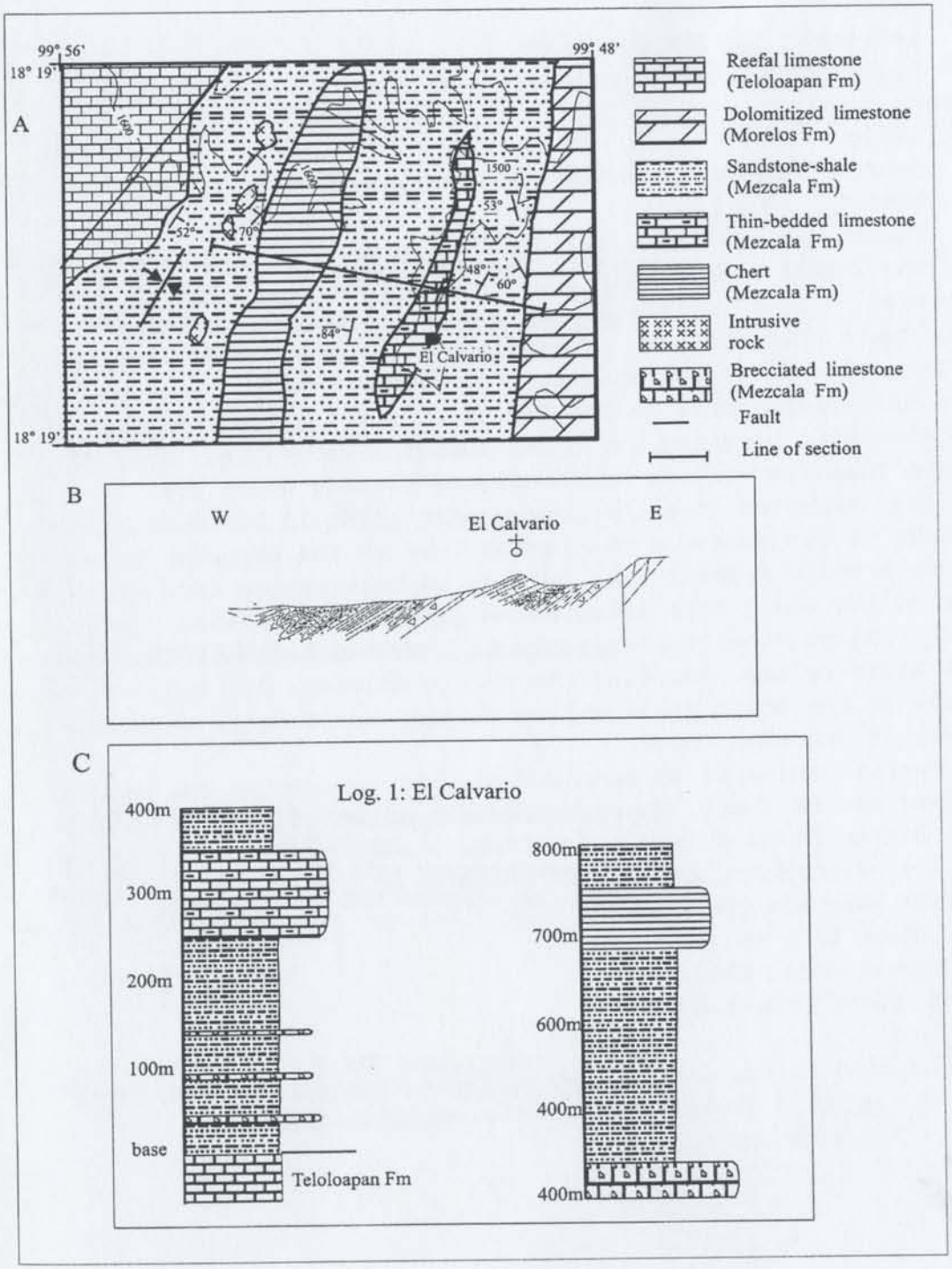

Figure 28. Mezcala Formation: (A) geologic map, (B) schematic structural section, and (C) composite section.

lithoclasts and bioclasts (Figure 28). Finally, the uppermost part (680–800 m in column, Figure 28C) of the formation is characterized by very thin-bedded chert and thin-bedded, fine-grained sandstone.

d. Boundaries and distribution

The base of the Mezcala Formation was previously described (see § 2.3.3) and the top boundary is not exposed in the study area. The Mezcala Formation is mainly exposed in the Pachivia Valley where it shows an elongated north–south trend (Figures 3 and 28A). The thin-bedded limestone facies is discontinuous and pinches out to the south and north (Figure 28A).

e. Fauna and age

Beds of the lower portion of the Mezcala Formation were sampled to determine the age of its gradational contact with the Teloloapan Formation. Planktonic foraminifera include *Favusella* sp., *Favusella washintensis*, *F. hedbergellaeformis*, *Hedbergella* sp., *Praeglobotruncana* sp., *Praeglobotruncana* cf. *stephani*, *Rotalipora* sp., and *Thalmanninella* cf. *Appeninica* (González-Casildo, 1999 written communication, and Guerrero et al., 1993). These fauna are typical of the lower Cenomanian (González-Casildo, 1999 written communication).

The thin-bedded black limestones were also sampled. Unfortunately, severe recrystallization prevents a precise age determination. The fauna are also planktonic foraminifera and include *Favusella* sp., *Hedbergella* sp., *Praeglobotruncana* sp., and *Rotalipora* sp. that have been reported from the Albian–Cenomanian (González-Casildo, 1999; written communication). However, Ontiveros (1973) reported a Turonian age for

the same lithology based on *Calcisphaerula innominata* (Bonet), *Pithonella ovalis* (Kauffman), *Pithonella trejoi* (Bonet), *Hedbergella* sp., *Stomiosphaera conoidea* (Bonet), and *Stomiosphaera cardiiformis* (Ayala and Seiglie).

Based on these fauna an early Cenomanian to post-Turonian age is interpreted for the Mezcala Formation in the study area. The early Cenomanian age is the oldest age yet reported for this formation in the region.

3.2.2. The Miahuatepec Formation

The name Miahuatepec Formation is proposed for a sequence of predominately thick bedded, coarse- to medium-grained sandstone interbedded with siltstone and rare thin-bedded limestone (Appendix 9). The unit is highly folded and exclusively exposed in the westernmost part of the thesis area (Figure 3).

a. History and name

No previous studies have differentiated this siliciclastic unit from the volcanosedimentary sequences exposed in the Teloloapan and Arcelia areas.

Campa et al. (1974) included this unit in their metasedimentary unit of the "Secuencia volcanosedimentaria de Telolopan-Ixtapan de la Sal", and described it as a gray-green, foliated, coarse- to fine-grained metasandstone. De Cserna et al. (1978) originally incorporated the sandstone and interstratified shale into the Mezcala Formation. Subsequently, De Cserna (1983) included this unit in the lower member of the Xochipala Formation, which is composed of andesitic lavas with pillow structures associated with sandstones, conglomerates, tuffs, and graywackes, all of Late Jurassic to

Early Cretaceous age. Ramírez et al. (1990) informally described this siliciclastic unit as the Miahuatepec Formation. They differentiated this unit from the siliciclastic rocks of the Mezcala Formation and volcanic and volcaniclastic units of the Arcelia sequence because of its stratigraphic position and severe deformation. Cabral (1995) described, in the same area, a monotonous package of well-foliated phyllites that weather to a light brown color, associated with thin intervals of black chert. He informally termed these rocks the Almoloya Phyllite.

The name for this unit is taken from the town of Miahuatepec, located between San Martin and Las Ceibas on Federal Road 51, where the unit is well exposed (Figures 3 and 29). The name Almoloya Phyllite, proposed by Cabral (1995), is rejected because in the town of Almoloya, where he originally described this unit, the exposed rocks are volcanic and volcaniclastic rocks belonging to the Villa Ayala and Acapetlahuaya formations. Although the Miahuatepec Formation contains foliated rocks, it is lithologically distinct from the arc-related succession, and is considered to be younger. Also, this unit is differentiated from the volcaniclastic rocks in the Arcelia region that are assigned to the Arcelia – Palmar Chico subterrane.

b. Type section and thickness (see Appendix 9)

The Miahuatepec Formation is highly folded at all localities in the study area and no continuous sections were measured. Hence, the complete sequence is difficult to document. However, a regional section measured along Federal Road 51 between the towns of San Martin and Las Ceibas, west of the thesis area, is designated as a composite type section for this formation (Figures 3 and 29). In this area, the lower contact with the

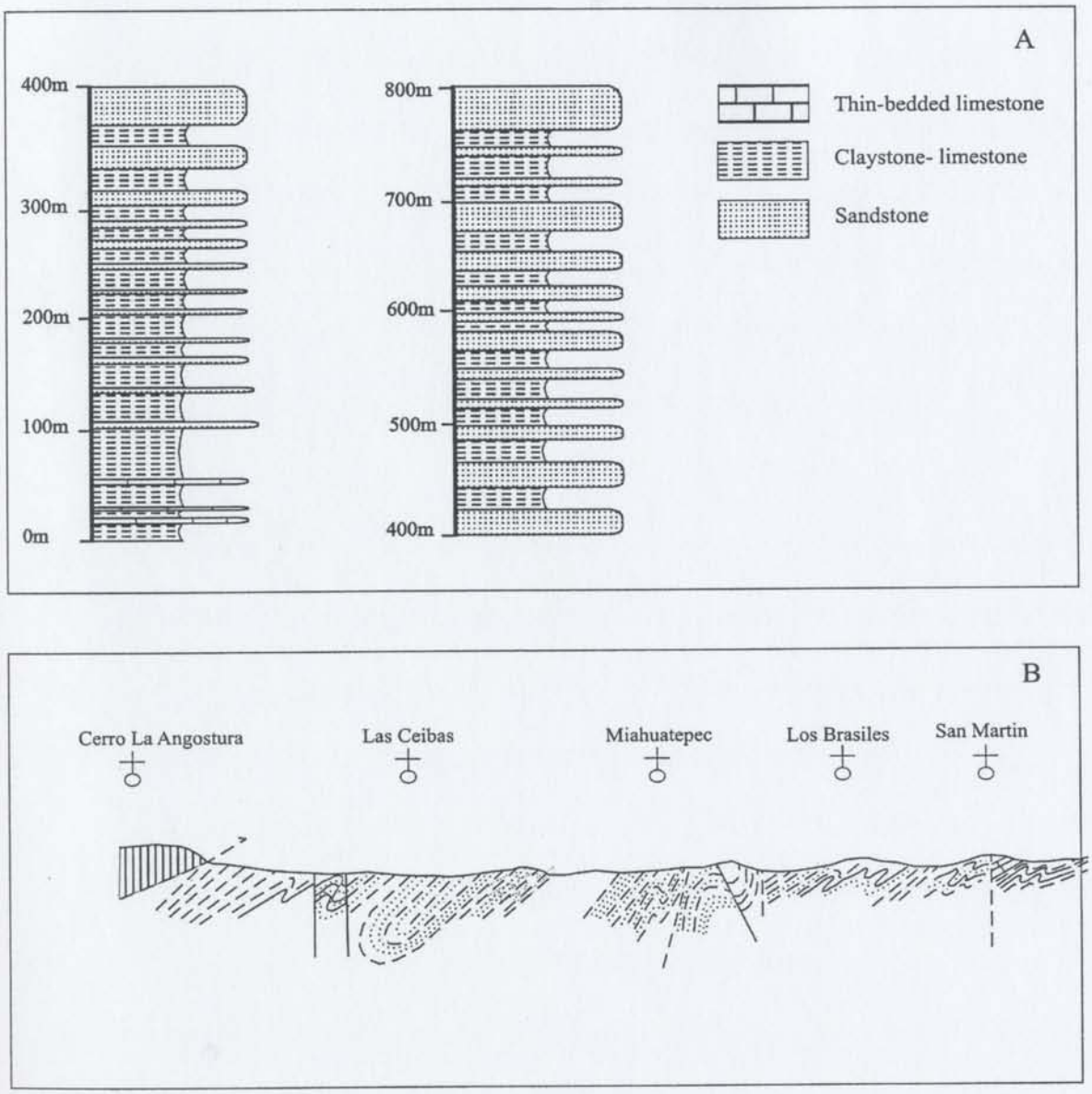

Figure 29. Miahuatepec Formation: (A) schematic composite type section; and (B) schematic structural section. See Figure 41 for localities location.

thin-bedded black limestone of the Amatepec Formation is exposed, while the upper contact is nowhere exposed.

The thickness of the Miahuatepec Formation is difficult to measure because of the lack of a continuous undeformed section. However, an estimated thickness of 800 m is proposed (Figure 29A) based on bedding attitudes from San Martin to Miahuatepec towns. In the same area, De Cserna (1983) reported a thickness of 250–400 m for the lower member of his Xochipala Formation, while Cabral (1995) estimated a structural thickness of 800 m for the sequence termed by him as the Almoloya Phyllite.

c. Lithology

The siliciclastic rocks of the Miahuatepec Formation are distinguished from the Mezcala Formation by stronger deformation and different lithostratigraphical relationships with the surrounding formations (Arcelia sequence and Amatepec Formation). Although some authors have assigned the unit to the Arcelia sequence (De Cserna, 1983; Cabral, 1995), it is compositionally unlike the volcanic and volcaniclastic rocks of the Arcelia sequence. The Miahuatepec Formation is a coarse- to fine-grained siliciclastic unit with minor thin-bedded limestone toward the base.

In the type area, light brown and micaceous siliciclastic rocks are characteristic the Miahuatepec Formation. The lower levels of the unit, between San Martin and Los Brasiles, contain siltstone beds interbedded with scattered thin-bedded limestone and fine-grained sandstone. This set of facies, in the town of Miahuatepec, changes upward to an interval of fine-grained sandstone and siltstone. The sandstone/siltstone ratio is about 2:1. The sandstone beds are 15–20 cm thick and medium to coarse grained.

The uppermost levels of the Miahuatepec Formation, in Las Ceibas town, show an upward thickening trend in sandstone bed thicknesses. Thick-bedded (40–100 cm) and coarse- to medium-grained lithic sandstone are predominant. Thin to medium interbeds (5–20 cm) of finely laminated siltstone are present between the sandstone beds. Bouma Tab and Tabc sequences are frequently found associated with intervals rich in rip-up clasts.

d. Boundaries and distribution

The Miahuatepec Formation rests on the thin-bedded limestone of the Amatepec Formation. This contact is well exposed in the San Martin and Peña el Organo localities, in the west-central and northwest parts of the study area, respectively (Figures 3 and 29). At these localities, a 5–10 m highly deformed zone, where very thin beds of limestone are interbedded with siltstone and fine-grained sandstone of the Miahuatepec Formation, characterizes the boundary.

The top of the Miahuatepec formation is not exposed in the study area and it has not been reported from other areas. In the western part of the thesis area, the Miahuatepec Formation is overthrust by the volcanic rocks of the Arcelia sequence (Figures 3 and 29).

e. Fauna and age

The Miahuatepec Formation has an unknown age. Despite sampling for this thesis project, no microfossils were found. A Late Cretaceous age is assumed based exclusively on stratigraphic criteria (i.e, superposition). Despite strong deformation, outcrop quality is sufficient to demonstrate that this siliciclastic unit overlies the Albian–Cenomanian

carbonates of the Amatepec Formation. This would make the Miahuatepec Formation post-Cenomanian in age.

3.3. FACIES OF THE SEDIMENTARY COVER SUCCESSIONS

3.3.1. The Mezcala Formation

The Mezcala Formation consists of eight facies. These fall naturally into three groups based on dominant lithologies. The first group is heterolithic, and includes limestone breccia, thin-bedded limestone, and chert; the second group is sandstone dominated, and includes thick- to medium-bedded sandstone facies; and the third group is sandstone-shale, and includes medium-bedded sandstone and shale, thin-bedded sandstone and shale, shale and thin-bedded sandstone, and laminated shale. Appendix 10 contains a summary of the facies in the Mezcala formation.

3.3.1.1. Heterolithic Facies

3.3.1.1.1: Facies MF1: Limestone breccia

Facies MF1 constitutes <5 % of the Mezcala Formation. Limestone breccia occurs in beds that form units 3 cm to 40 m thick (columns E and G in Figures 30, as well as Figure 31A). Granule- to boulder-sized clasts are typically reworked rudist bioclasts and mudstone–wackestone lithoclasts derived from the neighboring limestones of the Morelos Formation and the Teloloapan Formation. There are also rare intraformational clasts of sandstones or shales derived from the Mezcala Formation itself. Clast diameter is 2 mm to 45 cm but most are granules. Clast shape is subangular to subrounded.

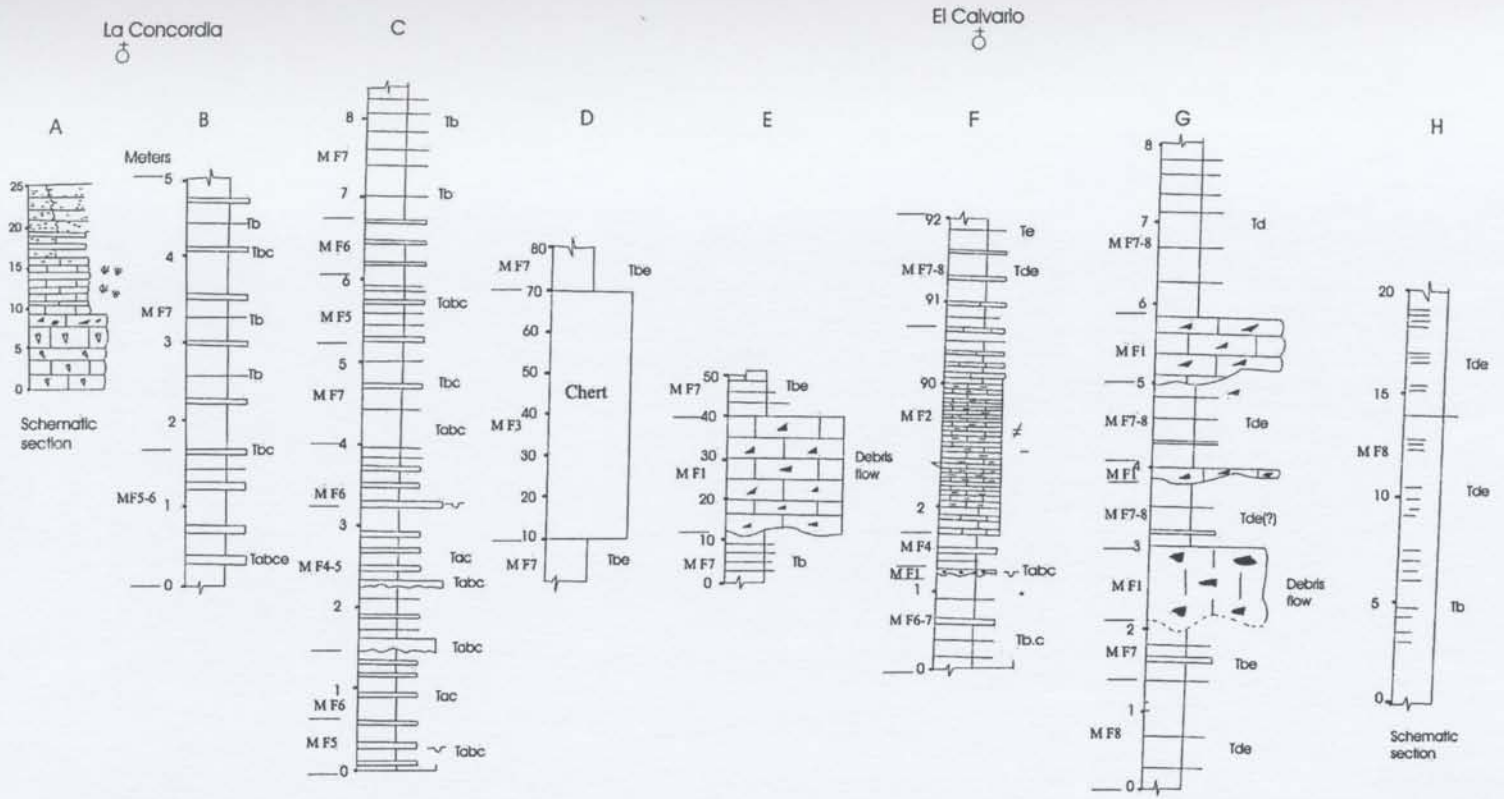

Figure 30. Sedimentary logs measured between La Concordia and El Calvario towns in the Mezcala Formation. Each log is located in Figure 40B. All the scales are in meters. Logs D and E illustrate facies MF3 and MF1. Log F shows facies MF2 and the scale change in the middle of the column because of the thickness of the facies. Column H is a schematic section of the strong deformed shale of facies MF8. There is not time or lithology correlation among the different logs because of the deformation in the formation.

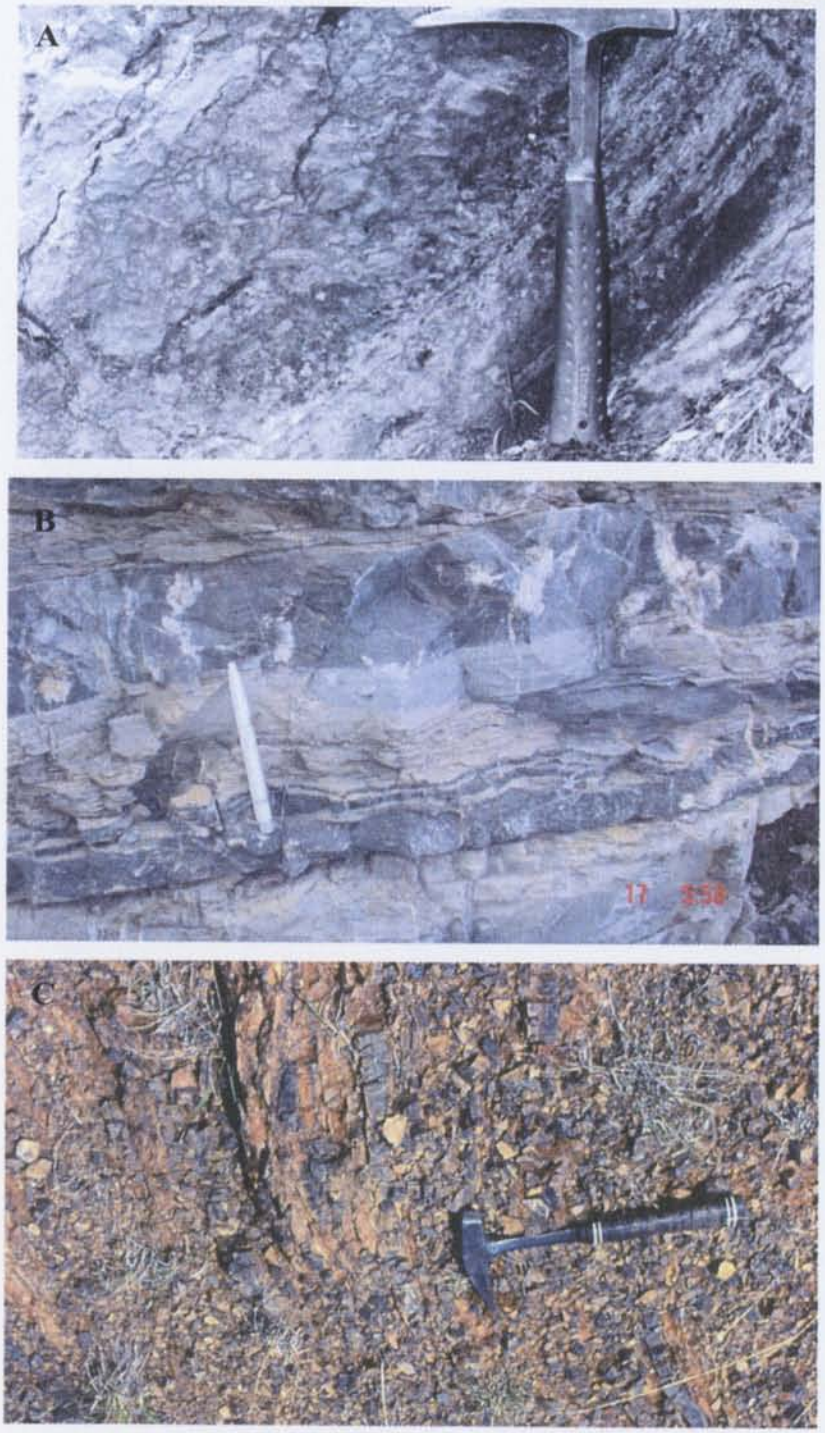

Figure 31. Representative Mezcala Formation lithofacies: (A) Limestone breccia (MF1); (B) Thin–bedded limestone (MF2); (C) Chert beds (MF3). All pictures from El Calvario area. Pen and hammer are 14 cm and 25 cm long, respectively.

Some thick and medium beds are lenticular at outcrop scale. Although clast-supported deposits are present, the facies is mainly matrix-supported. Most beds are disorganized, but some beds show normal or inverse grading. Lower and upper bed boundaries are usually sharp and wavy (columns E and G in Figure 30). Intense dolomitization and recrystalization are observed in this facies.

Limestone breccia is present at the contact with the Morelos and Teloloapan formations, as well as interbedded with sandstone and shale facies in the El Calvario, Romita, and Pachivia localities, (columns E and G in Figure 30 and column G in Figure 32).

Textural features of the limestone breccia beds suggest that they are debris-flow deposit. They are assigned to facies A.1.1 (disorganized gravel) of Pickering et al. (1998). Debris-flow deposits are typically matrix-supported and disorganized. Most of the lithoclasts and bioclasts are believed to have been derived from the Morelos and Teloloapan formations, which are in contact with the Mezcala Formation in the area.

3.3.1.1.2: Facies MF2: Thin-bedded limestone

Facies MF2 forms ~10% of the Mezcala Formation. Thin-bedded limestone is black in color, contains bioclasts, and has a mudstone to packstone texture (Dunham, 1962). Beds are 1–10 cm thick, forming units up to 90 m thick in some areas (column F in Figure 30, column D in Figure 32, and Figure 31b). Thin-bedded limestone is host to abundant nodular and lenticular black chert. It also exhibits normally graded laminae, which are composed by abundant planktonic fauna (radiolaria, foraminifera, and

calcispherulids). Where in contact with shale and thin-bedded and very fine-grained sandstone, this facies becomes interbedded with these other rocks and is locally mixed with siliciclastic mud to become marl. The thin-bedded limestone crops out in the central Pachivia Valley (Figures 3, 30, and 32), where it forms a mapable north–south-trending belt from El Calvario town to the Pipincatla locality.

Facies MF2 is interpreted to represent pelagic and hemipelagic deposition. The presence of calcispherulids has been associated with high nutrient levels in the water column (Hernández, 1999; Aguilera, 2000). Nodular and lenticular black chert present in facies MF2 is interpreted as a product of diagenesis.

3.3.1.1.3: Facies MF3: Chert beds

Facies MF3 represents <5% of the Mezcala Formation. Chert beds are very thin to thin, and form units 10–70 m thick. These crop out exclusively in the southern part of the Pachivia valley (between El Calvario and La Concordia, column D in Figure 30). The facies consists of monotonous black and white chert in beds 1–5 cm thick. In thin section, scattered and recrystallized radiolaria, and microcrystaline quartz are observed.

Chert beds are interpreted to have been deposited in a basinal pelagic setting. Predominance of chert and the radiolarian fauna suggests deposition below the carbonate compensation depth (CCD). The black color of some beds might record temporary anoxia (cf. Pickering et al., 1989). This facies is assigned to facies G1.1. of Pickering et al. (1989).

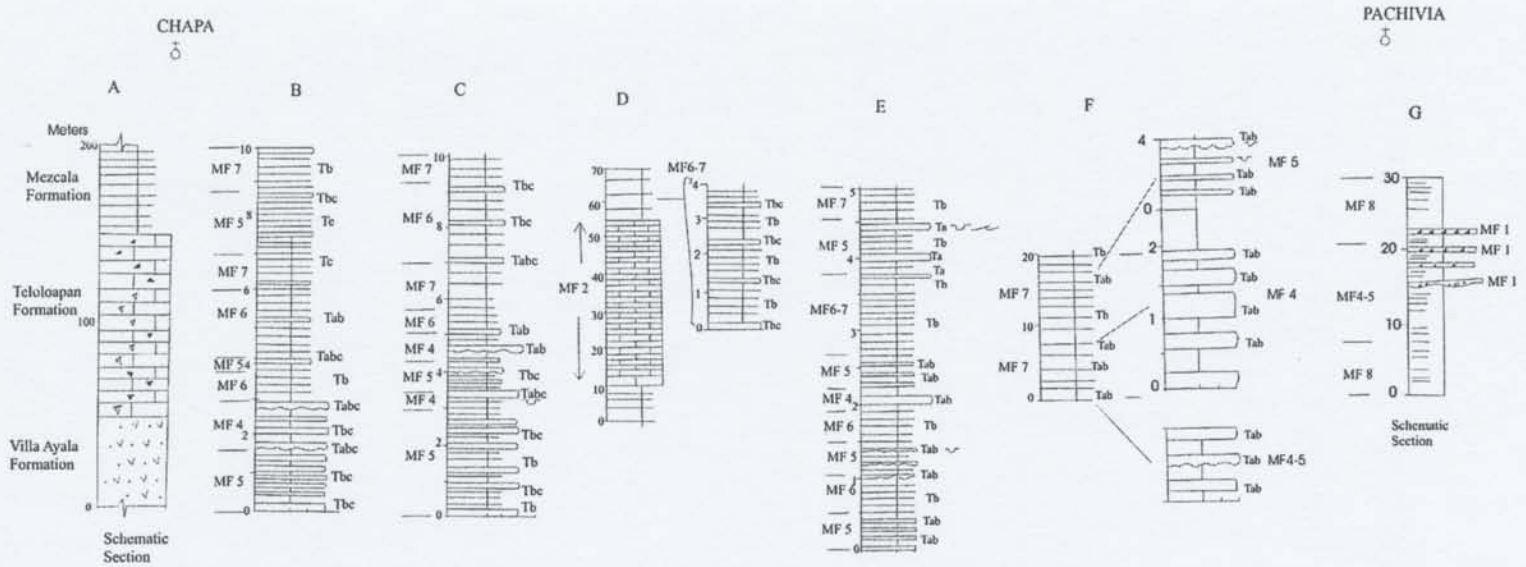

Figure 32. Sedimentary logs measured in the Mezcala Formation between Chapa and Pachivia towns. Each log is located in Figure 40B. Scales vary from one to the next but all are in meters. Column A is a schematic section showing the stratigraphic relationship among the formations. Column G is a schematic section from the strong deformed shale (MF8) and calcareous facies (MF2). There is not time or lithologic correlation among each log.

3.3.1.2. Sandstone Facies

3.3.1.2.1: Facies MF4: Thick- to medium-bedded sandstone

This facies forms ~15% of the Mezcala Formation. Facies MF4 is a medium-grained sandstone, and dominantly medium-bedded (10–30 cm) with scattered thick beds (30–40 cm) and minor pelitic intervals (5–10 cm thick; Figure 33A). The sandstones contain Tbc Bouma sequences (column F in Figure 32). No amalgamated beds are present in this facies. Sandstone beds exhibit sharp and erosional lower boundaries; upper boundaries are usually sharp also. Facies MF4 is associated with thin sandstone beds and minor shale of facies MF5 and MF6. The sandstone to mudstone ratio is approximately 10:1. This facies is mainly found in the El Calvario and Pachivia areas (columns C and F in Figure 30; column F in Figure 32).

Sedimentary structures are normal grading, parallel lamination, asymmetrical ripple marks and load casts. Rare grooves, prod marks, and scours marks were found in the Pachivia locality, usually associated with abundant carbonaceous material.

Based on locally preserved partial Bouma sequences and sole markings the sandstone beds are interpreted as turbidites. This facies corresponds with facies C2.1 and C2.2 of Pickering et al. (1989). The high sandstone to shale ratio and presence of Bouma Ta divisions suggests a proximal depositional site.

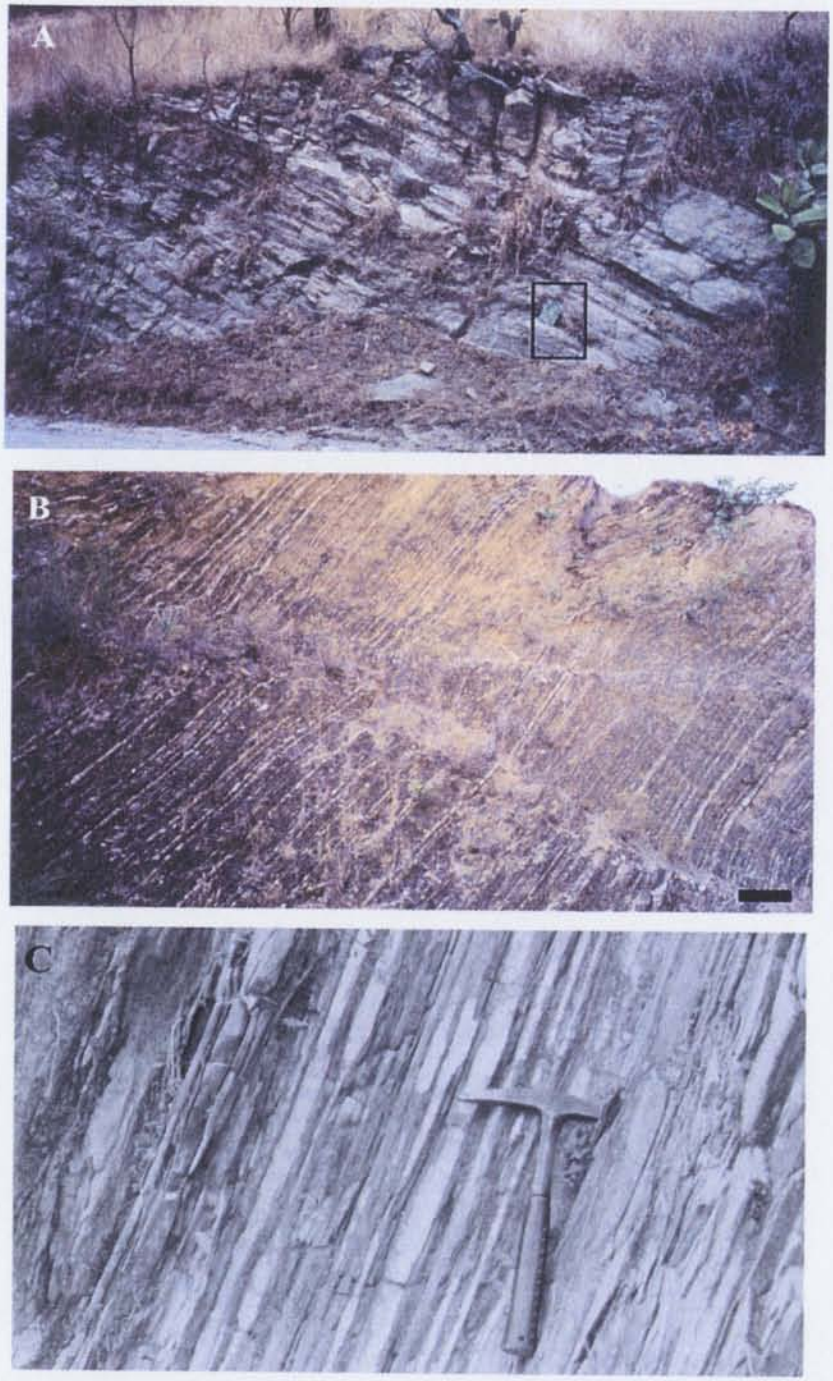

Figure 33. Representative lithofacies of the Mezcala Formation: (A) Thick- to medium-bedded sandstone (MF4), Pachivia locality; (B) Thin-bedded sandstone and shale (MF6), Pachivia locality; (C) Shale and thin-bedded sandstone (MF7), La Concordia locality. Hammer is 25 cm and notebook is 20 cm long. Bar scale in B = 1 m.

3.3.1.3. Sandstone-shale Facies

3.3.1.3.1: Facies MF5: Medium-bedded sandstone and shale

This facies represents ~15% of the Mezcala Formation. Facies MF5 is defined as interbedded sandstone and shale couplets, which contain Bouma sequences Tabc and Tab. This facies consists of brown and green, graded, planar and cross-lamination, medium- to fine-grained sandstone interbedded with shale. The sandstone-shale ratio is approximately 1:1 (see column C in Figure 30 and columns B, C, and E in Figure 32). Sandstone beds are 10–15 cm thick. This facies is found in sequences up to 10 m thick, but the deformation in the area prevents detailed sections thicker than 8 m from being measured. In general, deformation obscures sedimentary structures in the sandstones. Only less deformed sections exhibit more clearly the sedimentary structures that were measured for paleoenvironmental analysis. This facies is commonly in contact with facies MF6 (see columns B, C, and E in Figure 32).

Sole marks are rare, consisting of flutes and other scour marks. Load structures (ball and pillow) are locally well developed. Lenticular and flaser beds are also observed closed to the Pachivia and La Concordia localities (Figures 30 and 32). No upward-thickening or upward-thinning sequences were observed, perhaps because of the deformation and lack of lateral and vertical continuity, or maybe because they are indeed not present (cf. Chen, 2000).

Facies MF5 is inferred to have been deposited by high and low concentration turbidity currents. Waning tractive flows produced the lamination and subsequent fallout

of suspended mud deposits the shales. This facies has the characteristics of C.2.2 of Pickering et al. (1989).

3.3.1.3.2: Facies MF6: Thin-bedded sandstone and shale

This facies forms monotonous intervals up to 50 m thick of thin-bedded and fine- to very fine-grained sandstone interbedded with shale (Figure 33B). The sandstone-shale ratio is ~1:3. Deformation obscures the sedimentary structures in these fine-grained deposits, and some beds show tectonic "boudinage". Only a few detailed sections were measured because of the deformation (see Figures 30 and 32). However, Tab and Tbc Bouma sequences are locally present. Grading is not common. Lower and upper bed boundaries are usually sharp.

Facies MF6 is the most common facies in the Mezcala Formation at more than 25% of the sequence (columns B–C in Figures 30 and 32.) It is associated with almost all other facies, and forms thick intervals.

This facies is interpreted to have been deposited by low concentration turbidity currents, where fallout of suspended fine grains was dominant. Facies MF6 is correlated with facies C2.3 of Pickering et al. (1989).

3.3.1.3.3: Facies MF7: Shale and thin-bedded sandstone

Facies MF7 forms ~15% of the Mezcala Formation. This facies consists of very fine- to fine-grained, thin-bedded, graded and parallel laminated sandstone interbedded with thick intervals of shale. The shale to sandstone ratio is generally about 5:1, but in

some places it is higher. The facies occurs as units more than 40 m thick, although rarely can a complete section be measured because of stratigraphic repetition by folding. The deformation in this shaly facies is ductile. The deformation obscures sedimentary structures. It is locally difficult to differentiate very fine-grained sandstone from shale (Figure 33C). However, small detailed sections were successfully measured to show the internal facies characteristics (see Figures 30 and 32).

Sandstone occurs as tabular beds 0.5–5 cm thick interbedded with shales up to 20 cm thick. The graded Ta division is missing and the facies displays mostly incomplete Bouma sequences (Tb-e, Tc–e, and Td–e). Sharp upper and lower bed boundaries are characteristic.

Facies MF7 is interpreted to have been deposited by low-concentration turbidity currents, where fallout and limited traction prevailed. The dominance of shale might represent rapid settling of flocs formed in highly concentrated mud clouds (Pickering et al., 1989). This facies corresponds with C2.3 and C2.4 of Pickering et al. (1989).

3.3.1.3.4: Facies MF8: laminated shale

Facies MF8 forms <10% of the Mezcala Formation (columns H and G in Figures 30 and 32, respectively). It consists of highly deformed shale with sporadic very fine-grained and very thin-bedded sandstones. Like facies MF6 and MF7, this facies passes imperceptibly into associated facies. Laminated shales occur in packets up to 5 m thick. The thicker of the isolated sandstone beds are normally graded. Some sandstone beds show parallel lamination, but deformation generally obscures the sedimentary structures.

Despite the deformation in this facies, it seems to resemble facies D2.1 and D2.2 of Pickering et al. (1989). They interpreted the transport process of these facies as low concentration turbidity currents, with the deposits produced by grain-by-grain deposition from suspension, followed by traction transport of the silt load.

3.3.2. The Miahuatepec Formation

Seven facies constitute the Miahuatepec Formation. There are two sandstone facies, two sandstone and shale facies, two shales, and one calcareous facies. Appendix 11 contains a summary of the facies.

3.3.2.1. Sandstone Facies.

3.3.2.1.1. Facies MiF1: Pebbly and coarse sandstone

Facies MiF1 consists of light brown, predominantly very coarse- to medium-grained, and thick- to very thick-bedded sandstone (columns C and G in Figure 34 and column B and F in Figure 35). Bed thickness varies from 0.6–2 m, with sharp upper and lower boundaries. Erosional contacts are observed at the base of the formation. The facies forms less than 10% of the total exposures.

Sandstones of this facies occur as abruptly graded beds, with Ta, Tab, and scattered Tabc Bouma sequence. Some sandstone beds contain rip-up clasts of sandstone and shale concentrated toward the base of the beds. Sometimes, rip-up clasts are also distributed throughout the bed (column C in Figure 34 and column C in Figure 35). Deep scours are locally present, as are amalgamated beds (column C in Figures 34 and 36A)

forming stacked sequences from 3–5 m thick. Rare flutes were found at two localities. This facies usually passes upward into facies MiF2 and MiF3.

High concentration turbidity currents likely deposited this facies. Rapid deposition accounts for the thick- to very thick sandstones with their scattered rip-up clasts. Facies MiF1 is analogous to facies B1.1 and B2.1 of Pickering et al. (1989).

3.3.2.1.2. Facies MiF2: Thick-bedded sandstone

This facies is similar to facies MiF1 in color, but it is medium-grained and rarely coarse-grained. The thick-bedded (30–50 cm) sandstones exhibiting sharp lower and upper boundaries, and less common wavy and/or erosional lower contacts. The sandstones are interbedded with thin shales (1–5 cm). The sandstone to shale ratio is higher than 5:1. This facies forms ~20% of the formation (see Figures 34 and 35).

Despite the deformation, graded bedding and Bouma sequences (Tab and rare Tabc) are evident. Questionable sole marking might be tectonic striations. Rarely, rip-up clasts are present in this facies. Amalgamated beds are more common in this facies than in facies MiF1. Intervals up to 5 m thick occur (column D in Figure 34 and column B in Figure 35). This facies alternates with facies MiF3 (column F in Figure 34).

High concentration turbidity currents might have deposited facies MiF2. Rapid deposition of sediments was followed by tractional transport. The minor shale intervals (argillaceous levels) could represent fallout of silt and clay from the suspension cloud that remained after passage of the main flow. Facies MiF2 is analogous to facies B1.1 and B2.1 of Pickering et al. (1989).

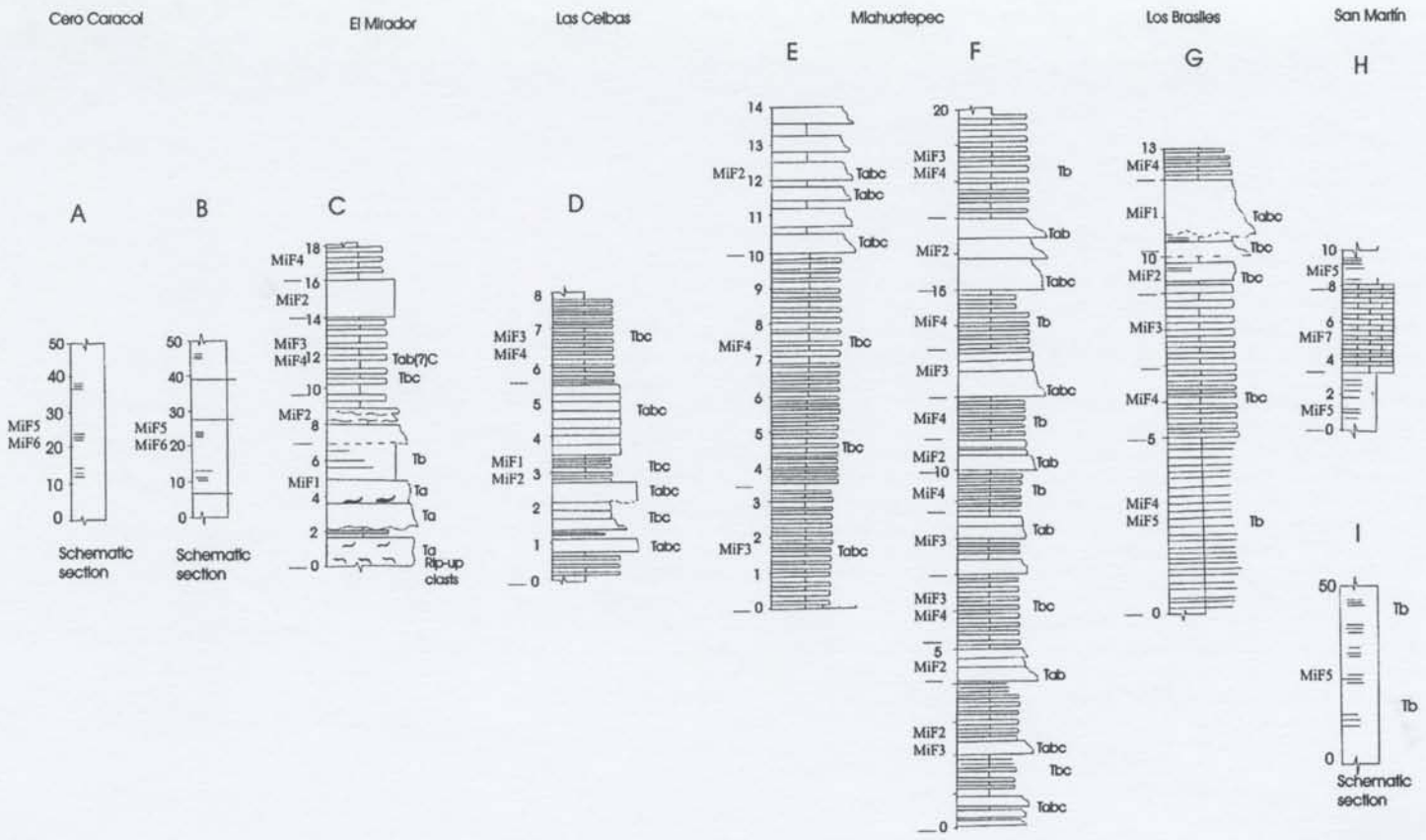

Figure 34. Miahuatepec Formation logs. Sedimentary logs measures between Cerro Caracol and San Martin localities. Scales vary, but are all in meters. Location of each log is shown in Figure 41B. There is no time or lithologic correlation suggested between each log.

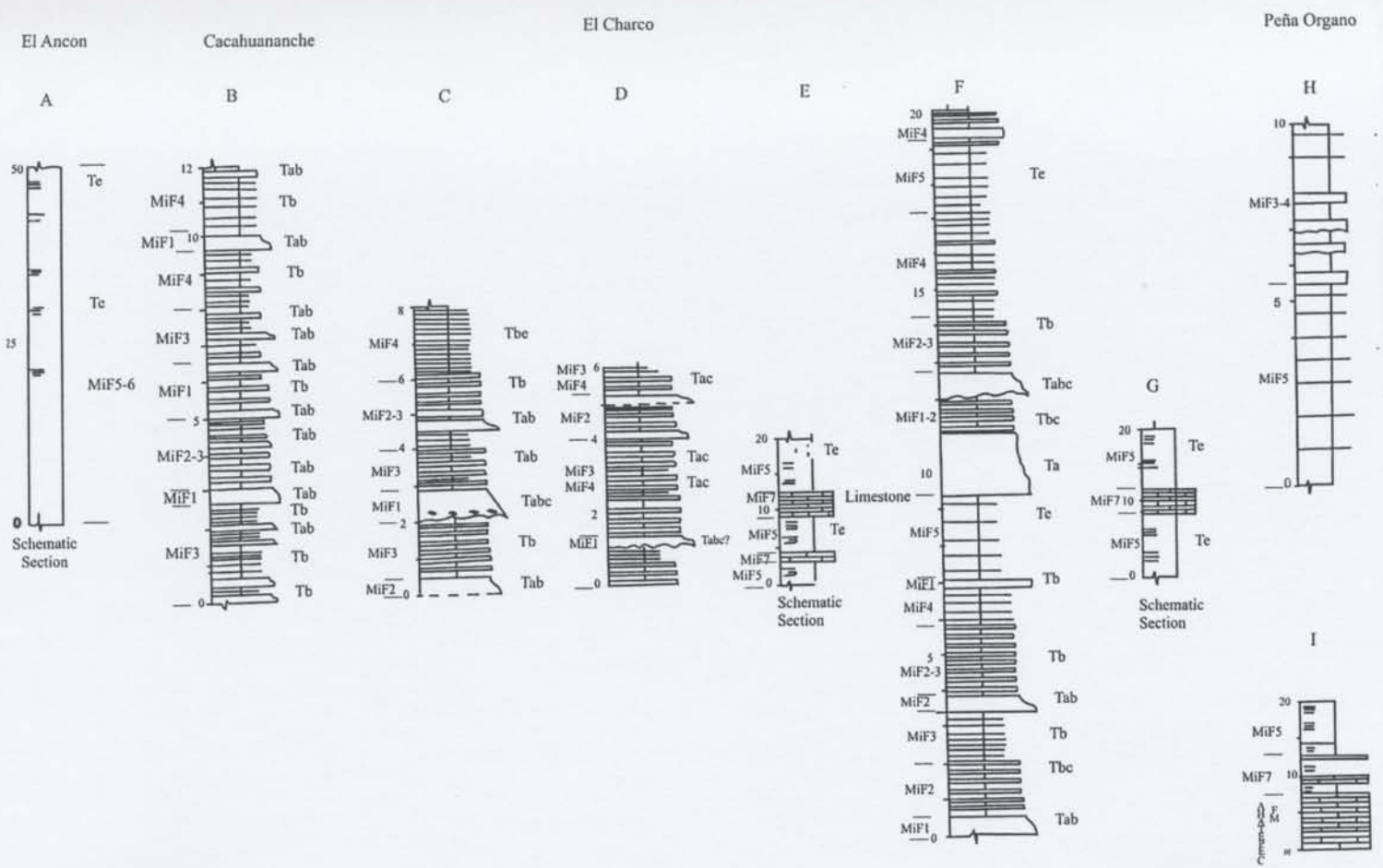

Figure 35. Miahuatepec Formation logs. Sedimentary logs measured between El Ancon and Peña Organo. Scales vary, but are all in meters. Location of each log is shown in Figure 41B. There is no time or lithologic correlation suggested between each log.

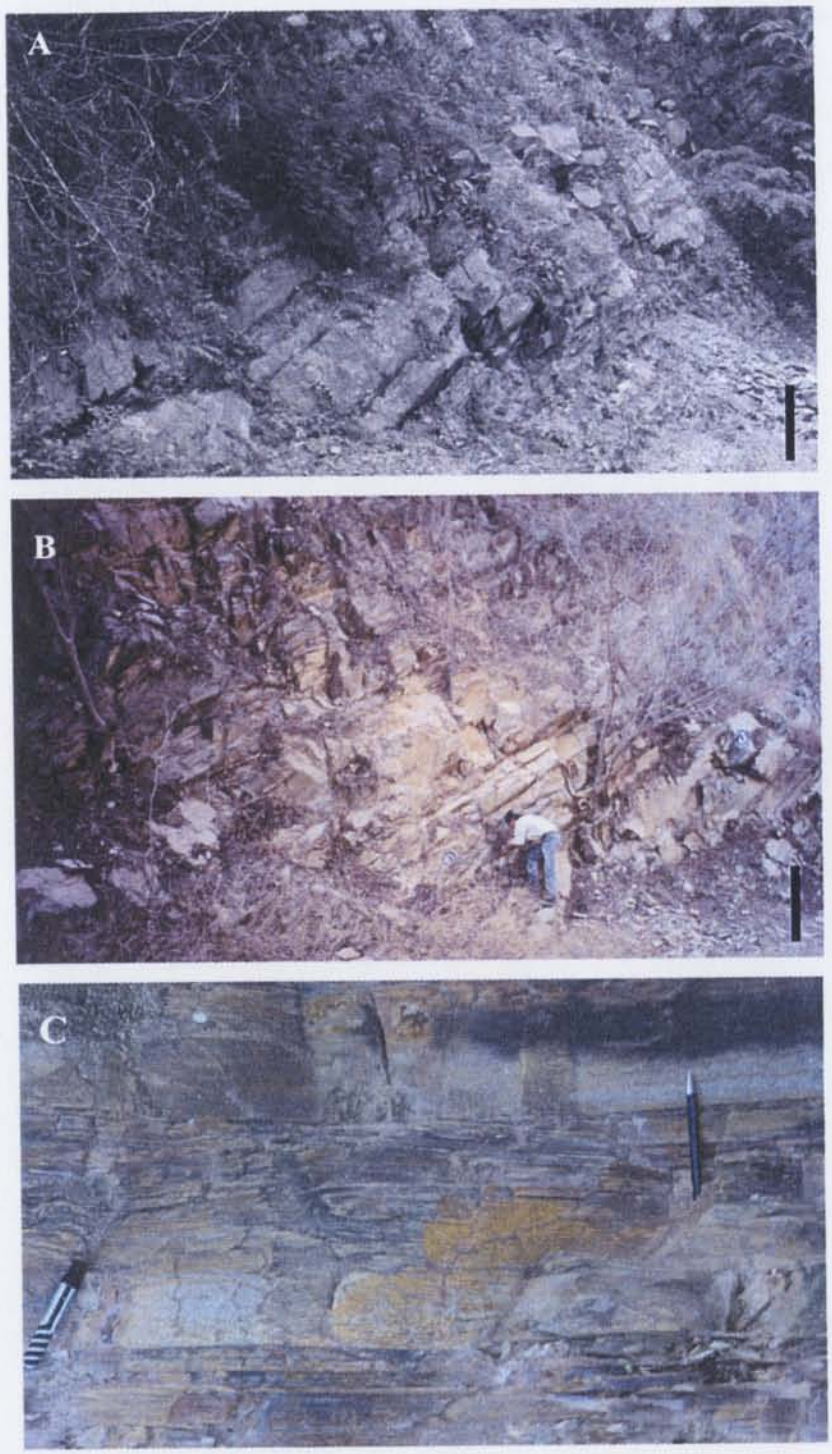

Figure 36. Representative lithofacies of the Miahuatepec Formation: (A) Pebbly and coarse sandstone, Peña Organo locality; (B) Thick-bedded sandstone, Cacahuananche locality; (C) Medium-bedded sandstone and shale, Las Ceibas locality. Bar scale = 1 m. Pencil is 14 cm long.

3.3.2.2. Sandstone-Shale Facies

3.3.2.2.1. Facies MiF3: Medium-bedded sandstone and shale

Bedding in this facies is more strongly affected by deformation than the other facies. However, sedimentary structures are not completely obscured. Facies MiF3 includes sandstone beds, 10–25 cm thick. These medium- to fine-grained sandstones exhibit normal grading associated with parallel and wavy lamination, and rarely cross-lamination (Tab and Tabc Bouma sequences; see columns, F–G in Figure 34 and column B in Figure 35). Facies MiF3, together with facies MiF4, is the most common lithofacies present in the Miahuatepec Formation. Facies MiF3 forms ~30% of the exposures in the study area (see Figures 34 and 35).

Upper and lower bed boundaries are sharp and locally loaded. Two or three graded beds can be stacked forming a sandstone package separated by 10–20 cm of shale (Figure 36C). The majority of the fine-grained sandstone beds intervals display planar lamination.

The presence of Bouma sequences indicates that the beds were deposited from turbidity currents. Beds showing Tab Bouma sequences are ascribed to high concentration flows with subsequent traction transport (Tb and Tc divisions). Facies MiF3 corresponds to facies C2.2 of Pickering et al. (1989).

3.3.2.2.2. Facies MiF4: Very thin- to thin-bedded sandstone and shale

This facies consists of medium- to fine-grained and very thin- to thin-bedded sandstone associated with thick interbeds of shale. Bedding geometry and contacts are partially modified by tectonic deformation. However, bed thickness is 3–10 cm, with sharp upper and lower boundaries and tabular bed geometry. Facies MiF4 comprises ~20% of the Miahuatepec Formation (columns E and G in Figure 34 and columns C and F in Figure 35). Sandstone to shale ratio is 1:3 or higher. This facies resembles MiF3 facies but is distinguished by its smaller bed thickness.

Sedimentary structures are not completely obscured by deformation, but they are rare. The sandstone beds are rarely graded. Tbc and Tbe Bouma sequences are present associated with load structures (Figure 37A).

Based on the presence of partial Bouma sequences, this facies is interpreted to have been deposited by turbidity currents. Facies MiF4 corresponds to facies C2.4 of Pickering et al. (1989).

3.3.2.3. Shale Facies

3.3.2.3.1. Facies MiF5: Laminated shale

Facies MiF5 constitutes ~10% of the Miahuatepec Formation. It consists of yellow and brown, parallel laminated shale (Figure 37B) and minor very thin beds (1–3 cm) of very fine-grained sandstone. Deformation is strong and parallel lamination is only locally observed. Some occurrences of this facies are up to 40 m thick (columns B and

G–I in Figure 34 and column F–I in Figure 35). This facies is mainly found along the west and east contacts of the Miahuatepec Formation.

Facies MiF5 is interpreted to have been deposited by turbidity currents as fallout of fine sediments from suspension. This interpretation is based on association with facies MiF3 and MF4, also interpreted as turbidites. Facies MiF5 resembles facies D2.2 of Pickering et al. (1989).

3.3.2.3.2. Facies MiF6: Black shale

This facies is highly deformed and the sedimentary structures, except parallel laminations, are obscure. Facies MiF6 is a black laminated shale. Some internal color variation parallels the lamination. Parallel and wavy laminations, as well as poor graded bedding, are locally discernable. However, the apparent graded bedding might be an artifact of the deformation. This facies sporadically contains radiolarian fauna. These microfossils are highly deformed in thin section. Facies MiF6 is observed exclusively along the western boundary of the formation. This facies forms less than 5% of the Miahuatepec Formation.

The presence of radiolaria and the muddy original composition suggest that these are pelagic and hemipelagic sediments deposited during a period of clastic sediment starvation. This facies resembles facies E1 and E2 of Pickering et al. (1989).

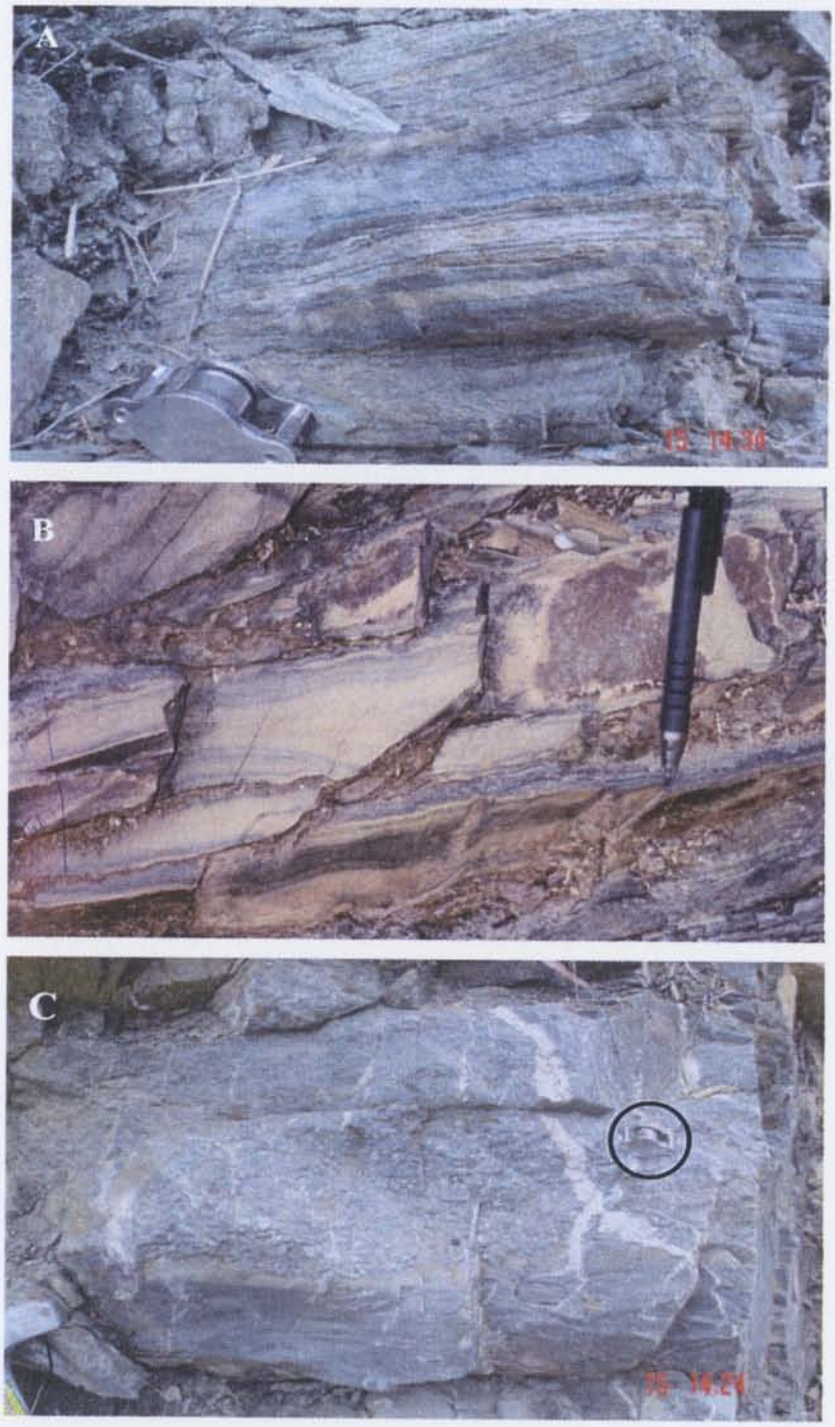

Figure 37. Representative lithofacies of the Miahuatepec Formation: (A) very thin- to thin-bedded sandstone and shale (MiF4), Miahuatepec locality; (B) laminated shale (MiF5), Los Brasiles locality; (C) calcareous beds (MiF7), Peña Organo locality. Handlens and pen are 2.5 cm and 14 cm long, respectively.

3.3.2.4. Calcareous facies

3.3.2.4.1. Facies MiF7: Calcareous beds

Calcareous beds consist of black, very thin- to thin-bedded mudstone–packstone (Figure 37C). These limestone beds range from 1–10 cm thick forming stacked levels 2–8 m thick in some areas (column H in Figure 34 and columns G and I in Figure 35) that are interbedded with laminated shale. These limestones are completely recrystallized and deformed. However, some bioclasts observed in thin section are interpreted as radiolarian and planktonic foraminifera. Thin-bedded black limestone crops out in the eastern part of the study area (Figures 34 and 35), where this facies is associated with the laminated shale (facies MiF5). This facies constitutes less than 5% of the Miahuatepec Formation.

Based on texture and fauna, this facies is interpreted to represent pelagic deposition during times of dramatically reduced clastic input.

3.4. REGIONAL CORRELATION AND DISCUSSION

Figure 11 (p. 53) shows a regional correlation of the sedimentary cover sucessions. A specific correlation between the carbonate-platform formations and the Upper Cretaceous siliciclastic sequences is illustrated in Figure 38. A Cenomanian–Turonian tie-line is plotted because it represents the most common boundary between these sequences. This correlation incorporates data collected during this thesis research and published stratigraphic data from other authors.

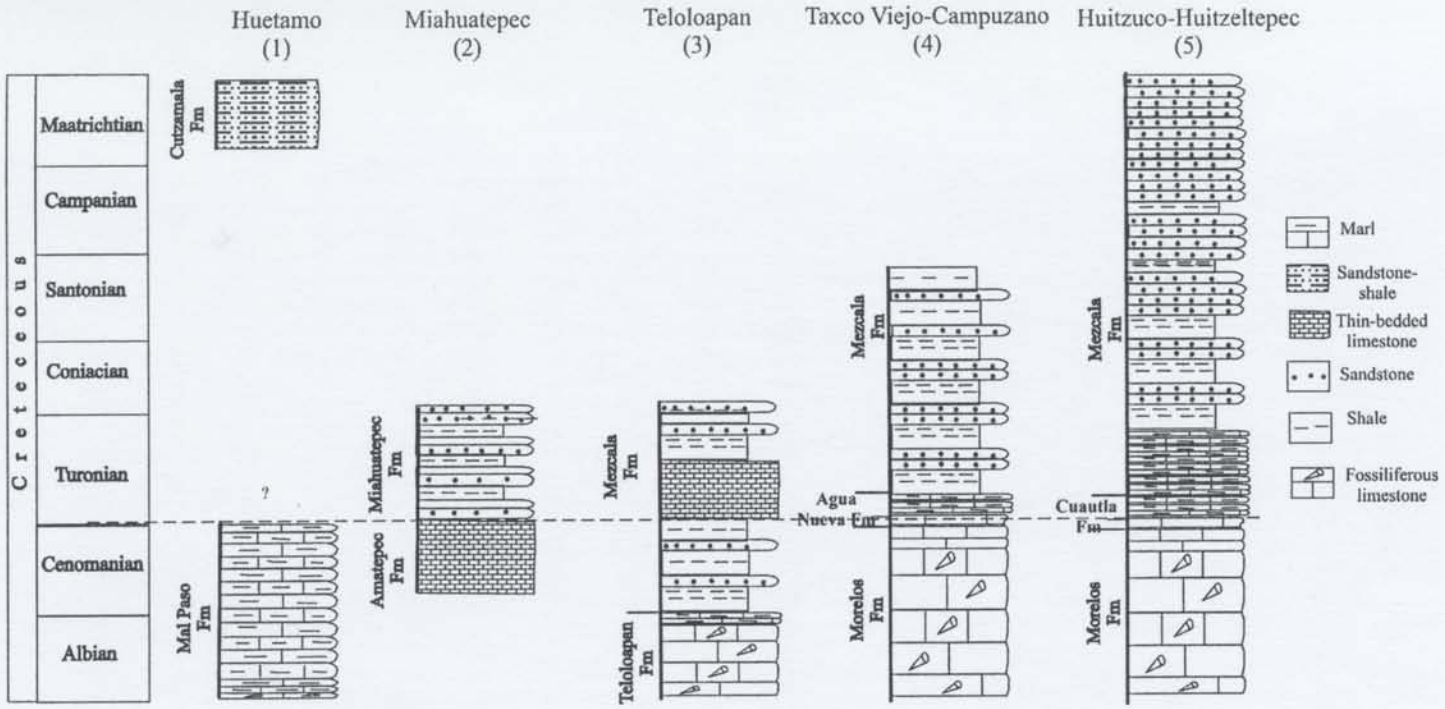

Figure 38. Generalized regional correlation of Upper Cretaceous sedimentary cover successions between the thesis area and neighboring areas. Data from each area: (1) Pantoja (1959), Campa (1977); (2) and (3) this work; (4) Estrada (1995), Ocampo (2004), Guerrero (unpublished), Garibay et al. (1999), Ocampo et al. (2002), Rosendo et al. (2002); (5) Gonzalez (1991), Aguilera et al. (1998), Hernandez et al. (1997).

As in chapter 2, a brief stratigraphic overview is provided for the sedimentary cover successions, which crop out in the thesis area, to the west (Huetamo area), and to the east (the Morelos-Guerrero Platform). Facies correlation is also presented, but a detailed interpretation of the sedimentary environment is deferred to chapter 4. Sedimentologic studies of other authors contribute to the correlation for the Cutzamala Formation to the west, and different authors in the Guerrero-Morelos Platform (González, 1991; Hernández, 1999; Aguilera 1995; 2000, for the boundary between the Morelos and Mezcala formations; Estrada, 1995; and Ocampo, 2004, for the Mezcala Formation).

3.4.1. Sedimentary Cover Successions in the Teloloapan area

Two highly deformed Upper Cretaceous siliciclastic sequences crop out in and adjacent to the study area: The Miahuatepec Formation (west, column 2 in Figure 38) and the Mezcala Formation (east, column 3 in Figure 38).

The Miahuatepec Formation is predominant very thick- to medium-bedded, coarse- to medium-grained sandstone, interbedded with shale in different proportions throughout the formation, as well as scattered limestone beds. The lower contact with Albian thin-bedded limestone of the Amatepec Formation (Ramírez et al., 1990), although highly deformed, is concordant. Facies analysis shows that the Miahuatepec Formation was deposited by high to low concentration turbidity currents with minor pelagic and hemipelagic deposits.

The Mezcala Formation is mainly thin- to medium-bedded, medium to fine-grained sandstone interstratified with shale, thin-bedded limestone, calcareous breccia

and chert. Based on planktonic fauna (calcispherulids and foraminifera), an Early Cenomanian–post-Turonian age is confidently established for this formation. The lower contact with the Teloloapan Formation is transitional and concordant (column 3). The lower contact with the Morelos Formation (columns 4 and 5) is always concordant with The Agua Nueva Formation. Facies analysis indicate that the Mezcala Formation was mainly formed by low concentration and relatively dilute turbidity currents, or is pelagic-hemipelagic deposits.

3.4.2. Western area (Huetamo area)

The Cutzamala Formation (Campa, 1977) forms the Upper Cretaceous sequence in the Huetamo area. The Cutzmala Formation is composed of almost 1500 m of thick- to very thick-bedded continental red sandstone and conglomerate with shale intervals (column 1 in Figure 38). This thick sequence covers the monotonous Albian–Cenomanian thin-bedded argillaceous limestone of the Mal Paso Formation. The age of the Cutzamala Formation was originally considered Late Cretaceous (Campa, 1977), but recent stratigraphic studies conclude a latest Cretaceous (Campanian–Maastrichtian) age for the unit, based on pollen and dinosaur tracks (Centeno, 2004 personal communication).

Lithology, age, facies and deformation are different between the Huetamo area and the Miahuatepec and Mezcala formations in the Teloloapan area. Hence, no correlation is proposed among the Cutzamala Formation and the Miahuatepec and Mezcala formations in the study area.

3.4.3. Eastern area (the Morelos-Guerrero Platform)

In the eastern area (the Morelos-Guerrero Platform), The Mezcala Formation occurs in two area: the Taxco el Viejo-Campuzano and the Huitzuco-Huitziltepec areas, in the north and north-central part of Guerrero State, respectively (see Figure 38). These are described separately because different lithostratigraphic and facies characteristics have been reported in these areas.

3.4.3.1. Taxco el Viejo-Campuzano area. In the Taxco el Viejo-Campuzano area (column 4 in Figure 38), the Mezcala Formation is thick- to medium-bedded, coarse- to medium-grained sandstone and shale, associated with scattered conglomerate strata. There are also thin-bedded limestones in the lower part of the Agua Nueva Formation (Estrada, 1995; Ocampo, 2004). Based on macrofossils, a Late Cretaceous (Turonian) age has been postulated for the Mezcala Formation in this region (Garibay et al., 1999; Ocampo et al, 2002; Rosendo et al., 2002), although upper Cenomanian planktonic microfossils have been reported near the contact with the Morelos Formation (Estrada, 1995). The lower contact with the Morelos and Agua Nueva formations is transitional and concordant throughout the area, although tectonic contacts also occur. Ocampo (2004) reported high to low concentration turbidity current deposits associated with debris flows, pelagic-hemipelagic, and tempestite deposits in the Mezcala Formation in this area.

The base of the Mezcala Formation in the thesis area is older (early Cenomanian) than in the Taxco el Viejo-Campuzano area (see Figure 38). Thin-bedded and laminated

mudstone-packstone, assigned in the thesis area to the Mezcala Formation and to the Agua Nueva Formation in the Taxco el Viejo-Campuzano area, show similar textures in both areas. More chert is present in the latter area. The Mezcala Formation is predominatly pelagic and hemipelagic deposits in both the Teloloapan and Taxco el Viejo- Campuzano areas. However, Guerrero and Ramírez (1992) and Ocampo (2004) also interpreted tempestite deposits in the Taxco el Viejo-Campuzano area. Ocampo et al. (in prep.) have found the same equinoid-crinoid fauna in these strata from Teloloapan to Taxco el Viejo.

The Mezcala Formation in the Teloloapan area consists of medium- to fine-grained sandstone and ~40% shale, suggesting a distal setting. In the Taxco el Viejo-Campuzano area, in contrast, thick- to medium-grained sandstones are associated with minor shale (~30%). Tempestites are also common throughout the Mezcala Formation in the Taxco el Viejo-Campuzano area (Ocampo, 2004), while they are absent in the Teloloapan area. Paleocurrent data in the Taxco el Viejo-Campuzano area show a NE→SW and W→E trend for the Mezcala Formation (Ocampo, 2004).

The Upper Cretaceous formations of the Teloloapan area (especially the Mezcala Formation) and Taxco el Viejo area can be correlated with a certain level of confidence. Some stratigrapic and paleontologic data for the Turonian support this correlation. On the other hand, the Miahuatepec Formation (column 2 in Figure 38) does not show any lithogical and facies similarities with the contemporary Mezcala Formation as recognized in the Taxco el Viejo-Campuzano area.

3.4.3.2.Huitzuco-Huitziltepec area. In the Huitzuco-Huitziltepec area (column 5 in Figure 38), the "shallow member" of the Mezcala Formation is exposed (cf. González, 1991). In this area, the base of the Mezcala Formation consists of intercalations of thin-bedded bioclastic mudstone–wackestone and marls. The middle portion consists of intercalations of red siltstone, shale and sandstone displaying cross-stratification. The upper part of the formation is characterized by an intercalation of thick-bedded sandstone and conglomerate (González, 1991; Hernández, 1999). The age of the formation is late Cenonamian–Maastrichtian (Hernández, 1999; Aguilera et al., 1998; Aguilera, 2000). The lower contact with the limestone formations (the Cuautla and the Morelos formations) is concordant (González, 1991; Hernández, 1999). In this area, facies are interpreted as offshore to deltaic deposits.

No lithostratigraphic correlation is apparent between the Mezcala Formation in the Teloloapan area and rocks assigned to this formation in Huitzuco-Huitziltepec area. Lithology, age and facies are different in both areas. One exception is the Turonian thin-bedded limestone (named the Cuautla Formation in the Huitzuco-Huitziltepec area), which can be correlated with a certain degree of confidence.

The presence of similar sequences overlying the Mixteca and Guerrero terranes (and the Arcelia – Palmar Chico and Teloloapan subterranes) raises important questions about the timing of amalgamation and accretion of these terranes. This amalgamation is throught to have taken place in early Aptian time (Campa and Coney, 1983; Ramirez et al., 1991; Tardy et al., 1994). The stratigraphic and facies correlation among the three areas (Huetamo area, Teloloapan area and Guerrero-Morelos Platform) have fundamental

implications for the sedimentary and tectonic evolution of the area. These implications will be considered more fully in chapters 4 and 6.

3.5. SUMMARY

Two Upper Cretaceous siliciclastic sequences are recognized in the sedimentary cover successions: the Mezcala and Miahuatepec formations. The Mezcala Formation is characterized by interstratified shale and sandstone with minor thin-bedded limestone, chert and debris-flow deposits. The Miahuatepec Formation is formed by a thick interval of sandstone and shale with scattered thin-bedded limestone. The Cenomanian–post-Turonian age of the Mezcala Formation is documented using microfossils. This is the oldest age yet reported for comparable siliciclastic units in southwestern Mexico. In contrast, the age of the Miahuatepec Formation is poorly documented because of the lack of fossils.

Despite the strong deformation, eight lithofacies can be distinguished in the Mezcala Formation, grouped as heterolithic facies, sandstone facies, and sandstone-shale facies. Seven facies are recorded for the sandstones, shales and calcareous rocks in the Miahuatepec Formation. The facies in both formations suggest that the process of sediment delivering was mainly high- to low-concentration turbidity currents, punctuated by minor pelagic sedimentation.

Regional lithostratigraphic correlation with neighboring Upper Cretaceous deep-water sediments suggest that the Mezcala Formation in the study area is similar to the deep water-member of the Mezcala Formation in the Mixteca Terrane.

CHAPTER 4. ENVIRONMENTAL INTERPRETATION AND BASIN DEVELOPMENT

4.1. INTRODUCTION AND METHODOLOGY

Accretion and configuration of terranes in southern Mexico has been broadly documented and accepted (Campa and Coney, 1983; Ramírez et al., 1991; Talavera, 1993; Tardy et al., 1994; Dickinson and Lawton, 2001, and references therein). However, little is known about the sedimentary evolution and the basins developed in the Guerrero Terrane. This chapter describes the environmental and basin evolution of the arc-related and the sedimentary cover successions in the thesis area. The stratigraphy and facies described in chapters 2 and 3 are used to document this sedimentary evolution throughout the Cretaceous.

The interpretation of depositional environments for ancient volcanic arc sequences is difficult because of the lack of complete sections due to strong deformation and metamorphism, which develop during plate convergence and collision. Destructive processes in the arc itself (e.g., magmatism, explosive events, and erosion) further obscure early history. The pyroclastic and epiclastic deposits in arcs are commonly studied using concepts and methods of clastic sedimentology to interpret the diverse deposits of the volcaniclastic apron (Fisher, 1984; Fisher and Schmincke, 1984; Cas and Wright, 1987, 1991; Busby-Spera, 1987, 1988). Recently, Wright (1996) and Wright et al. (2002) studied volcaniclastic processes in the Kemadec arc, SW Pacific, and confirmed the applicability of classical clastic sedimentary methodology to the study of

post-eruptive events. Sedimentation and deposition in arc-related settings are controlled by eruption style and later periods of erosion and reworking of the pyroclastic and epiclastic products (post-eruptive processes).

Facies analysis and interpretation of the arc-related succession of the Teloloapan area (Villa Ayala, Acapetlahuaya and Teloloapan formations) reveal a history that extends from the beginning of arc construction, to the cessation of arc volcanism, to the development of a carbonate platform atop the arc. A similar history has been documented in other intra-arc settings (Larue et al., 1991; Smith and Landis, 1995). The arc-related succession of the Teloloapan area provide one of the best documented, longest histories of sedimentation in any intra-arc setting in southwestern Mexico, extending over ~33.5 my.

In order to document the depositional history of the Teloloapan area, the facies are integrated into facies associations following the model of sedimentation proposed by Larue et al. (1991) for tropical areas of the Caribbean region, and Smith and Landis (1995) for sedimentation in intra-arc settings.

Seven facies associations (FA) are recognized in the arc-related succession (Appendix 12). The Villa Ayala Formation represents volcanic-arc construction (FA1-volcanic and pyroclastic activity) and destruction (FA2-erosion and formation of submarine fans) near or on the arc vent/buildup. The lower calcareous levels interbedded with epiclastic rocks of the Villa Ayala Formation were likely deposited on an island-arc carbonate platform developed on extinct arcs (FA3). The Acapetlahuaya Formation and uppermost levels of the Villa Ayala Formation (FA4) consist of fine-grained sediments

deposited by distal pyroclastic and epiclastic processes. Finally, the Teloloapan Formation is composed predominantly of calcareous rocks (FA5–FA7) forming restricted platform, reef, and tempestite deposits. The facies associations document five phases of syn-eruptive and post-eruptive sedimentation in the arc-related successions. Two broad settings are recognized in the arc-related sequences: deep-marine environments (Acapetlahuaya-Villa Ayala area) and shallow-marine settings (Teloloapan-Ahuacatitlan area), central and east portions of the thesis area, respectively.

Structural disruption also limits application of sedimentary depositional models to the sedimentary cover successions (the Mezcala and Miahuatepec formations). Field observations in these successions are limited by poor lateral and vertical continuity because of the deformation. Despite this fact, general depositional trends can be inferred, and those facies recognized in these formations are interpreted using regional cross section. Facies associations are recognized based on the map distribution of facies, following the Underwood (1984) and Leverenz (2000) methodology. Well-preserved fauna help to partially constrain the vertical succession for the Mezcala Formation, but are not available in the Miahuatepec Formation. Short detailed sections assist the environmental interpretation, although lack of stratigraphic markers prevents the measured sections from being correlated. No major faults are recognized and mapped in the Mezcala and Miahuatepec formations, but strong deformation likely is responsible for an unknown amount of stratigraphic repetition.

Three facies associations have been recognized in the Mezcala Formation in an effort to interpret the sedimentary environment (see Appendix 13). FA1 includes the

sandstone and sandstone-shale facies (MF4, MF5, MF6, MF7, and MF8). The heterolithic thin-bedded limestones and chert beds, as well as part of the laminated shale (facies MF8) interbedded with these facies, are included in FA2 (pelagic and hemipelagic sediments). Finally, FA3 consists exclusively of limestone breccias (MF1); interpreted as debris-flow deposits.

A number of sedimentological features characterize the Mezcala Formation: (1) Fine-grained deposits comprise >50% of the sedimentary rocks (shales associated with thin- to medium-bedded sandstone in different proportions); (2) pelagic facies comprises ~20% of the succession; and (3) conglomerates and coarse-grained sandstone are rare. These features are believed to indicate deposition of the Mezcala Formation as a mud/sand-rich submarine-fan system (cf. Reading and Richards, 1994). The apparent lack of channels suggests a middle and lower fan setting.

Three facies associations are recognized in the Miahuatepec Formation (Appendix 14). FA1 includes the sandstone facies (MiF1 and MiF2). FA2 consists of sandstone-shale facies (MiF3, MiF4, and MiF5) and part of the MiF2 sandstone facies. Finally, pelagic-hemipelagic facies MiF6 and MiF7 are included in FA3, as is a portion of the laminated shale facies (MiF5). Facies of the Miahuatepec Formation are predominantly thick- to medium-bedded, coarse to medium-grained sandstone (~70%), interbedded with shale intervals (~25%), and scattered calcareous beds (~5%). The three facies associations observed in the Miahuatepec Formation can be interpreted in terms of the middle to lower submarine-fan model. Based on the overall sandstone-shale ratio for the Miahuatepec Formation, a mud/sand-rich submarine-fan system is inferred (cf. Reading

and Richards, 1994). Because of structural dismemberment during accretion, only remnants of the middle to outer parts of the submarine-fan system are preserved.

4.2. DEPOSITIONAL HISTORY FROM FACIES AND COMPOSITIONAL DATABASE

4.2.1. The arc-related succession

4.2.1.1. Berriasian–Aptian (The Villa Ayala Formation)

Interpretation of FA1. This facies association represents the main syn-eruptive processes in the study area (Figure 39A). The primary volcanic rocks were only studied where they are associated with pyroclastic and epiclastic rocks, so only a brief interpretation is presented here.

Syn-eruptive processes characterize large volumes of primary volcanic rocks distributed mainly in six areas (Huayatengo, Villa Ayala, Zacatlancillo, Alpixafia, Acatempan, and Ahuacatitlan localities; see Figures 3, 12, and 15). Primary volcanic rocks described of facies VA1 form FA1. The rocks form a thick accumulation of pillow and masive lava sheet flows, as well as scattered associated hyaloclastites. They resulted from subaqueous volcanic eruptions at fissures and vents during the construction of the arc (Figure 39A). FA1 is similar to the *central facies* proposed by Smith and Landing (1995) for intra-arcs, and the early edifice of the Caribbean arcs proposed by Larue et al. (1991).

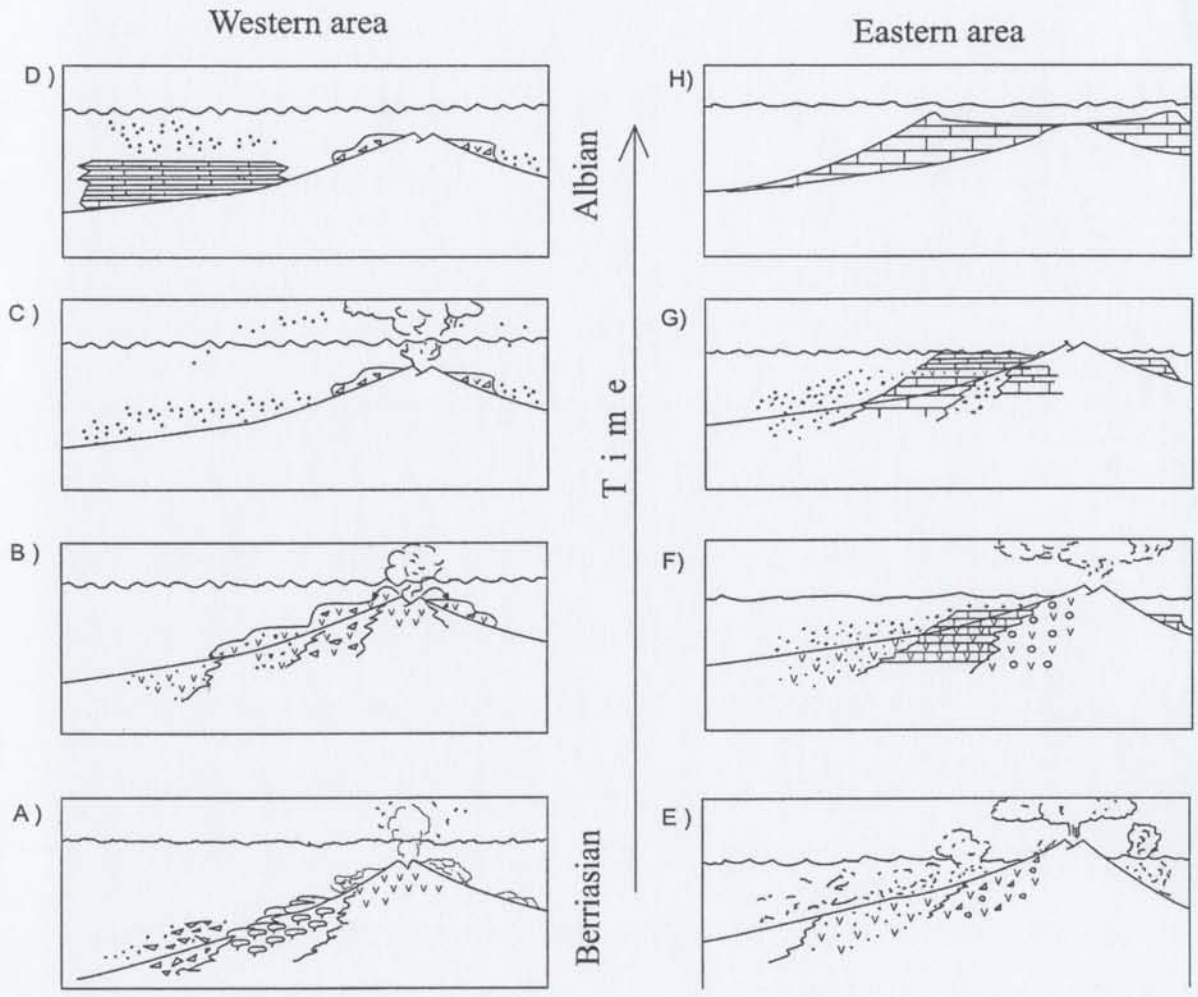

Figure 39. Schematic diagram illustrating the depositional histories of deep-water (A-D) and shallow-water volcanic/volcaniclastic and limestone lithofacies associations: A. Primary volcanic facies (FA1); B Pyroclastic – epiclastic facies (coarse grained tuff), FA2; C. Fine-grained tuff – epiclastic facies (FA4); D. Deep-water deposits of the Amatepec Formation; E. Hybrid sandtone – hybrid limestone facies (FA3); and F–H. Limestone facies (FA5–7).

The pillow lavas record periods of slow rates of effusion with rare non-explosive bursts of activity (cf. Carlisle, 1963; Yamagishi, 1991). The remaining lava flow units are interpreted to represent direct volcanism from vents. Finally, the hyaloclastite deposits represent quench brecciation and mechanical breakage of pillow lavas and lava flows. The relationship between pillow lavas and hyaloclastites records a decreasing effusion rate toward the end of each individual eruption (cf. Yamagishi, 1991). Furthermore, hyaloclastites may have formed by cooling, contraction and granulation by spalling of the masive lavas and pillow lavas (cf., Stix, 1991; Lajoie and Stix, 1992). Kokelaar and Busby (1992) reported that the water-lava interaction in deep-sea environments causes explosive fragmentation of the lavas to produce volcanic breccias.

Pillow lavas indicate subaqueous conditions. Radiolarian like those found in tuffs interbedded with the pillows of FA1 occur in water depths of 100–5000 m (Bignot, 1985). Features indicating hot emplacement (e.g., wisps and reaction corollas) are found in the proximal pyroclastic deposits. Depths of subaqueous explosive volcanism have been proposed to lie between 200 m and 1000 m (Fisher, 1984; Stix, 1991; Kokelaar and Busby, 1992). Recently, Wright et al. (2002) inferred depths of 600–800 m for basaltic effusion associated with pyroclastic rocks in the Kermadec arc, near New Zealand. Considering these modern occurrences, a depth of at least 100–500 m is suggested for eruption of the pillow lavas and masive lava flows of the Villa Ayala Formation.

Interpretation of FA2. Both the volcanic breccias and conglomerate lithofacies and some of the tuff and epiclastic lithofacies are grouped into FA2 (Figure 39B). Facies VA2–VA4 are considered to record proximal pyroclastic flows, debris flows and high-density turbidity currents in a deep-water setting. Facies VA6–VA10 (tuff and epiclastic lithofacies) are considered to document the development of slope-apron deposits. They mainly crop out in the Villa Ayala-Zacatlancillo and Alpixafia areas, where voluminous coarse-grained volcaniclastic rocks associated with fine- to medium-grained volcaniclastic rocks are exposed (see Figures 3, 12 and 15).

As a whole, FA2 is interpreted as proximal post-eruptive volcaniclastic deposits that accumulated under conditions of rapidly changing sediment supply. Pulses of enhanced sediment delivery are inferred after each pyroclastic eruption because of high levels of erosion on the volcano flanks (Figure 39B). Smith and Landis (1995) document similar features in the *central* and *apron* facies of an intra-arc setting. Larue et al. (1991) and Wright et al. (2002) assigned coarse proximal deposits to pulses of arc development in the Caribbean region and the Kermadec arc, respectively.

Volcano flanks are sites of initiation of mass movements such as debris flows, high- and low-density turbidity currents, and slumps. The coarse-grained volcaniclastic rocks in FA2 are likely the result of intense proximal pyroclastic processes and derived mass flows.

Matrix-supported textures in conglomerates of VA4 indicate remobilization of the products of pyroclastic eruptions by subaqueous debris flows (cf. Busby-Spera, 1988; Wright, 1996). This remobilization is more evident at the Zacatlancillo and Alpixafia

localities (Figures 12 and 15, and reconstruction in Figure 39C) where thick levels of matrix-supported conglomerates are found interbedded with pyroclastic facies and lavas. There appear to have been periods of pyroclastic eruption produced by explosive activity, followed by mass- or debris-flow activity, both of which alternated with quiescent basalt effusion.

Clast-supported conglomerates of facies VA3 with their erosive bases, grading, channelized zones, and monogenetic clast lithology were deposited from high-density turbidity currents closed related and interstratified between the pyroclastic and debris-flow events. Relationships observed in facies VA3 clearly indicate that pyroclastic flows, debris flows and other mass flows were common during arc development in the Teloloapan area.

FA2 also records relatively quiet periods of sedimentation, representing deposits of pyroclastic and epiclastic flows produced by low concentration turbidity currents developed on the flanks of the arc. Facies VA6 and VA7 were deposited from turbidity currents while facies VA10 was produced from subaqueous fallout and and turbidity currents. Facies VA9 consists of the deposits of debris flows or high-density turbidity currents, most common in the Villa Ayala Formation. The best exposures of FA2 are in the Alpixafia section (Figure 15).

Wright (1996) has concluded that volcaniclastic facies are largely proximal and confined to the edifice of the volcano morphology. In contrast, Busby-Spera (1988) and White and Busby-Spera (1987) reported that volcaniclastic aprons derived from adjacent volcanic centers fill the deeper area between volcanoes, and that they are characterized by

"random" facies patterns. Abundant syndepositional deformational structures indicate the unstable conditions of high slopes and ash-rich primary deposits.

Interpretation of FA3. Pillow lavas, massive lava flows, and peperites constitute the primary volcanic rocks in FA3. These formed by shallow-water volcanism in the eastern area (Teloloapan-Ahuacatitlan area, see Figures 3 and 39E). The main characteristic of FA3 is the direct interbedding of volcanic rocks with the hybrid sandstone and hybrid limestone (facies VA12–VA14) at the top of the Villa Ayala Formation.

FA3 was examined in two localities: (a) the Acatempan area, and (b) the Ahuacatitlan area (Figures 14 and 21). The Acatempan locality contains pillow lavas, massive lavas flows, and peperite rocks. These rocks, especially the peperites, are associated with hybrid limestones (facies VA13). According to White and Busby-Spera (1987), peperites are produced by ascent of magma throughout wet sediments causing steam explosions in shallow water depths. At the same locality, massive lavas are interbedded with facies VA14, which contains a rich assemblage of reworked and *in situ* shelly fauna (rudists, corals, and nerineids). The presence of peperites and shelly fauna confirm a shallow-water setting in the Acatempan locality.

The Ahuacatitlan area is one of the best localities to observe subaqueous volcanic rocks deposited in a shallow-water setting. In this area, homogenized, mixed limestone and lava flows (peperites) are associated with abundant *in situ* shallow water fauna (corals and algal mats). The massive lava flows show extreme vesicularity. Lithoclasts in

the hybrid sandstone facies (VA13) display angular shapes indicating limited transport. Channels are present in the hybrid sandstone facies.

Facies VA12 and VA14, associated with primary volcanic rocks (VA1), reflect shallow-water deposition in a littoral zone, close to the arc which provided the lithoclasts of tuff and lava. Wave action is believed to have been responsible for the erosion and concentration of lithics and shells during deposition of FA3. The sediments could have been supplied from erosion of the volcano flanks to form scouring features. Comparable features have been documented elsewhere in similar shallow-water volcaniclastic deposits (Pirrie, 1989; Fritz and Howell, 1991; Mángano and Buatois, 1996, among others). They have documented that volcaniclastic deposits in shallow conditions are closely related to downslope contemporaneous deposits emplaced by high-density turbidity currents. The character of inter-eruptive deposits is controlled by shelf hydrodynamic regime, sea-level change and tectonics of the basin. These facies show many similarities to those in non-volcanic settings.

4.2.1.2. Late Aptian (The Acapetlahuaya and Villa Ayala formations)

Interpretation of FA4. Facies VA5, VA8, VA10, and VA11 are tuff and epiclastic lithofacies assigned to FA4. FA4 is a very fine- to fine-grained tuff and epiclastic succession produced by distal ash fallout and low concentration turbidity currents. FA4 mimics the distal facies proposed by Smith and Landis (1995) for intra-arc sedimentological evolution, while Larue et al. (1991) described similar deposits in the last stage of evolution of volcanic arcs in the Caribbean region.

FA4 is restricted to the Acapetlahuaya Formation and the uppermost levels of the Villa Ayala Formation. Distal marine deposits of FA4 are mainly distributed along the central part of the study area (Figures 3, 20 and 39C). There are two possible explations for this distribution. First, the paleogeography of the area might have been controlled by high arc edifices that acted as a barrier to the transport of ash and fine suspensions to the eastern area. Second, there might have been bottom currents that concentrated the fine-grained deposits in specific areas.

FA4 represents diminishing ash dispersal during waning stages of pyroclastic eruption, as well as erosion and remobilization of ash by low-density turbidite currents. Some authors (Yamada, 1984; Orton, 1996; and Wright, 1996; among others) suggest that fine-grained post-eruptive deposits are formed not only by pyroclastic processes but also by strong bottom currents that redistribute this sediment.

4.2.1.3. Late Aptian–late Albian (The Teloloapan Formation)

Interpretation of FA5. FA5 is only observed in the eastern area (Teloloapan-Ahuacatitlan area, Figure 3). FA5 includes the uppermost level of the Villa Ayala Formation and the lower portion of the Teloloapan Formation.

After, and partly contemporaneously with the volcaniclastic sedimentation represented by FA3 (latest Aptian–earliest Albian), an isolated shelf/platform began to develop over the slopes and crests of partly or completely inactive volcanic highs (Figure 39F-G). This evolution is documented by FA5 that includes facies VA14 (fossiliferous tuffaceous sandstone), TE1 (algal bindstone), and TE2 (mollusk and benthic foraminifera

wackestone). VA14 and TE1 are interbedded and they record the first stage of platform construction in a shallow-water setting. The abundant fauna and hybrid limestone beds suggest that facies VA14 accumulated during periods of relatively quiescence in the shallow-water area.

In the Teloloapan locality and north of the Ahuacatitlan locality (Figure 21), fossiliferous tuffaceous sandstone (facies VA14) and algal bindstone (facies TE1) rich in fauna record an extraordinary period of quiescence in the area. However, tuffaceous matrix in facies VA14 and very thin beds of tuff within facies TE1 record nearby volcanism. Nerineid fauna (facies VA14) marks the first stage of stabilization in the platform while algal laminites in facies TE1 suggest high energy in a tidal setting. Subsequent restricted and low-energy conditions in the platform are represented by facies TE2. The platform flourished, and the relatively protected shallow-marine and low-energy the platform developed as a shelf "lagoon" (Figure 39H).

Faunal proliferation and ashfall deposits associated with periods of subdued volcanism have been reported in other Cretaceous sequences (Matthews et al., 1974; Coates, 1977; Polsak, 1981; Camoin et al., 1988; Shiba, 1993; Soja, 1996; Masse et al., 1996; Upadhyay, 2001). Polsak (1981) described an Upper Cretaceous barrier reef to lagoon setting made up of rudists and coral bioherms, associated with nerineids on the slopes of island arcs in the Inner Dinarides, Yugoslavia. Camoin et al. (1988) reported rudists and coral frameworks associated with submarine volcanism in the Maastrichtian of the Pachino area in Sicily (Italy), and suggested a shallow-marine high-energy environment in restricted ecological conditions. Some authors (Matthews et al., 1974;

Shiba, 1993; and Masse et al., 1996) reported Aptian–Cenomanian barrier-reef carbonate banks on the top of seamounts/guyots at the western Pacific, as well as in the Caribbean region (Coates, 1977) and India (Upadhyay, 2001). In general, the carbonate banks of the Teloloapan area are composed of rudists, nerineids, and benthic fauna deposited as buildups or in shelf lagoons. The same facies distribution has been suggested by Soja (1996) to characterize the pioneer stages of formation of carbonate platforms on island arcs of a number of Paleozoic–Mesozoic sequences.

FA5 exhibits some features similar to the above examples: (1) a contemporaneous relationship with pyroclastic and epiclastic rocks; (2) fauna which are relatively monogenetic (*Cossmanea (Eunerinea) hicoriensis* in nerineids, and *Toucacia* sp. in rudists), associated with algal mats (TE1) and benthic foraminifera (TE2); and (3) a shallow-water setting on a restricted shelf/platform. The lack of a reef framework during the early development of the carbonate shelf/platform (FA5) suggests that the environment was relatively sheltered. Nerineids and toucacid rudists did not form "wave resistant features" (cf. Camion et al., 1988; Gili et al., 1995). Instead, biostromal monopleurid buildups (bafflers) are common in lagoons during Aptian–Albian time (Gili et al., 1995). Rudists and nerineids assemblages in FA5 are believed to have stabilized the substrate for the later development of "rudist reefs" or "rudist frameworks" (see FA6, below). Abundant nerineids (facies VA14) and scattered rudists (facies TE1) suggest that the former acted as more efficient colonizers than the latter. Finally, the monogenetic faunal association implies a restricted ecological conditions and limited temperature fluctuations during this time (cf. Camoin et al., 1988; Soja, 1996).

Interpretation of FA 6. FA6 includes facies TE3–TE7, and forms more than 60% of the Teloloapan Formation. This facies association is broadly exposed throughout the eastern part of the thesis area wherever carbonates crop out (Figures 3 and 23).

FA6 suggests that conditions became favorable for the formation of organic rudist-dominant frameworks during the middle Albian. These rudist framework/reef deposits are exposed throughout the area, and include backreef to forereef sediments. Rudists are the dominant frame builders, while other fauna (e.g. corals and nerineids) are subordinate.

Some authors (Masse and Phillip, 1981; Kauffman and Johnson, 1988; Scott, 1988) have suggested that during the Early Cretaceous rudists began to play a dominant role as reef builders, because of their apparent tolerance to fluctuations in seawater chemistry, temperature, and clastic supply. The hypothesis that rudists were gregarious sediment dwellers and did not form typical reefs has also been suggested (Gili et al., 1995), because they are generally sediment supported and not true bioconstructions. Caprinid-caprotinid structures are usually found in intrashelf environments, monopleurid-requieniid-radiolitid assemblages colonized shelf lagoons, and caprinid biostromes are found around the margins of the shelf (Masse and Phillip, 1981; Scott, 1988; Kauffman and Johnson, 1988; Gili et al., 1995).

FA6 might be interpreted as the record of rudist-dominant frameworks/reefs, which formed across a spectrum of marginal to restricted environments in the carbonate shelf/platform of the Teloloapan Formation. In this interpretation, facies TE3 (bioclast and intraclast rudstone and grainstone) dominated the forereef. Finally, facies TE4 and

TE5 (thick- shelled caprinid-radiolitid rudists assemblages) constituted the reef front. Facies TE6 and TE7 (thin- and thick-shelled requienid-monopleurid-caprinid rudist assemblage associated with corals, nerinea, and benthic foraminifera) formed the reef crest to the restricted environment of the backreef.

Interpretation of FA7. Facies TE8–TE10 form FA7. This facies association overlies the rudist frameworks/reefs of FA6, and constitutes almost 15% of the Teloloapan Formation (Figure 23).

These storm deposits accumulated during the last stage of development of the calcareous platform in the Late Albian. They formed at the margin of the platform where wave action was intense. Guerrero et al. (1991, 1993) have previously documented this final stage of the development of Teloloapan platform, so this overview will be brief.

Bourgeois (1980) and Dott and Bourgeois (1982) proposed a model for storm deposits. They recognized a composite, typical hummocky-bedded-to-burrowed sequence which includes the following features from base to top: (1) a sharp, erosional base with pebble or intraclast lags; (2) a division of hummocky-bedded fine sandstone in which laminae thickness and sediment grain size decrease upward, whereas horizontality of laminae and organic content increase upward; (3) sets of symmetrically-rippled fine to very-fine cross-laminated sandstone; (4) a zone very rich in plant fragments; and (5) burrowed, medium-gray, very fine silty sandstone.

Aigner (1982) also proposed a similar ideal sequence for calcareous tempestites that include, from base to top: (1) an erosional base with basal shell lag followed by

graded bedding; (2) planar lamination; (3) wave-ripple lamination; and (4) a pelitic division. Bed tops show biological modification.

Facies FA7 resembles storm deposits described by these authors. Textures of facies TE8–TE10 suggest storm deposits in periplatform conditions (Coniglio and Dix, 1992). Facies TE8 might represent the peak storm flows and highly erosive waves in the proximal area, because of the presence of conglomeratic beds containing disarticulated or broken rudists, ammonites and gravel-sized pieces of limestone. Boulders indicate an intense wave-dominated setting (cf. Bourgeois, 1980). The amalgamated hummocky cross-stratified beds of facies TE9 imply water depths sufficiently shallow so that storms of average intensity erode the substrate to a depth that would destroy evidence of faunal activity (cf. Bourgeois, 1980; Aigner, 1982). Facies TE10 is believed to represent periplatform oozes deposition (cf. Coniglio and Dix, 1992).

4.4. THE SEDIMENTARY COVER SUCCESSIONS

4.4.1. Cenomanian–Post Turonian

4.4.1.1. The Mezcala Formation

Interpretation of FA1. FA1 includes MF4–MF8, and is interpreted as middle- to lower-fan deposits of a submarine-fan depositional system. Evidence for this interpretation includes the presence of Bouma sequences, the variable sandstone to shale ratios, vertical profiles, and facies distribution (see Appendix 13 and Figures 30, 32, and 40).

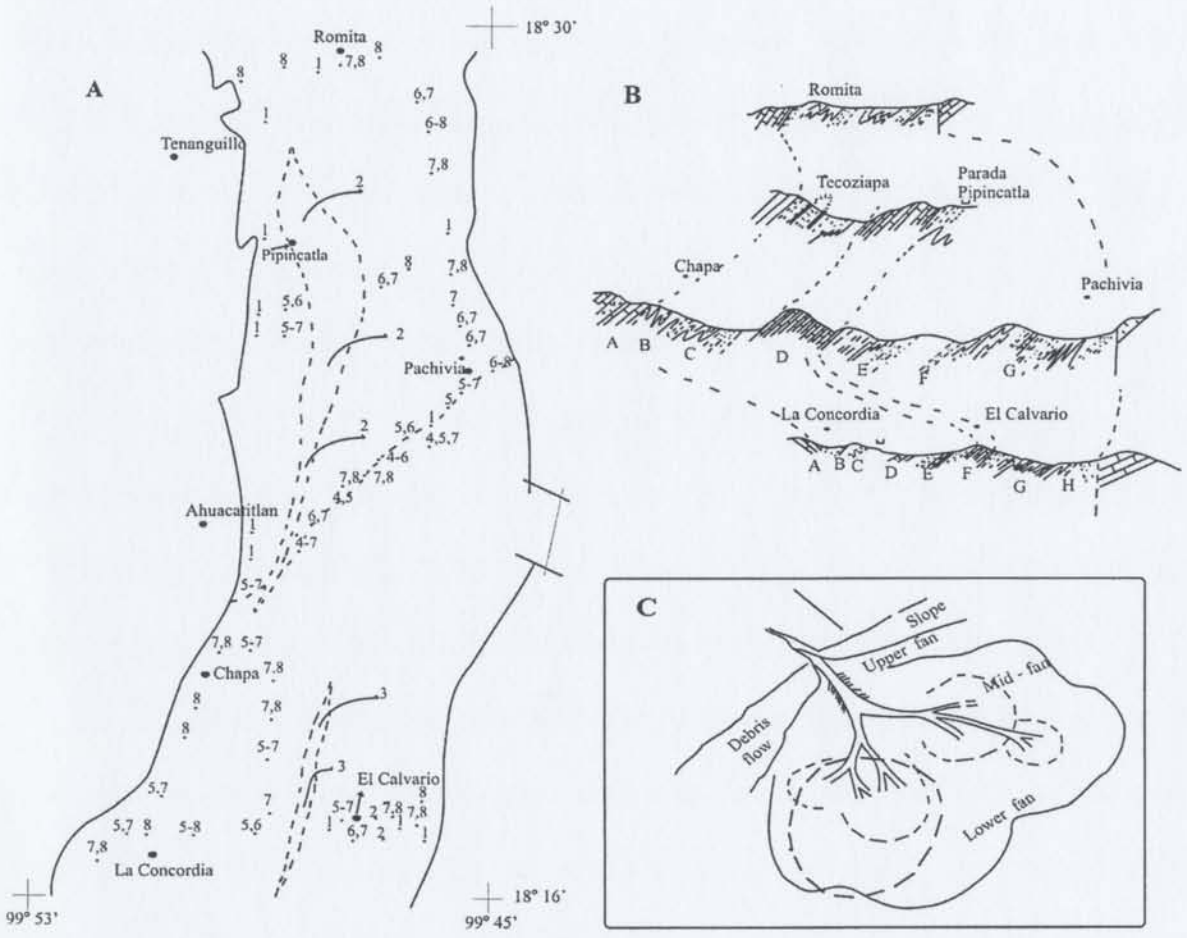

Figure 40. The Mezcala Formation. A. Distribution of the dominant facies. Numbers correspond to the code used in the Mezcala Formation (e.g. MF1=1). B. Structural section showing deformation and facies distribution. Letters correspond to logs in Figures 30 and 32. Inferred submarine-fan environment; circle emcompasses the setting recognized.

Mutti and Normark (1987) characterized overbank deposits in ancient systems as generally fine-grained, thin-bedded, and current-laminated deposits resulting from lateral spreading from confined turbidity currents; graded mudstone units are generally abundant. Overbank deposits can occur in many parts of a turbidite system associated with various types of channels. Mutti and Normark (1987) described lobes in ancient sequences as non-channelized and tabular bodies, which range from 3–90 m thick and which are composed of thick-bedded sandstone alternating with thinner-bedded and finer-grained interlobe facies. The association of lobes and interlobe deposits is considered diagnostic of a lower fan depositional environment although lobe deposits also have been reported from upper and middle fan environments (see Mutti and Normark, 1987).

The thick- to medium-bedded sandstone of facies MF4 (mainly exposed in the western area of the Mezcala Formation, see columns C and F in Figure 32) could represent minor channelized deposits in a middle-fan position. Evidence comes from the presence of beds with a Bouma Ta division, the medium-sand grain size, and local erosional contacts (cf. Mutti and Normark, 1987). Scarcity of thick-bedded and coarse-grained sandstone and no large erosional cuts suggest that larger fan channels are not preserved.

Two interpretations are proposed for the sandstone-shale intervals (facies MF5–MF7) which form ~55% of the facies in the Mezcala Formation. These intervals commonly show thin- to medium-bedded, medium-grained sandstones associated with shale intervals. Shale intervals are minor in MF5–MF6 and more abundant and thicker in MF7 (Appendix 10).

First, where thick-bedded sandstone is associated with medium- to thin-bedded sandstone and minor shale-dominated facies, a channel-overbank system might be inferred (cf. Mutti and Normark, 1987). According to Nelson et al. (1978), abrupt changes from channel to overbank areas are represented by distinct breaks in bed thickness and sedimentary structures. Chen and Hiscott (1999) suggest that thick and sandy beds and thin and variable muddy deposits are organized into packets, representing channel deposits, and levee or channel-margin or interchannel deposits. This interpretation is consistent with the suggestion of some minor channelized sandstone, as well as the abrupt changes in bed thickness and sandstone-shale ratio in this facies association (see Figures 30 and 32). Bouma sequences also change as bed thickness decreases. Only the thicker beds have Ta divisions.

Second, thick and monotonous sandstone-shale intervals showing occasional sandstone-dominated "packets" might be interpreted as middle fan deposits with occasional submarine-fan lobes and/or lobe-fringe deposits (cf. Mutti and Normark, 1987). Mutti (1977) reported that turbidites of the lobe-fringe deposits in the Hecho Group display base-missing Bouma sequences (e.g., Tb-e, Tc-e, Td-e and Te). Piper (1978) and Stow and Shanmugam (1980) argued that fine-grained turbidites with E_1 and T_0–T_4 divisions, respectively, can occur on fan lobes. Pickering (1981) reported that lobe-fringe deposits are thin-bedded Bouma Td-e turbidites containing less sand than associated lobe deposits.

Finally, the laminated shale facies with minor sandstone intervals of facies MF8 is interpreted as a hemipelagic drape over interlobe or overbank deposits formed during

periods of inactivity in the submarine-fan system (cf. Hiscott, 1980; Chen and Hiscott, 1999). Some areas show a transition from facies MF7 to MF8, especially in the central and southern Pachivia valley (Figure 40A). These areas could represent interlobe or overbank deposits in the submarine-fan system.

Interpretation of FA2. The thin-bedded limestone (MF2) and chert beds (MF3) represent predominantly pelagic deposits in the Mezcala Formation. FA2 forms ~15% of the Mezcala Formation (see Figure 40). The composition (planktonic foraminifera, calcispherids, and radiolaria) and texture indicate deposition by pelagic setting. Calcareous planktonic fauna (planktonic foraminifera and calcisphaerids) suggest deposition above the Carbonate Compensation Depth (CCD), while radiolarian fauna in the chert beds favor their deposition below the CCD (Bignot, 1985).

Pelagic sediments suggest that clastic influx was negligible. Hayward (1984) suggested that pelagic (and hemipelagic) sediments are accumulated on submarine fans during times of slow accumulation of clastic sediments, or starvation in the basin. Today, the Amazon Fan and many other modern fans are blanketed by pelagic to hemipelagic foraminiferal muds, as a consequence of high global sea level (Flood et al., 1995).

Interpretation of FA3. FA3 constitutes ~5% of the Mezcala Formation (see Figure 40). Limestone breccia of FA3 is interpreted as debris-flow deposits. Evidence in support of this interpretation is the chaotic fabric, the reworked fragments from

neighboring formations, and the lenticular shapes of the beds (cf. Hiscott and James, 1985).

Deposition of limestone breccia might reflect tectonic pulses in the basin or simply unstable and steep slopes in the calcareous rocks that supplied the calcareous lithoclasts and bioclasts. Concentration of these deposits along the contacts with the underlying carbonate platforms suggests that these are proximal slope deposits. Some debris flows reached the middle fan area because some breccias are interbedded with sandy turbidites (see columns E–G in Figure 30).

4.4.1.2. The Miahuatepec Formation

Interpretation of FA1. FA1 forms 30% of the Miahuatepec Formation, and includes facies MiF1 and MiF2 (Figure 41). This facies association is mainly distributed in the central part of the Miahuatepec Formation (see Figure 41A). It is interpreted to represent accumulation of sediments in the channel-lobe transition of a submarine-fan system (cf. Mutti and Normark, 1987).

Mutti and Normark (1987) define the channel-lobe transition as a region, which separates well-defined channels or channel-fill deposits from well-defined lobes or lobe facies. The channel-lobe transition includes thick-bedded, and commonly conglomeratic and sandstone facies which are typically amalgamated and characterized by extensive shallow scouring.

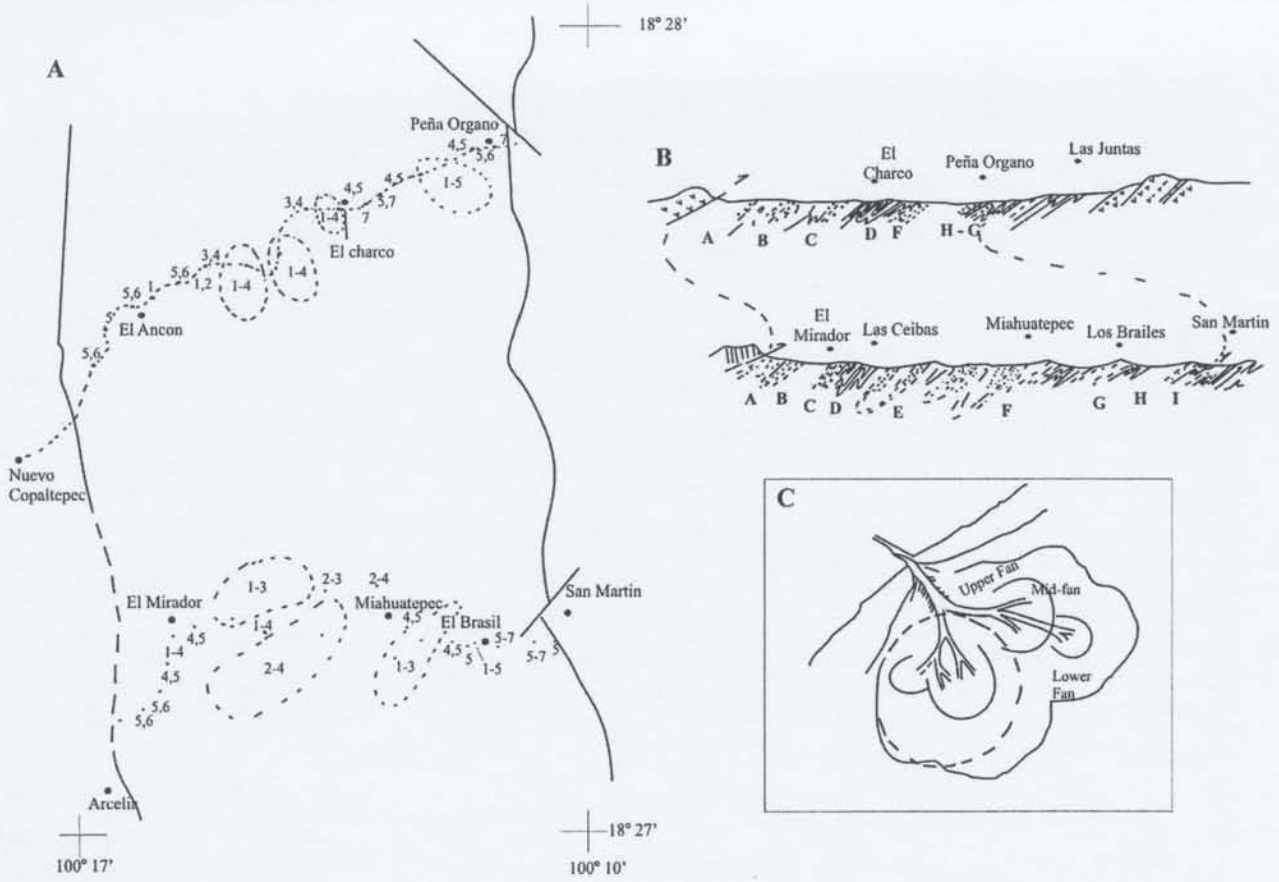

Figure 41. The Miahuatepec Formation. A. Distribution of dominantt facies. Numbers correspond to the code used in the Miahuatepec Formation (e.g. MFi1=1). B. Structural section showing deformation and facies distribution. Letters correspond to logs in Figures 34 and 35. Inferred submarine-fan environment; circle emcompasses the setting recggnized.

Mutti and Normark (1987) used the term "scours" for isolated, roughly equidimensional cut-and-fill features where the erosion and fill are produced by the same flow. Scours vary in size and geometry, ranging from small-scale flute casts to large and deep scour pits. The scours are associated with abundant shale rip-up clasts.

FA1 displays features similar to those described by Mutti and Normark (1987) for the channel-lobe transition. The lack of conglomeratic facies suggests that FA1 accumulated in small or minor channels or in scour zones in the channel-lobe transition. Evidence for this interpretation includes the limited erosional features in facies MiF1, Tabc Bouma sequences (mostly Ta and Tab), the size grain, as well as the amalgamation in facies MiF1 and MiF2. The rip-up clasts observed in this FA suggest high concentration turbidity currents and local erosion. The best example of this FA is in the regional section El Mirador-San Martin (column C and D in Figure 34).

The limited occurrence of FA1 in the area might indicate that the depositional site was far from the source area.

Interpretation of FA2. FA2 dominates the Miahuatepec Formation forming up to 50% of the outcrops (see Appendix 14). The sandstone-shale facies included in FA2 might have formed lobes deposits associated with the distributary channels of the channel-lobe transition of FA1 (cf. Mutti and Normark, 1987). Evidence for this interpretation includes the relationship with FA1 and the presence of monotonous sandstone-shale intervals with tabular bedding and Tabc Bouma sequences.

Non-channelized bodies of thick-bedded sandstone alternating with thin-bedded and fine-grained facies characterize ancient lobes (Mutti, 1977; Hiscott, 1980; Pickering, 1981; Mutti and Normark, 1987). Mutti (1977) and Pickering (1981) suggest that the alternation of thick-bedded and thin-bedded sandstones represents lobe and lobe-fringe deposits. Lobe-fringe deposits show cyclic vertical variation in the sandstone-shale ratio and bed thickness, as well as Tb-e, Tc-e, and Tc Bouma sequences. Lobes occur as amalgamated, medium- to very thick-bedded, fine- to very coarse-grained sandstone beds in packets typically 2–15 m thick. Sandstone beds are predominant but shale is present. Bouma Tab or Tc divisions are common, and grooves and flutes are well developed. Chen and Hiscott (1999) demonstrate that sandstone packets in submarine-fan successions are not characterized by either asymmetrical upward-thickening or -thinning cycles. They summarize the main characteristics of lobe deposits as: (1) common amalgamation, rare basal scours, and sand beds with parallel or wavy bases; (2) scattered mud clasts which "float" in the upper part of the bed; (3) near-absence of pebbles and granules; (4) Ta dominant, with minor Tc and/or Td-e; and (5) most beds are thin to thick bedded.

Strong deformation and limited lateral and vertical exposure in the Miahuatepec Formation prevents the measurement of long series of bed thicknesses in FA2 for statistical study. Hence, no trends can be demonstrated in facies MiF3–MiF5, which form FA2. Lobe and lobe-fringe deposits in FA2 are interpreted where monotonous and abundant sandstone-shale beds alternate with FA1 (see column G in Figure 34, as well as column B, C and F in Figure 35, and Figure 41).

The medium-bedded sandstone of facies MiF3, locally associated with thick-bedded sandstone of MiF2, could represent lobe deposits. Evidence comes from the presence of beds with a Bouma Ta division, the typical medium- to fine-grained sandstone texture, amalgamated beds, rare basal scours, and the sandstone-shale ratio (cf. Mutti and Normark, 1987). The thin-bedded, medium- to fine-grained sandstone interbedded with variable amounts of shale (facies MiF4) might represent lobe-fringe deposits (cf. Mutti, 1977, and Pickering, 1981). The sandstone-shale ratio, Tbc and Tbe Bouma sequences, and bed thickness support this interpretation. Finally, thick shale intervals and sporadic thin beds of sandstone in MiF5 suggest mud drapes on top of abandoned lobes and lobe-fringes (cf. Mutti, 1977, and Hiscott, 1980; Figure 41).

Interpretation of FA3. FA3 is composed of black shale (MiF6), calcareous beds (MiF7), and minor laminated shale (MiF5). It is interpreted to be pelagic and hemipelagic sediments interfingered with lower submarine-fan deposits.

The strong deformation in the thesis area largely obscures the sedimentary structures in FA3. Hence, only the very fine-grained character and isolated presence of this facies along the eastern and western boundaries of the Miahuatepec Formation (see Figure 41A) are used to infer a distal setting. Monotonous and thick sequences of shale associated with thin-bedded limestone suggest that clastic influx was negligible.

4.5. DEPOSITIONAL HISTORY, REGIONAL CORRELATION AND DISCUSSION

Depositional studies in the Guerrero Terrane have been sporadic and have yielded crude regional models that did not consider the tectonic complexity (De Cserna, 1983; De Cserna et al., 1978; Johnson et al., 1991; Cabral, 1991). Only Centeno (1994) and Guerrero (1997) developed sedimentary depositional models for the Zihuatanejo-Huetamo subterrane in the Arteaga and Huetamo areas, respectively. In this section, the depositional history of the Teloloapan area will be clarified using stratigraphic information from chapters 2 and 3 and the facies associations described and interpreted above.

A regional correlation is difficult among the different tectonic assemblages neighboring the Teloloapan area, because of a lack of detailed sedimentological studies in the Arcelia area (belonging to the Arcelia – Palmar Chico subterrane, to the west) and the Tejupilco area (straddling the Arcelia – Palmar Chico and the Teloloapan subterranes, to the north). Only the sedimentary depositional setting of Huetamo area (to the far west) has been documented (Guerrero, 1997), and it is clearly different (see Figure 11). The successions in the Teloloapan and Huetamo areas were both deposited during the Early Cretaceous in arc-related settings. However, the Huetamo area was a back-arc setting, while the Teloloapan area was an intra-arc setting. Limestone sequences in the Guerrero Terrane, from west to east, are island-arc carbonates with different ages: (1) late Aptian-Albian in the Zihuatanejo area; (2) early Barremian–Albian in the Huetamo area; and (3) late Aptian-Albian in the Teloloapan area. Limestones in the Morelos-Guerrero platform

range from Albian–Cenomanian. Finally, sedimentologic studies conducted in the deformed Upper Cretaceous (Mezcala Formation) turbidites of neighboring areas by Ocampo (2004), and other studies in progress help with the correlation of the Mezcala and Miahuatepec formations.

Deposition in the Teloloapan subterrane began with intra-arc sedimentation during the Early Cretaceous, followed by carbonate accumulation above the island-arc deposits (Villa Ayala, Acapetlahuaya, and Teloloapan formations). During the Late Cretaceous, sedimentary cover successions accumulated as submarine-fan systems (Mezcala and Miahuatepec formations). The size and shape of the basins where these sequences were deposited is unknown because of the deformation, and because different structural levels are exposed across the Teloloapan area. However, rapid facies and thickness changes suggest that the area was an active margin during the Early Cretaceous. Likewise, the Late Cretaceous submarine-fan systems are typical of active margins (cf. Leverenz, 2000; Shanmugam et al., 1988; Barnes, 1988; Underwood, 1984; Nielsen, 1985, among others).

Early Cretaceous: from intra-arc to island-arc carbonates settings

Hauterivian–early Aptian. During the Hauterivian–early Aptian, volcanic and volcaniclastic rocks of the Villa Ayala Formation were deposited in an intra-arc setting (Figure 39).

Larue et al. (1991) and Smith and Landis (1995) developed a depositional model for intra-arc sedimentation. Both models are almost identical with some differences during

the evolution of the depositional systems. The lowermost part is oceanic arc basement consisting of oceanic crust (**depositional system I**, not considered in the model of Smith and Landis, 1995). Built atop the oceanic crust is the arc sequence (**depositional system II**, termed central facies by Smith and Landis, 1995). This depositional system contains lava flows, pillow lavas, autoclastic and pyroclastic breccias associated with feeder dikes and plutons, as well as peperites. Relatively steep initial dips characterize the flanks of volcanoes. **Depositional system III** (the apron and distal facies of Smith and Landis, 1995) has coarse- to fine-grained pyroclastic and epiclastic rocks. This depositional system represents pyroclastic fallout events and the remobilized material deposited on the flanks of the arc by gravity-flow processes. Intercalations of pelagic, biogenic sediments, and chert may occur in depositional systems II and III. **Depositional system IV** is the cessation of the arc volcanism and contains reworked volcanic material (epiclastic deposits) and shallow-water reefal limestones. The carbonate island-arc deposits will be discussed later.

Depositional systems II–IV are present in the arc-related succession of the Teloloapan subterrane. The initial primary volcanic deposition is documented in the Villa Ayala Formation (FA1) and is closely related to proximal pyroclastic events and epiclastic deposition documented in FA2; these are depositional systems II and III of Larue et al. (1991). The first depositional system of the Villa Ayala Formation was characterized by high eruptive rates (fissures and vents) providing the materials for a variety of gravity flows on the unstable and steep flanks of the volcanoes (Figure 39A). These characteristics have been documented in ancient arc-related sequences where thick

successions of primary volcanic rocks are interstratified with volcanic conglomerates, breccias, and thick-bedded lapilli tuffs (Busby-Spera, 1987; Busby-Spera, 1988; Houghton and Landis, 1989).

The thickness and interstratification of syn- and post-eruptive deposits in FA1 and FA2 (e.g., Villa Ayala, Ranchos Nuevos, Alpixafia, and Zacatlancillo localities, see Figures 12 and 15) suggest that volcanism and gravity-flows deposition were contemporaneous. Coarse- to medium-grained pyroclastic and epiclastic deposits of FA2 were emplaced by mass flows (pyroclastic flows, turbidity currents, debris flows), in accord with the volcano/submarine-fan sedimentation model (cf. Busby-Spera,1988; Smith and Landis,1995; Wright,1996).

Previously (Berriasian–Valanginian) and during the Hauterivian–early Aptian in the Huetamo area, very thick- to medium-bedded predominantly conglomerate, coarse-grained sandstone, and tuff facies were deposited in an submarine-fan system; followed by deltaic deposits and shallow-water rudist reefs (Guerrero, 1997). Except for a 3 m thick pillow lava interval, no primary volcanic rocks occur in the Huetamo region. Considering their contracting environmental settings during Early Cretaceous time, no lithostratigraphic correlation is possible between the Huetamo and the Teloloapan regions.

In the Tejupilco area, the lack of sedimentological studies does not allow a comparison to be made with the thesis area, whereas to the west of the study area, rocks of equivalent age have not been reported.

Late Aptian–late Albian. During late Aptian, two different depositional systems developed in the Teloloapan area (Figure 39). In the western part of the area (Figure 39C), the uppermost levels of the Villa Ayala and the Acapetlahuaya formations consist of distal pyroclastic-epiclastic deposits (depositional system III in the model above) represented by very fine-grained tuff-epiclastic facies of FA4. FA4 depositional features are interpreted to have resulted from fallout of subaqueous ash, and resedimentation by turbidity currents (cf. Fisher, 1984; White and Busby-Spera, 1987; Busby-Spera, 1988; Houghton and Landis, 1989). Wright (1996) documents that fine-grained ash can be extensively transport and redistributed by bottom currents. The deformation and lack of sedimentary structures in these deposits prevents a unique interpretation of the depositional processes.

During the latest Aptian in the eastern area (Teloloapan–Ahuacatitlan region), a mature stage of evolution of the arc-related sequence is recorded by hybrid facies with abundant reworked shallow-marine fauna mixed with volcaniclastic materials (FA3). This marked the beginning of the formation of an isolated carbonate platform (FA5–FA7) during the Albian (see Figure 39E).

Hybrid and carbonate rocks of the Villa Ayala and Teloloapan formations are similar to depositional system III in the model above. Soja (1996) proposed a detailed evolutionary model for such island-arc carbonates. There are four stages: (1) incipient colonization of organisms in shallow subtidal environments during inactive volcanism and tectonic quiescence and then resumption of volcanism; (2) carbonate platform stabilization, subsidence and formation of fringing reefs or sand shoal; (3) formation of a

restricted-platform (shallow lagoon) and redesimentation of reef detritus downslope; and (4) formation of an atoll, rapid uplift by faulting and formation of extensive debris flows, and rapid rise in eustatic sea level leading to drowning of the carbonate platform.

FA5–FA7 in the Teloloapan Formation resemble some of the evolutionary stages in the island-arc carbonate model of Soja (1996). With the end of volcanism (primary volcanic and pyroclastic rocks), epiclastic deposits accumulated with a variety of hybrid facies (FA3) in the latest Aptian. During the earliest Albian, a carbonate platform was initiated in a subtidal restricted lagoon, associated with pioneering nerinea and rudist framestones (FA5). In the middle Albian, the carbonates flourished rudist-dominanted reefs/frameworks. Finally, during the late Albian, storm deposits were produced at the platform margin. Facies and facies associations of the Teloloapan Formation fit the Read (1985) model of an isolated platform.

During the latest Albian–early Cenomanian, thin-bedded limestone of the Amatepec Formation was deposited as basinal storm deposits (Guerrero and Ramírez, 1992) in the central part of the thesis area (Figure 39D). The lime mudstones are interpreted as "periplatform oozes" (Coniglio and Dix, 1992). This sequence is exposed in the thesis area, but it was not study.

Early Cretaceous limestones with abundant fossils have been extensively reported throughout the Guerrero Terrane (Bonneau, 1972; Cojan, 1973; Alencaster and Pantoja, 1986; Alencaster, 1986; Guerrero et al., 1990, 1991; Pantoja, 1993). These limestones are interbedded with volcanic and/or volcaniclastic rocks forming rudist patches/frameworks. Nerinea concentrations are also present. The different areas from Zihuatanejo to

Teloloapan (except the Arcelia area) share lithological, faunal, and sedimentological similarities to the rocks described in the Teloloapan area. Some endemism in this region has been proposed with the western Pacific region (Masse et al., 1996). However, more paleontologic studies would be required to demonstrate such endemism for the island-arc carbonates of the Guerrero Terrane.

In the Guerrero-Morelos Platform (to the east), intertidal to supratidal carbonates accumulated during the Aptian (Chilacachapa Formation, cf. Campa and Ramírez, 1979; see column 5 in Figure 11). Marls with abundant orbitolinids, oncoids and local tidal channels are predominant. During the Albian–Cenomanian, very thick- to thick-bedded limestone with abundant rudists, corals, algal mats, and benthic foraminifera formed reef deposits, which are capped by ooid grainstone deposited in carbonate sand shoals (González, 1991). The facies and facies associations suggest that the Guerrero-Morelos platform developed as a carbonate ramp (González, 1991).

Faunal associations suggest that both the island-arc carbonate (Teloloapan Formation) and the Guerrero-Morelos Platform (the Chilacachapa and Morelos formations) were deposited in the tropics. However, there are sedimentological differences between these sequences. (1) The facies and facies associations in the Teloloapan Formation are small in scale and change faster, while in the Guerrero-Morelos Platform the facies are extensive and several meters thick. For example, tidal deposits are thicker in the Chilacachapa Formation (>100 m) and thinner in the Teloloapan Formation (~30 m). The same is observed for reef deposits (~200 m compared with ~60 m, respectively). (2) Storm deposits cap the reefs in the Teloloapan

Formation, while no storm deposits have been reported from the Morelos Formation. (3) The Teloloapan Formation developed in an isolated platform, whereas the Morelos Formation forms a carbonate ramp. It appears that although both carbonate sequences shared the same tropical conditions, different depositional conditions prevailed, at an active margin in the Teloloapan area, and along a passive margin for the Guerrero-Morelos Platform.

Early Cenomanian–post Turonian: the submarine-fan systems

During the early Cenomanian to post-Turonian, submarine-fan systems were developed in the Teloloapan area (Miahuatepec and Mezcala formations) and the neighboring area to the east (Mezcala Formation). No similar sequences have been reported to the west where continental deposits of the Cutzamala Formation (cf. Campa, 1977) were deposited in post Turonian, perhaps Maastrichtian time (Centeno, personal communication 2004)

During the Cenomanian–post-Turonian, submarine fans of the Mezcala Formation consist of medium- to thin-bedded, medium- to fine-grained sandstone interbedded with abundant shale intervals deposited in overbank areas and lobes (FA1), associated with scattered debris-flow deposits (FA3). Turonian thin-bedded limestone and chert beds (FA2) record off platform (periplatform ooze) transport and pelagic deposition.

Post Turonian submarine fans of the Miahuatepec Formation are dominantly thick- to medium-bedded, coarse- to medium-grained sandstone and shale intervals

interpreted as the deposits of channel-lobe transitions and lobes (FA1–FA2), associated with minor pelagic and hemipelagic deposits (FA3).

Grain size and sediment volume have been correlated with transport processes, facies character, architecture and scale in submarine-fan systems (Mutti, 1985; Mutti and Normark, 1987: Reading and Richards, 1994). Mutti (1979) developed the concept of efficient and inefficient fan systems based on their ability to transport sand long distances. He suggested that turbidity currents in mud-rich systems transport sand efficiently over long distances, while current sand-rich systems move sand only short distances basinward. Reading and Richards (1994) used relative amounts of grain-size classes to classify deep-water systems into mud-rich, mud/sand-rich, sand-rich, and gravel-rich. Each class is further divided based on the type of feeder system into submarine-fan point source, multiple-source ramps, and slope-apron linear source. Mutti (1985) proposed three types of turbidite system. A Type I system is thick-bedded sandstone that alternates with thin-bedded sandstone and mudstone and forms lobe deposits. Type II is extensively scoured and locally channelized sandstone and pebbly sandstone and contains deposits of channel-lobe transitions and lobes. Type III is predominantly muddy and thin-bedded sandstone or thin-bedded and graded mudstone and is associated with channel-levee complexes.

Sediments in the Mezcala and Miahuatepec formations in the study area are predominantly sand- and mud-sized. Facies in the Mezcala Formation have a sandstone:shale ratio of 1:2 to 1:1 and are predominantly C2.2–C2.4 in the Pickering et al. (1989) scheme (Appendix 10). In contrast, the Miahuatepec Formation contains more

sandstone than shale beds, and is dominated by facies B1.1–B2.1 and C2.2–C2.4 in the scheme of Pickering et al. (1989, see Appendix 11).

In terms of the Mutti (1979) scheme, the submarine-fan systems in the Mezcala and Miahuatepec formations are mud-rich and sand-rich, respectively. Following the scheme of Reading and Richards (1994), the Mezcala and Miahuatepec formations are mud/sand-rich turbidite systems. A point-source turbidite system (cf. Reading and Richards, 1994) appears to apply best to both formations. Using the scheme of Mutti (1994), the Mezcala Formation is a type II system and the Miahuatepec Formation is a type III system. However, poor chronology and strong deformation prevent any inference to be drawn concerning the role of sea-level changes in controlling evolution of these deep-sea systems (cf. Mutti, 1994).

According to Reading and Richards (1994), the shape of mud/sand-rich submarine fans should be radial, but because they develop mainly in small, confined, tectonically active basins, they tend to conform to basin topography and be affected by syndepositional tectonic movements. In the study area, petrographic data (chapter 5) show that the Mezcala Formation contains volcanic detritus from the Villa Ayala Formation and carbonate particles possibly derived from the Teloloapan and Morelos formations. The Miahuatepec Formation contains significant volcanic detritus from the Teloloapan and Arcelia arc sequences. These petrographic observations indicate that uplift and unstable conditions predominated during the deposition of the submarine-fan systems.

Regional correlation among the different Upper Cretaceous submarine-fan systems is ambiguous because of strong deformation observed in the sequences, although west of the study area the Mezcala Formation is less deformed. In general, there are no time or lithologic markers. An exception is the Turonian thin-bedded limestone sequence, which is present in the Mezcala Formation in the study area and in the Agua Nueva Formation to the west. Ocampo (2004) and studies in progress show that the Mezcala Formation in the east is composed of a number of turbidite complexes (cf. Mutti and Normark, 1987). Each turbidite complex is formed by two or three turbidite systems containing channel-overbank, channel-lobe and/or lobe deposits, associated with debris-flow and storm deposits throughout the formation. The turbidite systems range from sand-rich to mud/sand-rich types. Paleocurrents measured by Ocampo (2004) suggest that each turbidite system trends NE-SW and E-W. The presence of a succession of lithologically similar turbidite complexes is certain to confound any long-distance correlations, because complex turbitite system in one area could not be distinguished from complex turbidity systems in another area. The only hope for improved correlations is the discovery of new markers horizons, either lithologic or biostratigraphic.

4.6. SUMMARY

Lithofacies of the Lower Cretaceous arc-related succession (Chapter 2) and the Upper Cretaceous sedimentary cover successions (Chapter 3) record sedimentation in an intra-oceanic arc and submarine-fan systems, respectively. This chapter provides the first

detailed environmental interpretation and basin analysis for the highly defomed Cretaceous rocks of the Teloloapan subterrane.

Facies associations in the Villa Ayala and Acapetlahuaya formations document the evolution of an intra-oceanic arc with intensive volcanism and coarse-grained volcaniclastic deposition (early arc development), followed by pulses of pyroclastic activity associated with slope-apron deposits formed by high- to low-concentration turbidity currents and debris flows. The pyroclastic activity was diminished and airfall deposits have been documented in the central part of the thesis area (Villa Ayala and Acapetlahuaya formations). In the eastern part of the thesis area, the volcanic activity ended entirely and upper Aptian–Albian carbonate platform deposits of the Teloloapan Formation accumulated on the top of the arc volcanoes.

During the Late Cretaceous, deep-water sedimentation dominated, and formed the submarine-fan deposits of the Mezcala and Miahuatepec formations. These formations are mud/sand-rich submarine-fan systems deposited in middle to upper fan environments. Facies associations indicate that the Mezcala Formation contains channel-overbank and lobe-fringe deposits, whereas the Miahuatepec Formation shows channellized lobe and lobes deposits. Both formations contain scattered pelagic deposits.

CHAPTER 5. PETROGRAPHY, GEOCHEMISTRY AND PROVENANCE

5.1. INTRODUCTION AND METHODS

Petrographic and geochemical data are used to document the detrital composition and provenance of the medium-grained tuff and epiclastic rocks of the arc-related and sedimentary cover successions. The arc-related succession (Villa Ayala and Acapetlahuaya formations) is composed of volcanic and very fine- to coarse-grained volcaniclastic rocks. The coarser siliciclastic rocks of the sedimentary cover successions (the Mezcala and Miahuatepec formations) are epiclastic sandstones.

Two hundred and thirty-five samples of coarse- to medium-grained sandstone and tuff were collected from the arc-related succession. These cover the entire succession, and are used to characterize the petrofacies of the formations. Based on a preliminary examination, nineteen representative samples of the entire succession were selected for point counting (Table 2). Thin sections of primary volcanic rocks were also examined to characterize the mineralogy and textures, which contributed detritus to the volcaniclastic rocks.

Two hundred samples of coarse- to fine-grained sandstone were collected in the Mezcala and Miahuatepec formations, one hundred samples in each formation, to characterize the petrofacies. Sixteen of these samples were selected for point counting (Tables 3 and 4).

Four to five hundred points were counted for each thin section following the Gazzi-Dickinson method (Ingersoll et al., 1984). Appendix 15 shows the grain

parameters used. Volcanic grains were classified according to Dickinson (1970) and Marsaglia and Ingersoll (1992). Some samples were stained for plagioclase and K-feldspar using the method of Marsaglia and Tazaki (1992). To avoid obscuring important features during the staining process, only one third of the thin sections were stained. The more altered samples were not stained.

Using the petrographic features, twenty-eight samples from the arc-related succession were selected for whole rock chemical analysis (20 in the Villa Ayala Formation and 8 in the Acapetlahuaya Formation). Thirteen of these were further analyzed for trace and rare earth elements (REE) using inductively coupled plasma-source mass spectrometry (ICP-MS). For the sedimentary cover successions, only the sandstones of the Miahuatepec Formation were selected for geochemistry. Fifteen samples were selected for whole rock analysis and eight of these were further analyzed by ICP-MS. Appendices 16 and 17 show the whole-rock major elements for the arc-related succession and Miahuatepec Formation, respectively.

All chemical analyses were performed at the Department of Earth Sciences of Memorial University of Newfoundland, Canada. First, the weathered surface was removed from all samples. They were then crushed and powdered in an agate puck mill. Major elements (reported as weight percent, %) along with trace elements (reported as parts per million, ppm) were determined for pressed powder pellets (5 grams) by X-ray fluorescence (XRF), using an ARL Model 8420 instrument. Selected trace elements, including the rare earth elements (REE), were analyzed by ICP-MS, submitted as < 200 mesh powders, (see Jenner et al., 1990, for the full analytical method).

Despite the known mobility of major elements during processes such as weathering, diagenesis, and metamorphism (Taylor and McLennan, 1985; McLennan et al., 1993; Johnsson, 1993), major elements can be used to establish a general lithologic classification of the studied rocks, using the classification of Pettijohn et al. (1987). Some major elements, trace elements, and REE provide a more robust indication of source and tectonic setting. Controversy exists as to whether mudstones or sandstones are better indicators of source in active margins. Some authors (Bhatia, 1985; McCann, 1991, among others) support the use of fine-grained sediments because they reflect the active continental margin signature while sandstones carry a "memory" of the relict passive margin signature in their recycled grains. However, it has been suggested that volcaniclastic sandstones preserve a significant portion of the geochemical characteristics of their primary source material and therefore information about the tectonic setting (Floyd and Leveridge, 1987; McLennan et al., 1990; Hiscott and Gill, 1992). Considering this fact, medium-grained sandstones were selected for geochemical analysis from the Villa Ayala, Acapetlahuaya and Miahuatepec formations. This permits a comparison of chemistry and detrital mineralogy in the same samples.

5.2. PETROGRAPHY, GEOCHEMISTRY, AND PROVENANCE OF THE ARC-RELATED SUCCESSION

5.2.1. Petrographic description, petrofacies and source

Petrography. Volcaniclastic sandstones and tuffs of the arc-related succession are compositionally uniform, moderately to poorly sorted, feldspathic litharenites (cf. Folk, 1974; Figure 42A and Table 2). These rocks have been metamorphosed to the greenschist and prehnite-pumpellyite metamorphic facies (Talavera, 1993). In addition, diagenesis affects most of the original detrital textures. However, detrital textures in most of the samples are sufficiently well preserved to identify the primary composition of the rocks. An effort was made to establish original detrital composition even in the most altered samples.

The mean values for framework grains are 11% quartz, 32% feldspar, and 57% lithic fragments (Table 2 and Figure 42A). Ferromagnesian grains, point counted as dense minerals, are also present throughout the succession ranging from 0–6%, with a mean value of 4%; some levels close to volcanic rocks reach almost 15%. Matrix is difficult to distinguish because compaction and alteration of lithic fragments form a pseudomatrix (Dickinson, 1970), but petrographic analysis shows that most of the apparent "matrix" is crushed and altered lithic fragments (Figure 43A). Very fine, highly altered matrix is believed to be volcanic ash, but this is difficult to verify because of the degree of alteration of the samples (Figure 43B). Matrix percentage in Table 2 reflects true matrix of depositional origin.

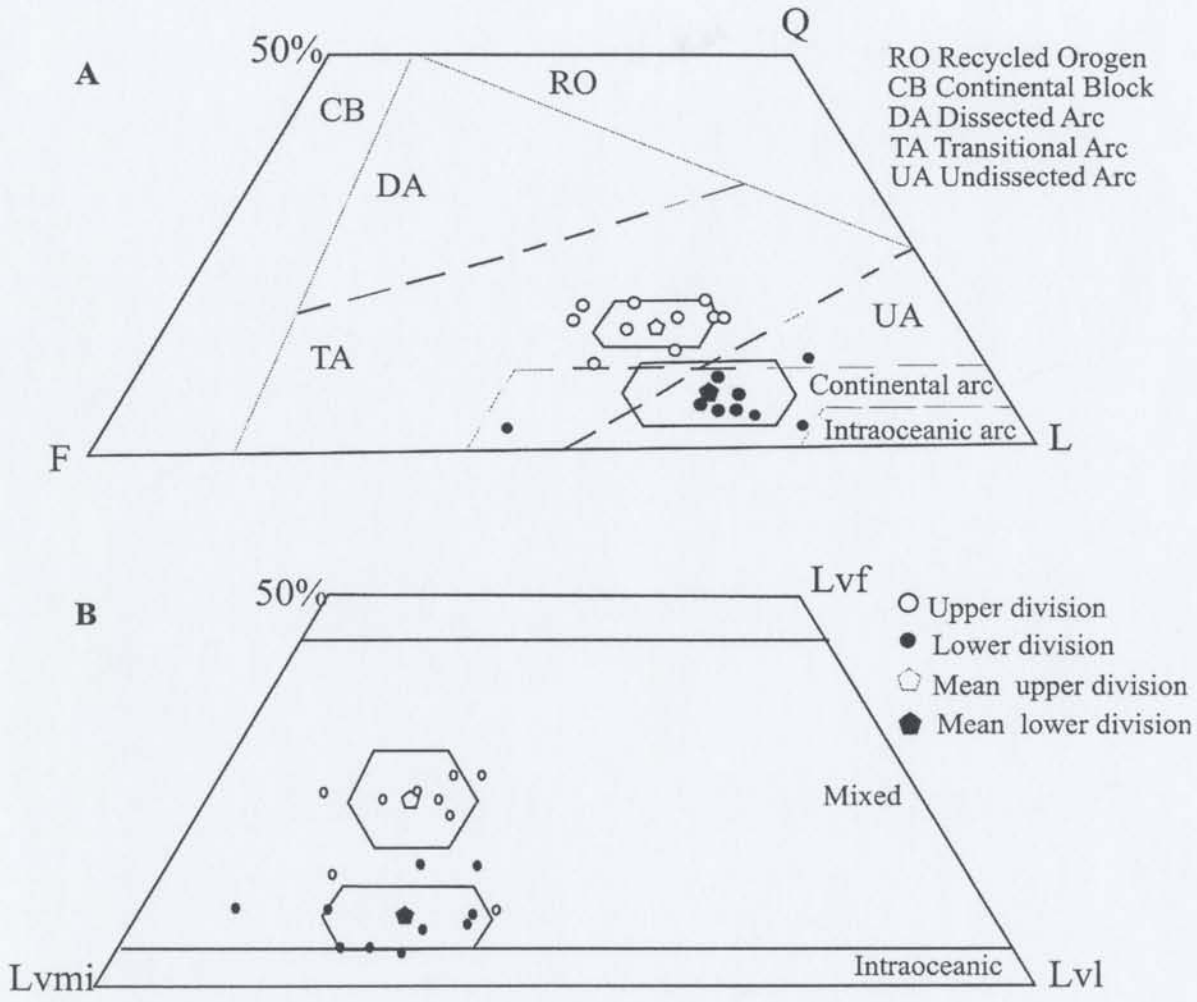

Figure 42. Ternary plots of the arc-related succession. A, QFL plot. B. LvfLvmiLvl plot. The upper part of each triangle is not shown because no data plot there. Polygons show standard deviation. Filled and open small polygons in both diagrams show lower and upper division, respectively. Major fields from Dickinson (1985). Continental, intraoceanic, and mixed subfields from Marsaglia and Ingersoll (1992).

Table 2. Recalculated modal point counts of the arc-related succession. Numbers in brackets are the points on which each recalculation to 100% is based. Note: L = Lv in theses rocks.

Sample	QFL%			QmFLt%			QmPK%			LvmiLvlLvf%			Lvv
	Q	F	L	Qm	F	Lt	Qm	P	K	Lvmi	Lvl	Lvf	
Lower													
J10	3	54	43 (400)	3	54	43 (400)	5	89	6 (165)	80	10	10 (126)	0
TMX77	16	35	49 (417)	1	42	57 (355)	2	66	32 (151)	68	27	5 (204)	0
J68	3	23	74 (405)	3	23	74 (405)	10	72	18 (104)	56	36	8 (247)	18(301)
J71	12	18	70 (420)	2	18	80 (420)	12	70	18 (126)	61	32	7 (263)	6(276)
J63	5	31	64 (402)	0	31	69 (402)	0	75	25 (123)	55	36	9 (233)	10(258)
J62	9	29	62 (446)	4	29	67 (446)	12	65	23 (147)	54	41	5 (257)	7(275)
J77	7	28	65 (402)	4	28	68 (402)	11	80	9 (139)	65	31	4 (219)	16(261)
TMX132	5	29	66 (472)	2	29	69 (472)	7	71	22 (147	70	20	10 (311)	0
J12	4	28	68 (520)	4	28	68 (520)	12	67	21 (166)	51	33	16 (354)	0
TMX127	6	32	62 (428)	6	32	62 (428)	17	71	12 (162)	57	27	16 (266)	0
Mean	7	31	62	3	31	66	9	72	19	62	29	9	
Standard Deviation	4	9	9	2	10	10	5	7	8	9	9	4	
Upper													
J90	11	41	48 (425)	7	41	52 (425)	15	68	17 (206)	52	38	10 (202)	2(205)
TMX17	19	38	43 (450)	19	38	43 (450)	33	55	12 (256)	53	22	25 (181)	7(1940
J05	19	33	48 (423)	15	32	53 (423)	31	52	17 (200)	57	19	24 (192)	6(205)
TMX118	17	29	54 (464)	2	29	59 (464)	30	55	15 (189)	67	18	15 (235)	6(251)
TMX122	17	24	59 (435)	12	24	64 (435)	33	54	13 (155)	63	12	25 (207)	15(245)
TMX31	17	40	43 (424)	13	40	47 (424)	25	54	21 (225)	48	25	27 (183)	0
TMX15	19	25	56 (455)	13	24	63 (455)	34	51	15 (170)	51	25	24 (224)	13(256)
J21	17	25	58 (406)	11	25	64 (406)	30	56	14 (147)	51	27	22 (191)	20(237)
TMX33	12	32	56 (449)	8	32	60 (449)	21	56	23 (182)	45	28	27 (251)	0
Mean	16	32	52	12	32	56	28	56	16	54	24	22	
Standard deviation	3	7	6	3	6	7	6	5	4	7	7	6	

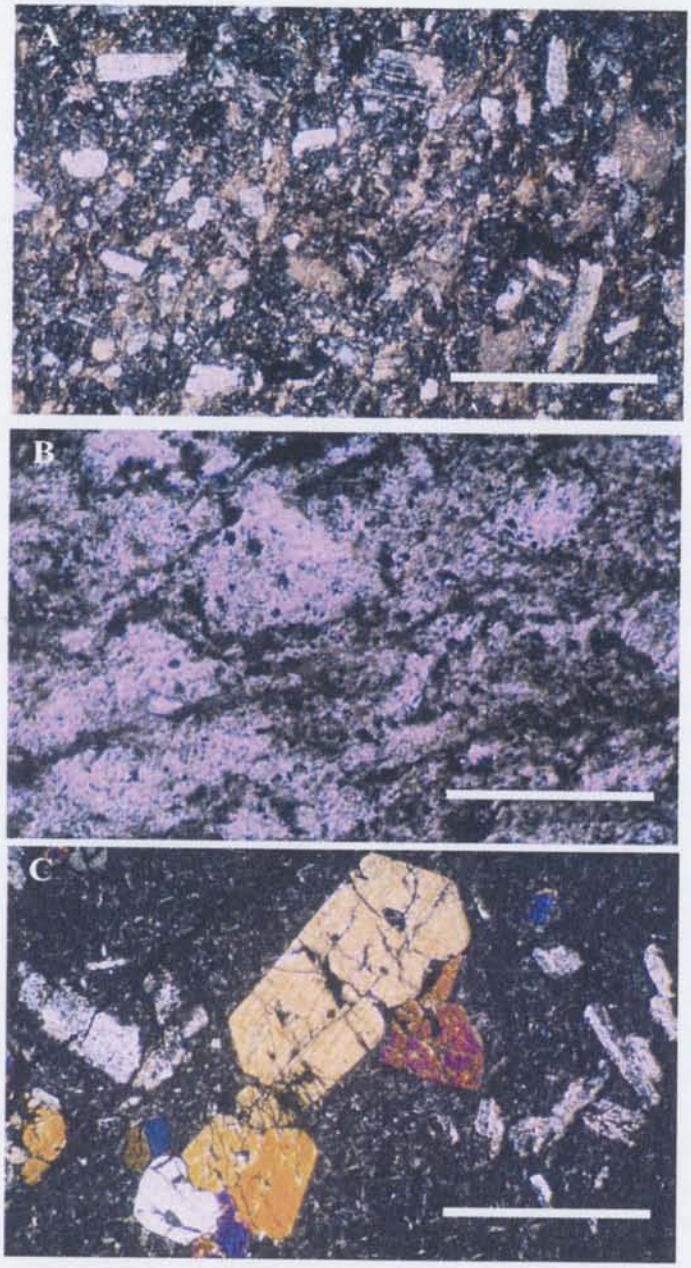

Figure 43. Photomicrographs of the arc-related succession. A, General view of lithic fragments and feldspar in a pseudomatrix (J11). B, Devitrified fine-grained matrix (J08). C, Ferromagnesian and plagioclase crystals within the microlitic groundmass of a volcanic lithic grain (J15). Scale bars = 0.25 mm. Number of sample in parentheses.

Volcanic lithic fragments are the dominant component in the arc-related succession. No fragments of sedimentary or metamorphic rocks were observed in the analyzed samples. Volcanic lithic grains are mafic in composition (basalt to andesite, Figure 43C), and show microlitic, lathwork, felsitic and vitric textures.

Microlitic volcanic lithic fragments (Lvmi; Figures 42B, 44C, 45A) are grains containing microlites of plagioclase and represent mainly an intermediate type of lava (Dickinson, 1970). Andesites, basalts and basalt andesites contain microlitic textures. In the arc-related succession, microlitic texture is characterized by plagioclase microlites within a black or devitrified groundmass. The microlitic texture observed in the samples is similar to the intersertal textures in basalts and andesites of the Villa Ayala Formation. Felsic microlitic fragments are present throughout the succession but are minor. Microlitic volcanic lithic fragments are the principal component in the arc-related succession and form, on average, >55% of the volcanic lithic population (Table 2 and Figure 42B).

Lathwork volcanic lithic fragments (Lvl; Figure 45B) are plagioclase laths (as first defined by Dickinson, 1970) and other sand-sized phenocrysts in an intergranular, intersertal or devitrified groundmass. They are derived from basaltic lavas. In the arc-related succession tuffs and sandstones, the phenocrysts are laths of plagioclase, pyroxene and amphibole, while the groundmass is microlitic or black or brown devitrified glass. These fragments are similar to the textures observed in basalts and basaltic andesites of the Villa Ayala Formation.

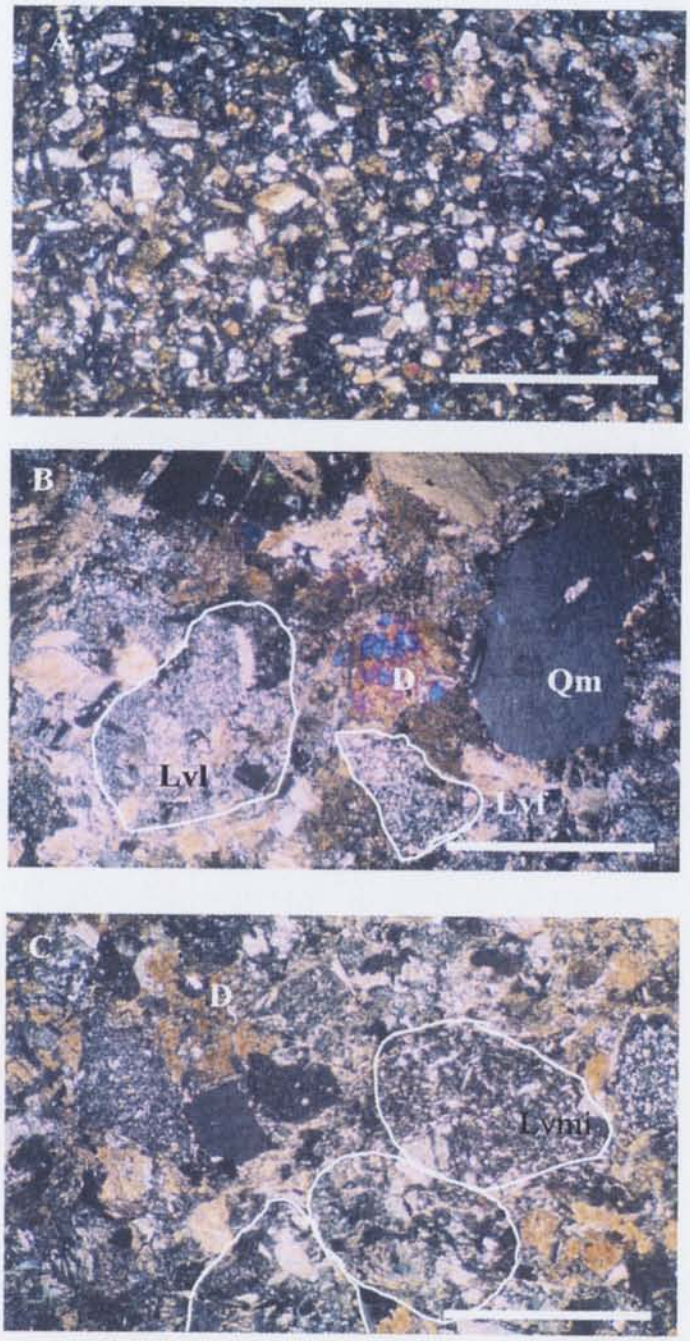

Figure 44. Photomicrographs of grain textures in the arc-related succession. A, Plagioclase and dense minerals (TMX30). B, Monocrystalline quartz (Qm), volcanic lathwork (Lvl) and felsitic (Lvf) grains (J12), C, Volcanic microlitic grains (Lvmi) and dense minerals (D), J62. Scale bars = 0.25 mm. Number of samples in parentheses.

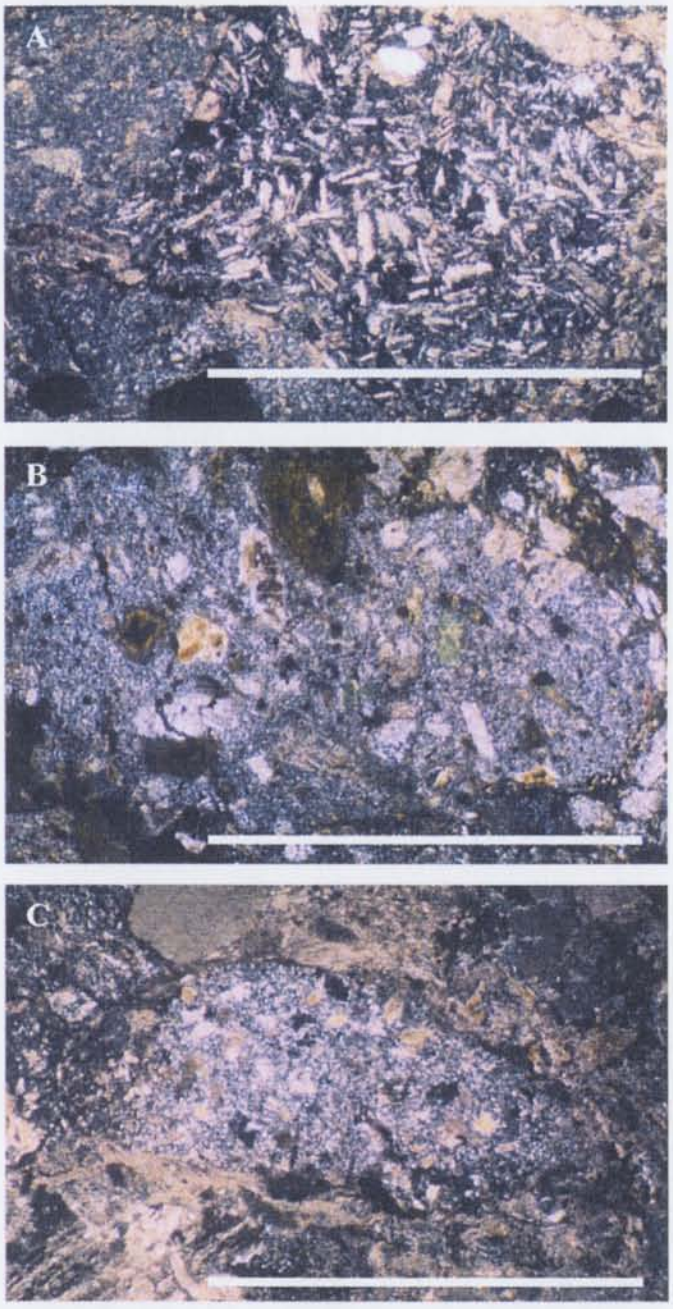

Figure 45. Photomicrographs of the arc-related succession. A, Volcanic lithic grain with microlitic texture (J63). B, Lathwork texture, showing andesite grain with ferromagnesian and feldspar laths (J63). C, Volcanic fragment with felsitic texture (TMX15) . Scale bars = 0.25 mm. Number of sample in parentheses.

Lathwork volcanic lithic fragments are the second most abundant volcanic lithic grains in the arc-related succession, comprising >24% of the volcanic lithic population (Table 2 and Figure 42B).

Felsitic volcanic lithic fragments (Lvf; Figures 42B and 45C) consist of a microcrystalline mosaic of granular or seriate, anhedral quartz and feldspar. They represent silicic volcanic rocks, although felsitic seriate textures have been reported in andesites (Critelli et al., 2002). In the arc-related succession, felsitic volcanic lithic fragments contain very fine-grained feldspathic material. The presence of microphenocrysts of ferromagnesian minerals and feldspars in andesite flows suggests that some felsitic volcanic lithic fragments could be felsic microlitic fragments derived from andesitic rocks, although rhyolites also have been reported in the Villa Ayala Formation (Talavera et al., 1995). Felsitic volcanic lithic fragments comprise ~10% of the volcanic lithic population in the arc-related succession (Table 2 and Figure 42B).

Vitric volcanic lithic fragments (Lvv) are glass shards, and pumice or scoria, as well as partially to completely altered glass (Dickinson, 1970; Marsaglia and Ingersoll, 1992). Vitric fragments in the arc-related succession are composed of very fine, highly altered clay or zeolite minerals, brown or black in color. Bubble-wall shards are rare. Vitric fragments are similar to the textures in vitric tuff petrofacies and the altered glass observed in basalt and andesite flows of the Villa Ayala Formation. Vitric volcanic lithic fragments form less than 5% of the volcanic lithic fragments in the arc-related succession. In Table 2, the Lvv population is reported individually with the total lithic grain counted in parenthesis.

Feldspars crystals are mainly euhedral to subhedral plagioclase and minor potassium feldspar. The plagioclase shows a high degree of alteration to sericite, albite or clays, which cloud the crystals (Figure 44A). Microscopic identification of plagioclase composition is difficult because of the considerable diagenesis in the samples. However, andesine has been chemically identified (Talavera, 1993; Talavera et al., 1995).

Monocrystalline quartz grains are mostly subangular, although some subrounded grains are also present (Figure 44B and C). Quartz grains show straight and undulose extinction. The quartz generally lacks mineral inclusions, while embayments are present in some samples. Polycrystalline quartz grains are mainly chert (Ch).

Ferromagnesian minerals, counted as dense minerals, are present throughout the arc-related succession (mean ~4%, see Table 2). They are composed of clinopyroxene, orthopyroxene, and amphibole (Figures 43C, 44A and C). Oxides are also observed in some levels.

Petrofacies. Petrographic analysis suggests that volcaniclastic rocks of the arc-related succession can be informally divided into lower and upper division (see Figure 42A). The lower division roughly corresponds with the lower and middle parts of the Villa Ayala Formation, while the upper division is considered similar to the Acapetlahuaya Formation and the upper part of the Villa Ayala Formation. According to this division, three petrofacies can be recognized in the arc-related succession. They are: (1) tuff; (2) epiclastic sandstone; and (3) hybrid sandstone. Appendix 16 contains geographic and stratigraphic location of the samples. The tuff and epiclastic rocks are shown in Table 2. Hybrid sandstones were not point counted.

Tuff petrofacies. This petrofacies is mainly found the lower part of the arc-related succession, and is characterized by very fine to very coarse tuff and subordinate vitric tuff. Some tuff plots in the lower parts of the QFL and QmFL ternary diagrams (Figures 42A and 46A). The tuff petrofacies is interbedded with primary volcanic rocks and breccias.

Tuff contains dominantly subangular to angular volcanic lithic fragments, showing microlitic and lathwork textures and scattered vitric and felsitic textures. Feldspar crystals (mean 35%) are mostly plagioclase and subordinate monocrystalline quartz (6%) and pyroxenes (3–6%). The grains are contained in a fine brown devitrified groundmass. When coarse-grained and fine-grained tuffs are interbedded, a microscopic load structure is developed (Figure 47A). Abundant oxides are frequently found in the tuff petrofacies.

Vitric tuff shows pseudomorphed shards with angular, cuspate, and arcuate finely granular material, possibly replacing the original glassy ash (Figure 47B). The recognition of vitric material is ambiguous, because is replaced by clay or a light brown alteration product that could be chlorite.

Epiclastic sandstone petrofacies. Thirteen of the nineteen samples point-counted are epiclastic sandstones (see Table 2). This petrofacies is mainly found in the upper part of the arc-related succession, although similar samples (not point counted) were collected from some levels of the lower part of the succession. The epiclastic sandstones plot in the lower middle portion of the standard QFL and QmFL ternary diagrams (Figures 42A and 46A).

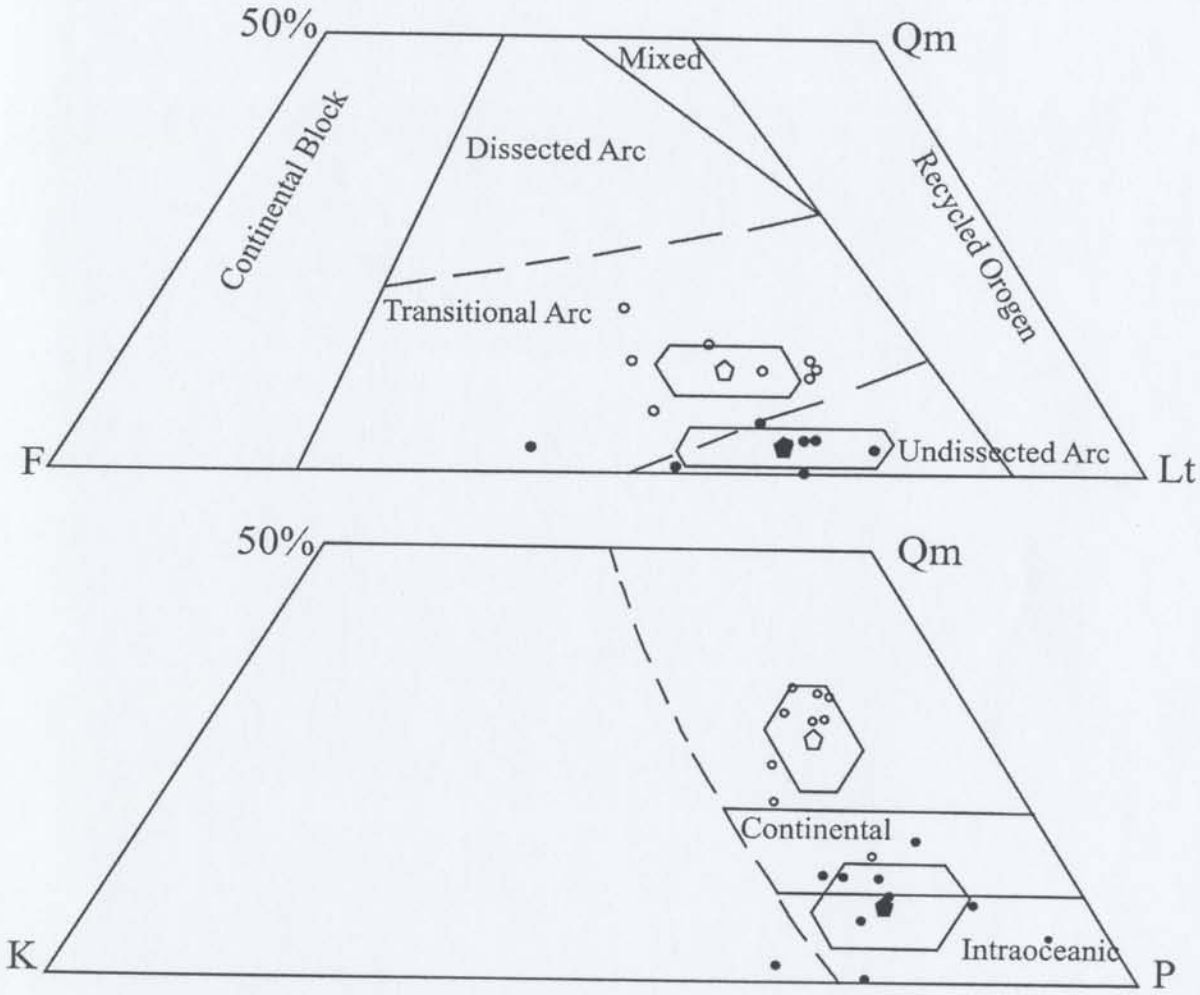

Figure 46. Ternary plots of the arc-related succession. A, QmFLt plot. Tectonic settings and their boundaries are from Dickinson (1985). B. QmKP plot. Fields from Marsaglia and Ingersoll (1992). The upper part of each triangle is not shown because no data plot there. Polygons show standard deviation. Filled and open small polygons in both diagrams show lower and upper division, respectively. Samples plot as black and white circles for the lower and upper division, respectively.

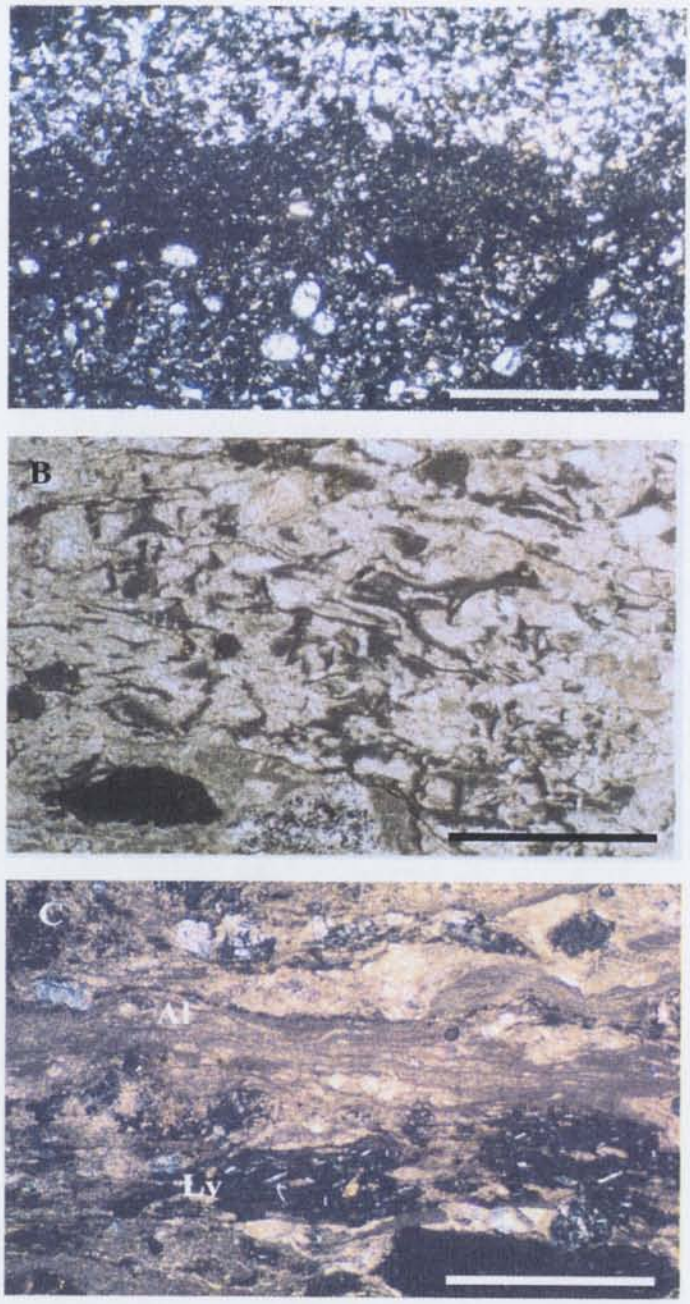

Figure 47. Photomicrographs of petrofacies of the arc-related succession. A-B. (A) Tuff petrofacies, showing interstratification of fine- to medium-grained tuff (J07) and (B) shard structure in vitric tuff (TMX32). C, Hybrid petrofacies, showing mixture of volcanic (Lv) and algal material (Al), J50. Scale bars = 0.25 mm.

The epiclastic sandstone petrofacies contains volcanic lithic fragments with microlitic, felsic, lathwork, and vitric textures. However, felsitic textures are more abundant in this petrofacies than they are in the tuff petrofacies (see Table 2 and Figures 42 and 47). Monocrystalline quartz is also more abundant in this petrofacies, while plagioclase abundance is similar to that of the tuff petrofacies. Ferromagnesian grains, point counted as dense minerals, and oxide minerals are less abundant (at 1–2%) than they are in the tuff petrofacies. Grains are contained in a silt-clay-sized matrix.

Hybrid sandstone petrofacies. The term hybrid sandstone is used here for mixtures of clastic and calcareous material (Zuffa, 1985). The hybrid sandstone petrofacies is only found in the upper part of the Villa Ayala Formation. This petrofacies contains abundant intrabasinal volcanic and calcareous lithic grains (Figure 47C). Volcanic lithics mostly have microlitic and felsitic microlitic textures, while lathwork and glomeroporphyric textures are rare. Intrabasinal calcareous fragments include bioclast fragments of mollusks, corals, and algal laminites, as well as intraclasts of benthic foraminifera and peloidal wackestone–packstone. Plagioclase and potassium feldspar are highly altered to calcite, clay minerals, and possibly zeolites. The grains are contained in a clay matrix, which is altered to chlorite and other unidentified fine grain material. Silicification and calcification are usually present in the rims of the fragments.

Source. The compositional modes for the volcaniclastic rocks of the arc-related succession plot consistently in the lower and middle portion of the QFL and QmFLt ternary diagrams, indicating a volcanic source (Figures 42A and 46A). Volcanic lithic

fragments are the dominant components, having mean values of 62% in the lower part and 56% in the upper part of the succession. Furthermore, microlitic, felsic microlitic and lathwork volcanic lithic fragments constitute almost 80% of the volcanic grains, while felsitic fragments form ~20%. The high proportion of microlitic and lathwork fragments suggests that the volcaniclastic rocks of the arc-related succession were mainly derived from basaltic and andesitic sources. The increase of felsic fragments in the upper part of the arc-related succession signals the availability of a new felsic source. This might be the result of a change in magma composition of contemporary volcanoes.

5.2.2. Geochemistry and source

Major elements. Whole rock analyses of major elements are shown in Appendix 16, while Table 5 contains volatile-free percentages, where the data are recalculated to 100%, ignoring LOI, as well as trace and rare earth elements.

Despite the known mobility of major elements during weathering, diagenesis and metamorphism (Taylor and McLennan, 1985), the chemical classification of Pettijohn et al. (1987), using log (SiO_2/Al_2O_3) vs. log (Na_2O/K_2O), shows the rocks of the arc-related succession to be graywackes, except one sample (J34) which plots near the arkose-lithic arenite boundary (Figure 48). This is the expected rock type, based on petrographic observations.

Table 5. Recalculated major-elements data for sandstones from the arc-related succession (wt %; volatile-free).

Sample	SiO_2	TiO_2	Al_2O_3	Fe_2O	MnO	MgO	CaO	Na_2O	K_2O	P_2O_5	CIA
J11	53.29	1.05	15.73	11.30	0.16	8.43	3.55	5.66	0.68	0.14	48.8
J12	66.03	0.52	14.98	4.30	0.04	2.00	7.22	1.78	3.05	0.07	43.6
J10	53.02	1.04	15.98	10.97	0.14	8.57	3.54	5.93	0.66	0.15	48.6
TMX77	54.03	0.91	15.30	9.60	0.10	12.64	3.29	2.72	1.26	0.15	56.4
TMX32	49.77	1.39	17.25	9.63	0.15	5.57	10.07	3.51	2.41	0.24	39.2
TMX136	49.28	1.11	17.66	9.68	0.18	12.33	4.29	2.88	2.40	0.19	53.8
J71	48.41	0.96	15.37	11.31	0.16	14.11	5.03	3.10	1.42	0.17	49.3
TMX79	44.82	0.99	14.34	12.41	0.17	19.32	5.53	1.85	0.44	0.12	99.0
TMX116B	61.62	0.76	14.86	7.68	0.11	5.94	2.61	5.03	1.27	0.12	50.7
TMX116	61.08	0.91	18.33	3.81	0.06	2.23	6.66	3.97	2.85	0.10	45.7
TMX17	73.65	0.41	16.12	1.28	0.01	1.14	2.03	2.69	2.62	0.05	59.5
TMX18	73.13	0.42	16.50	1.19	0.01	1.22	2.01	2.87	2.51	0.05	59.7
TMX123	58.57	0.58	12.70	4.07	0.12	1.41	18.18	2.60	1.70	0.07	27.1
TMX122	62.06	0.60	14.58	2.59	0.05	1.94	11.81	2.20	4.09	0.08	33.0
TMX118	72.06	0.54	16.49	3.42	0.03	1.92	0.54	1.67	3.22	0.10	8.5
TMX15	70.74	0.39	14.15	1.63	0.03	1.74	6.57	1.88	2.82	0.05	43.8
TMX38	55.96	0.97	15.45	7.24	0.04	11.41	1.74	2.20	4.86	0.13	56.1
TMX34	65.75	0.55	15.13	4.79	0.05	3.51	4.82	1.34	3.99	0.07	32.3
TMX127	55.27	1.06	13.00	6.80	0.16	8.43	5.87	0.34	8.84	0.22	46.3
TMX19	65.52	0.39	14.62	3.75	0.07	2.69	7.54	3.00	2.36	0.06	53.1
J90	47.74	1.06	14.03	12.47	0.18	13.54	6.78	2.34	1.67	0.19	43.8
J87	46.81	1.08	14.14	12.33	0.18	14.07	7.30	2.40	1.51	0.18	42.8
J21	60.72	0.78	14.65	3.28	0.07	1.84	13.78	2.46	2.37	0.05	31.6
J25	61.72	0.60	14.55	2.67	0.07	1.97	12.06	2.15	4.13	0.08	32.7
J34	59.92	0.78	14.65	3.17	0.07	1.83	14.68	2.56	2.27	0.07	30.5
TMX31	53.30	1.06	17.41	10.37	0.12	9.99	1.81	4.24	1.57	0.13	59.2
TMX33	51.68	1.21	17.77	10.80	0.12	10.60	1.94	4.31	1.44	0.13	59.3
TMX30	70.60	0.56	16.51	2.70	0.03	1.36	2.97	2.45	2.74	0.08	57.1

Table 5 (Continued). Trace and rare earth elements data for sandstones from the arc-related succession (ppm). ICP-MS Data. * trace element analyzed by XRF. La/Y = La_N/Y_N

	J10	TMX77	TMX132	TMX136	J71	J34	TMX33	TMX116	TMX18	TMX118	TX34	TMX127	J87
Rb	4.8	34	82	24.6	32.7	80	47	43	90	147.5	156.3	135.8	49.3
Sr	216	152	207	289	281	390	222	157	373	180	482	198	260
Ba	39	235	366	337	221	321	715	343	2655	537	1019	1050	583
Zr	82.3	86.1	165.5	92.8	82.5	213.1	188.8	164.3	173.9	174.8	169.8	202	99.6
Nb	12.3	10.9	11.6	10.4	12.2	10.7	7.5	7.4	7.8	7.9	8.7	14.0	7.0
Hf	1.72	1.78	3.77	2.17	2.59	2.51	2.98	2.87	2.39	2.94	4.41	7.07	1.9
Ta	1.24	1.27	1.22	1.24	1.19	1.1	0.78	1.41	3.76	1.06	1.88	1.73	0..6
Th	1.91	2.20	4.84	2.07	2.28	6.26	5.65	5.28	5.99	6.45	9.1	6.85	2.99
U	0.60	0.65	1.67	0.78	0.68	1.75	1.78	1.63	2.09	1.87	2.95	3.53	1.0
Cs*	22	32	43	37	26	18	36	27	9	13	14	24	49
Y	23.9	16.2	22.0	23.2	16.3	20.4	26.9	23.0	44.1	27.8	25.5	27.9	20
Pb	7.8	2.3	6.3	3.8	5.5	12.4	10.1	9.9	10.1	9.9	10.1	7.6	2.2
V*	259	211	288	272	217	68	252	171	29	65	78	147	329
Cr*	432	315	108	269	349	27	45	65	11	39	34	18	449
Cu*	55	44	36	43	37	6	27	31	---	7	5	11	88
Sc*	22	32	43	37	26	18	36	27	9	13	14	24	49
La	13.2	14.03	23.4	14.23	13.22	38.7	19.9	17.5	41	27.5	21.4	28.7	15.5
Ce	31	28.4	48.6	30.6	27.9	67.3	41.7	38.4	59.5	47.3	44.4	62.6	36.5
Pr	4.24	3.63	6.33	4.11	3.57	7.64	5.56	5.17	8.51	6.07	5.39	7.93	4.98
Nd	18.4	15.1	26.3	18.22	14.96	26.64	23.03	21.14	32.45	24.16	20.53	32.63	21.16
Sm	4.56	3.53	5.69	4.51	3.42	5.36	5.31	4.75	6.88	5.14	4.56	6.70	4.78
Eu	1.19	1.03	1.402	1.416	1.089	1.233	1.616	1.176	2.108	1.266	1.027	1.576	1.077
Gd	4.77	3.45	5.22	4.79	3.39	4.59	5.34	4.64	7.39	5.06	4.51	6.2	4.48
Tb	0.737	0.53	0.749	0.717	0.525	0.674	0.839	0.714	1.233	0.79	0.75	0.888	0.66
Dy	4.61	3.22	4.33	4.38	3.305	3.991	5.11	4.382	7.719	4.985	4.834	5.284	3.982
Ho	0.88	0.65	0.849	0.899	0.647	0.765	1.024	0.875	1.545	1.022	1	1.046	0.758
Er	2.37	1.80	2.32	2.52	1.80	2.14	2.98	2.45	4.29	2.98	2.97	2.97	2.06
Tm	0.31	0.255	0.321	0.348	0.257	0.313	0.42	0.372	0.602	0.434	0.448	0.42	0.282
Yb	1.84	1.57	2.12	2.21	1.58	2.01	2.63	2.37	3.69	2.86	2.86	2.65	1.83
Lu	0.254	0.221	0.302	0.302	0.225	0.295	0.373	0.352	0.507	0.42	0.418	0.397	0.262
Eu/ Eu*	0.77	0.76	0.90	0.92	0.77	0.71	0.76	0.69	0.90	0.74	0.78	0.93	0.98
La/Y	4.85	6.08	7.47	4.38	5.60	13.08	5.14	4.98	7.54	6.51	5.07	7.37	5.76
La/Th	6.91	6.38	4.83	6.88	5.8	6.18	3.53	3.31	6.85	4.26	2.35	4.2	5.19
Th/U	3.17	3.38	2.89	2.65	3.35	3.58	3.18	3.25	2.87	3.45	3.08	1.94	2.98

Table 5 (continued). Trace elements data for sandstones from the arc-related succession (ppm). XRF Data.

Sample	Sc	V	Cr	Cu	Zn	Ga	Rb	Sr	Y	Zr	Ba	Pb
J11	32	254	395	39	59	20	13.6	219	25.6	81.3	167	7
J12	94.6	74	34	10	35	15	94.6	204	21.2	145	515	9
TMX79	40	239	592	44	68	14	12	283	17.3	67.5	102	12
J21	14	65	26	6	13	11	69	387	20	92.4	431	---
J25	13	67	28	---	---	14	13	176	27	146	551	7
TMX31	26	202	99	18	45	19	39	223	29	147	811	12
TMX30	15	61	21	---	12	13	72	145	29	175	713	9
TMX116B	19	136	48	11	26	15	40.3	157	24	145	371	--
TMX17	10	25	17	---	---	10	85	372	46	135	3132	--
TMX123	21	7	18	11	22	11	47	384	26	152	517	7
TMX122	14	58	24	5	---	13	131	178	58	145	107	5
TMX15	11	35	25	---	--	12	82	189	25	152	828	5
TMX38	23	265	107	47	18	11	42	64	15	132	805	--
J90	48	290	367	75	40	17	--	265	22	90	1249	46
TMX19	15	54	27	--	---	16	61	219	25	127	1130	5

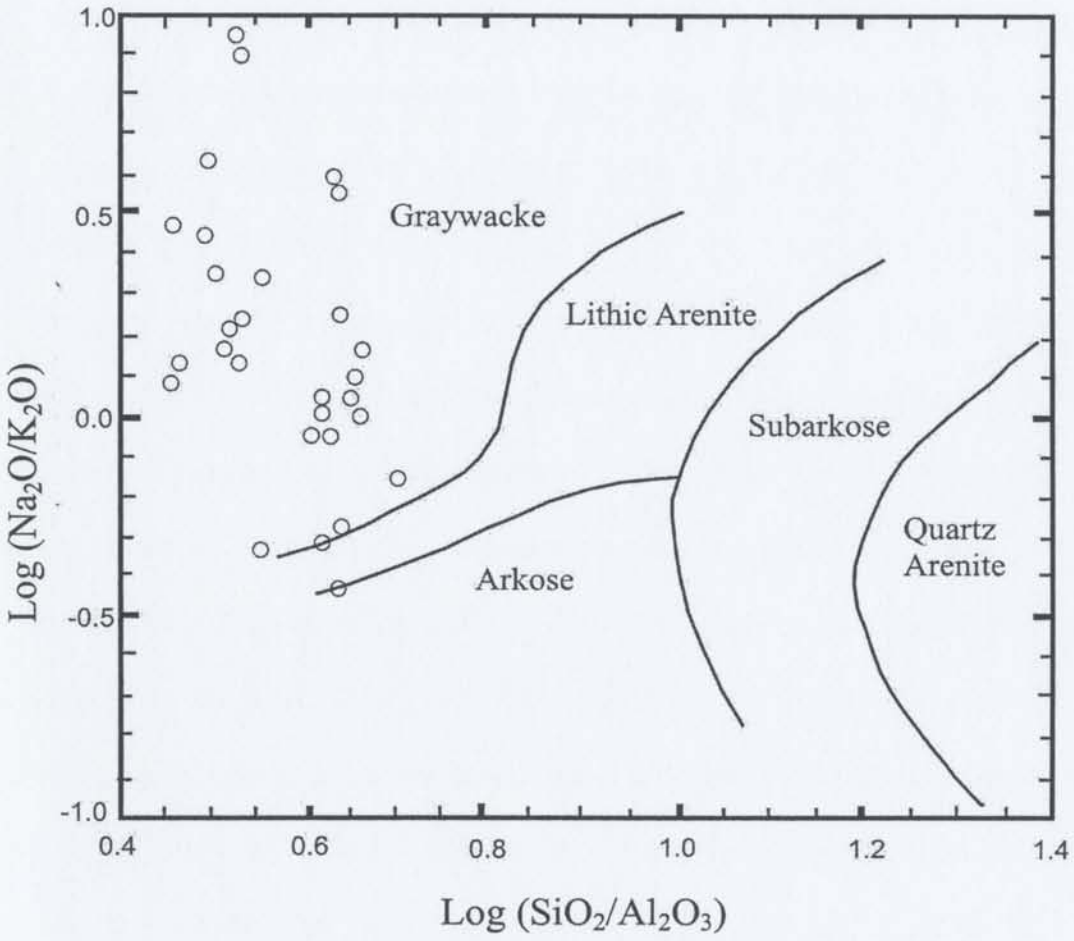

Figure 48. Chemical classification of volcaniclastic sandstones of the arc-related succession from Pettijohn et al. (1980). Data plotted from Table 5.

The major-element composition is also similar to that of sandstones from oceanic island arcs (Bhatia, 1983). FeO+MgO contents range from moderate to high, with mean values of 12.41 wt%. SiO_2 contents vary from 44–73 wt% with a mean of 56 wt%, while Al_2O_3 contents range from12–18 wt% with a mean of 15 wt%. SiO_2/Al_2O_3 ratio in the arc-related succession is relatively constant from 3.11–5 (mean 3.8). SiO_2/Al_2O_3 ratio is an indicator of maturity in clastic rocks (Bhatia, 1983; McLennan et al., 1993). Based on this indicator, rocks of the study area are chemically immature. Potassium and sodium are highly mobile during diagenesis and weathering in volcanic rocks (Nesbitt and Young, 1984). Na_2O and K_2O in the samples show variable abundances, ranging from 0.3–5.7 wt% and 1.7–5.7 wt%, respectively. This variability confirms the considerable alteration observed in thin sections. The K_2O/ Na_2O ratio is highly variable from 0.11–3.0 (mean 0.9). The chemical index of alteration (CIA) has been established as a guide to the degree of weathering of the source rocks and diagenesis (Nesbitt and Young, 1984). Unweathered igneous rocks have values of 50 (McLennan et al., 1993). The CIA for samples of the arc-related succession (Table 5) ranges from 27–59 with a mean of 46.8, indicating a moderate (51–59) to low (<50) degree of alteration.

Because the CIA values indicate limited alteration, major elements might be useful indicators of source-rock composition for the arc-related succession. On a K_2O vs. SiO_2 (Figure 49A), the samples plot in the calc-alkaline field for rocks with medium to high potassium. An FeO/MgO vs. SiO_2 plot (Figure 49B) shows that the igneous source rocks fall in the calc-alkaline and tholeiitic fields. Volcaniclastic sands and sandstones of the Izu-Bonin arc studied by Hiscott and Gill (1992) show a similar pattern to the

samples from the arc-related succession. Finally, an MgO vs. SiO_2 plot (Figure 49C) shows that the samples are predominately basaltic to andesitic in composition, while some samples plot in the dacite to rhyolite field.

The major-element geochemistry suggests that volcaniclastic rocks of the arc-related succession were derived from a calc-alkaline and tholeiitic, basalt to andesite source. The source also contained minor dacite and rhyolite. Talavera (1993) studied the mineral chemistry and geochemistry of the lavas in the Teloloapan area, and recognized mainly basalt and andesite compositions, with scattered dacite-rhyolite rocks. However, a calc-alkaline affinity for the lavas was recognized. Petrographic data gathered for this thesis research also illustrate that volcanic lithic fragments in the arc-related succession were derived predominately from basalt and andesite sources (microlitic and lathwork textures). Minor amounts of felsitic grains indicate a less important felsic source.

Trace and rare earth elements. Trace elements and rare earth elements (REE) have been used as indicators of source and degree of fractionation of the source in volcaniclastic sequences (Floyd and Leveridge, 1987; McLennan et al., 1990, 1993; McLennan and Taylor, 1991). Two cross-plots (La/Th vs. Hf and Th/Sc vs. Zr/Sc) and the REE spidergram are used to infer the source and fractionation of the source in the arc-related succession.

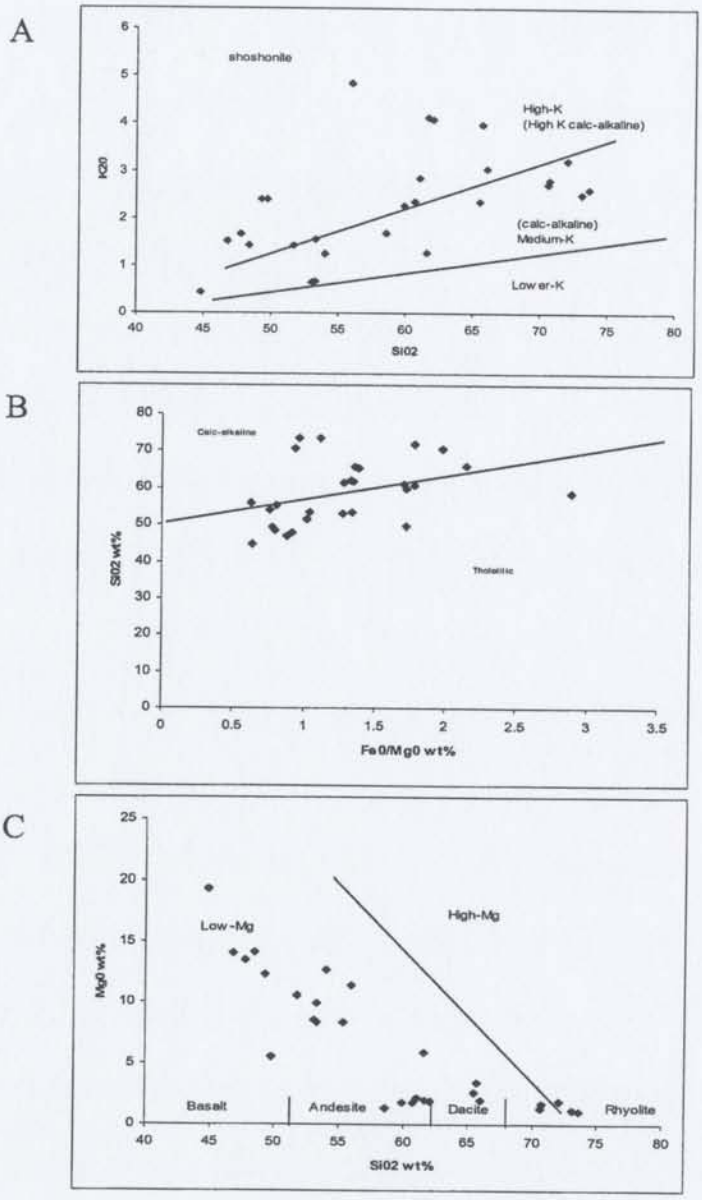

Figure 49. A. Potash vs. silica. The dividing lines between fields are from Pecerillo and Taylor (1976). B. Silica vs. FeO/MgO. The dividing line between tholeiitic and calc-alkaline are from Miyashiro (1974). C. MgO vs. Silica. Boundaries between volcanic rocks are from Taylor (1969). The boundary between the low- and high-Mg fields is from Taylor, Fujioka, et al. (1990). Data plotted from Table 5.

Floyd and Leveridge (1987) used the La/Th versus Hf diagram to discriminate among different arc components and sources for Devonian sandy turbidites. In Figure 50A, the samples fall in the field of andesitic arc and mixed felsic/basic sources, showing moderate La/Th ratios and low contents of Hf. The diagram illustrates an evolution from a predominately mafic source to a minor felsic source in the arc-related succession.

McLennan et al. (1993) used a plot of Th/Sc against Zr/Sc as a good indicator of igneous chemical differentiation processes and zirconium enrichment, respectively. The Th/Sc vs. Zr/Sc diagram (Figure 50B) shows a clear trend of igneous differentiation of the source rocks from basalt to dacite. There was no zirconium addition during the evolution of the rocks (cf. McLennan et al., 1993), suggesting no reworking to concentrate sedimentary zircon.

Results from REE analysis support a predominantly mafic source for the samples of the arc-related succession (Figure 51). These show an enriched light REE pattern (La_N/Yb_N = 4.38–13.08, mean 6.46), a strong negative Eu anomaly (Eu/Eu*=0.69–0.93, mean 0.82), and a relatively flat and uniform concentration of heavy REE. The Eu anomaly is the typical result of plagioclase fractionation in the source magmatism. Eu/Eu* represents the Eu value expected for a smooth chondrite-normalized REE pattern and Eu-anomalies are calculated as $Eu_N/[(Sm_N)(Gd_N)]^{1/2}$ (McLennan et al., 1990).

The REE patterns are characteristic of basalts and andesites from medium- to high-K calc-alkaline magmatic suites (Gill, 1981; McLennan et al., 1990, 1993).

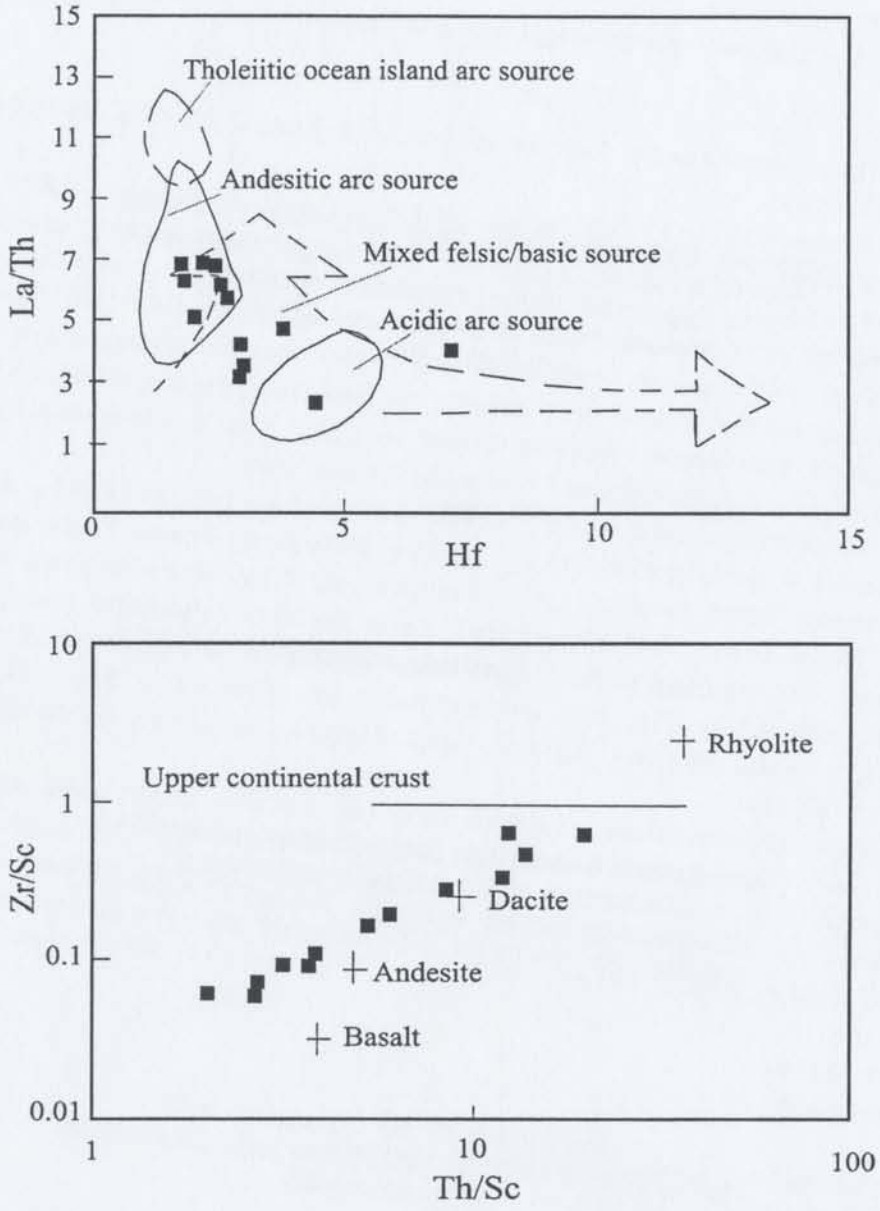

Figure 50. Source rock discrimination diagrams. A. La/Th vs. Hf from Floyd and Leveridge (1987). B. Zr/Sc vs. Th/Sc from McLennan et al. (1993). Plutonic equivalents from Wallin (2003). Data plotted from Table 5.

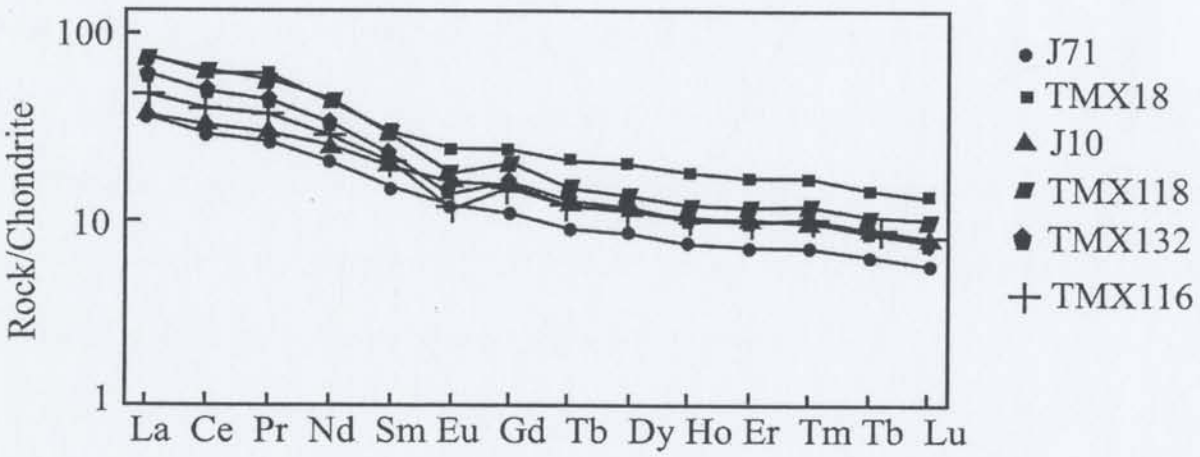

Figure 51. Chondrite-normalized REE pattern for the arc-related succession. Normalizing values from Taylor and McLennan (1985). Data plotted from Table 5.

5.2.3. Arc evolution

Talavera (1993) and Talavera et al. (1995) documented that volcanic rocks in the Teloloapan subterrane are mainly basalts in the lower stratigraphic levels (petrographically, the lower division, which is the lower and middle part of the Villa Ayala Formation), while the upper levels (here the upper division, which is the upper part of the Villa Ayala and the Acapetlahuaya formations) are basalts and andesites with minor rhyolites. Petrography and geochemistry of volcaniclastic rocks reported in this thesis confirm this evolution. Volcaniclastic sandstones in the lower part of the succession are compositionally derived from basalts and andesites, while the upper division is mainly derived from basaltic andesites–rhyolites.

The vertical evolutionary trend in the arc-related succession is well defined using petrography and geochemistry. Stratigraphy of the arc-related succession (see chapter 2) shows that the lower stratigraphic levels are predominantly primary volcanic rocks: basaltic pillow lavas and other flows. These lavas are interbedded with tuffs and epiclastic sandstones of the petrographic lower division, which mainly mimic the basaltic composition of the source (lithic grains with microlitic textures) with a small contribution from andesites (lathwork and microlitic textures). Petrographically, the upper division shows a decrease in microlitic volcanic fragments, while lithic grains with lathwork textures persist. Felsitic volcanic fragments increase as a proportion of the volcanic lithic fragments, suggesting that a felsic source was added to the basalt-andesite source, which supplied the lower division. Ternary diagrams clearly show this change in grain population in the arc-related succession (Figures 42 and 46).

Geochemical data support the petrographic evolution. Major elements of the volcaniclastic rocks in the lower division show a basic composition (SiO_2=48–55%, Al_2O_3=13–17%, FeO=10–12%, MgO=9–14%, volatile free basis; see Figures 49 and 50). The chondrite-normalized REE patterns are highly enriched in LREE similar to the patterns for andesites and basalts from medium- to high-K calc-alkaline magmatic series (Figure 51). K_2O versus silica diagram (Figure 49A) supports a volcanic source with these characteristics. In contrast, volcaniclastic samples from the upper division are more felsic in composition (SiO_2=66–72%, Al_2O_3=14–16%, F_2O=2–4%, MgO=1–3%, volatile free basis; see Figures 49 and 50). REE patterns for the felsic source are likely similar to those for basic rocks. However, samples that could be assigned to a felsic source show a strong negative Eu anomaly, attributed to fractionation of plagioclase in the source.

Sandstone provenance and geochemical data in the arc-related succession can be interpreted as indicators of an intra-oceanic arc, consistent with the results of facies analysis (see chapter 4). An intra-arc setting is likely similar to that of an immature back-arc basin. Intra-arc basins are located within or on the spine of the arc, while back-arc basins are situated behind the arc front (cf. Smith and Landis, 1995). Considering that only few examples of ancient intra-arc settings have been reported, the rocks of the arc-related succession are instead compared with those of back-arc basins. Petrography and geochemistry of the volcaniclastic samples of the arc-related succession share features with backarc settings reported in the literature (Marsaglia and Ingersoll, 1992; McLennan et al., 1990; Hiscott and Gill, 1992). The petrographic lower division represents the early evolution of mafic volcanism in the arc, showing the same characteristics reported for

intraoceanic arcs by Marsaglia and Ingersoll (1992), while the more felsic composition of the upper division can be interpreted as a change to an evolved or mature intra-oceanic arc with calc-alkaline affinity. Trace elements and REE (Th/Sc=0.1–0.67; Th/U=1.94–3.45; La_N/Yb_N=4.38–13.08; Eu/Eu*=0.69–0.93) in the arc-related succession show features similar to those observed in back-arc settings as reported by McLennan et al. (1990) and Hiscott and Gill (1992).

5.3. PETROGRAPHY AND GEOCHEMISTRY OF THE SEDIMENTARY COVER SUCCESSIONS

5.3.1. The Mezcala Formation

Petrography. Sandstones of the Mezcala Formation are moderately to poorly sorted mainly feldespathic litharenites and minor litharenites (Q30; F23; L47, cf. Folk, 1974; Table 3) and calclithites (>64% carbonate fragments; cf. Folk, 1959; Table 3).

Volcanic and sedimentary fragments are the dominant lithic component in the Mezcala Formation. Volcanic lithic fragments (Lv) form ~30% of the lithic population, and show microlitic and felsitic textures (Figures 52A and 53A). There are subordinate volcanic lithic lathwork fragments. Volcanic lithic microlitic texture shows plagioclase microlites contained in an aphanitic groundmass. Volcanic lithic fragments showing felsitic microlitic texture are also found in the samples of the Mezcala Formation. Felsitic texture consists of a microgranular groundmass of feldspar and quartz. Finally, lathwork

volcanic grains show plagioclase laths in a seriated, microlitic, and microgranular groundmass.

Sedimentary lithic fragments (Ls) are common throughout the Mezcala Formation (Figures 52B and 53C). They are predominately carbonate (Lsc) and scattered sandstone and siltstone fragments. Lithic carbonate fragments form ~15% of the quartzolithic sandstones, but they are higher (65–90% of the lithic population) in the calclithites (see Figure 54). Lithic carbonate fragments include fine-grained limestone and dolostone. Microfossils are also commonly found (Figure 53C).

Quartz (~30%, Figures 52A and 53A) is mainly subangular transparent grain with undulose and straight extinction, sometimes showing embayments and without inclusions. This variable also includes subordinate microcrystalline quartz (chert, Ch) and polycrystalline quartz (Qp).

Feldspar crystals are both altered and unaltered euhedral and subhedral plagioclase and minor potassium feldspar (Figure 53B). Microscopic identification of plagioclases is difficult because of the high alteration in the samples, but in unaltered samples plagioclases vary from bytownite to labradorite based on the Michel-Levy method.

Petrofacies. Sandstones of the Mezcala Formation can be divided into quartzolithic and calclithite suites (Figure 54). No vertical trend is proposed in the Mezcala formation because of the strong structural deformation.

Table 3. Recalculated modal point counts (as percents) for the Mezcala Formation. Geographic and stratigraphic location of each sample is presented in Appendix 12. Numbers of grains counted in parentheses.

Sample	QFL			QpLvLs			QmLssLsc			QpLssLsc		
Number	Q	F	L	Qp	Lv	Ls	Qm	Lss	Lsc	Qp	Lss	Lsc
TMX09	43	26	31(404)	20	40	40(165)	74	6	20(248)	–	–	–
TMX06	37	27	36(420)	17	38	45(174)	67	3	30(219)	24	7	69(103)
TMX23	33	28	39(4160	9	37	54(174)	54	7	39(247)	14	15	71(110)
TMX143	29	18	53(439)	11	40	49(252)	51	7	42(248)	12	13	75(140)
TMX03	29	15	56(427)	12	46	42(278)	52	8	40(128)	18	13	69(142
TMX148	31	25	44(426)	14	57	29(236)	68	3	29(213)	32	7	61(102)
TMX146	35	28	37(461)	20	71	9((187)	89	8	3(159)	–	–	–
TMX46	34	36	30(408)	17	79	4(148)	95	2	3(118)	–	–	–
TMX47	15	22	63(400)	8	59	33(284)	40	9	51(158)	18	12	70(116)
TMX112	32	21	47(404)	9	61	30(213)	67	6	27(158)	–	–	–
TMX145	23	13	64(427)	10	65	25(303)	56	13	31(173)	29	21	50(107)
TMX09A	26	21	53(404)	14	64	22(250)	65	3	32(160)	–	–	–
TMX143A	26	15	59(406)	9	59	32(264)	55	5	40(188)	–	–	–
TMX11	4	1	95(400)	1	3	96(384)	3	2	95(380)	1	2	97(372)
TMX12	5	3	92(400)	0	4	96(368)	5	0	95(372)	0	0	100
TMX147	8	13	79(400)	0	19	81(316)	11	0	89(288)	0	0	100

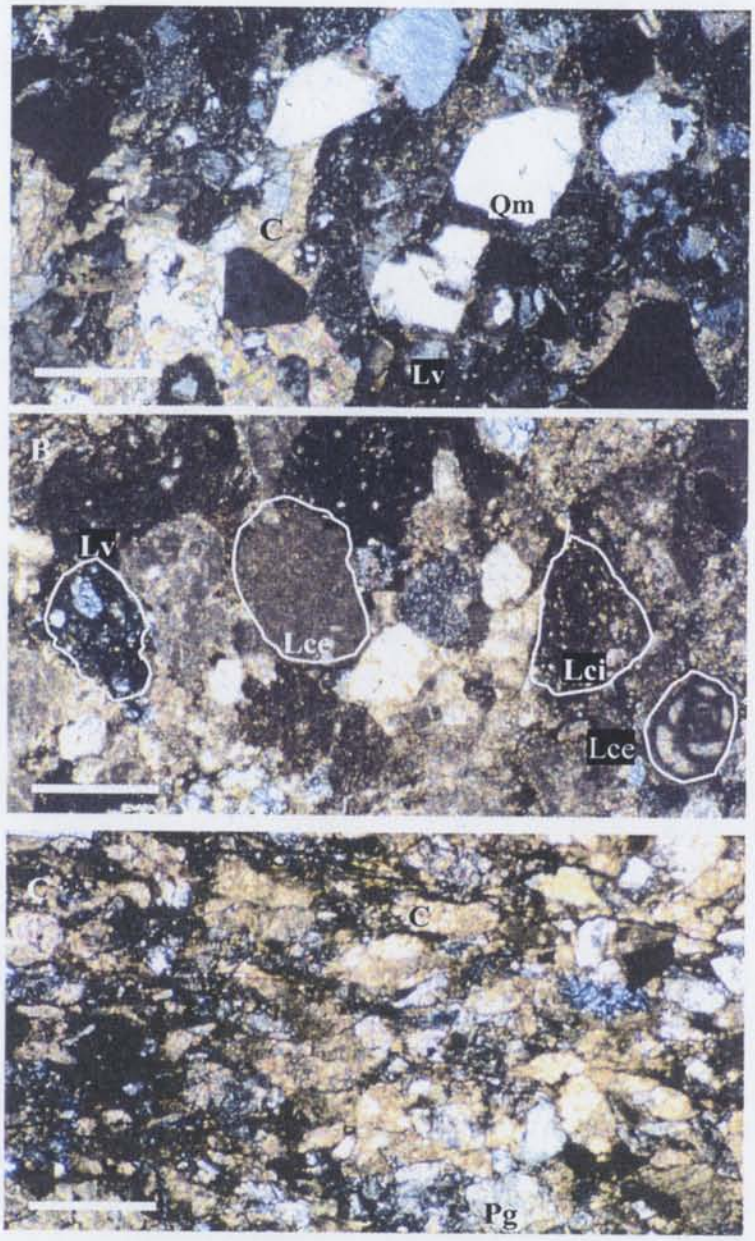

Figure 52. Photomicrographs of sand grains from the Mezcala Formation. Scale bars = 0.25 mm. A. Monocrystalline quartz (Qm) and volcanic fragments (Lv) in the quartzolithic suite (TMX146). B. Intrabasinal (Lci) and extrabasinal (Lce) carbonate grains in the quartzolithic suite. (TMX03). C. Altered plagioclase (pg) and calcite cement (C). (TMX07). Calcite cement is present in all the photomicrographs.

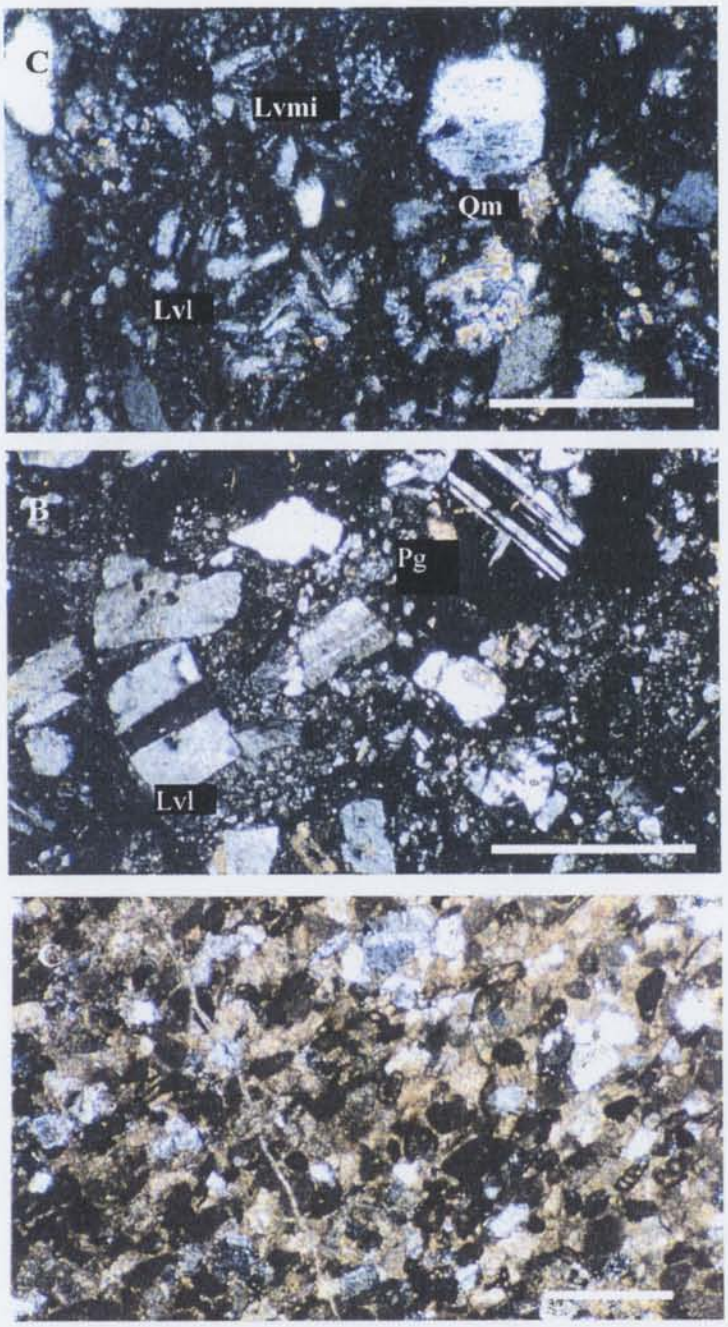

Figure 53. Photomicrographs of sand grains from the Mezcala Formation. Scale bars = 0.25 mm. A. Volcanic lathwork texture within microlitic (Lvl and Lvmi) groundmass of grains (outlined).. B. Plagioclase (Pg) in felsitic groundmass and monocrystalline quartz. (TMX147). C. Extrabasinal carbonate fragments and monocrystalline quartz in the calclithite suite (TMX03).

Quarzolithic suite. Sandstones of the quartzolithic suite are dominant in the Mezcala Formation and they are mainly found in the north and central area of the Pachivia valley. This suite plots in the middle area of a standard QFL ternary diagram (Figure 54A; Q30;F23;L47). The predominance of volcanic over sedimentary lithic fragments is illustrated in a QpLvLs ternary diagram (Figure 54B), where two main populations are observed: volcanic-rich and sedimentary-rich (see Table 3). Most of the samples point counted (13) show a high amount of volcanic lithic fragments with microlitic, felsitic and minor lathwork volcanic textures, while five samples are dominated by lithic sedimentary fragments, mainly carbonate and scattered sandstone and siltstone fragments.

Volcanic lithic fragments vary from 14–46% in the quartzolithic suite, while lithic carbonate ranges from 1–25%. The anomalous amount of carbonate fragments observed in the Mezcala Formation is not usual in quartzolithic rocks. Ingersoll et al. (1987) described similar carbonate proportions in sandstones from southwestern Montana, and suggested the term impure calclithite for sandstones containing less than 50% carbonate grains.

Calclithite suite. Folk (1959) defined a "calclithite" as a terrigenous sandstone containing more than 50% carbonate fragments derived by erosion of preexisting limestones. In contrast, Zuffa (1980) proposed the term "hybrid arenite" for a sandstone containing intrabasinal and extrabasinal detritus. Although a predominant extrabasinal origin is expected for the carbonate fragments in the calclithites of the Mezcala

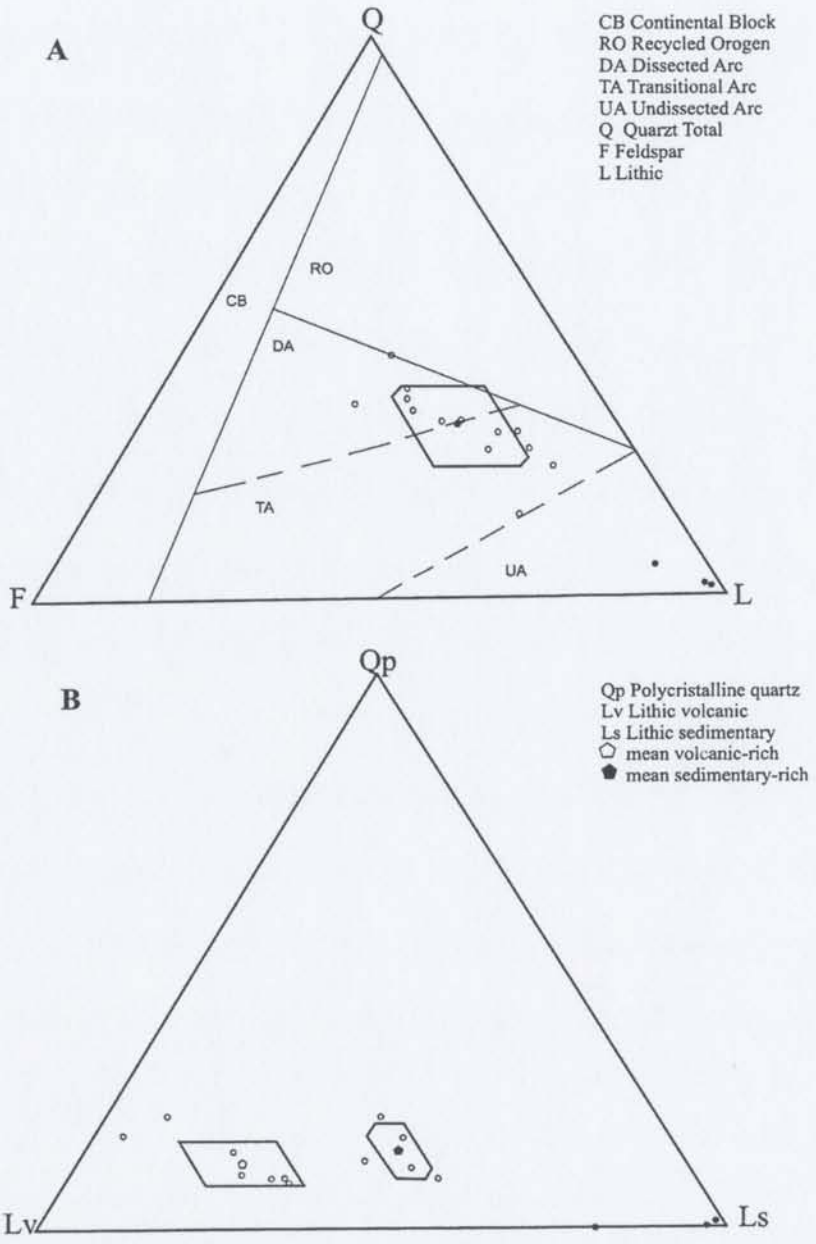

Figure 54. Ternary diagram for the Mezcala Formation sandstones from Table 3 data. Polygons show mean and standard deviation of the quartzolithic suite (white circles). Calclithite proposed samples are black circles. Tectonic settings are from Dickinson (1985). In B polygons show volcanic- and sedimentary-rich populations.

Formation no attempt was made to fully document the intrabasinal and extrabasinal origin of the carbonates, following Zuffa (1980). For this reason, the more generic term calclithite is preferred instead of using the hybrid arenite classification

The calclithite suite has a random occurrence throughout the Mezcala Formation, although it is mainly found in the central and southern parts of the Pachivia Valley. This suite was extensively sampled (30 samples) but because of their homogeneous petrographic features only three samples were point counted. Those plot in the L apex of the QFL and QpLvLs ternary diagrams (see Figure 54). These samples contain a dominant percentage of carbonate lithic population (65–90%) of the whole rock with variable amounts of monocrystalline and polycrystalline quartz grains (1–8%), plagioclase (1–13%) and volcanic lithic fragments (3–15%). Calcite cement is wide spread in the sandstones of the Mezcala Formation; however, carbonate fragments in the calclithite suite can be distinguished from the cement based on textural relationships with surrounding grains, composition (altered versus pristine cement), and presence of included fossils older than the host rock (see Figures 52B and 53C; cf. Zuffa, 1980; Ingersoll et al., 1986).

Source. Petrographic analysis is applied to suggest that sandstones of the Mezcala Formation were derived from older formations exposed in the Teloloapan subterrane and surrounding areas. Volcanic lithic fragments are texturally similar to the basic and felsic rocks observed in the arc-related succession. Characteristics observed in monocrystalline quartz such as euhedral shape, embayments and clear transparency, as well as

composition of plagioclases, support derivation from a mafic to intermediate volcanic source. Volcanic lithic felsitic fragments were derived from a felsic source.

Petrographic features of the carbonate lithic fragments suggest they were derived from an extrabasinal carbonate source, likely preexisting carbonate-platform rocks of the Morelos and Teloloapan formations, which underlie the Mezcala Formation. Some carbonate fragments show textures similar to the thin-bedded limestone member of the Mezcala Formation, suggesting that some carbonate grains are intrabasinal in origin. An intrabasinal source is also inferred for the scattered lithic sandstone and siltstone fragments.

5.3.2. Petrographic description, petrofacies, geochemistry and provenance of the Miahuatepec Formation

5.3.2.1. Petrographic description, petrofacies, and source

Petrography. Sandstones of the Miahuatepec Formation are poorly to moderate sorted, medium- to very coarse-grained feldespathic litharenites (Q35; F21; L44; cf. Folk, 1974), highly altered, with petrographic matrix ranging from 10–16%.

Lithic fragments are the predominant grain type in sandstones of the Miahuatepec Formation, varying from 39–50%. Approximately 95% of the lithic population is volcanic, the rest being sedimentary lithic (Table 4). Volcanic lithic fragments show mainly microlitic and felsic microlitic textures, subordinate lathwork and felsitic textures (Figure 55). Because of the degree of alteration, there is some uncertainty as to whether

some grains counted as felsic microlitic and felsitic grains might be chert. Even if chert is more abundant than what is reported in Table 4, these rocks would never be volcanolithic sandstones.

Lithic sedimentary fragments form <5% of the lithic population. They are mainly carbonate, sandstone and siltstone fragments. Carbonate fragments (Figure 56C) were recognized following petrographic criteria recommended by Zuffa (1980), such as textural relationships with surrounding grains, alteration of the grains which distinguish them from pristine cement. A separation of intrabasinal and extrabasinal carbonate fragments was not attempted because the thin-bedded limestone of the Miahuatepec Formation (intrabasinal source) is petrographically similar to limestones of the Amatepec Formation (likely extrabasinal source). However, the former is characterized by more intense diagenesis, such as recrystallization. Sandstone fragments show fine grains of quartz and feldspar within a clay matrix, while siltstones contain silt- and very fine sand-sized quartz and feldspar with abundant clay matrix (Figure 55B). Some sedimentary grains (<1%) show an advanced degree of pressure solution and an incipient planar foliation. However, they are assigned to the sedimentary population instead of a metamorphic category because of the lack of metamorphic minerals.

Quartz grains (28–42%) are subangular to subrounded, monocrystalline quartz with undulose to straight extinction. Because of the deformation, some monocrystalline quartz shows sutured contacts and pressure shallows parallel to the foliation of the rock (Figures 55A and 56A).

Table 4. Recalculated modal point counts (as percentages) for the Miahuatepec Formation. Geographic and stratigraphic location of each sample is presented in Appendix 18. Numbers of grains counted in parentheses.

	QFL			QmFL			QpLvLs		
Sample	Q	F	L	Qm	F	L	Qp	Lv	Ls
TMX69	28	23	49(500)24	23	53(500)		9	91	0(266)
TMX67	38	21	41(500)31	21	48(500)		13	81	6(239)
M32B	31	24	45(500)25	24	51(500)		12	84	4(256)
TMX52	37	21	42(500)30	21	49(500)		14	81	5(246)
TMX58	28	25	47(500)23	25	52(500)		11	86	3(262)
TMX70	36	23	41(500)26	23	51(500)		20	70	10(255)
TMX57	35	20	45(500)28	20	52(500)		13	80	7(234)
TMX51	40	18	42(500)27	18	55(500)		24	65	11(278)
TMX164A	42	19	50(470)32	19	49(470)		21	73	6(232)
TMX162A	39	22	39(500)32	22	46(500)		15	81	4(323)
TMX160	31	19	50(440)23	19	58(440)		12	85	3(254)
TMX65	35	23	42(500)27	23	50(500)		16	80	4(250)
M34A	38	16	46(457)31	16	53(457)		13	76	11(241)
TMX68	39	17	44(486)33	17	50(486)		12	79	9(243)
TMX53	36	20	47(423)29	17	54(423)		12	81	7(227)
TMX55	33	20	47(464)27	20	53(464)		12	83	5(245)
Mean	35	21	44	28	21	52	14	80	6
Standard Deviation	4	3	3	3	3	3	4	6	3

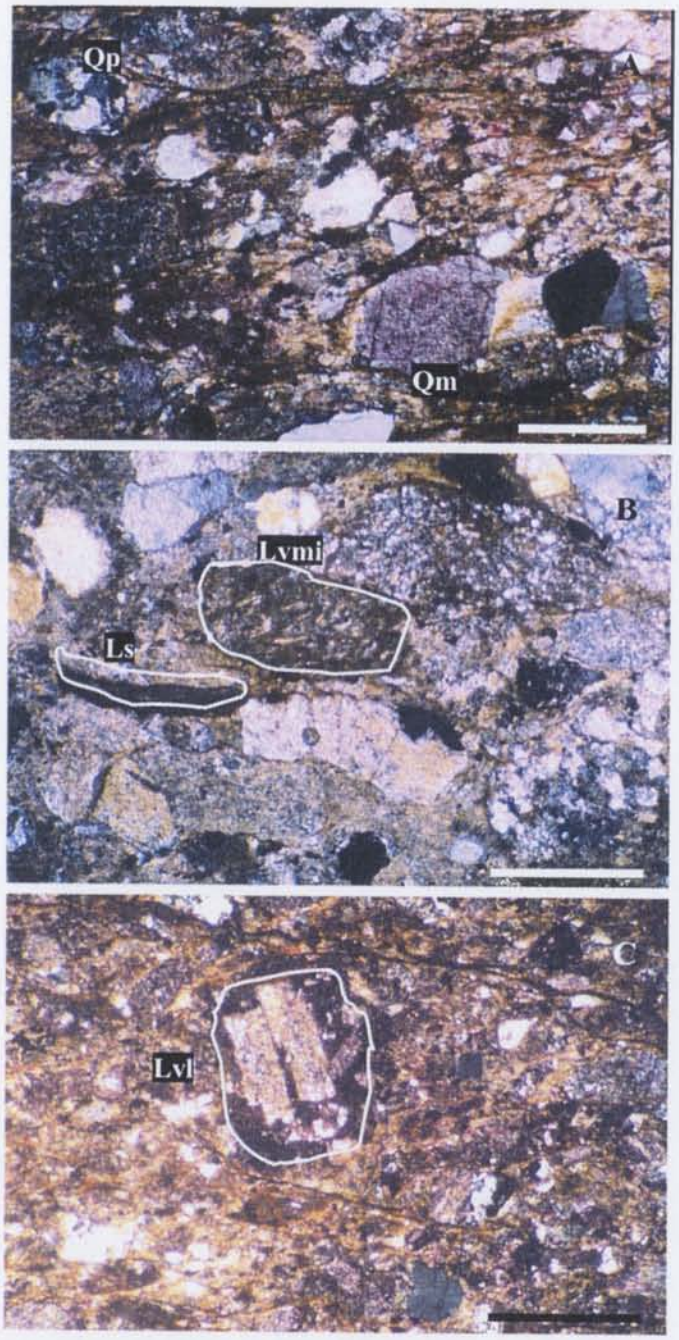

Figure 55. Photomicrographs of sand grains from the Miahuatepec Formation. A, Monocrystalline (Qm) and polycrystalline quartz (Qp). Sample TMX51. B, Volcanic lithic fragments with microlitic (Lvmi) texture. Sample TMX53. C.,Volcanic lithic grain with lathwork texture (Lvl). Sample TMX65. Scale bars = 0.25 mm.

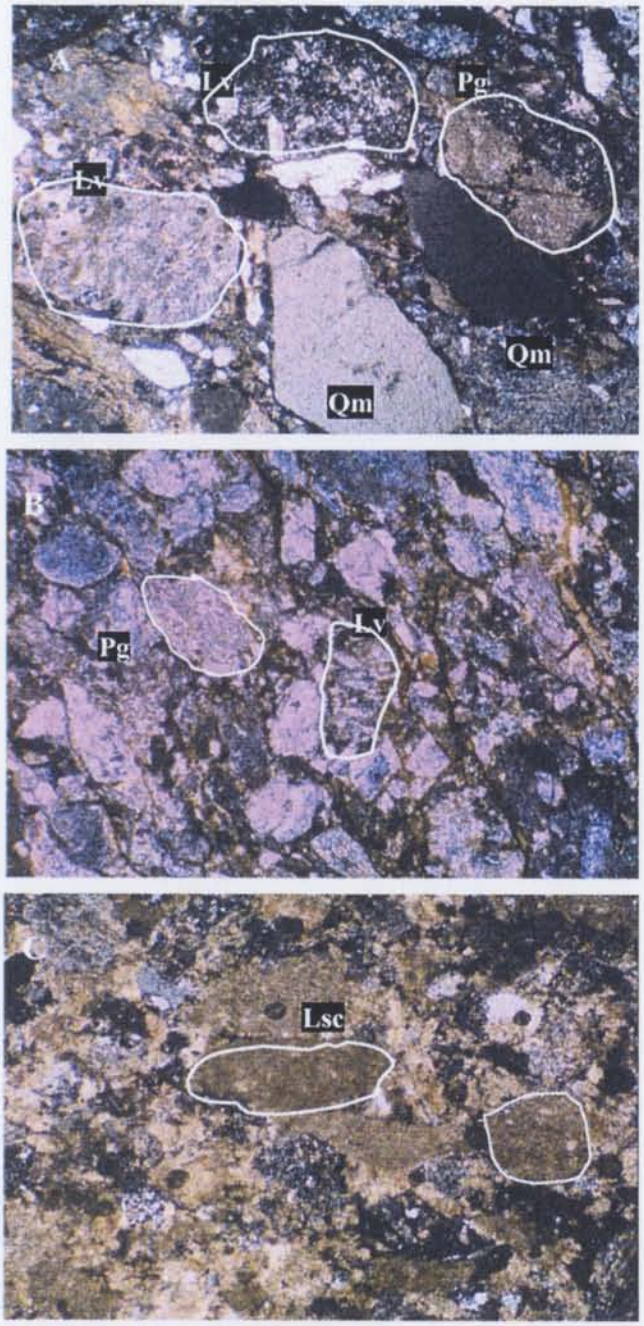

Figure 56. Photomicrographs of sand grains from the Miahuatepec Formation. A, Monocrystalline quartz (Qm), lithic volcanic grain (Lv) and altered feldspar (Pg). Sample TMX67. B, Altered feldspars (Pg) and lithic volcanic grains (Lv). Sample TMX52. C, Lithic carbonate fragments (Lsc). Sample TMX164A. Scale bars = 0.25 mm.

Microcrystalline quartz (chert) and polycrystalline quartz are also found in minor proportions (see Table 4). Some polycrystalline quartz shows crystal elongation, which is interpreted as the result of deformation of the sandstones. No metamorphic features such as foliation and development of micas were observed in these grains.

Feldspar crystals form 15–25% of the grain population. They are mainly highly altered plagioclase and minor potassium feldspars (Figure 56A and B). Microscopic identification of the variety of plagioclase is difficult because of the strong alteration and deformation in the samples. The alteration makes the crystals appear cloudy. Albitization and seritization is the most common alteration in feldspars.

Petrofacies. Based on the significant amounts of quartz, feldspar, and lithic fragments, sandstones of the Miahuatepec Formation are assigned to one dominant quartzolithic petrofacies (Figure 57). The samples of this quartzolithic suite plot in the middle area of a standard QFL ternary diagram, close to the Q–L join (Figure 57). A similar pattern is observed on the QmFLt ternary diagram (Figure 58A), where chert and polycrystalline quartz grains are included in the lithic category. The predominance of volcanic lithic fragments over polycrystalline quartz and sedimentary lithic fragments is well illustrated on a QpLvLs ternary diagram (Figure 58B), where the samples predominantly plot close to the Lv pole.

The lack of fossils and the strong deformation observed in the Miahuatepec Formation does not provide the stratigraphic control needed to illustrate a vertical petrographic trend. Most of the sandstones with >35% quartz were sampled in the

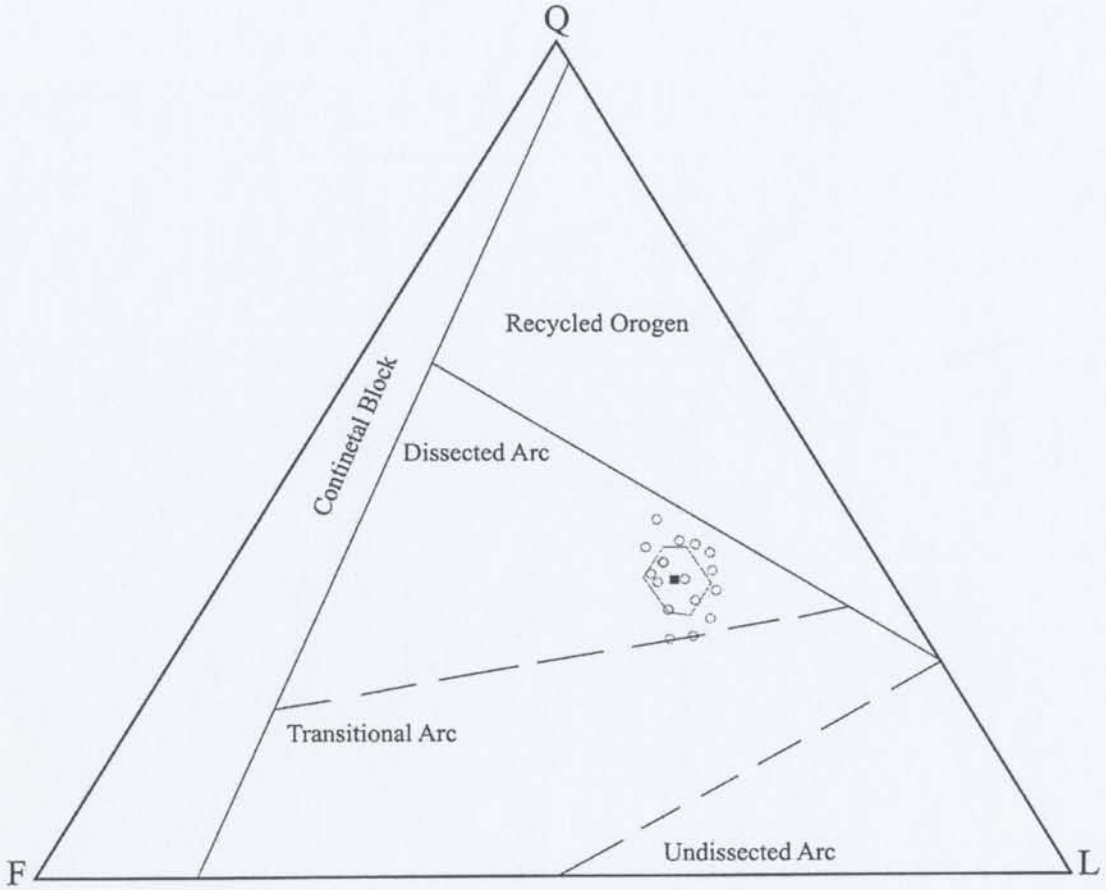

Figure 57. QFL ternary diagram of the Miahuatepec Formation sandstones. Data from Table 4. Polygons show mean (filled square) and one standard deviation for the quartzolitic petrofacies (open circles). Tectonic settings from Dickinson (1985).

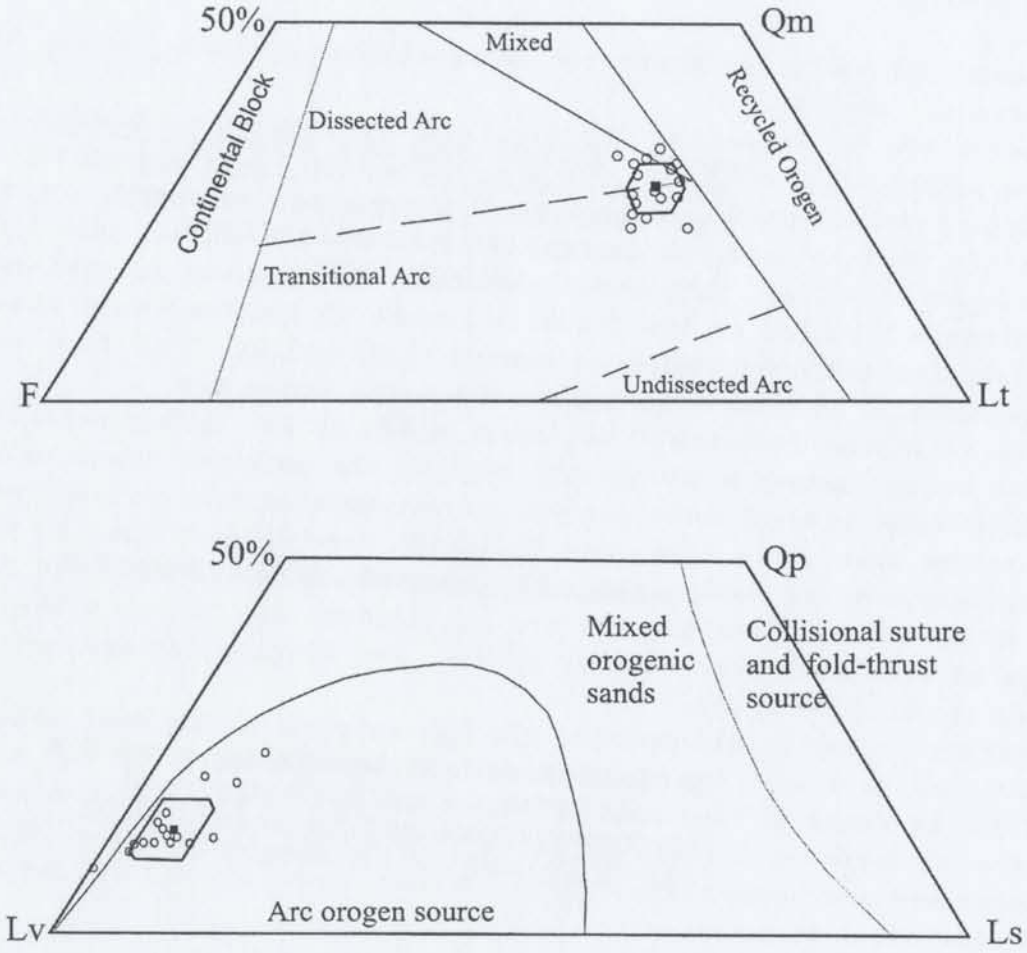

Figure 58. Ternary diagram plots of the Miahuatepec Formation sandstones. Data from Table 4. A. QmFLt plot. B. QpLvLs plot. Polygons show standard deviation and full squares mean of the quartzolithic petrofacies (open circles). Fields from Dickinson (1985).

northern portion of the Miahuatepec Formation, while samples with <35% quartz were sampled in the southern part of the formation. This spatial variation might result from the exposure of different stratigraphic levels in the two areas.

Source. The predominance of lithic volcanic fragments associated with moderate amount of quartz and less feldspar in the sandstones of the Miahuatepec Formation suggests a mostly volcanic source with a minor contribution from the erosion of sedimentary rocks. Volcanic lithic fragments are predominantly grains with microlitic and felsic microlitic textures. These volcanic textures have been reported in basalts through andesites (Dickinson, 1970; Critelli et al., 2002). The minor amounts of volcanic lithic fragments with lathwork textures also suggest an andesitic source, while felsitic textures are indicative of rhyolites. The Miahuatepec Formation is in between two volcanogenic areas, the Teloloapan subterrane to the east and the Arcelia – Palmar Chico subterrane to the west. Both sequences are made up of volcanic rocks with basalt–andesite composition.

Petrographic features observed in monocrystalline quartz also support a volcanic origin for the quartz population, while the polycrystalline quartz (chert fragments) might be derived from the uppermost level of the Arcelia – Palmar Chico subterrane that is composed of radiolarian chert. The same level contains black shale that could account for the scattered siltstone fragments identified in the sandstones of the Miahuatepec Formation. Carbonate fragments are derived either from the Amatepec Formation or from the thin–bedded limestone of the Miahuatepec Formation itself, as intrabasinal particles.

Finally, the scattered sedimentary siliciclastic fragments are considered to be intraformational in origin.

5.3.2.2. Geochemistry and source

Major elements. Major elements whole rock analyses of are shown in appendix 17. Table 6 lists volatile-free percentages, where the data are recalculated to 100% ignoring LOI. The CIA values for sandstones of the Miahuatepec Formation vary from 25–90 with a mean of 53. These values indicate that almost half of the sandstones of the Miahuatepec Formation have a high degree of alteration (see Table 6), which is consistent with the petrographic observations. The major elements are only used in a general way to illustrate the lithologic classification and variation of the major elements in the Miahuatepec Formation. On subsequent diagrams, samples with values of CIA greater than 60 are shown with a different symbol

Following the chemical classification of Pettijohn et al. (1987), the sandstones of the Miahuatepec Formation fall in the greywacke field, while two samples with high CIA values plot in the arkose field (Figure 59). The considerable scatter of Na_2O/K_2O in Figure 59 illustrates the high mobility of these major elements, while SiO_2/Al_2O_3 show little variation in samples of the Miahuatepec Formation. The relatively low and uniform values of SiO_2/Al_2O_3 and widely variable K_2O/Na_2O suggest an immature composition for sandstones of the Miahuatepec Formation (cf. Bhatia, 1983; McLennan et al., 1993).

Table 6. Recalculated major-elements (wt %; volatile-free), trace and rare earth elements (ppm) data for sandstones of the Miahuatepec Formation.

Sample	TMX51	TMX55	TMX162A	TMX57	TMX164A	TMX68	TMX160	TMX65	TMX70	TMX69	TMX53	TMX58	TMX67	M34	M33B
SiO_2	53.26	72.10	60.59	58.80	73.99	70.72	65.90	73.61	58.65	61.06	74.09	65.10	70.13	62.57	58.09
TiO_2	1.1	0.52	0.76	0.59	0.37	0.56	0.53	0.40	1.11	0.90	0.37	0.70	0.60	0.70	0.67
Al_2O_3	15.72	16.65	14.60	12.74	15.89	16.54	15.05	16.11	18.30	18.3	15.94	16.31	16.42	16.42	14.75
Fe_2O	11.42	3.34	3.29	4.07	2.95	2.66	4.29	1.28	4.47	3.82	2.94	6.93	4.01	4.60	7.08
MnO	0.16	0.03	0.05	0.12	0.03	0.03	0.04	0.01	0.08	0.06	0.03	0.04	0.03	0.06	0.09
MgO	8.43	1.89	2.00	1.42	1.75	1.36	2.02	1.20	2.21	2.21	1.64	3.28	1.69	1.96	4.68
CaO	3.57	0.50	13.68	17.90	0.73	2.88	7.26	2.05	8.50	6.66	0.67	2.11	1.38	9.94	9.35
Na_2O	5.50	1.70	2.44	2.60	1.51	2.46	1.76	2.68	3.49	4.06	1.54	3.41	3.22	2.15	3.90
K_2O	0.69	3.19	2.42	1.68	1.51	2.72	3.07	2.60	3.06	2.83	2.71	2.03	2.44	2.40	1.26
P_2O_3	0.14	0.08	0.06	0.07	0.07	0.07	0.07	0.05	0.12	0.10	0.07	0.08	0.07	0.08	0.13
CIA	49	70	32	25	70	58	44	91	43	46	70	58	61	39	37
Rb	13.5	106	70	49	78	82	101	84	81	84	79	67	79	72	24
Sr	221	136	389	378	132	143	202	211	211	213	133	194	502	237	438
Ba	168	502	413	393	750	566	410	621	778	750	618	464	502	531	203
Zr	82	76.30	157	70.8	155	84	59.3	70	151	152	71	68	82	157	102
Nb	13	9	11	7.5	7.5	9	7	7.3	9.3	10	8	8	8.2	8.4	3.7
Hf	-	2.60	-	2.4	-	2.94	1.99	2.85	-	-	3.14	3.57	3.76	-	-
Ta	-	1.28	-	1.3	-	1.64	0.89	2.42	-	-	1.62	1.27	1.98	-	-
Th	-	7.23	7	6.42	7	7.11	5.53	5.2	8	6	6.27	4.37	6.22	-	-
U	-	1.99	-	1.6	-	1.9	1.50	1.54	1.5	4	1.98	1.43	2.02	-	-
Cs	-	6.39	-	3	-	3.53	5.79	5	-	-	5.24	3.8	4.85	-	-
Y	-	21.89	20	25	23	28	22	18	18.6	18	24	22	23	25	16.5
Pb	10	15	12	10	11	11	11	7	5	5	11	9	11	8	8
V	250	63	73	74	65	54	70	31	180	177	64	136	4	81	154
Cr	401	21	34	18	35	16	28	24	113	64	28	90	156	29	30
Cu	35	6	7	9	11	-	9	-	27	33	11	20	2.5	6	6
Sc	30	15	14	18	14	11	18	13	27	24	11	17	9	14	19
Zn	58	21	12	21	31	12	37	-	45	45	30	34	25	19	34
Ga	19	14	10	11	13	13	14	9	13	16	12	18	15	14	15
La	-	12.62		18	-	27	19.65	19.6	-	-	20.5		23.5	-	-
Ce	-	43.91		36.1	-	47.3	41.04	42.31	-	-	33.53		46.96	-	-
Pr	-	3.63		4.84	-	6.75	5.37	5.45	-	-	5.45		5.86	-	-
Nd	-	14.89		19.79	-	26.69	21.51	21.65	-	-	21.19	-	23.03	-	-
Sm	-	3.57		4.44	-	5.67	4.865	4.61	-	-	4.71	-	4.87	-	-
Eu	-	0.702		0.938	-	1.36	1.041	1.31	-	-	0.916	-	1.135	-	-
Gd	-	3.707		4.48	-	5.51	4.48	4.20	-	-	4.37	-	4.65	-	-
Tb	-	0.627		0.713	-	0.865	0.694	0.63	-	-	0.704	-	0.695	-	-
Dy	-	4.106		4.411	-	5.2	4.196	3.72	-	-	4.396	-	4.194	-	-
Ho	-	0.849		0.887	-	1.048	0.822	0.711	-	-	0.889	-	0.812	-	-
Er	-	2.65		2.55	-	2.92	2.29	1.893	-	-	2.581	-	2.255	-	-
Tm	-	0.379		0.36	-	0.419	0.322	0.269	-	-	0.381	-	0.326	-	-
Yb	-	2.404		2.266	-	2.619	1.996	1.629	-	-	2.449	-	2.113	-	-
Lu	-	21.889		0.323	-	0.387	0.286	0.217	-	-	0.335	-	0.32	-	-

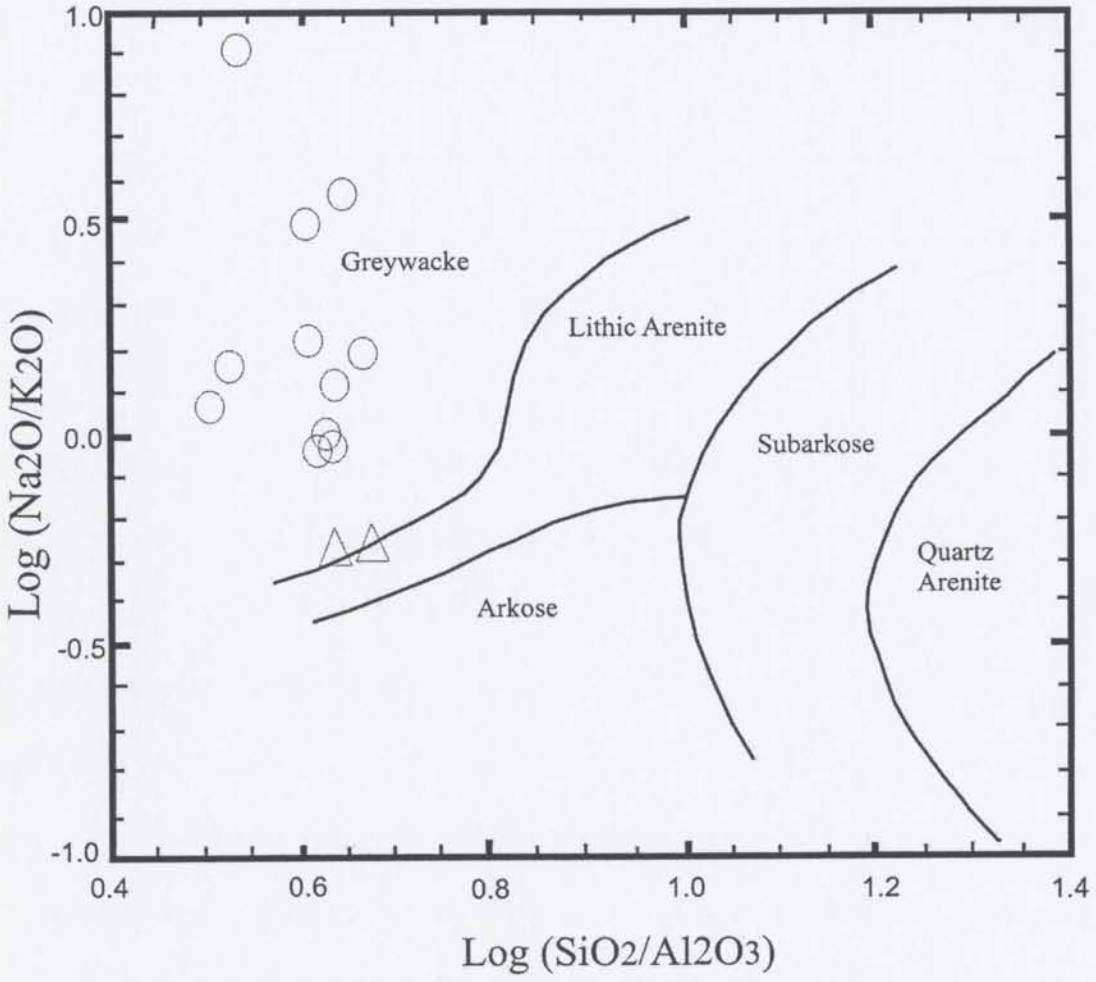

Figure 59. Chemical classification of Pettijohn et al. (1987). Triangles show samples of the Miahuatepec Formation with CIA values >60. Data from Table 6.

Considering that most of the lithic fragments in the Miahuatepec Formation are volcanic, two discriminant diagrams are used to investigate the source, although caution is required because of the mobility of major elements during diagenesis and alteration. On an MgO versus SiO_2 plot (Figure 60A), the samples of the Miahuatepec Formation have a mafic to felsic source typical of calc-alkaline volcanic rocks (Figure 60B). However, if the abundant quartz in the sandstones were not from the same volcanic source, then volcanic rocks would be more mafic.

Trace and rare earth elements. Trace elements and REE patterns can help to identify the source area and its degree of fractionation (McLennan et al. 1990, 1993; McLennan and Taylor, 1991). Here, the source of the Miahuatepec Formation is inferred using a cross-plot of La/Th versus Hf proposed by Floyd and Leveridge (1987), as well as chondrite-normalized plots. A more comprehensive description and interpretation of the trace elements and REEs will be provided in the provenance discussion in chapter 6.

Sandstones of the Miahuatepec Formation plot in the field for a mixed felsic–basic source on a La/Th versus Hf diagram (Figure 61A). Most data show low to moderate La/Th ratios (mean 3.5) and low contents of Hf (mean 2.9 ppm). The La/Th mean value for the sandstones is in between fields from oceanic island arcs (predominantly mafic) and continental island arcs (mixed mafic and felsic) reported by Bhatia and Crook (1986).

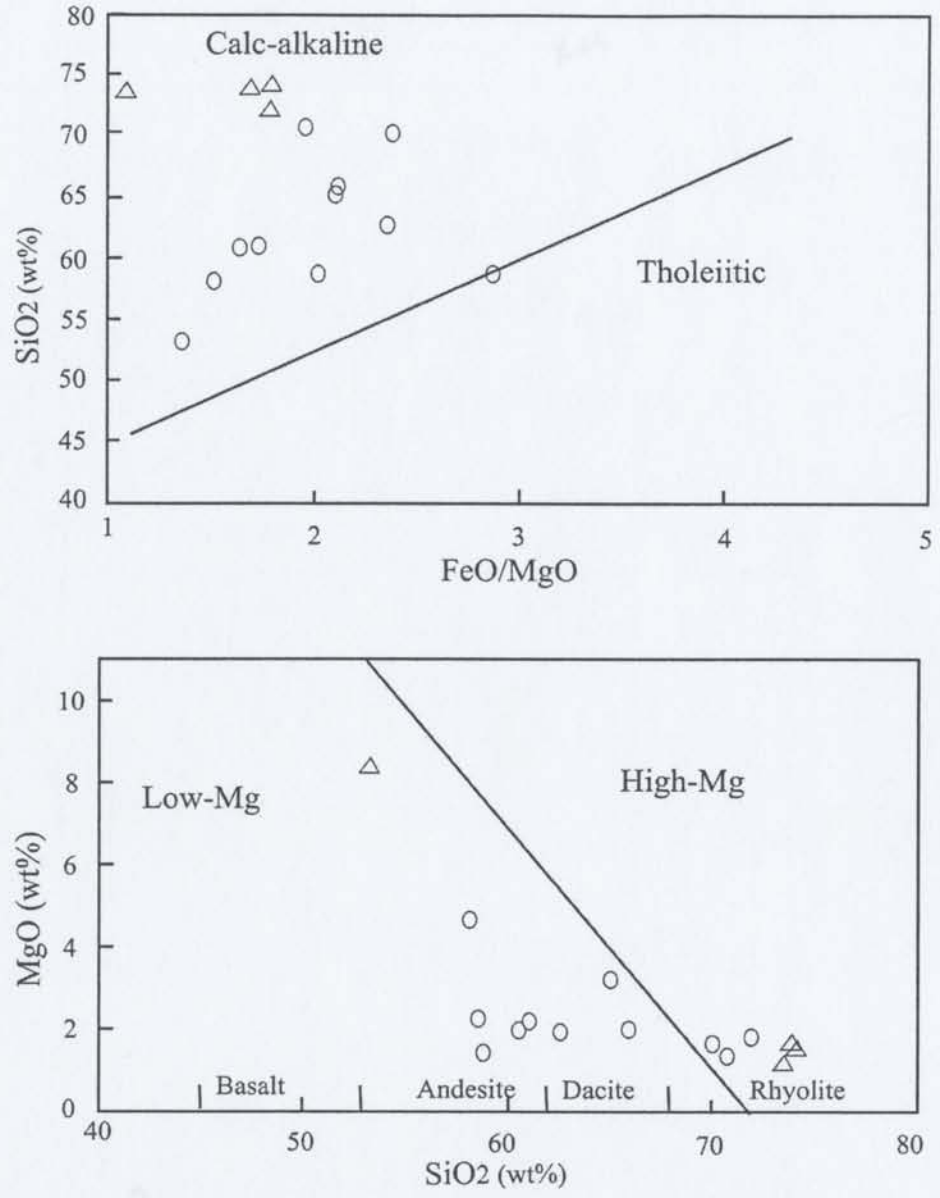

Figure 60. Discriminant diagrams for sandstones of the Mihauatepec Formation using data from Table 6. A. MgO vs. Silica. Boundaries between volcanic rocks are from Taylor (1969). Boundary between the low-Mg and high-Mg field is from Taylor, Fujioka, et al. (1990). B. Silica vs. FeO/MgO. The dividing line between tholeiitic and calc-alkaline are from Miyashiro (1974). Triangles show samples >60 CIA values.

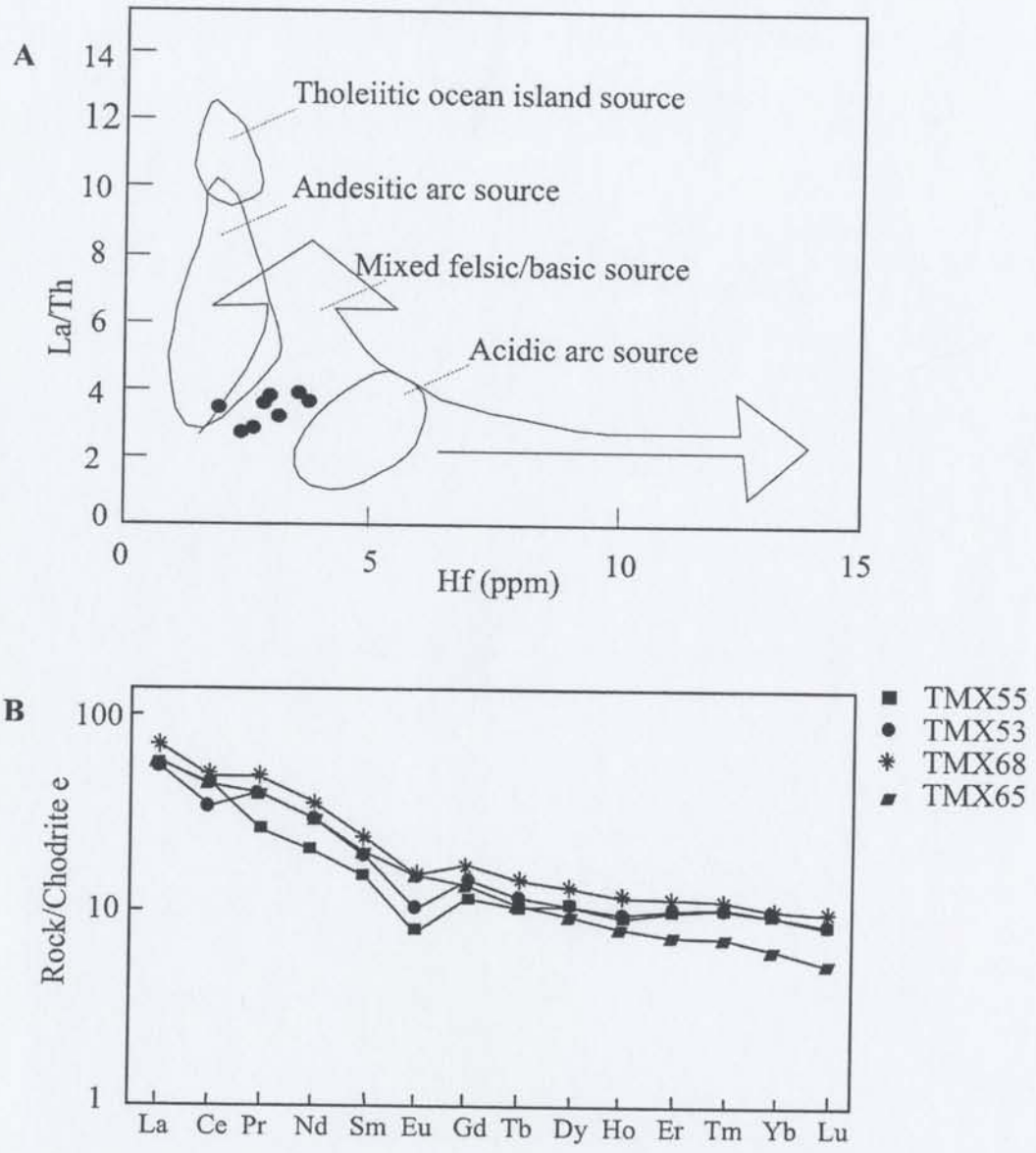

Figure 61. Source rock discrimination diagrams for the Miahuatepec Formation sandstones. A, La/Th versus Hf from Floyd and Leveridge (1987). B, Chondrite-normalized REE pattern. Normalizing values from Taylor and McLennan (1985). Data plotted from Table 6.

The REE pattern is enriched in light rare earth elements (LREE). There is a strong negative Eu anomaly, and a relatively flat trend for the heavy rare earth elements (HREE). The La_N/Yb_N ratio is between 5.39 and 8.13 with mean of 6.48, and Eu/Eu* values range from 0.58–0.90 (mean 0.72) indicating a strong fractionation of plagioclase in the magma chambers of the source area. The REE patterns are characteristic of evolved volcanic arcs with medium- to high-K, calc-alkaline magmatic suites (Gill, 1981; McLennan et al., 1990, 1993).

5.5. SUMMARY

The evolution of the arc-related succession (Villa Ayala and Acapetlahuaya formations) of the Teloloapan subterrane and its Upper Cretaceous sedimentary cover successions are reconstructed in this chapter using new petrographical and geochemical data.

The arc-related succession is volcanic lithic-rich sandstone and tuff, including epiclastic sandstone. In addition, a hybrid sandstone petrofacies (mixed siliciclastic and carbonate grains) is documented in the upper part of the Villa Ayala Formation. The sandstones and volcaniclastic rocks of the Villa Ayala Formation show a homogeneous population of volcanic fragments of basaltic to andesitic composition in the lower and middle parts. A rhyolitic source might have contributed to the upper part of the succession. The detrital composition indicates an undissected to transitional arc provenance. Geochemical data support this interpretation. Major elements indicate a mafic to felsic igneous source, while trace and rare earth elements confirm derivation

from medium- to high-K calc-alkaline rocks. The contribution of the arc-related succession most closely resembles modern back-arc settings, but intra-arc settings likely have the same characteristics but are less well known. The hybrid sandstone petrofacies records the initiation of the contemporaneous carbonate platform of the Teloloapan Formation.

The petrographic composition of the Mezcala and Mihauatepec formations is mainly volcanic lithic fragments with minor feldspar and quartz. This composition indicates a source in the intraoceanic successions of the Teloloapan and Arcelia – Palmar Chico subterranes, respectively. Major-elements geochemistry of the Miahuatepec Formation support derivation from a volcanic source, while the trace and rare earth elements imply a mixed felsic/basic source with strong plagioclase fractionation in the magma chambers of the source area. REE patterns indicate that the sources were evolved volcanic arcs with medium- to high-K calc-alkaline compositions. Carbonate-rich sandstones (calclithite petrofacies) in the Mezcala Formation record the erosion of the carbonate platforms of the Teloloapan and Morelos formations. The petrographic composition of the two Upper Cretaceous siliciclastic sequences is compatible with uplift and erosion of the underlying units. The volcanic source, in particular, change from a transitional to dissected arc provenance.

CHAPTER 6. TECTONIC EVOLUTION OF THE TELOLOAPAN SUBTERRANE AND IMPLICATIONS FOR ORIGIN OF THE GUERRERO TERRANE

6.1. INTRODUCTION

It is broadly accepted that western Mexico originated as a series of accreted island-arc terranes. The Guerrero Terrane plays an important role in the evolution of western Mexico during the latest Late Jurassic–Early Cretaceous. It is the largest and most complex arc-related sequence along the Pacific margin (Figure 1, p. 3). However, there is a debate about the tectonic mechanism for its formation, as well as the timing of the amalgamation and accretion to the "cratonal-continental" margin of Mexico of the collage of volcanic-volcaniclastic rocks that compose this terrane (Campa and Ramírez, 1979; Campa and Coney, 1983; Coney, 1983; Ramírez et al., 1991; Talavera et al., 1993; Centeno et al., 1993; Tardy et al., 1994; Elías and Ortega, 1998; Dickinson and Lawton, 2001, and references therein).

The term "terrane" is used for an area characterized by rocks having a stratigraphy that is diagnostic of a particular tectonic setting and different from that of neighboring areas or terranes. Each terrane is surrounded by fault boundaries or marked by thick and highly deformed deep-water sequences called "sutures zones" (Coney et al., 1980). The evolution of terranes is controlled by collisional tectonics, during amalgamation (the joining of terranes in an oceanic setting) and accretion (the joining along a continental margin) reflecting the complexity of one or several tectonic phases (Howell, 1995).

Pickering et al. (1988) suggest that initial collision may be "soft", that is without associated major orogenesis across the collision suture(s), followed by "hard collision" with high regional deformation over tens of millions of years. The terms "soft collision" and "hard collision" are used here as initial and later stages during accretion of terranes.

East of the study area, the Mixteca Terrane forms the "cratonal-continental" margin (Campa and Coney, 1983, see Figures 1 and 62). The Mixteca Terrane (see column 6 in Figure 11, p. 53) contains a metamorphic Paleozoic basement termed the Acatlan Complex (Ortega, 1978) disconformity covered by Upper Permian carbonate-platform and siliciclastic deltaic sequences with abundant fauna (Flores y Buitrón, 1980). Triassic?–Middle Jurassic? ignimbritic rocks overlie the Permian sequences (Corona, 1983, Las Lluvias Formation), and are in turn covered by Middle Jurassic conglomerates and coarse- to fine-grained sandstone and siltstone formed in a deltaic setting (Tecocoyunca Group) with abundant fossils of plants and ammonites (Erben, 1956). Lower Cretaceous rocks range from continental beds (Zicapa Formation) to marls and evaporitic rocks (Nejapa and Huitzuco formations, respectively). Finally, Middle Cretaceous carbonates of the Morelos–Guerrero Platform (Morelos Formation) and Upper Cretaceous siliciclastic rocks (Mezcala Formation) complete the succession in the Mixteca Terrane.

In general, two tectonic models have been suggested for the formation of the Guerrero Terrane. Some authors recognized a single but complex intra-oceanic island arc either with east-dipping subduction (Campa and Ramírez, 1979; Elias and Ortega, 1998; Dickinson and Lawton, 2001) or west-dipping subduction (Coney, 1983; Urrutia and

Valencio, 1986; Tardy, et al., 1994; Freydier et al., 1996). Others authors prefer a series of intra-oceanic arcs separated by oceanic basins forming complex multi-arc systems similar to the present-day western Pacific (Ramírez et al., 1991; Talavera et al., 1993; Centeno et al., 1993; Mendoza and Suastegui, 2000).

The presence of uppermost Lower Cretaceous carbonate sequences and Upper Cretaceous siliciclastic sequences throughout both the Guerrero Terrane (Zihuatanejo–Huetamo, Arcelia – Palmar Chico, and Teloloapan subterranes), as well as in the Mixteca Terrane raises important questions about the timing of amalgamation and accretion of these terranes and subterranes, which is thought to have taken place during the late Early Cretaceous (Tardy et al., 1994; Freydier et al., 1996, and 1997) or Late Cretaceous (Campa and Ramírez, 1979; Campa and Coney, 1983; Coney, 1983; Salinas, 1994).

In this chapter, a summary of stratigraphy and facies analysis (chapters 2–4) is combined with data from petrographic and geochemistry studies in the Teloloapan area (Teloloapan subterrane) to create a tectonic model for the arc-related and sedimentary cover successions in the thesis area. The model accounts for stratigraphic, sedimentologic, geochemical, and provenance data acquired during the thesis research, and selected isotopic and geochemical data published previously for other parts of the Guerrero Terrane.

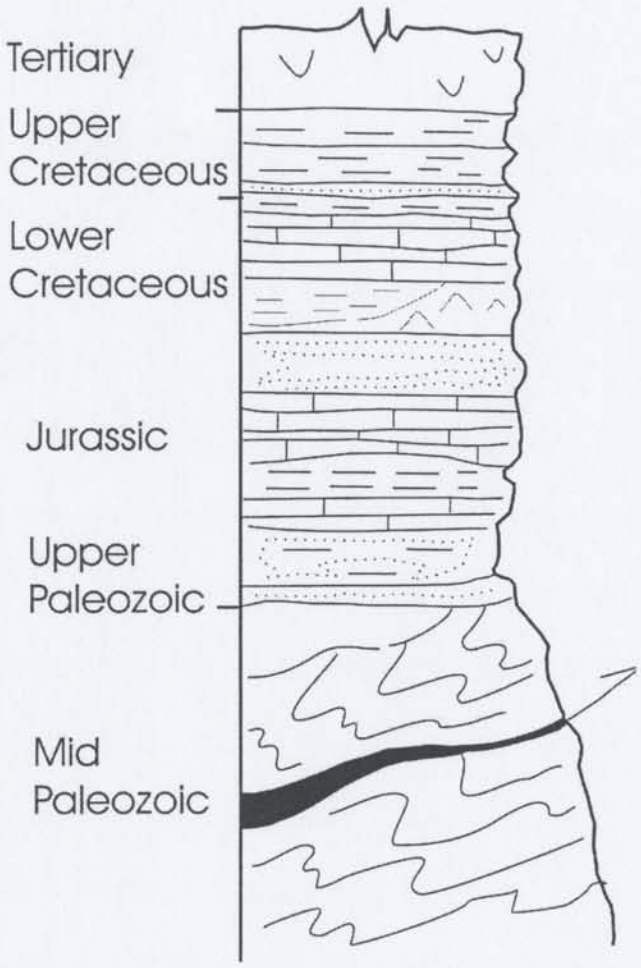

Figure 62. Composite stratigraphic column of the Mixteca Terrane (From Campa and Coney, 1983).

6.2. MODEL FOR TECTONIC DEVELOPMENT OF THE GUERRERO TERRANE

6.2.1. Overview and essential trends to be satisfied by the model

Ramírez et al. (1991) divided the Guerrero Terrane in southwestern Mexico into three distinctive subterranes, termed (from the Pacific margin toward the east) the Zihuatanejo–Huetamo, Arcelia – Palmar Chico and Teloloapan subterranes (see Figure 2, p. 4). Evidence from stratigraphy, sedimentology, volcanic and sedimentary petrography, structural geology and geochemistry from the different subterranes suggest that they formed different intraoceanic arcs throughout the latest Late Jurassic to Early Cretaceous (Ramírez et al., 1991; Guerrero et al., 1993; Guerrero, 1997; Guerrero et al., 2003; Talavera et al., 1993; Talavera, 1993; Talavera, 1995; Salinas, 1994; Salinas et al., 2000; Mendoza and Suastegui, 2000; and references therein)

The Zihuatanejo–Huetamo subterrane (columns 1–3 in Figure 63) includes four lithological assemblages. (1) Triassic? – Jurassic? metamorphic rocks form the basement (Vidal, 1986; Centeno, 1994; Garcia and Talavera, 1994). (2) Lower Cretaceous calc-alkaline to tholeiitic andesitic and dacitic lavas interbedded with tuff and volcanic breccia are covered by Albian–Cenomanian limestones and continental red beds interpreted as an intra-oceanic island arc (Ferrusquia et al., 1978; Vidal, 1986; Talavera, 1993; Freydier et al., 1997; Mendoza and Suastegui, 2000). (3) Tectonic mélange associated with fine-grained, micaceous intensely deformed sandstone and shale represents the subduction zone and trench-fill deposits (Vidal, 1986; Talavera, 1993, 2000). (4) Valanginian–Hauterivian conglomerate and sandstone, interbedded with tuffs and siltstones with

abundant fauna, which are overlain by highly fossiliferous Barremian–Cenomanian limestones. The siliciclastic deposits formed submarine-fan and deltaic settings in a back-arc basin (Pantoja, 1959; Campa, 1977; Guerrero, 1997).

The Arcelia – Palmar Chico subterrane (column 4 in Figure 63) is formed of Albian–Cenomanian tholeiitic pillow basalts associated with serpetinized gabbros and ultramafic dikes, overlain by intercalations of volcaniclastic sediments, radiolarian chert, and black shales deposited in intra-oceanic arc and back-arc basins (Delgado et al., 1990; Davila and Guerrero, 1990; Ortiz and Lapierre, 1991; Mendoza and Suastegui, 2000).

The Teloloapan subterrane consists of Berriasian–Aptian calc-alkaline basalts, andesites and scattered rhyolites interbedded with tuff, epiclastic sandstone, and shale, covered by Upper Aptian–Albian carbonate rocks (coumns 6–8 in Figure 63). The succession is interpreted as an intra-oceanic arc and a carbonate platform, which developed atop arc volcanoes (Guerrero et al., 1990; Talavera, 1993; and data in this thesis).

6.2.2. History of development of the Guerrero Terrane

The data presented in chapters 2–5 of this thesis and other studies can be used to trace the historical development of the Guerrero Terrane in southwestern Mexico. In an attempt to illustrate the tectonic evolution along the length of the Guerrero Terrane, a series of schematic cross-sections are presented in Figure 64. A precise paleogeographic

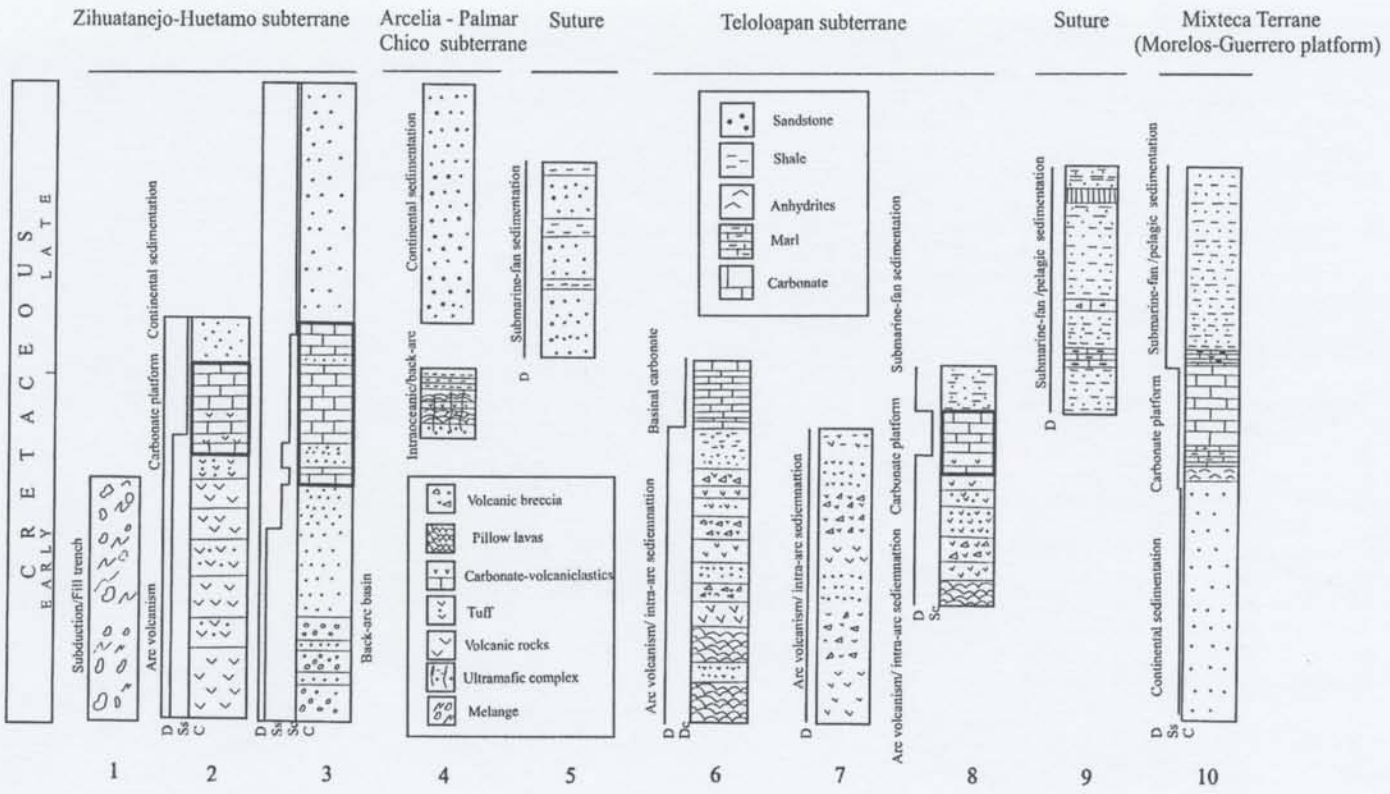

Figure 63. Generalized stratigraphic columns and environmental interpretation for the Guerrero Terrane, suture sequences and the Mixtexa Terrane. 1. Las Ollas sequence; 2,. Zihuatanejo area; 3. Huetamo area; 4. Arcelia – Palmar Chico subterrane; 5 Miahuatepec Formation; 6–8. Teloloapan subterrane in Villa Ayala (6), Alpixafia (7) and Ahuacatitlan–Acatempan (8) areas; 9. Mezcala Formation (Pachivia Valley); 10 Morelos–Guerrero Platform in the Chilacachapa area. Note that island-arc carbonate deposits are marked with coarse squares. D= deep; Dc= deep carboante; Sc = shallow carbonates; Ss = shallow sandstones; C = continental.

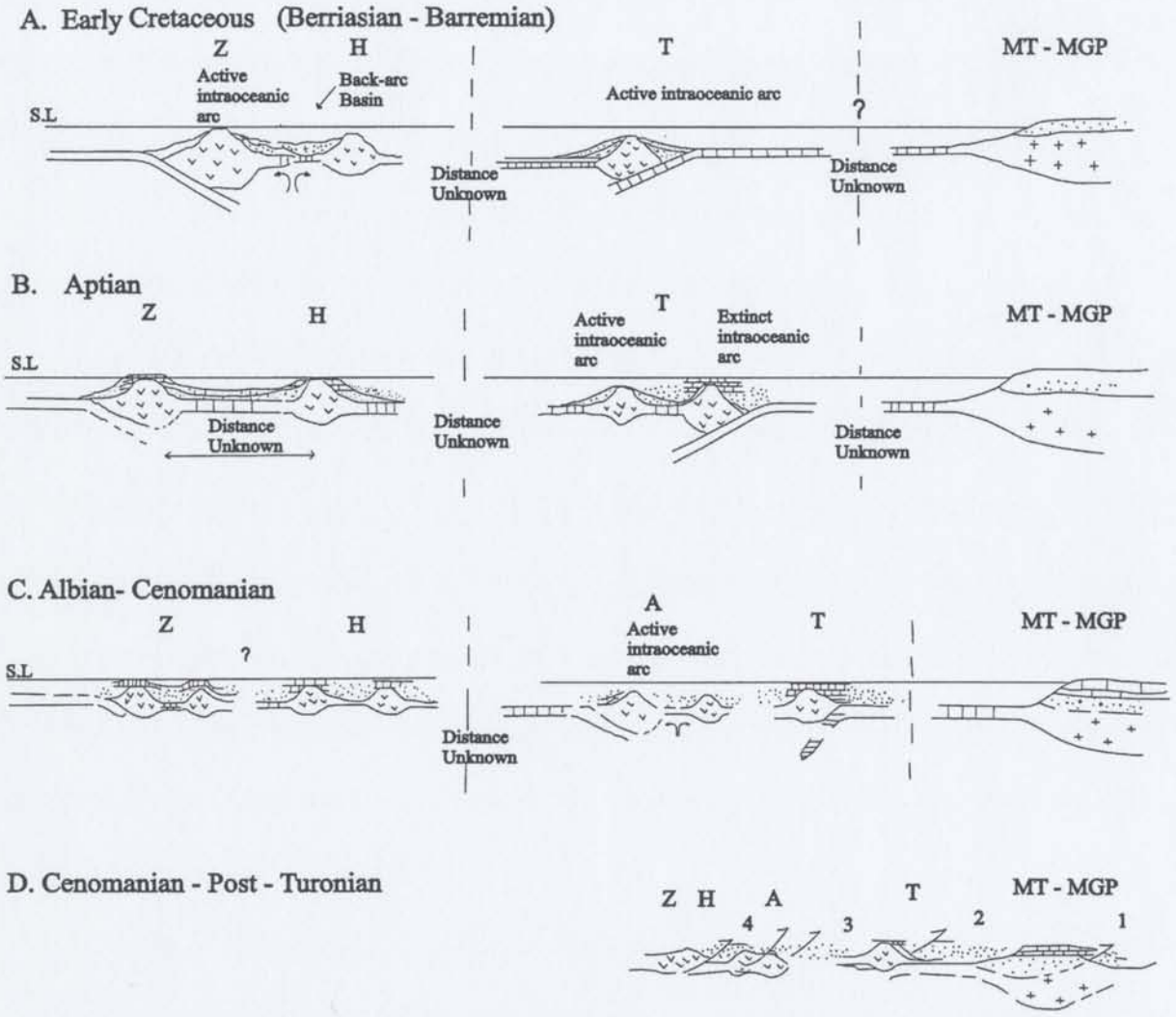

Figure 64. Tectonic evolution during the Cretaceous, including the Guerrero and Mixteca terranes. Z = Zihuatanejo; H = Huetamo; T = Teloloapan; A = Arcelia; MT-MGP = Mixteca Terrane – Morelos Guerrero Platform. S.L = Sea Level. In D 1 = Mezcala Formation in Mixteca Terrane; 2 = Mezcala Formation in Teloloapan subterrane; 3 = Miahuatepec Formation; 4 = Cutzamala Formation

reconstruction of the different subterranes within the Guerrero Terrane is not possible at this time, but multiple and contrasting intra-oceanic basins and episodes of amalgamation-accretion are documented. The tectonic reconstruction is restricted to the Cretaceous and shows the tectonic evolution of the different basins, flexural and subsidence events, and amalgamation and accretion among the volcanogenetic subterranes and between the Guerrero and Mixteca terranes.

During the latest Late Jurassic and Early Cretaceous, a series of intraoceanic arcs developed along the southwestern Pacific margin of Mexico (Figure 64). Over this time interval the Farallon plate had a sinistral oblique convergent margin with NW→SE movement, which later changed to W→E (Engebretson et al., 1985). The earliest stage of subduction began during the latest Late Jurassic (Tithonian) to earliest Early Cretaceous (Berriasian–Valanginian) in the western part of the Guerrero Terrane, and formed the intraoceanic–mélange-backarc system of the Zihuatanejo-Huetamo subterrane (Columns 1–3 in Figure 63 and Figure 64A).

Rocks of the subduction-intraoceanic arc system crop out in the Zihuatanejo area, and are represented by the highly deformed and serpentinized sequence of the Las Ollas Complex and the tholeiitic and calc-alkaline basalts–dacites of the Zihuatanejo Formation, respectively (Vidal, 1986; Talavera, 1993, 2000). Rocks of the back-arc basin are exposed in the Huetamo area. There, a thick sequence of deep-water siliciclastic rocks (Angao and San Lucas formations) is overlain by a shallow-water carbonate platform sequence (Comburindio Formation). Volcanic and sedimentary geochemistry, and sandstone petrography support this interpretation (Talavera, 1993; Guerrero, 1997;

Mendoza and Suastegui, 2000; see Figure 65). REE patterns of the Zihuatanejo lavas show enrichment in LREE relative to HREE, with La_N/Yb_N values ranging from 2.47 to 9.83, typical of medium- to high-K calc-alkaline suites (Mendoza and Suastegui, 2000, Figure 65A). The same REE pattern is observed in volcanic pebbles and sandstones from the Huetamo area (Figure 65B and C), suggesting that these rocks shared a common magma source. Mendoza and Suastegui (2000) reported also that volcanic pebbles in the Huetamo area are derived from tholeiitic, calc-alkaline, and shoshonitic lavas similar to the source composition for modern back-arc settings. Geological characteristics of the Zihuatanejo-Huetamo subterrane are consistent with the paleogeography proposed by Dickinson and Lawton (2001) for the Guerrero Terrane and tectonic models from Baja California (Busby et al, 1998; Umhoefer, 2003), both of which suggest an east-dipping subduction zone and an outboard intraoceanic arc system.

Contemporaneously during Berriasian–Aptian time, an intraoceanic arc system developed in the eastern part of the Guerrero Terrane (the Teloloapan subterrane; Figure 64). An intra-arc basin composed of volcanic buildups and arc aprons with abundant basalts–andesites and minor rhyolites and volcaniclastic rocks developed above a west-dipping subduction zone (columns 6–8 in Figure 64; see chapter 2 for evolution of the intra-arc basin). A west-dipping subduction zone is interpreted because the magmatic activity took place on its western side (the Teloloapan subterrane) and no volcanism has been reported in the Mixteca Terrane, which was located on the eastern side of the eventual suture between terranes. During the Early Cretaceous, the Mixteca Terrane is considered to have been far to the east of the Guerrero Terrane, and characterized

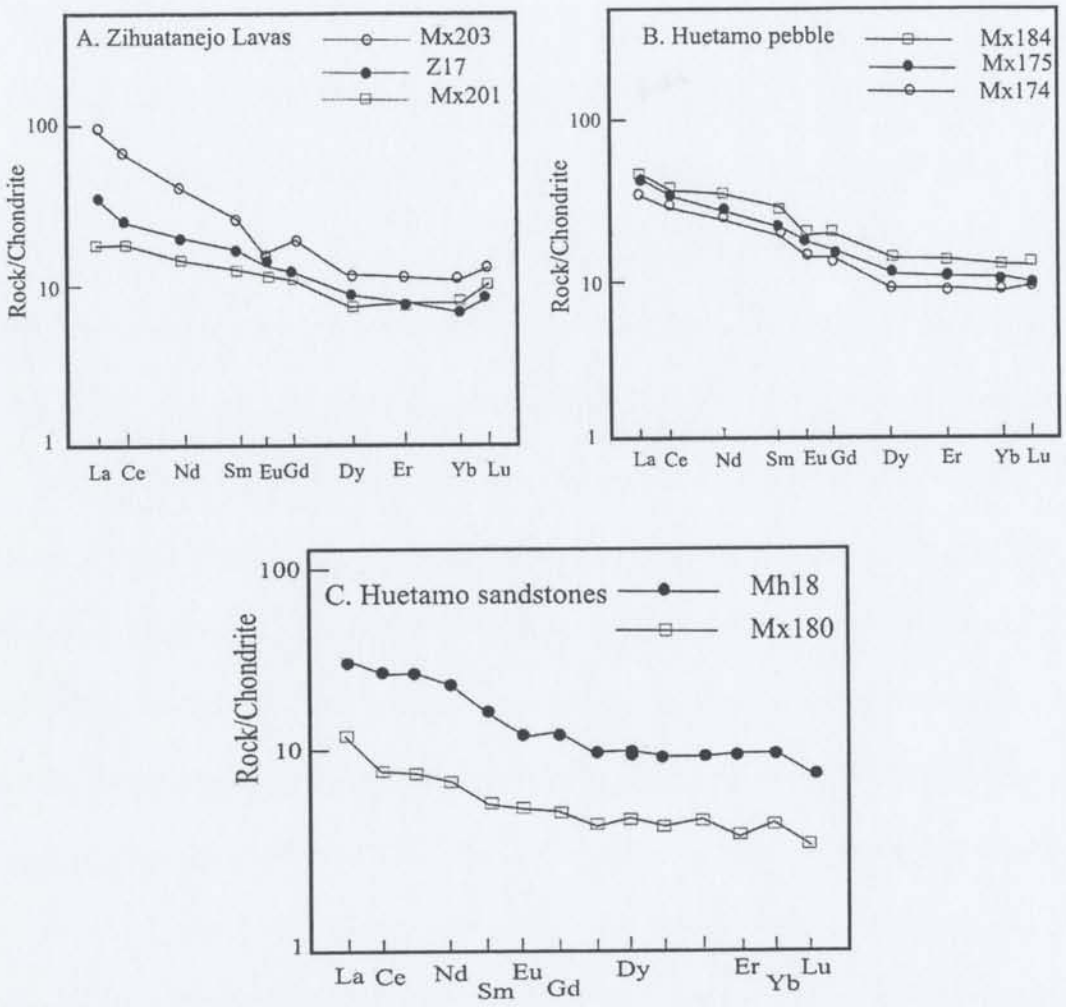

Figure 65. Chondrite-normalized rare earth elements for the Zihuatanejo-Huetamo subterrane: (A) Zihuatanejo volcanics; (B). Huetamo volcanic pebbles, and (C) Huetamo sandstones. Normalizing values for volcanic flows and pebbles are from Eversen et al. (1978), and for sandstones are from Taylor and McLennan (1985). Data for volcanic rocks and volcanic pebbles are from Mendoza and Suastegui (2000).

by continental red beds and shallow-water and evaporitic sedimentation in a passive margin.

The isotopic composition of the Teloloapan lavas has ε_{Nd} = +1.6 to +4.6 and ε_{Sr} = -14.3 to +2.3. These compositions are similar to those of Island Arc Basalts (IAB) and Ocean Island Basalts (OIB) (Talavera et al., 1995). Centeno (1994) reported ε_{Nd} =+3.6 to +7 in the Guerrero terrane, values observed in island arcs. The isotopic data suggest that basement rocks were not involved in magma generation in the Teloloapan subterrane.

The geochemistry of basalts in the Teloloapan subterrane shows that the REE patterns are very homogeneous and characterized by enrichment of LREE relative to HREE and a moderate Eu anomaly. REE patterns in rhyolites show a strong Eu anomaly and relatively flat HREE trend, similar to medium- to high-K calc-alkaline suites typical of mature intra-oceanic arcs (Talavera, 1993; Talavera et al., 1995; Mendoza and Suastegui, 2000; Figure 66A and B). The REE patterns of the volcaniclastic rocks studied in this thesis are similar to those observed for the primary volcanic rocks (Figure 66C; see also chapter 5). The volcaniclastic rocks show variable Th/Sc ratios (0.1–0.67, mean 0.25) and Th/U ratios (1.94–3.45), and a moderate to high negative Eu anomaly (Eu/Eu*= 0.69–0.90, mean 0.82). These geochemical features of the volcaniclastic rocks most closely resemble the young differentiated arc component of McLennan et al. (1990), specifically from back-arc basins of the Bering Sea which are associated with the relatively evolved Aleutian island arc.

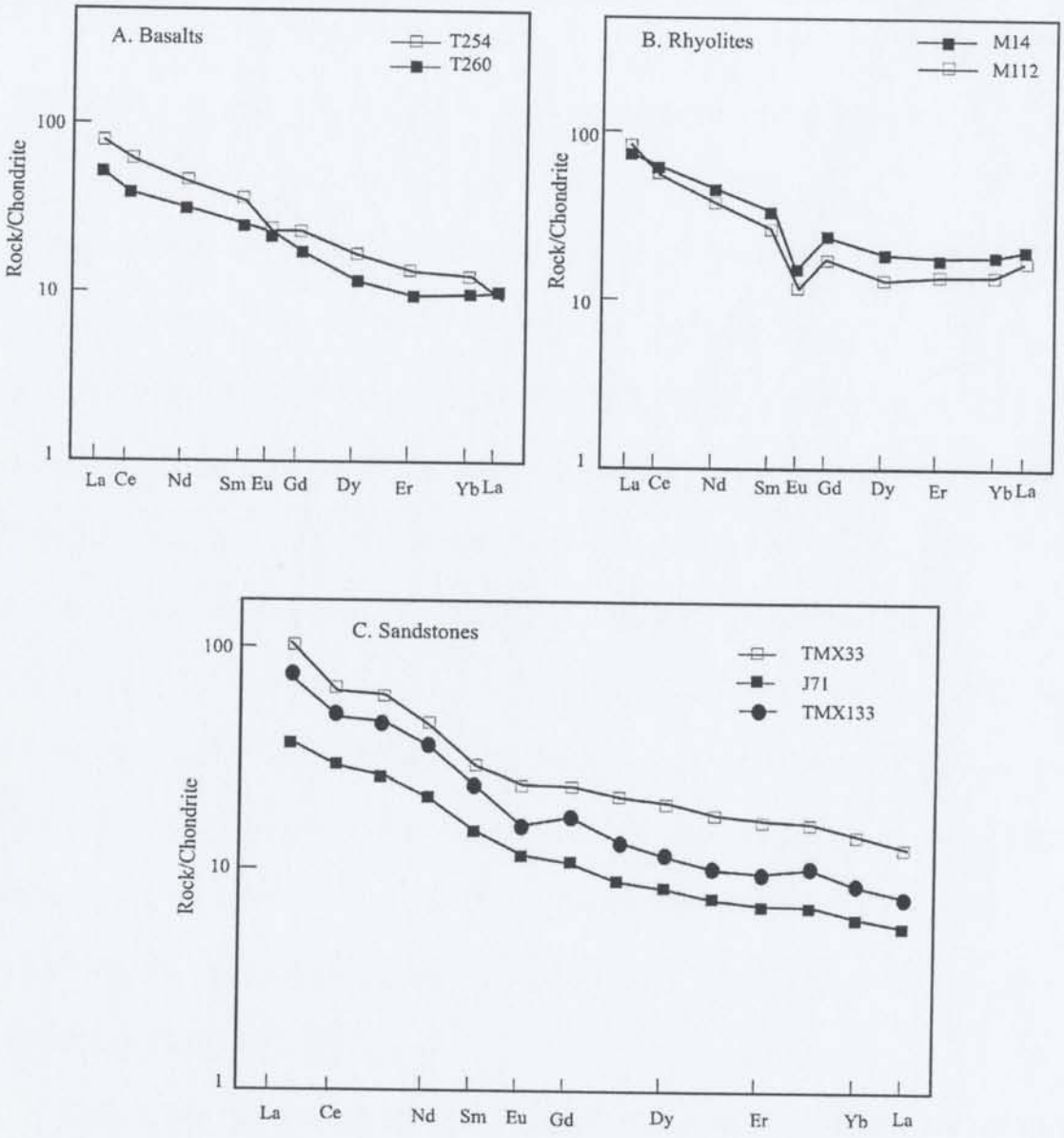

Figure 66. Chondrite-normalized REE patterns for the Teloloapan subterrane. A and B, volcanic lavas. C, sandstone and tuff. Normalizing values for volcanic rocks are from Eversen et al. (1978), and for sediments are from Taylor and McLennan (1985). Volcanic rock data from Mendoza and Suastegui (2000).

Using the elements La, Th, and Sc to discriminate tectonic settings, most of the volcaniclastic samples plot in the oceanic island-arc field (cf. Bhatia and Crook, 1986; Figure 67B). The samples of the arc-related succession have low La/Sc ratios (mean 1.19) and Th/Sc ratios (mean 0.25), which are characteristic of oceanic island-arc sandstones (Bhatia and Crook, 1986). Furthermore, samples show a relatively linear trend on a La/Th/Sc diagram, similar to the back-arc deposits studied by McLennan et al. (1990). Sandstone provenance data agree with this assessment. Samples of the arc-related succession show a clear evolution from an undissected to transitional arc provenance (Figure 67A; see chapter 5). The provenance of the volcaniclastic rocks of the Teloloapan subterrane can be explained in terms of the evolution of the volcanic activity and erosion in the intra-oceanic arc (see § 5.4.2.3). The composition of the volcanic lithic fragments and their association with lava flows suggest that they were derived from the erosion of mostly mafic pyroclastic products. This interpretation is supported by the abundance of microlitic and lathwork textures in the volcanic lithic fragments. In terms of grains components, the volcaniclastic rocks are similar to sandstones from the Bering Sea (Marsaglia and Ingersoll, 1992).

During the late Aptian–early Albian, volcanic activity largely ceased and only sporadic pyroclastic events took place in the Guerrero Terrane. Carbonate platforms began to develop on top of the island-arc edifices (Figures 63 and 64B). There was a high rate of deposition in the carbonate platforms (300–500 m in thickness) signifying a high rate of subsidence to generate the necessary accommodation space.

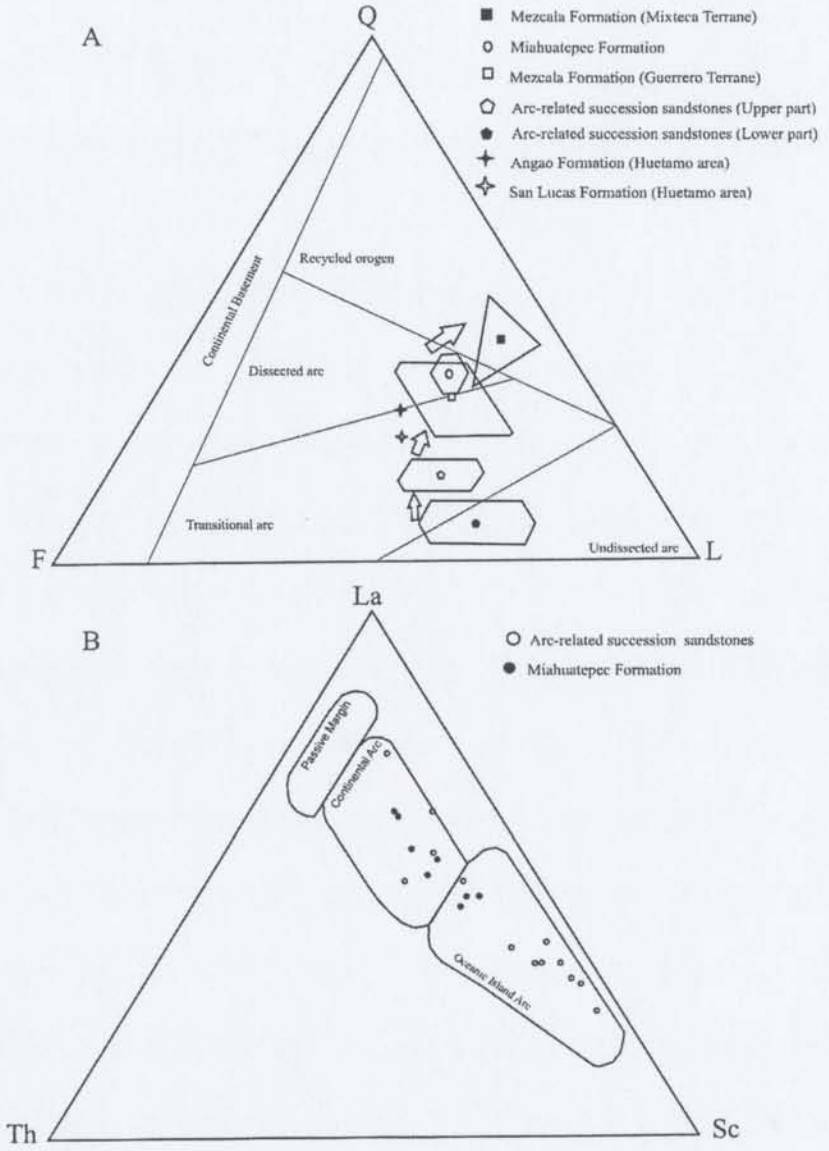

Figure 67. Sumary ternary diagrams. A, QFL plot showing mean and standard deviation of the different arc-related and sedimentary cover successions in the Guerrero and Mixteca terranes. Fields from Dickinson (1985). B. La/Th/Sc discriminant diagram from Bhatia and Crook (1986), showing sandstones of the arc-related succession and the Miahuatepec Formation.

Such conditions in carbonate deposits suggest rapid vertical crustal movements leading to rapid relative sea-level fluctuations. The crustal movements might have been the result of tectonic instability in the region possibly during flexural deformation of the subducting plate.

Later, during the Albian–Cenomanian, a new immature intraoceanic arc associated with a back-arc basin was initiated between the Zihuatanejo-Huetamo and Teloloapan subterranes, forming the mafic volcanic rocks of the Arcelia – Palmar Chico subterrane (Mendoza and Suastegui, 2000; column 4 in Figure 63 and Figure 64C). Geochemistry of volcanic rocks of the Arcelia – Palmar Chico subterrane is similar to oceanic island-arc to backarc basins (Mendoza and Suastegui, 2000; Figure 68). The REE patterns in the inferred back-arc rocks show relatively flat patterns (La_N/Yb_N = 2.10–4.63), while REE patterns in the oceanic island-arc rocks are enriched in LREE relative to HREE with La_N/Yb_N ratios of 2.10–4.63 and a moderate Eu anomaly (Figure 68).

The inferred westward jump in the position of subduction to account for the formation of rocks of the Arcelia – Palmar Chico subterrane might suggest that, during Albian–Cenomanian time, "soft collision" (cf. Pickering et al., 1988) occurred between the Teloloapan subterrane and the Mixteca Terrane (formed by the Morelos-Guerrero Platform) (cf. Bustamante et al., 2004). This accretion event should have produced either a change in sedimentation or an unconformity. However, neither interruption in sedimentation nor unconformity has been recognized in the region during this time. Instead, the carbonate sedimentation, which was initiated during the late Aptian (in the

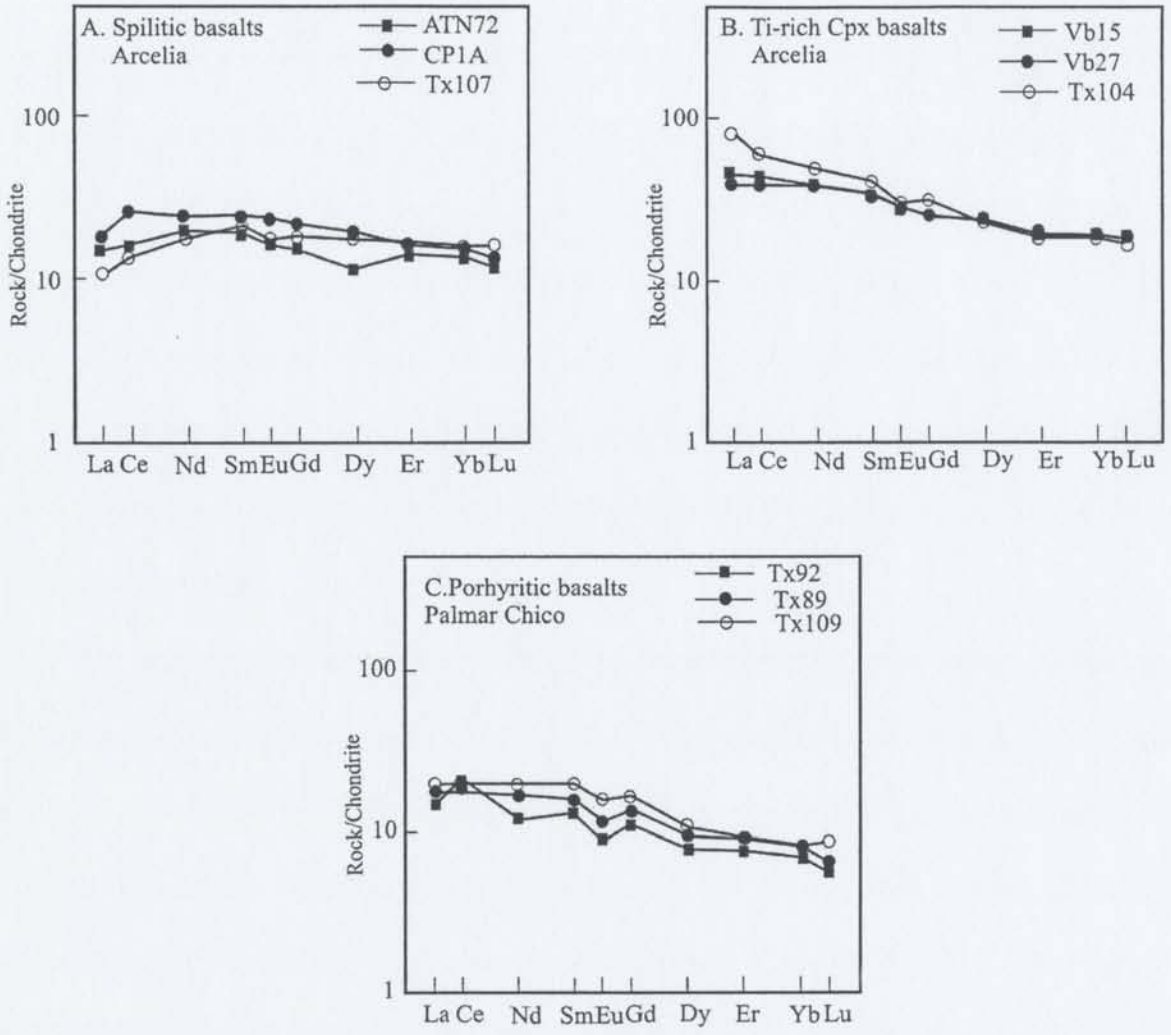

Figure 68. Chondrite-normalized rare earth elements for the Arcelia – Palmar Chico subterrane: (A and B) Arcelia volcanics; (C). Palmar Chico volcanics. Normalizing values for basalts are from Eversen et al. (1978). All Data from Mendoza and Suastegui (2000).

Huetamo area since the Barremian), continued throughout the Albian in the different parts of the Guerrero Terrane. The storm deposits of the Teloloapan Formation record the only change in sedimentation during this time. Storm deposits have also been reported from deep-water black carbonates of the Amatepec Formation (Guerrero and Ramírez, 1992) and from some intervals of the Morelos Formation (González, 1991). This link in sedimentary processes might indicate that the two carbonate-platforms were geographically close at this time, but this type of paleoenvironmental evidence is weak. However, contemporary storm deposits are not present in the Huetamo area (Zihuatanejo-Huetamo subterrane).

The apparent lack of deformation and no interruption in sedimentation at this time of possible "soft collision" might be explained by oblique convergence. Support comes from the northern part of Baja California, where from 125 to 105 Ma the oceanic arc of the Guerrero Terrane collided with the continent in a transpressional regime associated with strike-slip movements (Engebretson et al., 1985; Umhoefer, 2003). Alternatively, the westward jump in subduction might reflect an interregional reorganization of plate motions, so that no local cause (e.g. "soft collision" and locking of the subduction zone) is required. Whatever the cause, the Teloloapan arc became inactive as arcs to the west came to life.

In contrast, Cretaceous history of the Mixteca Terrane started with deposition of the Morelos-Guerrero high-energy carbonate platform during Aptian time (see column 10 in Figure 63). This carbonate platform persisted through the Albian–Cenomanian along the Mixteca passive margin.

During the Late Cretaceous, uplift and thrusting of the Guerrero Terrane began, shedding detritus for submarine-fan deposits into the suture zones between the Arcelia – Palmar Chico and Teloloapan subterranes, and between the Guerrero Terrane and the Mixteca Terrane (columns 5 and 9 in Figure 63 and Figures 64D). In this interpretation, Upper Cretaceous units such as the Miahuatepec and Mezcala formations are attributed to deformation during the Laramide orogeny in southern Mexico. The rocks of the study area are strongly deformed showing fold axes and faults which strike NW-SE, associated with east-verging folds and thrust faults related to the Laramide deformation (Salinas, 1994; Salinas et al., 2000).

Although sandstones of the contemporaneous Upper Cretaceous Mezcala and Miahuatepec formations do not plot in the recycled-orogen compositional field (collisional basins of Dickinson, 1984; Figure 67A), their detrital composition does suggest uplift and erosion of several of the underlying units in the region. Sandstone petrography of the Mezcala Formation indicates that lithic fragments are the most abundant component (Q30%;F23%;L47%). The lithic grains are volcanic (mean 30%) and sedimentary (mean 17%, mostly carbonate). The abundance of carbonate fragments results locally in carbonate-rich sandstones (calclithite petrofacies, see chapter 5) throughout the Mezcala Formation; these plot in between the transitional and dissected arc fields (Figure 67A). In contrast, sandstones of the Miahuatepec Formation contain more quartz and lithic grains (Q35%;F21%;L44%), forming a quartzolithic petrofacies. These samples plot along the boundary between the dissected arc and the recycled orogen compositional fields (see Figure 67A).

Provenance evaluation suggests that sandstones of the Miahuatepec and Mezcala formations represent the mixed influence of volcanic arcs (the Miahuatepec Formation), and volcanic-arc and carbonate-platform sources (the Mezcala Formation). Similar variable sandstone composition has been documented in basins related to collisional events in the Appalachians, Apennines, and New Guinea (Hiscott, 1978; Critelli and Le Pera, 1995; Abbott et al., 1994). The fact that the samples do not plot in the recycled-orogen field of Dickinson (1985) might result from the lack of a cratonic basement source, which is normally an important contributor of quartz. Farther east on the craton, sandstones of the Mezcala Formation in the Mixteca Terrane are more quartzose, and do fall in the recycled-orogen field (Centeno, 1994; Guerrero unpublished data; Figure 67).

The similarity of REE patterns for the Miahuatepec Formation and rocks of the Arcelia – Palmar Chico subterrane (see Figures 61B and 68) suggests that this formation might have been derived by erosion of that subterrane. Sandstone geochemistry of the Miahuatepec Formation shows moderate Th/Sc ratios (0.26–0.69, mean 0.46), variable La/Sc ratios (0.84–2.61, mean 1.55), and a strong negative Eu anomaly (Eu/Eu*= 0.58–0.90, mean 0.72). Similar geochemical data are associated with the young differentiated arc component of McLennan et al. (1990), specifically data from volcanogenetic sequences such as the Aleutians. In the La, Th, Sc tectonic discriminant diagram, the samples of the Miahuatepec Formation fall in the continental-arc and oceanic island-arc fields (cf. Bhatia and Crook, 1986; Figure 67B).

The Late Cretaceous amalgamation-accretion event (Figure 64D) is interpreted to have induced uplift of the arc-related sequences and the carbonate-platform rocks,

providing detritus for the different siliciclastic sequences in the study area. The early Cenomanian–Turonian age documented for the Mezcala Formation (see fauna and age description in §3.2.1) constrains the timing of this uplift. For example, the contact between the Teloloapan and the Mezcala formations is transitional and is early Cenomanian in age in the study area, while the contact between the Morelos and Mezcala formations east of the study area (the Mixteca Terrane) is slightly younger (late Cenomanian–early Turonian). These dates suggest a somewhat diachronous final amalgamation-accretion.

The clastic sequence of the youngest Cutzamala Formation (at the top of columns 3–4 in Figure 63) is attributed to continental deposition during the final docking between the Zihuatanejo-Huetamo and the Arcelia – Palmar Chico subterranes, forming a successor basin, which existed during post-Turonian time.

Paleomagnetic data suggest that the Guerrero Terrane, in southwestern Mexico, experienced some tectonic rotation but no change in paleolatitude relative to North America (Böhnel et al., 1989). The cratonic Mixteca Terrane, including its Mezcala and Morelos formations, completed a small counterclockwise rotation (~20°) with no change in paleolatitude relative to North America (Böhnel, 1999; Molina et al., 2003). However, Urrutia and Valencio (1986) have suggested that rocks of the Guerrero Terrane experienced a northwestward movement. They measured both normal and reverse polarities and infer remagnetization during the deformation of these rocks.

Based on their paleomagnetic data, Böhnel et al. (1989) suggested that the Guerrero Terrane formed relatively near the continental margin followed by minor

movements during the Cretaceous. An alternative interpretation might be that the different arc-related sequences (Zihuatanejo–Huetamo, Arcelia – Palmar Chico and Telolopan subterranes), which constitute the Guerrero Terrane, traveled along W→E tracks (which cannot be established using paleomagnetism) and they were only relatively close to one another during the late Cretaceous to produce "hard collision" (cf. Pickering et al., 1988). The geologic data (stratigraphy, sedimentology, geochemistry, and structural geology) support multiple arc-related successions during the Late Jurassic–Early Cretaceous and formation of suture zones (Miahuatepec and Mezcala Formation) where strong deformation thrusting were focused during Late Cretaceous compression. Additional paleomagnetic data might clarify the geometry of the major accretional events during this time in southwestern Mexico. The existing data, however, are not adequate to constrain the assembly of the terranes and subterranes.

6.3.SUMMARY

The available data indicate the following sequence of events: (1) formation of multiple open-ocean intra-arc basins during the Early Cretaceous; (2) cessation of volcanic activity and development of carbonate platforms on top of the former island arcs of the Guerrero Terrane during Aptian–Albian time; (3) renewal of volcanic activity and formation of a more westerly intra-oceanic arc and back-arc basins during the Albian–Cenomanian after possible "soft collision" of the Guerrero and Mixteca terranes; and (4) development of thrust-belt basins and accretion of the different volcanogenic subterranes,

as well as final accretion of the Guerrero Terrane to the Mixteca cratonic block during the Late Cretaceous.

CHAPTER 7. CONCLUSIONS

7.1. STRATIGRAPHIC CONCLUSIONS

1. The arc-related succession, in the Teloloapan subterrane, is composed of three Berriasian to Albian formations. The Villa Ayala Formation (Berriasian–Aptian) is a thick sequence of volcanic and volcaniclastic rocks (breccias, conglomerates, tuffs, and epiclastic rocks). The Acapetlahuaya Formation (Upper Aptian) contains fine- to medium-grained tuff and epiclastic sandstones, as well as shale, and the Teloloapan Formation (Aptian–Albian) consists of carbonate rocks.
2. Field mapping and section measurement suggest that the arc-related succession forms a continous succession without stratigraphic interruption. Neither disconformities between formations nor basement rocks were recognized in the study area. Fauna and flora found in the formations support this interpretation.
3. The sedimentary cover successions consist of two Upper Cretaceous siliciclastic units. The Miahuatepec Formation (Post-Cenomanian and higher), to the west, consists of coarse- to fine-grained sandstones and shale, with minor thin-bedded limestones. The Mezcala Formation (Lower Cenomanian–Coniacian and higher), to the east, is fine- to medium-grained sandstone, shale, minor radiolarian chert, and thin-bedded limestone.

4. Based on microfauna, The Mezcala Formation has an early Cenomanian age, which is the oldest age reported for the sedimentary cover successions in the region. Furthermore, a concordant and transitional contact is recognized between this formation and the Teloloapan Formation.

7.2. SEDIMENTOLOGICAL CONCLUSIONS

1. Facies analysis in the arc-related succession indicates the evolution of an intra-oceanic arc characterized by primary volcanic products, volcanic breccias and conglomerate, tuff, epiclastic, hybrid, and carbonate facies. The facies record the initiation of submarine arc volcanism and buildups of volcano structures, with contemporaneous destruction and remobilization of the volcano structures and development of fan-aprons characterized by the deposits of high- to low-density turbidity currents and minor debris-flows, as well as pyroclastic eruptions.
2. Volcanism was contemporaneous with deposition of the different volcaniclastic facies. Carbonate and hybrid facies are contemporaneous with the formation of a high- to low-energy shallow-water carbonate platform atop the volcano structures. The last stage of evolution of the arc-related succession is defined by shallow-water and rudist reefs/framework deposits, followed by storm deposits.
3. Facies analysis in the sedimentary cover succession (the Miahuatepec and Mezcala formations) shows the development of mud/sand-rich submarine-fan

systems. Overbank, channel-overbank and lobe-fringe turbidity-current deposits, associated with pelagic sediment, and scattered debris-flow deposits, characterize the Mezcala Formation submarine-fan system. In contrast, the submarine-fan system in the Miahuatepec Formation contains deposits of channel-lobe transitions, lobes and lobe-fringe areas associated with predominantly high-density turbidity currents and deposited in the middle to upper part of the fan system.

7.3. PETROGRAPHIC, GEOCHEMICAL AND PROVENANCE CONCLUSIONS

1. Sandstone petrography and geochemistry of the arc-related succession (Villa Ayala and Acapetlahuaya formations) show a tuff and epiclastic sandstone petrofacies derived from a medium- to high-K calc-alkaline volcanic source within an undissected–transitional but evolved intra-oceanic arc. Based on petrography, the sandstone evolution of the intra-oceanic arc is documented by the tuff and epiclastic sandstone petrofacies. A third petrofacies consists of hybrid sandstone, which documents the mixture of detritus from volcanic and carbonate rocks.
2. Sandstone petrography of the Mezcala Formation reveals quartzolithic and calclithic suites, which were shed from volcanic and carbonate-platform sources. Sandstone petrography and geochemistry of the Miahuatepec Formation show it to be quartzolithic in composition and derived predominantly from an arc source.

3. Sandstone provenance results for the Miahuatepec Formation suggest the uplift and erosion of volcanic units mainly from the Arcelia-Palmar Chico subterrane, while sandstones of the Mezcala Formation have a mixed provenance from the carbonate platform (Teloloapan and Morelos formations) and volcanic rocks of the arc-related succession. This distinctive provenance in the two Upper Cretaceous siliciclastic formations points to a transitional–dissected arc provenance for the Mezcala Formation and a dissected arc provenance for the Miahuatepec Formation.

7.4. TECTONIC CONCLUSIONS

1. The stratigraphy, sedimentology, petrography and geochemistry of the different units in the Guerrero Terrane, together with data from other studies, allow to be recognized four tectonic stages in the Guerrero Terrane and the Mixteca Terrane to the east: (1) formation and evolution of multiple long-lived intra-oceanic arcs during the Early Cretaceous; (2) partial interruption of the volcanic activity and formation of island-arc carbonates during the Aptian–Albian, possibly promoted by the flexural and vertical movement of the subducting plate during accretion of the Guerrero and Mixteca terranes; (3) reactivation of volcanic activity and development of the short-lived intra-oceanic and back-arc system of the Arcelia-Palmar Chico subterrane during Albian–Cenomanian time; and (4) amalgamation-accretion events producing

uplift, erosion, thrust belts, and thick siliciclastic sequences during the Late Cretaceous.

REFERENCES

Abbott, L. D., Silver, E.A., Thompson, P.R., Lewicz, M. V., Scneider, C., and Abdoerrrias. A., 1994. Stratigraphic constraints on the development and timing of arc-continent colission in Northern Papua New Guinea. Jour. Sed. Res. V., B64, p. 169–183.

Aguilera, F. N., 1995; Litofacies, paleoecología y dinámica sedimentaria del Cenomaniano-Turoniano en el área de Zotoltitlan-La Esperanza, Estado de Guerrero, Inédito, master in science thesis, División de estudios de Posgrado, Facultad de Ingeniería, UNAM, 137p.

Aguilera, F. N., 2000. High resolution stratigraphy and palaeoecology of the Cenomania–Turonian successions, southern Mexico. University of London, Imperial College of Science Technology and Medicine. T.H. Huxley Scool of Environment, Earth Sciences and Engineering. Ph. D. thesis. 202 p.

Aigner, T., 1982. Calcareous Tempestites: Storm-dominated Stratification in Upper Muschelkalm Limestones (Middle Trias, SW-Germany). *In* Einsele G. and Seilacher A. (eds) Cyclic and event stratigraphy. Springer-Verlag. p. 180–198.

Alencaster, G. 1986. Nuevo rudista (Bivalvia-*Hippuritacea*) del Cretácico Inferior de Pihuama, jalisco. Bol. Soc. Geol. Mex., V. XLVII, p. 47–60.

Alencaster, G. and Pantoja, A. J., 1986. *Coalcomana ramosa* (Bochm) (Bivalvia-*Hippuritacea*) del Albiano Temprano del Cerro de Tuxpan, Jalisco. Bol. Soc. Geol. Mex. V. XLVII, p. 33–46.

Barnes, Ph. M., 1988. Submarine fan sedimentation at a convergent margin: the Cretaceous Mangapokia Formation, New Zealand. Sedimentary Geology, v. 59, p. 155–178.

Bhatia, M.R., 1983. Plate tectonics and geochemical composition of sandstones. Jour. Geology, v. 91, p. 611–627.

Bhatia, M.R., 1985. Rare earth geochemistry of Australian Paleozoic graywackes and mudrocks: Provenance and tectonic control. Sed. Geology. V. 45, p. 91–113.

Bhatia, M.R. and Crook, K.A.W., 1986. Trace elements characteristics of graywackes and tectonic setting discrimination of sedimentary basins. Contr. Mineral. Petr., v. 92, p. 181–193.

Bignot, G. 1985. Elements of Micropalaeontology. IHROC. 217 pp.

Böhnel, H., 1999. paleomagnetic study of Jurassic and Cretaceous rocks from the Mixteca terrane (Mexico). J. South Am. Earth Sci., v. 21, p. 545–556.

Böhnel, H., Alva, V.L.., Gonzalez, H.S., Urrutia, F. J, Moran, Z. D.J., and Schaaf, P., 1989. Paleomagnetic data and the accretion of the Guerrero terrane, southwestern Mexico continental margin, In Deep structure and past kinematics of accreted terranes, AGU Geophysical Monogran,n. 50, p. 73–92.

Bonneau, M., 1972. Données nouvelles sur les séries crétacées de la cote Pacifique du Mexique. Bull. Soc.Geol.France, 14, p. 15–65.

Bourgeois, J. 1980. A transgressive shelf sequence exhibiting hummocky stratification: The Cape Sebastian Sandstone (Upper Cretaceous), southwestern Oregon: Jour. Sed. Petrol., v. 50, p. 681–702.

Buitrón, B.E. and Rivera, C.E., 1985. Nerineidos (gastropoda-nerineidae) cretácicos de la región de Huetamo-San Lucas, Michoacán. Boletin Sociedad Geológica Mexicana, v, 46, p. 65–78.

Buitrón B.E. and Barceló D.J., 1988. Nerineidos (Mollusca-Gastropoda) del Cretácico Inferior de la region de San Juan Raya, Puebla. Revista Soc. Geol. Mex., v. 4, n.1, p.

Burckard, C., 1930. Etude synthetique sur le Mesozoique Mexicain. Mem. Soc. Pal. Suisse, 49–50, 280 p.

Busby-Spera, C.J. 1987. Lithofacies of deep marine emplacent on a Jurassic Backarc apron, Baja California (México). Jour. Geology, v. 95, p. 671–686.

Busby-Spera, C.J. 1988. Evolution of a Middle Jurassic back-arc basin, Cedros Island, Baja California: Evidence from a marine volcaniclastic arpón. Geol. Soc. Amer. Bull., v. 100, p. 218–233.

Busby, C., Smith, D., Morris, W., and Fackler-Adams, B., 1998. Evolutionary model for convergent margins facing large ocean basins: Mesozoic Baja California, Mexico. Geology, v. 26, p. 227–230.

Bustamante, G. J., Ramírez, E.J., and Miranda, H, A., 2004. Carta Geológica-Minera Taxco (E14 – A68), Estados de Guerrero, México y Morelos, Escala 1:50 000. Informe Interno COREMI-UAG. 50 p.

Cabral, C.E., 1995. Tectonostratigraphic assessment of the Tierra Caliente Metamorphic Complex, Southern Mexico. Ph. D. Dissertation. University of Miami. 140 p.

Camoin, G., Bernet–Rollande, M.C., and Phillip, J. 1988. Rudist-coral frameworks associated with submarine volcanism in the Maastrichtian of the Pachino area (Sicily). Sedimentology, v. 35, p. 123–138.

Campa, M.F., 1977. Estudio tectónico. Prospecto Altamirano-Huetamo. Pemex. Informe inedito. 94 p.

Campa, M.F., Campos, M., Flores, R., and Oviedo, R., 1974. La secuencia mesozoica volcánica-sedimentaria metamorfizada de Ixtapan de la Sal, Mex.-Teloloapan, Gro. Bol. Soc. Geol. Mex., 3, p. 7–28.

Campa, M.F. and Ramirez, E.J., 1979. La evolución geológica y metalogénetica del noroccidente de Guerrero. Serie Técnico-Científica. Universidad Autonóma de Guerrero. Tomo 1, 102 p.

Campa, M.F. and Coney, P.J, 1983. Tectono-stratigraphic terranes and mineral resources distributions in Mexico. Can. Jour. Earth Sci., v. 20, p. 1040–1051.

Campa, M.F., Ramirez, E.J., Flores, L.R., and Coney, P.J., 1980. Terrenos tectonoestratigráficos de la Sierra Madre del Sur, región comprendida entre los estados de Guerrero, Michoacán, México y Morelos. Serie Técnico-Científica 2. Univeridad Autonóma de Guerrero. 29 p.

Campa, M.F. and Iriondo, A., 2003. Early Cretaceous protolith ages for metavolcanic rocks from Taxco and Taxco Viejo in Southern Mexico. 99th Annual Meeting of the Geol. Soc. America Assoc., Cordillera Section. p. 31.

Carlisle, D., 1963. Pillow breccias and their aquagene tuffs, Quadra Island, British Columbia. Jour. Geol., v. 7, p. 48–71.

Cas, R. A.F. and Wright, J.V. 1987. Volcanic Successions. Modern and Ancient. Allen & Unwin, London, 528 pp.

Cas, R.A.F. and Wright, J.V. 1991. Subaqueous pyroclastic flows and ignimbrites: an assessment. Bull. Volcanol. , v. 53, p. 357–380.

Centeno, G.E., 1994. Tectonic evolution of the Guerrero Terrane, western Mexico. Ph.D. thesis. University of Arizona, 220 p.

Centeno, G. E., García, J. L., Guerrero, M., Ramírez, J., Salinas, J.C., and Talavera, O., 1993. Geology of the southern part of the Guerrero Terrane, Ciudad Altamirano-Telolopan area. Procceding First Circum-Pacific and Circum-Atlantic Terrane Conference, Guanajuato, Mexico. Field trip guide II, p. 22–33.

Chen, C. 1997. Statistical analysis of turbidite cycles in submarine fan successions. Unpublished PH. D. thesis. Memorial University of Newfoundland, Canada, 365 p.

Chen, C. and Hiscott, T.N., 1999. Statistical analysis of facies in submarine clustering in submarine-fan turbidite successions. Jour. Ser. Res., v. 69, n. 2, p. 505–517.

Chough, S.K. and Sohn, Y.K., 1990. Depositional mechanics and sequences of base surges, Songaksan tuff ring, Cheju Island, Korea. Sedimentology, v. 37, p. 1115–1135.

Coates, A.G., 1977. Jamaican Coral-Rudist frameworks and their geological setting. In: Stanley. H.F. et al., (eds) Reef and related carbonates–ecology and sedimentology. Studies in Geology, n. 4. A.A.P.G.

Coniglio, M. and Dix, G.R., 1992. Carbonate slope. In Walker, R.G. and James, N.P. (eds). Facies Models response to sea level change, p. 349–373. Geol. Assoc. Canada.

Coney, P.J., Jones, D.L., and Monger, J.W.H., 1980. Cordilleran suspect terranes. Nature, v. 288, p. 329–333.

Coney, P.J., 1983. Un modelo tectónico de México y sus relaciones con América del Norte, América del Sur y el Caribe. Revista Instituto Mexicano del Petróleo, v. 15, n.1., p. 6–15.

Coogan, A. H., 1973. New rudists from the Albian and Cenomanian of Mexico and adjacent South Texas. Rev. Inst. Mex. Petrol. V. 5, p. 1–83.

Corona, R., 1983. Estratigrafía de la región de Olinalá-Tecocoyunca, Noreste del Estado de Guerrero, Rev. Inst. Geol. U.N.A.M., vol. 5, no. 1, pp. 17-24.

Critelli, S., and Le Pera, E., 1995. Tectonic evolution of the Southern Apennines Thrust-Belt (Italy) as Reflected in Modal Compositions of Cenozoic Sandstone. Jour. Geol., v. 103, p. 95–105.

Critelli, S., Marsaglia, K.M., and Busby, C.J., 2002. Tectonic history of a Jurassic backarc-basin sequence (The Gran Cañon Formation, Cedros Island, Mexico), based on compositional modes of tuffaceous deposits. Geol. Soc. Am. Bull., v. 114, p. 515–527.

Davila, V. M. and Guerrero, M. 1990. Una edad basada en radiolarios para la secuencia volcánica-sedimentaria de Arcelia, Edo. de Guerrero. X Conv. Geol. Nal. Soc. Geol. Mex., abstracts, p. 83.

De Cserna, Z., 1965. Reconocimiento geológico de la Sierra Madre del Sur de México entre Chilpancingo y Acapulco, Estado de Guerrero. Bol. Inst. Geol. UNAM, 62, 76 p.

De Cserna, Z., 1983. Hoja Tejupilco 14Q-g(9), con resumen de la geología de la hoja Tejupilco, estados de Guerrero, México y Michoacán. UNAM, Inst. de Geol., Carta Geológica de México, serie 1: 100 000. 28 p.

De Cserna, Z. and Fries, C. Jr., 1981. Hoja Taxco 14Q-h (7) con resumen de la geología de la Hoja Taxco, Estados de Guerrero, México y Morelos. Univ. Nal. Autón. México, Instituto de Geología. Serie 1:100 000, 47 p.

De Cserna, Z., Palacios, M., and Pantoja, J., 1978. Relaciones de facies de las rocas cretácicas en el noreste de Guerrero y en areas colindantes de México y Michoacán. Sociedad Geológica Mexicana. Libro-guia de la excursion geológica a Tierra Caliente, p. 33–43.

Delgado, A. L., Lopez, M. M., York, D., and Hall, C. M., 1990. Geology of ultramafic localities in the Cuicateco and Tierra Caliente Complexes, southern Mexico. Gol. Soc. Am. Annual Meet., Abst. with Progr., 32 p.

Dickinson, W.R., 1970. Interpreting detrital modes of greywacke and arkose. Jour. Sed. Petr., v. 40. p. 695–707.

Dickinson, W.R., 1985. Interpreting provenance relations from detrital modes of sandstones, in Zuffa, G.G. ed. Provennace of arenites: Proceeding of the NATO Advanced Study Institute on Reading Provenance from Arenites, Cosenza, Italy, p. 333–362

Dickinson, W.R. and Lawton, T. F., 2001. Carboniferous to Cretaceous assembly and fragmentation of Mexico. Geol. Soc. America Bull., 113, no. 9, p. 1142–1160.

Dott, R.H. and Bourgeois, J. 1982. Hummocky stratification: Significance of its variable bedding sequences. Geol. Soc. Amer. Bull., v. 93, p. 663–680.

Dunham, R.J. 1962. Classification of carbonate rocks according to depositional textures. *In* Classification of carbonate rocks, a symposium. Ham, W.E. (ed) Amm. Assoc. Petr. Geol. Mem. 1, p. 108–121.

Elias, H. M., 1981. Geología del área de Almoloya de las Granadas-San Lucas del Maiz, Minicipio de Tejupilco, Estado de México. M.Sc.thesis, Fac. Ciencias U.N.A.M. 177 p.

Elias H.M., 1989. Geología Metamórfica del área de San Lucas del Maíz, Estado de México.U.N.A.M., Inst. Geología, Boletín 105. 79 pp.

Elias, H. M. and Sánchez, Z. J. L., 1992. Tectonic implications of a milonitic granite in the lower structural levels of the Tierra Caliente Complex (Guerrero state, southern Mexico). Rev. Inst. Geología, UNAM, 9, p. 113–125.

Elias H. M. and Ortega, G. F., 1997. Petrology of high-grade metapelitic xenoliths in an Oligocene rhyodacite plug-Precambrian crust beneath the southern Guerrero Terrane, Mexico?. Rev. Mex. Ciencias Geol., 14, 1, p. 101–109.

Embry, A.F. and Klovan., 1971. A Late Devonian ref. tract of northeastern Bank Island, N.W.T., Bull. Can. Petrol. Geol., v. 19, p. 732–736.

Engebretson, D.G., Cox, A., and Gordon, R.G., 1985. Relative motions between oceanic and continental plates in the Pacific basin: Boulder, Colorado, Geol. Soc. Am. Sp. Paper 206, 59 p.

Erben, H. K., 1956. El Jurásico Medio y el Calloviano de México. Cong. Geol. Internal. XX. México. Monografía.

Estrada, F. R., 1995; Análisis, distribución e interpretación de las facies turbiditicas de una porción de la Formación Mexcala, Escuela Regional de Ciencias de la Tierra. Universidad Autónoma de Guerrero, Bachelor thesis, 52p.

Eversen, N.M., Hamilton, P.J., O'nions, R.K., 1978. Rare earth abundances in chondritic meteorites. Geochemica et Cosmochmica Acta, v. 42, p. 119–1212.

Ferrusquia, I., Applegate, S.P., and Espinosa, L., 1978. Rocas volcanosedimentarias mesozoicas y huellas de dinosaurios en la region suroccidental pacifica de Mexico. Revista Inst. Geologia U.N.A.M., v. 2, n. 2, p. 150–162.

Fisher, R.V. 1984. Submarine volcaniclastic rocks. Geol. Soc. London, Special Publ. 16, p. 5–27.

Fisher, R.V. and Schmicke, H.U. 1984. Pyroclastic Rocks. Springer, New York, 472 p.

Fisher, R.V. and Smith, G.A., 1991. Volcanism, tectonic and sedimentation. In Fisher, R.V. and Smith, G.A. eds. Sedimentation in Volcanic Settings. SEPM Sp. Paper, No. 45. p. 1–5.

Flood R. D., Piper, D.J. W., Klaus, A. et al., eds., 1995. Proceeding of the Ocean Drilling Program, Initial Reports, 155: College Station, Texas (Ocean Drilling Program).

Flores, L. y Buitron, B. E. 1982. Revisión y aportes a la estratigrafía de la Montaña de Guerrero. UAG, Serie Tecnico Científica. no. 12, 28 p.

Floyd, P.A. and Leveridge, B.E., 1987. Tectonic environment of the Devonian Gramscatho basin south Corwall: Framework mode and geochemical evidence from turbiditic sandstone. Jour. Geol. Soc. London, v. 144, p. 531–542.

Folk, R.L., 1959. Practical petrographic classification of limestones, Amm. Assoc. Petroleum Geol. Bull., v. 43, p. 1–38.

Folk, R. L., 1974. Petrology of Sedimentary Rocks. Hwmphill Publ. Austin Tx. 182 p.

Freydier, C., Martínez, R.J., Lapierre, H., Tardy. M., and Coulon, C., 1996. The early Cretaceous Arperos oceanic basin (Western Mexico) Geochemical evidence for an aseismic ridgw formed near a spreading center. Tectonophysics, 259, p. 343–367.

Freydier, C., Lapierre, H., Tardy. M., Coulon, C, and Martínez, R.J., 1997. Volcaniclastic sequences with continental affinities within the late Jurassic–Early Cretaceous Guerrero Terrane intra-oceanic arc terrane (Western Mexico). Jour. Geology, 105, p. 483–503.

Fries, C. Jr., 1960. Geología del estado de Morelos y de partes adyacente de México y Guerrero, región central meridional de México. Bol. Inst. Geología, UNAM, 60, 236 p.

Fritz, W.J. and Howells, M.F. 1991. A shallow marine volcaniclastic model: an example from sedimentary rocks bounding the subaqueously welded Ordovician Garth Tuff, North Wales, U.K. Sedimentary geology, v. 74, p. 217–240.

García, D. J.L. and Talavera, M.O., 1994. Comparación litoestratigráfica entre las secuencias de Telolopan, Guerrero y Tejupilco, Estado de México. XII Conv. Nal. Soc. Geol. Mex. Abstracts, p. 60–61.

Garibay R. L.M., Sabanero S. M.E., and Sánchez R. L.E., 1996. Nerineidos (Gasteropoda= Nerinellidae Nerineidas) del Cretácico Inferior del Cerro del Gato, Chiautla, Estado de Puebla. Resumenes XIII Convención Geológica Nacional, Soc. Geol. Mex. La Paz, B.C.S. p. 52.

Garibay, R. L. M., Beltrán, S. A., Torres de L. H. R., 1999, Nueva Localidad con Inocerámidos (Mollusca Bivalvia) del Cretácico Superior del Estado de Guerrero, Primera Reunión Nacional de Ciencias de la Tierra, Simposio sobre el Sur de México, Conjunto Amoxcalli, UNAM. Abstracts.

Gill, J.B., 1981. Orogenic andesites and plate tectonics. Minerals and rocks 16, 360 p.

Gili, E., Masse, J.-P., and Skelton, P.W., 1995. Rudists as gregarious sediments-dwellers, not reef-builders, on Cretaceous carbonate platforms. Palaeogeogr. Palaeocl.,Palaeoecol., v. 118, p. 245–267.

Gómez, M.E., Contreras, M.B., Guerrero, M, and Ramírez, J., 1994. Amonitas del Valanginiano Superior y Barremiano de la Formación San Lucas, Huetamo, Michoacán. Bol. Soc. Paleont. Méx., v. 6, n. 1., p. 57–65.

González, P. V.V., 1991. Evolución sedimentológica y diagénesis del Cretácico de la porción norte del estado de Guerrero. M.Sci. Dissertation, División Estudios de Posgrado, UNAM.

Gradstein, F.M., Agterberg, F.P., Ogg, J. G., Hardenbol, J., Van Veen, P. Thierry, J. and Huang, Z. 1995. A Triassic, Jurassic and Cretaceous time scale. *In* Berggren, W.A., Kent, D.V., Aubry, M.-P., and Hardenbol, J. (eds). Geochronology, time scale and global stratigraphic correlation. SEPM Sp. Pub. 54. p. 95–126.

Guerrero, S. M., 1997. Depositional history and sedimentary petrology of the Huetamo sequence, southwestern Mexico. M.S. Dissertation. University of Texas at El Paso, USA. 120 p.

Guerrero, M., Ramírez, J., and Talavera, O., 1990. Estudio estratigráfico del arco volcánico Cretácico inferior de Teloloapan, Gro. X Conv. Nal. Soc. Geol. Méx. Abstracts. p. 67.

Guerrero, S. M. and Ramírez E. J., 1992. Depósitos de tormenta en el límite de la sedimentación de carbonatos y terrígenos (Cretácico Medio) en la región Norte de Guerrero. Memorias XI Convención Geológica Mexicana. Soc. Geol. Mex. p. 100–103.

Guerrero, M., Ramírez, J., Talavera, O., and Campa M.F., 1991. El desarrollo carbonatado del Cretácico Inferior asociado al arco de Telolopan, Noroccidente del Estado de Guerrero. Conv. Evolución Geológica de México. p. 67–70.

Guerrero, M., Ramírez, J., Gómez, M.E., González, V., and Martínez Cortes A., 1993. Depósitos de tormenta y fauna fósil asociada del Albiano Superior "Formación Teloloapan" Noroeste del Estado de Guerrero. IV Congr. Nal. Paleont. Soc. Méx. Paleont. p. 93–97.

Guerrero, S. M., Ramírez, E. J., and Hiscott N. R., 2003. Stratigraphy, sedimentology, and provenance evolution of early creataceous arcs, the Guerrero Terrane (SW Mexico): based on details studies of the Huetamo and Teloloapan areas. Cordilleran Section Meeting GSA. Vol.35., n.4.

Hayward, A.B. 1984. Hemipelagic chalks in a clastic submarine fan sequence: Miocene SW Turkey. *In* Stow, D.A.V. and Piper, D.J.W. (eds) Fine–grained sediments: deep–water processes and facies, p.453–467.

Hernández, R. Ulises., 1999. Facies, stratigraphy, and diagenesis of the Cenomanian–Turonian of the Guerrero-Morelos Platform, southern Mexico. Postgraduate Research Institute for Sedimentology, University of Reading. Ph. D. Thesis. 324 p.

Hernández, R. U., Aguilera, F. N., Martinez, M.M., and Barcelo, D. J., 1997. Guerrero-Morelos platform drowning at the Cenomanian – Turonian boundary, Huitziltepec area, Guerrero state, southern Mexico. Cretac. Res., v. 18, p. 661–686.

Hiscott, R.N., 1978. Provenance of Ordovician deep-water sandstones, Tourelle Formation, Quebec, and implications for inition of the Taconic orogeny. Can. Jour. Earth Sci., v. 15, p. 1579–1597.

Hiscott, R.N., 1980. Depositional framework of sandy mid-fan complexes of Tourelle Formation, Ordovician, Quebec. Am. Asoc. Petrol. Geol. Bull. V.64, n. 7, p. 1052–1077.

Hiscott, R.N. and James, N.P., 1985. Carbonate debris flows, Cow Head Group, western Newfoundland. Jour. Sed. Petrol., v. 55, p. 735–745.

Hiscott, R.N. and Gill, J.B., 1992. Major and trace elements geochemistry of Oligocene to Quaternary volcaniclastic sands and sandstones from the Izu-Bonin arc. In Taylor, B., Fujioka, K. et al., Proceedings of the Ocean Drilling Program, Scientific Results, v. 126, p. 467–485.

Hougthton, B.F. and Landis, C.A. 1989. Sedimentation and volcanism in a Permian arc–related basin, southern New Zealand. Bull. Volcanology, v. 51, p. 433–450.

Howell, D.G., 1995. Principles of Terrane Analysis New applications for global tectonics. Second edition. Chapman and Hall. 245 p.

Ingersoll, R., Bullard, T.F., Ford, R.L., Grimm J.B., Pickle, J.D., and Sares, S.W., 1984. The effect of grain size on detrital modes: a test of the Gazzi-Dickinson point-counting method. Jour. Sed. Petr. V. 54, p. 103–116.

Ingersoll, R., Cavazza, W., Graham S.A, and others participants, 1987. Provenance of impure claclithites in the Laramide foreland of Southwestern Montana. Jour. Sed. Petr., v. 57, p. 995–1003.

Ingram, R.L., 1954. Terminology for the thickness of stratification units and parting units in sedimentary rocks. Geol. Soc. Am. Bull., v. 65, p. 937–938.

James, N.P., 1984. Reefs. *In* Walker, R.G. (ed). Facies Models. Second edition. Geoscience Canada, reprint serie 1. p. 229–244.

Jenner, G.A., Longerich, H.P., Jackson, S.E., and Fryer, B.J., 1990. ICP-MS: a powerful tool for high-precision trace element analysis in earth sciences: evidence from analysis of selected U.S.G.S. reference samples. Chem. Geol., v. 83, p. 133–148.

Johnson, C., Lang, H., Cabral, C.E., Harrison, C., and Barros, J., 1991. preliminary assessment of stratigraphy and structure, San Lucas region, Michoacán and Guerrero states, SW Mexico. The Mountain Geologist, v. 28, n. 2-3, p. 125–135.

Johnsson, M., 1993. The system controlling the composition of clastic sediments. In: Johnsson, M.J. and Basu, A. eds. Processes Controlling the Composition of Clastic Sediments: Boulder, Colorado, Geol. Soc. Am. Special Paper 284, p. 1–19.

Kauffman, E.G. and Jonson, C.C., 1988. The morphological and ecological evolution of middle and upper Cretaceous reef–building rudists. Palaios, v. 3, p. 194–216.

Kokelaar, P. and Busby, C. 1992. Subaqueous explosive eruption and welding of pyroclastic deposits. Science, v. 257. p. 196–201.

Lajoie, J. and Stix., J. 1992. Volcaniclastic rocks. *In* Walker, R.G. and James N.P., Facies Models: Response to sea level change. Geol. Assoc. Canada. p. 101–118.

Larue, D.K., Smith, A.L., and Schellekens, J.H. 1991. Oceanic island arc stratigraphy in the Caribbean region: don't take it for granite. *In* R. Cas and C. Busby–Spera (editors). Volcaniclastic sedimentation. Sediment. Geol., v. 74, p. 289–308.

Leverenz, A. 2000. Trench–sedimentation versus accreted submarine fan – an approach to regional–scale facies analysis in a Mesozoic accretionary complex: "Torlesse" terrane, northeastern North Island, New Zealand. Sedimentary Geology, v. 132, p. 125–160.

Lorinczi, G. I and Miranda, V. 1978. Geology of the massive sulfide deposits of Campo Morado, Guerrero, Mexico. Economic Geology, v. 73, p. 180–191.

Mángano, M.G. and Buatois, L.A. 1996. Shallow marine event sedimentation in a volcanic arc–related setting: the Ordovician Suri Formation, Fatima Range, Northwest Argentina. Sediment. Geol., v. 105, p. 63–90.

Marsaglia, K.M. and Ingersoll, R.V., 1992. Compositional trends in arc-related, deep-marine sand and sandstone: A reassessment of magmatic-arc provenance. Geol. Soc. Am. Bull., v. 104, p. 1637–1649.

Marsaglia, K.M. and Tazaki, K., 1992. Diagenetic trends in ODP Leg 126 sandstones: Procceding of the Ocean Drilling Program, Scientific results, v. 126, p. 125–138.

Masse, J-P. and Phillips, J. 1988. Cretaceous coral-rudist buildups of France. *In* Toomey, D. F. (ed) European Fossil Reef Models. SEPM Special Publ. No. 30. p. 399–426.

Masse, J-P., Villeneuve, M., Tumanda, F., Quiel, C., and Diegor, W., 1996. Plates-formes carbonatées à orbitolines et rudistes du Crétacé inférieur dans l'île de Cebu (Philippines). C.R. Acad. Sci. Paris, t. 322, série Iia, p. 973–980.

Matthews, J.L., Heezen, B.C., Catalano, R., Coogan, A., Tharp, M., and Rawson., 1974. Cretaceous drowning of Reef on Mid-Pacific and Japanese Guyots. Science. V. 184, p. 462-464.

McCann, T., 1991. Petrological and geochemical determination of provenance in the southern Welsh Basin. In Morton, A.C., Todd, S.P., and Haughton, P.D.W., (eds). Developments in Sedimentary Provenance Studies. Geol. Soc. Sp. Paper, 57, p. 215–230.

McLennan, S.M. and Taylor, S.R., 1991. Sedimentary rocks and crustal evolution: Tectonic setting and secular trend. Jour. Geology, v. 99, p. 1–21.

McLennan, S.M., Taylor, S.R., McCulloch, M.T., and Maynard, J.B., 1990. Geochemical and Sm-Sr isotopic composition of deep sea turbicites: Crustal evolution and plate tectonics association. Geochemica et Cosmochimica Acta, v. 54, p. 2015–2050.

McLennan, S.M., Hemming, D.K., McDaniel, D.K., and Hanson, G.N., 1993. Geochemical approaches to sedimentation, provenance, and tectonics. In Johnsson, M.J. and Basu, A. (eds). Processes controlling the composition of clastic sediments. Boulder, Colorado. Geol. Soc. Am. Sp. Paper 284. p. 21–40.

Mendoza, O.T. and Suastegui, M.G., 2000. Geochemistry and isotopic composition of the Guerrero Terrane (western Mexico): implications for the tectono-magmatic evolution of southwestern North America during the Late Mesozoic. Jour. South America Earth Sci., v. 13, p. 297–324.

Miyashiro, A., 1974. Volcanic rock series in island arcs and active continental margins. Am.. J.Sci., v. 274, p. 321–355.

Molina, G. R.S., Böhnel, H, and Hernandez T., 2003. Paleomagnetism of the Cretaceous Morelos and Mezcala formations, southern Mexico. Tectonophysics, v. 361, p. 301–317.

Monod, O., Busnardo, R. and Guerrero, S.M., 2000. Late Albian ammonites from the carbonate cover of the Teloloapan arc volcanic rocks (Guerrero State, Mexico). South Am. Earth Sci., v. 13, p. 377–388.

Mortensen, J.K., Hall, B. V, Bissig, Th., Friedman, R.M., Danielson, Th., Olivier, J., Rhys, D.A., and Ross, K.V. 2003. U-Pb zircon age and Pb isotopic constraints on the age and origin of volcanogenic massive sulfides deposits in the Guerrero Terrane of Central Mexico. 99th Annual Meeting of the Geol. Soc. America Assoc., Cordillera Section. P. 24-4.

Mutti, E., 1977. Distinctive thin-bedded turbidite facies and related depositional environments in the Eocene Hecho Group (South-central Pyrenees, Spain). Sedimentology, v. 24, p. 107–131.

Mutti, E., 1979. Turbidites et cones sous-margin profound. *In* Homewood P. (ed). Sédimentation Détrique (fluviale, littorale et marine). Institut Geologie Université de Fribourgh. Fribourgh, Switzerland, p. 353–419.

Mutti, E., 1985. Turbidite systems and their relations to depositional sequences. *In* G.G. Zuffa (ed). Provenance of Arenites. D. Reidel Publ. Co. p. 65–93.

Mutti, E. and Ricci–Lucchi, F. 1975. Turbidites of the northern Appennines: Introduction to facies analysis. Intern. Geol. Rev., v. 20, p. 125–165.

Mutti, E. and Normark, W.R., 1987. Comparing examples of Modern and Ancient Turbidite Systems: Problems and Concepts. *In* Legget, J.K., and Zuffa, G.G. (eds). Marine Clastic Sedimentology. p. 1–38.

Nelson, C.H., Normark, W.R., Bouma, A.H., and Carlson, P.R., 1978. Thin–bedded turbidites in modern submarine canyons and fans. *In* Stanley, D.J. and Kelling, G. (eds). Sedimentation in submarine canyons, fans and trenches. p. 177–189. Dowden, Hutchinson and Ross Inc.

Nesbitt, H.W. and Young, G.M., 1984. Prediction of some weathering trends of plutonic and volcanic rock based on thermodynamic and kinetic considerations. Geochemica et Cosmochimica Acta, v. 48, p. 1523–1534.

Nielsen, T.H., 1985. Chugach Turbidite system, Alaska. *In* Bouma, A.H. and Barnes, N.E. (eds). Submarine fans and related turbidite systems. Springer, N.Y., p. 185–192.

North American Stratigraphic Code, 1984. Bull. Am. Assoc. Petrol. Geol., 67, p. 841–875.

Ocampo, D. Y.E., 2004. Análisis sedimentológico de la Formación Mexcala al Norte del estado de Guerrero. Unidad Académica de Ciencias de la Tierra. Universidad Autónoma de Guerrero. Bachelor thesis. 189 p.

Ocampo, D. Y. Z. E., Palacios, C. E., Rosendo, B. B., García, O. M., Buitrón, S. E. B. y Guerrero, S. M., 2002. Tres nuevas localidades fosilíferas de la Familia Inoceramidae dentro de la formación Mexcala al Norte de Guerrero., VIII Congreso Nacional de Paleontología, Abstracts, p. 117.

Ontiveros, T. G., 1973. Estudio estratigráfico de la porción noroccidental de la cuenca Morelos-Guerrero. Bol. Asoc. Mex. Geol. Petrol., 25, 189–234.

Ortega, G.F., 1978. Estratigrafia del Complejo Acatlan en la Mixteca Baja, Estados de Puebla y Oaxaca. UNAM, Rev. Inst. Geol., v. 2, n, 2., p. 112–131.

Ortega, G. F., 1981. Metamorphic belts of southern Mexico and their tectonic significance. Geofísica Internacional, 20, 177–202.

Ortiz, E. and Lapierre, H., 1991. Las secuencias toleíticas de Guanajuato y Arcelia, México centro-meridional: remanentes de un arco insular intra-oceánico del Jurásico superior-Crétacico inferior. Zbl. Geol. Palaeont. Teil I, 6, p. 1503–1517.

Orton, G.J. 1995. Facies models in volcanic terrains: time's arrow versus time's cycle. *In* Sedimentary Facies Analysis (Ed. A.G. Plint). P. 157–193. Blackwell Science, Oxford.

Orton, G.J., 1996. Volcanic environments. *In* Reading, H.G. (ed). Sedimentary environments: Processes, facies and stratigraphy. P. 485–567. Blackwell Science. Third Edition.

Pantoja, J.A., 1959. Estudio geológico de reconocimiento de la region de Huetamo, estados de Michoacán. Consejo de Recursos Naturales. Boletin 50, 36 p.

Pantoja, J.A., 1990. Redefinición de las unidades estratigráficas de la secuencia mesozoica de la región de Huetamo-Altamirano, estados de Michoacan y Guerrero. 10 a Convención Nacional, Resumenes, Soc. Geol. Mex., p.66.

Pantoja, J. A. 1993. Geology and rudist communities of the Huetamo region, State of Michoacan, Mexico. Guidebook of field trip B. Third Int. Conf. on Rudists, Mexico. 40 p.

Parga, P. J.J., 1981. Geología del area de Tizapa, Municipio de Zacazonapan, México. UNAM, Faculty of Science, M.S. Thesis, 135 p.

Pecerillo, A. and Taylor, S.R., 1976. Geochemistry of Eocene calc-alkaline volcanic rocks from Kastamonu area, northern Turkey. Contrib. Mineral. Petrol., v. 58, p. 63–81.

Pettijohn,F.J., Potter, P.E., and Siever, R., 1987. Sand and Sandstone. Springer-Verlag. 553 p.

Pickering, K.T., 1981. Two types of outer fan lobes sequence, from the late Precambrian Kongsfjord Formation submarine fan, Finmark, North Norway. Jour. Sed. Petrol., v. 51., n. 4., p. 1277–1286.

Pickering, K.T., Basset, M.G., and Siveter, D.J., 1988. Late Ordovician–early Silurian destruction of the Iapetus Ocean: Newfoundland, British Isles and Scandinavia–a discussion. Trasactions Royal Soc. Edimburgh. Earth Sciences, v. 79, p. 361–382.

Pickering, K.T., Hiscott, R.N., and Hein, F.J., 1989. Deep Marine Environments Clastic Sedimentation and Tectonics. Unwin Hyman, 416 p.

Pirrie, D., 1989. Shallow marine sedimentation within an active margin basin, James Ross Island, Antarctica. Sedimentary Geology, v. 63, p. 61–82.

Piper, D. J.W. 1978. Turbidite muds and silts on deep sea fans and abyssal plains. *In* Sedimentation in submarine canyons, fans and trenches. Stanley, D.J. and Kelling, G. (eds). Dowden, Hutchinson and Ross, Stroudsburg, PA. p. 163–176.

Polsak, A., 1981. Upper Cretaceous biolithitic complexes in a subduction zone: examples from the Inner Dinarides, Yugoslavia. *In* Toomey, D.F. (ed). European Fossil Reef models. SEPM Sp. Publ. 30., p. 447–472.

Ramírez, E.J., 1984. La acreción de los Terrenos Mixteco y Oaxaca durante el Crétacico inferior. Sierra Madre del Sur, México. Soc. Geol. Mex. Tomo XLV, 1–2, p. 7–20.

Ramírez, J., Guerrero, M., Talavera, O., and Salinas J.C., 1990. Los arcos magmáticos acrecionados del Occidente de México, Sierra Madre del Sur. Area Teloloapan-Arcelia, Gro. Internal Report Escuela Regional de Ciencias de la Tierra, U.A.G. 80 p.

Ramírez, J., Campa, M.F., Talavera, O., and Guerrero, M., 1991. Caracterización de los arcos insulares de la Sierra Madre del Sur y sus implicaciones tectónicas. Congreso Evolución Geológica de México. Soc. Mex. de Mineralogía. Inst. Geol., UNAM. Memory, p. 163-166.

Read, J.F., 1985. Carbonate platform facies models. Am. Assoc. Petrol. Geol. Bull., v. 66, p. 860–878.

Reading, H.G. and Richards, M., 1994. Turbidite systems in deep-water basin margins classified by grain size and feeder system. Am. Assoc.Petrol. Geol. Bull., v. 78, n. 5, p. 792–822.

Rodriguez, J., 1994. Estudio Petrográfico de la Secuencia Volcaniclástica de Telolopan, Gro. Bachelor Thesis. Escuela Regional de Ciencias de la Tierra, UAG. 84 p.

Rosendo, B. B., Ocampo, D. Y. Z. E., Buitrón, S. B. E y Garibay, R. L. M., 2002. Crinoides Planctónicos (Crinoide, Roveacrinidae) del Cretácico Superior de Cerro Gordo, Municipio de Taxco de Alarcón, Guerrero, VIII Cong. Nal. Paleont, Abstracts, p. 79.

Salinas, J.C., 1994. Etude structurale du Sud-ouest Mexicain (Guerrero). Analyse microtectonique des déformations ductiles du Tertiaire Infériour. Ph. D. Dissertation, Université D'Orléans, France, 211 p.

Salinas, J.C., Monod, O., and Faure, M., 2000. Ductile deformations of opposite vergence in the eastern part of the Guerrero Terrane (SW Mexico). Jour. South Am. Earth Sci., v. 13, p. 389–402.

Sanchez, Z. J.L., 1993. Secuencia volcanosedimentaria Jurásico superior-Cretácico inferior de Arcelia-Otzolapa (Terreno Guerrero) area Valle de Bravo-Zacazonapan, estado de México: Petrografía, geoquímica, metamorfismo e interpretación tectónica. M.Sci. dissertation, Fac. Ciencias, UNAM. 88 p.

Scott, R.W., 1988. Evolution of Late Jurassic and Early Cretaceous reef biotas. Palaios, v. 3, p. 184–193.

Shanmugam, G., Moiola, R.J., McPherson, J.G., and O'Connell, S. 1988. Comparison of turbidite facies associations in moder passive-margine Mississippi fan with ancient active-margin fans. Sedim. Geol., v, 58, p. 63–77.

Shiba, M., 1993. Middle Cretaceous Carbonate Banks om the Daiich-Kashima Seamount at the Junction of the Japan and Izu-Bonin Trenches. *In* Simo, J.A. T. et al (eds). Cretaceous Carbonate Platforms. AAPG. Memoir 56. p. 465–471.

Smith, G.A. and Landis, Ch. A., 1995. Intra-arc Basins. *In* Busby, C.J. and Ingersoll, R.V. (eds). Tectonics of Sedimentary Basins. Blackwell Science. p. 263–298.

Soja, C.M. 1996. Island–arc carbonates: characterization and recognition in the ancient geologic record. Earth Sci. Rev., v. 41, p. 31–65.

Stix, J., 1991. Subaqueous, intermediate to silicic–composition explosive volcanism: a review. Earth Sci. Rev., v. 31, p. 21–35.

Stow D.A.V. and Shanmugam G. 1980. Sequence of structures in fine–grained turbidites: comparison of recent deep–sea and ancient flysh sediments. Sedim Geol., v.24, p. 23–42.

Talavera, O., 1993. Les formations orogéniques mésozoiques du Guerrero (Mexique méridonal). Contributions a la connaissance de l'évolution géodinamique des cordilléres mexicaines. Thése de doctorat de l'Univ. Joseph Fourier-Grenoble I, France. 462 p.

Talavera, M. O., 2000. Melanges in southern Mexico: geochemistry and metamorphism of the Las Ollas complex (Guerrero terrane): Can. Jour. Earth Sci. , v. 37, p. 1309–1320.

Talavera, M.O., Ramirez, J., and Guerrero M., 1993. Geochemical evolution of the Guerrero Terrane: example of a Late Mesozoic multi-arc system. In Proceeding of the First Circum-Pacific and Circum-Atlantic Terrane Conference, Guanajuato, Mexico. P. 150–152.

Talavera, O., Ramirez, J, and Guerrero, M., 1995. Petrology and geochemistry of the Teloloapan Subterrane: a lower Cretaceous evolved intra-oceanic island arc. Geofisica Internacional, v, 34, p. 3–22.

Tardy, M., Lapierre, H., Bourdier, J. L., Coulon, C., Ortiz, E., and Yta, M., 1992. Intra-oceanic setting of the western Mexico Guerrero Terrane. Implications for the Pacific-Tethys Geodynamic Relationships. UNAM. Rev. Inst. Geol.

Tardy, M., Lapierre, H., Freydier, C., Coulon, C., Gill, J.B., De Lepinay, M., Beck, C., Martinez, R., Talavera, O., Ortiz, E., Stein, G., Bourdier, J.L., and Yta. M.,

1994. The Guerrero suspect terrane (western Mexico) and coeval arc terranes (Greater Antille and Western Cordillera of Colombia). A Late Mesozoic intra-oceanic arc accreted to cratonic America during the Cretaceous. Tectonophysicss, 230, p. 49-73.

Taylor, B., Fujioka, K. et al., 1990. Proceeding ODP, Initial Reports, v.126. College Station, TX (Ocean Drilling Program).

Taylor, S.R., 1969. Trace element chemistry of andesites and associated calc-alkaline rocks. In McBirney, A. R. (ed), Proceedings of the Andesite Conference, Bull. Oregon Dept. Geol. Mineral. Industries, v. 65, p. 43–64.

Taylor, S.R. and McLennan, S.M., 1985. The Continental Crust: Its Composition and Evolution. Oxford Blackwell Scientific. 312 p.

Tolson, G., 1993. Structural geology and tectonic evolution of the Santa Rosa area, SW Mexico State, Mexico. Geof. Int. v., 32, p. 397–413.

Umhoefer, P.J., 2003. A model for the North America Cordillera in the Early Cretaceous: Tectonic escape related to arc collision of the Guerrero terrane and a change in North America plate motion. In Johnson, S.E., Paterson, S.R., Fletcher, J.M., Kimbrough, D.L., and Martin-Barajas, A. (eds). Tectonic evolution of northwestern Mexico and the southwestern USA: Boulder, Colorado, Geol. Soc. Am. Sp. Paper 374, p. 117–134.

Underwood, M.B. 1984. A sedimentological perspective on strata disruption within sandstone–rich melange terranes. Jour. Geology, v. 92, p. 369–385.

Upadhyay, R., 2001. Middle Cretaceous carbonate build-ups and volcanic seamount in the Shyok suture, Northern Ladakh, India. Current Science, v. 81, n. 6., p. 695–699.

Urrutia F. J. and Linares, E., 1981. Dating of hydrothermal alteration, Ixtapan de la Sal, Mexico State, Mexico. Isochron West., v. 31, p. 15.

Urrutia, F.J. and Valencio, D.A., 1986. Paleomagnetic study of mesozoic rocks from Ixtapan de la Sal, Mexico. Geofisica Internacional, 25, p. 485–502.

Vidal, S.R., 1986. Tectonica de la región de Zihuatanejo, Gro. Sierra Madre del Sur. Bachelor thesis. I.P.N. - E.S.I.A. Mexico. 155 p.

Wallin, R.C.R., 2003. Provenance of Triassic–Cretaceous sandstones in the Antarctic Penincula: Implications for terrane models during Gondwana breakup. Jour. Sed. Res. V. 73. p. 1062–1077.

Wentworth, C.K., 1922. A scale of grade and class term for clastic sediments. Jour. Geology., v. 30, p. 377–392.

White, J.D.L. and Busby-Spera, C.J. 1987. Deep marine arc arpón deposits and syndepositional magmatism in the Alisitos Group at Punta Cono, Baja California, Mexico. Sedimentology, v. 34., p. 911–927

Wilson, J.L., 1975. Carbonate facies in geologic history. Springer-Verlag. 471 p.

Wright, I.C. 1996. Volcaniclastic processes on modern submarine arc stratovolcanoes: sidescan and photographic evidence from the Rumble IV and V volcanoes, southern Kermadec Arc (SW Pacific). Mar. Geol., v. 136, p. 21–39.

Wright, I.C., Stoffers, P., Hannington, M., de Ronde, C.E.J., Herzig,P. , Smith, I.E.M., and Browne, P.R.L. 2002. Towed–camera investigations of shallow–intermediate water–depth submarine stratovolcanoes of the southern Kermadec ar, New Zealand. Mar. Geol., v. 185, p. 207–218.

Yamada, E., 1984. Subaqueous pyroclastic flows: their development and their deposits. *In* Kokelaar ,B.P. and Howell, M.F. (eds). Marginal Basin Geology. Geol. Soc. London, p. 29–35.

Yamagishi, H., 1991. Morphological and sedimentological characteristics of the Neogene submarine coherent lavas and hyaloclastites in Southwest Hokkaido, Japan. *In* Cas, R. and Busby-Spera C. (eds). Volcaniclastic sedimentation. Sediment. Geol. V. 74, p. 5–23.

Zuffa, G.G., 1980. Hybrid arenites: their composition and classification. Jour. Sed. Petrol., v.50, p. 21–29.

Zuffa, G.G., 1985. Optical analyses of arenites: Influence of methodology on compositional results, in: Zuffa, G.G., ed. Provennace of arenites: Proceeding of the NATO Advanced Study Institute on Reading Provenance from Arenites, Cosenza, Italy, p. 165–190.

APPENDIX 1. TYPE SECTION OF THE VILLA AYALA FORMATION
MEASURED SECTION VILLA AYALA – RANCHOS NUEVOS

Location:

The section starts at Villa Ayala town (18º 24' N; 100º 02' W) and finishes at Ranchos Nuevos town (18º25' N; 100º 00' W). The section was measured along federal road 51 (Iguala–Altamirano) in different segments because of the poor vertical continuity and strong deformation. A general SW-NE line of section is followed.

Villa Ayala-Puerto El Aire locality

Thickness (m)	Description
0–100	Pillow lavas interval. The pillow lavas are dark to light green color with a basalt-andesite composition and a porphyritic texture. They show regular and uniform accumulations of cylindrical pillow lobes with hyaloclastic matrix. The pillow lobe can be individualized. Each pillow lava lobe is usually 1 m in diameter.
100–130	Volcanic breccia interval. The volcanic breccias contain monogenetic basalt fragments with variable size. The clasts are angular to subangular in shape. Clasts are contained in a fine to medium grained tuffaceous matrix that shows a pseudo fluidal texture. Small scale and poorly developed basalt "wisp" structures are observed in the contact between the matrix and the clasts, where foliation is less intense.
130–200	Tuff interval. The tuffs are very thin- to thin-bedded, fine- and very fine-grained with abundant radiolaria. The beds are stacked in sets up to 20 cm thickness. The beds are channelized, showing lateral continuity. Bed contacts are sharp and loaded. Sedimentary structures include parallel and ripple laminations, and rip-up clasts. Some beds show lenticular bedding. The main feature of this level is the high alteration to kaolinite.

200–230 Pillow lavas interval similar to above described in interval 0–100 m. Pillow lobes reach 1.5–2 m in diameter. They show an incipient mineralization and oxidation.

230–300 Volcanic breccia interval. Very thick-bedded volcanic breccia is similar to interval 100–130 m. This interval is poorly exposed and partially covered.

300–400 Tuff interval. Fine- grained and medium-grained tuffs are interbedded. Radiolarian fauna are mainly observed in the lower intervals. Tuff beds are stacked forming sets up to 600 cm thick. This interval shows graded beds and rip-up clasts. Bed contacts are sharp and erosive. Sedimentary structures include abundant parallel and ripple laminations associated with intervals of Bouma sequence Tbc and Tab. The uppermost level is dominated by very thin-bedded tuff with parallel lamination and lenticular stratification. The main alteration feature of this level is the high kaolinitization and oxidation.

400–500 Massive lava interval. Basalt-andesite lava flows show variable texture ranging from aphyric to porphyric basalt to porphyric andesite. phenocrytals include olivine, clinopyroxene, amphibole, and altered plagioclase. Fenocrystals in both basalts and andesites are contained in a microlitic groundmass. Some portions of the interval show high alteration.

Ranchos Nuevos locality

0–97 Poorly exposed volcanic breccia. The volcanic breccia shows angular to subrounded clasts of basalt and andesite. Volcanic breccia is interbeded with intervals (200-500 cm) of thick-bedded, medium-grained tuff.

97–110 Lava interval. Massive lava flow shows the same textural characteristics of the above described in the Villa Ayala-Puerto El Aire section.

110–182 Tuff interval. Thin- and medium-bedded tuff poorly exposed. The tuffs are highly altered. Parallel lamination is the usual sedimentary structure observed.

182–213 Clast- and matrix-supported volcanic conglomerate interval. The clast-supported volcanic conglomerate is 200 to 500 cm thickness. This interval contains basaltic-andesitic lava and fine-grained tuff fragments. The clasts are contained in a tuffaceous matrix. Clasts are subrounded to subangular in shape and range from 5 to 60 cm in diameter. The matrix-supported volcanic conglomerate contains angular basalt-andesite fragments and scarce tuff clasts. Bed contacts are generally sharp, erosive, and occasionally graded. Bed thickness is highly variable, with thick to very thick intervals from 2 to 10 m in thickness. Some levels in the Ranchos Nuevo town exhibit a partial gradation and pinch-out features in the uppermost level.

213–255 Tuff interval. Thick to medium-bedded, coarse- to fine-grained tuff is characteristic in this level. Individual beds are normally graded with parallel lamination near the top beds. This interval shows frequently sharp contacts, but also developed rip-up clast levels.

255–305 Clast-supported volcanic conglomerate interval. The clast-supported conglomerates contain subrounded to rounded volcanic and tuffs clasts in a coarse-grained tuffaceous matrix. Graded and parallel laminations are the usual sedimentary structures.

305–485 Very thin- to thin-bedded, fine- to medium-grained tuff interval. The interval is highly altered to kaolinite.

APPENDIX 2. REFERENCE TYPE SECTION OF THE VILLA AYALA FORMATION

MEASURED SECTION AT AHUACATITLAN LOCALITY

Location:

The section starts ~0.5 km SE of Ahuacatitlan town (18º22.5' N; 99º49' W). The section was measured along the slope of the Ahuacatitlan Hill in the west flank of an anticline. The outcrops are generally well exposed.

Thickness (m).	Description
0–17	Tuff interval. Thick and medium-bedded, medium- to coarse-grained structureless tuff and epiclastic sandstone predominate in this interval. The interval is poorly exposed.
17–23	Tuffaceous sandstone interval. Coarse- to very coarse-grained tuffaceous sandstone contains fossiliferous limestone clasts with corals and gastropods.
23–24	Tuff interval similar to interval 0–17 m.
24 –38	Limestone with volcaniclastic interval. Thin- to medium-bedded lithoclast wackestone is interbedded with abundant volcanic and volcaniclastic fragments. Reworked coral fragments are present.
38–44	Tuff interval. Thin-bedded, fine-grained tuff and fine-grained epiclastic sandstone interbedded with very thin-bedded bioclastic wackestone are observed in this interval.
44–47	Tuff and epiclastic sandstone interval. The interval contains thick-bedded, coarse-grained tuff and epiclastic sandstone similar to interval 17–23 m. Bed gradation is observed in the strata. Erosive contact beds are common.
47–53	Poorly exposed thin-bedded, fine-grained tuff.

53–56	Tuff interval. Coarse-grained tuff is associated with epiclastic sandstone. Both are partially covered.
56–62	Poor exposed thin-bedded, fine-grained tuffs and epiclastic sandstones interval.
62–68	Tuff interval. Very coarse-grained tuff and epiclastic conglomerate with volcanic and limestone fragments. The clast size ranges from granules to boulders. The interval does not show lateral continuity and is pinched-out. The conglomerate is decreasing in grain size toward the upper part of the interval.
68–77	Poorly exposed tuff interval.
77–88	Very thick-bedded granule conglomerate interval. Fragment composition in the conglomerate is volcanic with abundantly reworked limestone lithoclasts and bioclasts. The clasts are contained in a medium-grained epiclastic matrix. Laterally, the interval is interbedded with brecciated limestone.
88–93	Conglomerate interval. The conglomerate shows gradation. The base level contains homogeneous cobble–pebbly conglomerate. The top interval is chaotic, containing pebble to boulder conglomerate with abundant matrix.
93–94	Tuff interval. This interval is predominantly a medium-bedded, medium-grained, tuff-epiclastic sandstone interval.
94–100	Conglomerate interval. This interval is similar to the previously described in 88–93 m interval.

APPENDIX 3. FOSSILS OF THE VILLA AYALA AND ACAPETLAHUAYA FORMATIONS

Villa Ayala Formation

Radiolaria

Archaeodictyomyritra apiara Rust

Stradneria crenulata

Dyctyomitra sp. Foreman

Eucyrtis elido Schaaf

E. tenuis Rust

E. micropora Squibabol

Pantanellium corriganensis Pessagno

Pseudodictyomitra depresa Baumgartner

P. depresa

P. carphatica Lozyniak

Pseudopaskentaensis sp. Pessagno

Ristola boesii Parona

Sethocapsa hashimoto Tumanda

Thanarla pulchra Squinabol

T. conica

Xitus spicularis Aliev

Archaeodictyomitra puga Schaaf

A. vulgaris Pessagno

Holocryptocanium sp.

Obesacapsula rotunda

Pantanellium lanceola Parona

Calcareous nannoplancton

(Coccoliths)

Conusphaera sp

Watznaueria sp

Braanudosphaerids

Nerineids

Nerinella dayi (Blackenhorn)

Cosmannea (*Eunerinea*) titania

Plesioptyxis fleuriani D'Orbigni

Cosmannea (*Eunerinea*) *hicoriensis*

Acapetlahuaya Formation

Ammonites

Dufrenoya aff *turcata* Sow

Dufrenoya sp.

Parahoplites sp.

Hamites sp.

Acanthoplites sp.

APPENDIX 4. TYPE SECTION OF THE ACAPETLAHUAYA FORMATION
ACAPETLAHUAYA-HUAYATENGO SECTION

Location:

The section starts ~2.5 km NW of Acapetlahuaya town (18º 26' N; 110º 05' W). The section was measured along the road from Acapetlahuaya to Huayatengo localities. A continuous vertical section from the base to the top of the formation was not measured because of strong deformation. Only small sections were measured in detail. A composite stratigraphic column is proposed for the unit based on way-up criteria and regional structural trends.

Thickness (m).	Description
0–20	Tuff interval. The interval shows a very thick-bedded, coarse-grained tuff interbedded with small levels of thin-bedded, fine-grained tuff (1–5 cm). Some beds contain gradation and parallel lamination, but in general they are structureless.
20–25	Lava interval. Massive lava shows basalt-andesite composition with porphyritic texture, and intense weathering.
25–75	Tuff interval. Medium-bedded, medium-grained tuff alternating with thin bedded, fine to very fine-grained tuff. Tuffs form stacked beds up to 7 m thickness. The bed contacts are sharp and loaded. Graded beds and parallel lamination are common. Laminated, fine-grained tuff shows intervals up to 15 m thickness.
75–130	Tuff interval. This interval is similar in composition to the above described in interval 25–75 m, but the fine-grained- tuff is predominant, while thin- to medium-bedded, medium-grained tuff is minor. Fine-grained tuff is up to 20 m in thickness. Parallel lamination and graded beds are the usual sedimentary structures.

130–200	Tuff interval. The overall ratio of fine-grained tuff to medium-grained tuff is almost 5:1, with common intermitted laminated fine-grained tuff intervals.
200-375	Tuff interval. Laminated, very fine- to fine-grained tuff is predominant. Strong deformation is observed in the interval.
375–385	Sandstone interval. Thin- to thick-bedded epiclastic sandstone is interbedded with fine-grained tuff or siltstone. The epiclastic sandstone beds show abundant parallel lamination and scarce graded beds. The epiclastic sandstone is 30 to 60 cm in thickness, while siltstone is 5-8 cm in thickness.
385–415	Siltstone interval. The interval has similar sedimentary structures to the above described. However, grain size is finer (siltstone vs. sandstone)
415-435	Limestone interval. The interval is very thin-bedded limestone with interbedded siltstone. Limestone beds are recrystallized marls and carbonaceous limestone in the upper part.

APPENDIX 5. TYPE SECTION OF THE TELOLOAPAN FORMATION

TELOLOAPAN SECTION

Location:

The section starts ~ 2.5 km east of Teloloapan town (18º 22' N; 99º 55.8' W). The section was measured following a SE-NW line of section along the rural road between Teloloapan and Ahuacatitlan towns. A continuous vertical section contains the lower and middle parts of the Teloloapan Formation.

Thickness (m).	Description
0–28	Hybrid limestone interval. The interval shows thin- to medium-bedded packstone–wackestone interbedded with tuff. Volcanic material gives a light green color to the limestone. The limestone is recrystallized and dolomitized. Abundant fauna in this interval includes nerineids rudists (monopleurids and radiolitids), algae mats, and benthic foraminifera. Juvenile nerineids are concentrated in interval from 5 to 20 cm with shells orientated parallel to the stratification.
28–48	Packstone interval. Thin- to medium-bedded benthic foraminifera packstone. This interval is interbedded with mudstone and sporadic wackestone.
48–82	Wackestone interval. Limestones in this interval are thin- to medium-bedded dolomitized, benthic foraminifera wackestones and algae mats. Some beds show adult nerinea fauna up to 30 cm in size.
82–160	Packstone interval. This level is similar in composition to the above described in interval 28–48. The main characteristic of the packstone interval is the intense dolimitization and sporadic rudists fauna (monopleurids).

160–215 Rudstone-framestone interval. The interval contains thick- to very thick-bedded rudist rudstone–framestone that is partially dolomitized and recristallized. The caprinid- radiolitid assemblage is a common feature. Some beds are bioturbated.

215–380 Wackestone interval. Limestones in this interval are thin- to medium-bedded wackestone with dolomitization and recrystallization.

380–485 Dolomitized boundstone interval. The interval shows a massive to thick-bedded dolomized rudist boundstone characterized by abundant rudists (caprinids, radiolitids, and monopleurids) and scattered nerineids fauna. Bioturbated beds are commonly observed in this interval. Medium-bedded dolomitized lithoclastic and bioclastic packstone–wackstone intervals are also common observed in this level. The uppermost levels contain rudstone-floatstone textures associated to the dolomitized boundstone.

APPENDIX 6. REFERENCE TYPE SECTION OF THE TELOLOAPAN FORMATION

Location:

The reference section por the uppermost part of the Teloloapan Formation is located NW of La Concordia town (18º 17' N; 99º 51' W). The section was measured following a SE-NW. A continuous vertical section contains the upper part of the Teloloapan Formation and its contact with the Mezcala Formation..

Thickness (m).	Description
0–30	Dolomitized boundstone interval. The interval shows a massive to thick-bedded dolomized rudist boundstone characterized by abundant rudists (caprinids, radiolitids, and monopleurids), which show cluster and isolated rudists structure.
30–40	Limestone conglomerate. This part of the formation is composed of thick-bedded limestone comglomerates, which contain abundant reworked ammonites and rudits. The grain size is variable but predominate the boulders and pebble of lithoclast derived from the rudist boundstone level.
40–70	Packstone–mudstone interval. Thin- to medium-bedded laminated packstone to mudstone contain abundant fauna of ammonites and planktonic foraminifera, as well as hummocky cross-stratification.
70–80	Mudstone interval. The uppermost part of the Teloloapan Formation is predominantely mudstone interbedded with thin levels of laminated limestone (wackestones with abundant planktonic foroaminifera). This interval is overlain concordantly and transitional by marls and silstones of the Mezcala Formation.

APPENDIX 7. FOSSILS OF THE TELOLOAPAN FORMATION

Upper Aptian–Early Albian

Nerineids

Cossnannea (*Eunerinea*) *titania* Felix

Cosmannea (*Eunerinea*)*azteca* Alencaster

Cossmanea (*Eunerinea*) *hicoriensis* Cragin

Plesiptyxis fleuriani D'Orbigny

Plesiptyxis prefleuriani Delpey

Nerinella dayi Blackenhorn

Planktonic fauna

Microcalamoides diversus

Colomiella recta

Calpionella alpina

Middle Albian

Rudists

Coalcomana ramose

Caprinuliodea sp.

Toucasia sp

Texicaprina sp.

Praecaprina sp.

Nerineids

Nerinella (*Plesioptygmatis*) *tomatoensis*

Adiozoptyxis coquandiana D'Orbigni

Upper Albian

Ammonites

Mariella aff. camachoensis

Hamites cf. rotundus Sowerby

Turrilites (Turrilitoides) cf hugardianus

Manuaniceras peruvianus (von Bush)

multifidum (Steinmann)

Hysteroceras carinatum Spath

Mortoniceras (*Deiradoceras*) *cunninptoni* Spath

Puzosia (*Anapuzoisa*) sp.

Gaudryceras sp.

Hamites tenuis ?

Lechites sp.

Planktonic fauna

Favusella scitula ***Michel***

F. hiltermani (Loeblich and Tappan)

F. hedbergellaformis ***Longoria***

F. papagayoensis ? Longoria and Gamper

F. nitida Michel

F. pessagnoi Michel

F. cuadrata Michel

F. washitensis (Carsey)

F. hedbergellaensis ? Longoria and Gamper

F. orbiculata

F . wenoensis

Ticinella sp

T. multiloculata

APPENDIX 7. FOSSILS OF THE TELOLOAPAN FORMATION (CONTINUED)

Ammonites*

Hmamites sp. Gr. *intermedius*

Desmoceras latidorsatum

Lecchites moreli

Stoliczkaia sp. Gr. *notha*

S. cf. *tenuis*

S. (*Faraudiella*) cf. *blancheti*

Pervinquieria sp.

P. gr. *inflata*

P. juv. gr. *inflata*

P. rostrata

Oxytropidoceras cf. *cantianum*

Turrilitoides hugardianus

Fasciferela campae n.sp.

Puzosia aff. *mayoriana*

Hamites cf. *gardneri*

Hamites maximus

Planktonic fauna

Hedbergella trocoidea Gandolfi

H. delrioensis *(Carsey)*

Praeglobotruncana sp.

P. delrioensis ? (Plummer)

Heterohelix sp.

Globigerinelloides sp.

Rotalipora cf. *R. appenninica* (Renz)

Bishopella ornelasei Trejo

B. diazi Trejo

B. alata Trejo

Pithonella ovalis (Kauffmann)

P. trejoi Trejo

Calcisphaerula innominata Bonet

T. multiloculata

* Monod., et al. (2000)

APPENDIX 8. FACIES OF THE VILLA AYALA, ACAPETLAHUAYA, AND TELOLOAPAN FORMATIONS

Facies	Grain size	Other features	Process	Corresponding facies of Pickering et al.(1989)
VA1		Primary volcanic rocks formed of massive and pillow lava, hyaloclastite, and peperites.		
VA2	Block-granule	Very thick to thick beds. Contacts are sharp and erosional - Monogenetic clasts of basalt, usually angular-subangular. Poorly developed wisp structures	Debris flow to pyroclastic eruptions	
VA3	Block–granule	Clast-supported conglomerate, with very thick to thick beds showing erosional, channelized, wavy, and graded bases. Top contacts are sharp to gradational. Lava and tuff fragments with mostly subrounded to subangular shape	High-density gravity flow	A2.3
VA4	Block-granule	Matrix-supported and chaotic conglomerates. Bed contacts are sharp and erosional. scattered shard structures.	High-concentration turbidity currents to debris flows and pyroclastic flows	A1.1
VA5	Fine to very fine sand	Thin- to very thin-bedded, lami-nated radiolarian-rich tuff. Bed contacts are sharp and loaded. Parallel, ripple lamination, and lenticular bedding are common.	Low-concentration turbidity currents	D2.3

APPENDIX 8. FACIES OF THE VILLA AYALA, ACAPETLAHUAYA, AND TELOLOAPAN FORMATIONS (CONTINUED)

Facies	Grain size	Other features	Process	Corresponding facies of Pickering et al.(1989)
VA6	Fine to coarse Sand/ash	Medium-bedded tuff showing Tbc and sporadic Tabc Bouma sequences. Relict cuspate shards and fiamme are also present. Load cast and flame structures are common. Radiolarian are rare.	Low-concentration turbidity currents	C2.2
VA7	Coarse- to fine Sand/ash	Thick-bedded, coarse grained-tuff, Bed contacts sharp to gradational. Graded and laminated beds. Scattered rip-up clasts	High-concentration turbidity currents	B1.1
VA8	Fine sand	Thin-bedded epiclastic sand-stone. Contacts are sharp, loaded, or gradational. Asymmetric current ripples, cross and parallel lamination.	Low-concentration turbidity currents	D2.1
VA9	Block to Fine-grained lapilli	Thick to medium beds with folded and contorted clasts	Debris flows to overloading of wet depositional sediments.	F2.1
VA10	Medium sand	Thin- to medium-bedded epiclastic sandstone. Tabc and Tbce Bouma sequences. Rip-up clasts and bed amalgamation	High- concentration turbidity currents	C2.2

APPENDIX 8. FACIES OF THE VILLA AYALA, ACAPETLAHUAYA, AND TELOLOAPAN FORMATIONS (CONTINUED)

Facies	Grain size	Other features	Process	Corresponding facies of Pickering et al.(1989)
VA11	Very fine ash	Thin-bedded, laminated tuff interbedded with siltstone and thin to medium-bedded sandstone. Bed contacts are sharp to gradational. Abundant radiolaria	Dilute turbidity currents	D2.3
VA12	Medium sand	Thick- to medium-bedded hybrid sandstone with abundant litho- and bioclasts within a tuffaceous matrix. Bed contacts are sharp, flat, and loaded. Graded beds, nerineids fauna and bioclasts.		
VA13		Thick- to medium-bedded hybrid limestone with bioclasts and volcanic fragments. Corals abundant.		

Facies	Texture	Other features	Wave Energy	Corresponding facies of Wilson (1975)
VA14		Fossiliferous tuffaceous limestone with abundant nerineids. Beds range from 0.4–2.5 m.		
TE1	Bindstone	Thin to medium thickness beds. Algal lamination is locally dolomitized. Thin-shelled rudist	High-moderate	Restricted-platform

APPENDIX 8. FACIES OF THE VILLA AYALA, ACAPETLAHUAYA, AND TELOLOAPAN FORMATIONS (CONTINUED)

Facies	Texture	Other features	Wave Energy	Corresponding facies of Wilson (1975)
TE2	Wackestone	Thin to medium beds. Association of thin-shelled rudists with nerineids, and benthic foraminifera. Bioturbation is strong. Ostracod shells, red algae, and corals are scattered.	Low	Restricted-platform
TE3	Rudstone Grainstone	Very thick to thick beds Bioclast and intraclast of rudists, corals, and micritized mudstone to wackestone, angular- subrounded in shape. Planktonic fauna are scattered. Normal grading, cross-stratification, and soft-sediment deformation are common.	High	Marginal platform (reef)
TE4	Framestone	Very thick- to thick beds. Thick-shelled rudists (caprinid and radiolitid) with subordinate nerinea assemblage. Rudists form isolated and recumbent structures	High	Marginal platform (reef)
TE5	Floatstone	Very thick to thick beds Thick-shelled rudists in a bioclast/intraclast wackestone-packstone matrix. Rudists occur as upright clusters.	High	Marginal platform (reef)

APPENDIX 8. FACIES OF THE VILLA AYALA, ACAPETLAHUAYA, AND TELOLOAPAN FORMATIONS (CONTINUED)

Facies	Texture	Other features	Wave Energy	Facies according to Wilson (1975)
TE6	Framestone	Thick to medium beds. Thick- and medium-shelled rudists (requienids and monopleurids) form packed and isolated clusters. Benthic foraminifera abundant, nerineids and corals rare.	Low-moderate	Restricted-marginal platform
TE7	Framestone	Medium to thick beds. Thick-shelled caprinid rudists and corals with bioclast/lithoclast packstone matrix.	High–moderate	Marginal platform (reef)
TE8		Thick- to medium-bedded conglomeratic limestone with litho- and bioclasts of granule to boulder size. Bed contacts erosional.	High	Marginal platform
TE9	Packstone-Wackestone	Bed thickess is medium. Grains are planktonic fossils and ammonites. Contacts are sharp (base) to gradational (tops). Hummocky cross-stratification	High-moderate	Marginal platform
TE10	Wackestone-Packstone	Thin- to medium-bedded, laminated limestone with abundant planktonic fossils and scattered ammonites. Parallel and cross lamination associated with hummocky cross-stratification.	Low-moderate	Marginal platform

APPENDIX 9. COMPOSITE TYPE SECTION OF THE MIAHUATEPEC FORMATION

Location: The Miahuatepec Formation is highly folded in the study area and no continuous sections were measured along the unit. However, the region between the towns of San Martin and Las Ceibitas , along the Federal Road 51, is designed as the composite section of the Miahuatepec Formation.

Lithologic Description: Because of the strong deformation no continuous section can be measured. A lithologic description descripion of the Miahuatepec Formation is done in §3.2.2.

In the area from San Martin to Las Ceibitas towns, the Miahuatepec Formation is predominately thick-bedded, coarse – to medium-grained sandstone interbeded with siltstone and sporadic thin-bedded limestone. The main characteristic of the sandstones and shale interval of the Miahuatepec Formation is the light brown color and micaceous material and the strong deformation observed throughout the unit.

The thick- to medium-grained sandstone predominates over the siltstone and limestone. In some places, such as the Miahuatepec area, sandstones intervals show a well-developed Bouma sequence, where gradation is the predominant sedimentary structure. In the San Martin and Los Brasiles localities, the Miahuatepec Formation is mainly thin-bedded, mediun- to fine-grained sandtones with abundant siltstone and shale intervals. Near the town Arcelia, black shale is the dominant lithology.

APPENIDX 10. MEZCALA FORMATION FACIES

Facies	Grain size	Other features	Process	Corresponding facies of Pickering et al.(1989)
MF1 5%	Granule-boulder	Subangular-subrounded bioclasts and lithoclasts with mainly matrix-supported fabric, normal and inverse gra ding. Lower boundaries sharp and wavy	Debris flow	A.1.1
MF2 10%		Thin-bedded, laminated, mudstone-wackestone with nodular and lenticular black chert. Abundant planktonic fauna	Pelagic settling	
MF3 <5%		Very thin- to thin-bedded chert. Scattered radiolaria	Pelagic settling	G.1.1
MF4 15%	Medium sand	Minor shale intervals. Tabc Bouma divi sions. Sandstone boundaries sharp and erosional. Rare scour marks and load casts	Low-concentra-tration turbidity currents	C.2.1–C.2.2
MF5 15%	Medium to fine sand and muds	Sandstone-shale couplets. Medium bedded. Rare sole marks, load structures, lenticular and flaser bedding. Tabc & Tab Bouma sequence	High to low concentration turbidity c urrents	C.2.2

APPENDIX 10. MEZCALA FORMATION FACIES (CONTINUED)

Facies	Grain size	Other features	Process	Corresponding facies of Pickering et al.(1989)
MF6 25%	Fine to very fine sand and mud	Thick to thin bedded sandstones. Tab and rare Tbc. Bed contacts sharp	Low concentration turbidity currents	C.2.3
MF7 15%	Mud and fine to very fine sand	Thin bedded, graded and parallel laminated sandstone. Thick invervals of shale. Shale:sandstone ratio 5:1 or higher. Tb-e, Tc-e and Td-e common. Sharp bed boundaries.	Low concentration turbidity currents	C2.3–C2.4
MF8 <10%	Mud and minor very fine sand	Very thin-bedded sandstone, and laminated shale and sand-tone.	Low concentration turbidity currents	D2.1–D2.2

APPENDIX 11. MIAHUATEPEC FORMATION FACIES

Facies	Grain size	Other features	Process	Corresponding facies of Pickering et al.(1989)
MiF1 <10%	Very coarse to medium sand	Very thick- to thick-bedded. Sharp to erosional contacts. Ta, Tab abundant, scattered Tabc Bouma division. Rip-up clast and scour features. Amalgamated beds sporadic.	High concentration turbidity	B1.1 & B2.1
MiF2 20%	Medium to coarse sand	Thick- bedded. Sharp, wavy and erosional contacts. Sporadic shale levels. Tab and Tabc Bouma division. Rare sole markings. Amalgamated beds common. Sporadic rip-up clasts	High concentration turbidity	B1.1 & B2.1
MIF3 30%	Medium to fine sand, mud	Medium-bedded, grading, parallel, wavy and scattered cross- lamination. Bed contact sharp and load. Minor shale interval	High concentration turbidity	C2.2.
MiF4 20%	Medium to fine sand, mud	Thin- to very thin-bedded and thick shale intervals. Sharp contacts. Sandstone Shale ratio 1:3 or higher. Rare graded beds, Tbc and Te predominant.	Low concentration turbidity	C2.4

APPENDIX 11. MIAHUATEPEC FORMATION FACIES (CONTINUED)

Facies	Grain size	Other features	Process	Corresponding facies of Pickering et al.(1989)
MiF5 10%	Mud to very fine sand	Laminated shale and very thin-bedded sandstone. Parallel lamination Common.	Low and dilute turbidite.	D2.2
MiF6 5%	Mud and very fine sand	Predominantly wavy and parallel laminated shale	Low and dilute turbidite.	E1 &E2
MiF7 5%	Mud	Thin-bedded palnktonic limestone.	Pelagic settling	

APPENDIX 12. DEFINITION OF FACIES ASSOCIATIONS OF THE VILLA AYALA, ACAPETLAHUAYA, AND TELOLOAPAN FORMATIONS

Facies Association	Dominant facies	Interpretation of depositional environment
FA1	Exclusively primary volcanic (VA1) facies	Primary volcanic and pyroclastic activity
FA2	Clast- and matrix- supported and chaotic conglomerate; volcanic breccia (VA2–4)	Ejecta and slope-aprons on flanks of volcanic buildups.
FA3	Hybrid facies and minor primary Volcanic facies (VA12–14 and VA1)	Early evolution of island-arc carbonate platform in restricted and open conditions
FA4	Thin- to medium- bedded tuff and epiclastic sandstone (VA5–11)	Distal pyroclastic and distal epiclastic slope-apron
FA5	Thin- to medium- bedded limestone with abundant algal mats, mollusks and benthic foraminifera (TE1–2)	Restricted to open platform
FA6	Very thick- to thick- bedded rudist framestone to float-stone(TE3–7)	Reef
FA7	Conglomeratic limestone, Medium- to thin-bedded packstone-wackestone with abundant planktonic and ammonite fauna and hummocky cross-stratification (TE8–10)	Storm deposits at shelf marginal

APPENDIX 13. DEFINITION OF FACIES ASSOCIATIONS OF THE MEZCALA FORMATION

Facies Association	Dominant facies type	Interpretation of depositional environment
FA1 sandstone and sandstone-shale facies	Thick- to medium- bedded sandstones (MF4 and MF5) and thin-bedded sandstone-shale sequences (MF6, MF7, MF8) in variable proportions.	Minor channelized and channel-overbank and lobes system in middle to lower fan setting
FA2 Heterolithic facies	Consisting primarily of thin-bedded limestone (MF1) and chert beds (MF2), including minor amount of laminated shale facies (MF8)	Pelagic deposits drape on inactive submarine fan
FA3 Minor heterolithic facies	Dominated by limestone breccia (MF3).	Debris-flow deposits within middle fan sector of a submarine fan

APPENDIX 14. DEFINITION OF FACIES ASSOCIATIONS OF THE MIAHUATEPEC FORMATION

Facies Association	Dominant facies	Interpretation of depositional environment
FA1 Sandstone (30%)	Consisting of thick- to medium-bedded, pebbly to medium-grained sandstone (MiF1 and MiF2).	Deposition of channel-lobe transition in mid-fan position.
FA2 Sandstone-shale (60%)	Dominated by medium- to thin-bedded, medium- to fine- grained sandstone with minor shale levels (MiF3 and MiF4), and dominant shale intervals (MiF5).	Fan lobes and lobe-fringe within mid- to outer-fan position
FA3 10%	Consisting primarily of thin-bedded limestone (MiF7) and black shale intervals (MiF6), and less frequently laminated shale (MiF5).	Pelagic and hemipelagic deposits

APPENDIX 15. COUNTED AND RECALCULATED PARAMETERS

Counted Parameters

Qm	Monocrystalline quartz
Qp (1)	Polycrystalline quartz
Ch	Chert
P	Plagioclase feldspar
F	Potassium feldspar
Lv	Volcanic lithic
Lvv	Vitric volcanic lithic texture
Lvmi	Volcanic lithic with microlithic texture
Lvf	Volcanic lithic with felsitic texture
Lvl	Volcanic lithic with lathwork texture
Lsc	Sedimentary carbonate and bioclast lithic
Lsst	Sedimentary sandstone lithic
D	Dense minerals
M	Matrix

Q= Total quarzose grains

Qp= Polycrystalline quartz grains

Lt= Total lithic grains

Lv= Total volcanic lithic grains

Ls= Total sedimentary grains

Q= Qp+Qm+Ch

L=Lv+Ls

Lv= Lvv+Lmi+Lvf+Lvl

Ls= Lsc+Lscl

F= P+F

APPENDIX 16. WHOLE ROCK MAJOR ELEMENTS OF THE ARC-RELATED SUCCESSION. GEOGRAPHIC AND STRATIGRAPHIC LOCATION OF EACH SAMPLE IS SHOWN IN APPENDIX 18.

	Oxides percentages											
Sample	SiO2	TiO2	Al2O	MnO	MgO	CaO	Na2O	K2O	P2O5	Fe2O	LOI	Total
J11	47.99	0.95	14.17	0.14	7.59	3.20	5.10	0.61	0.13	10.18	10	100
J12	63.41	0.50	14.39	0.04	1.92	6.93	1.71	2.93	0.07	4.13	4.5	100
J10	51.64	1.01	15.56	0.14	8.35	3.45	5.78	0.64	0.15	10.68	2.60	100
TMX77	50.71	0.85	14.36	0.09	11.86	3.09	2.55	1.18	0.14	9.01	5.84	100
TMX132	46.87	1.31	16.25	0.14	5.25	9.48	3.31	2.27	0.23	9.07	5.86	100
TMX136	46.64	1.05	16.72	0.17	11.67	4.06	2.73	2.27	0.18	16.72	5.59	105
J71	42.80	0.85	13.59	0.14	12.48	4.45	2.74	1.26	0.15	10.00	11.50	100
TMX79	40.36	0.89	12.91	0.15	17.40	4.98	1.67	0.40	0.11	11.17	10	100
J21	55.4	0.71	13.37	0.06	1.68	12.57	2.24	2.16	0.05	2.99	8.68	100
J25	55.76	0.54	13.15	0.06	1.78	10.90	1.94	3.73	0.07	2.41	9.45	100
J34	58.03	0.76	14.19	0.06	1.77	14.22	2.48	2.22	0.06	3.07	1.87	100
TMX31	46.11	0.92	15.06	0.10	8.64	1.57	3.67	1.36	0.11	8.97	4.00	101
TMX33	50.41	1.18	17.33	0.12	10.34	1.89	4.2	1.41	0.13	10.53	2.53	100
TMX30	69.35	0.55	16.22	0.03	1.34	2.92	2.41	2.69	0.07	2.65	2.56	100
TMX116B	56.9	0.70	13.72	0.10	5.49	2.41	4.64	1.17	0.11	7.09	7.79	100
TMX116	59.24	0.88	17.78	0.06	2.16	6.46	3.85	2.76	0.10	3.70	3.00	100
TMX17	70.40	0.39	15.41	0.01	1.09	1.94	2.57	2.51	0.05	1.22	3.19	101
TMX18	74.14	0.42	16.51	0.01	1.22	2.02	2.87	2.53	0.05	1.19	3.25	104
TMX123	54.75	0.54	11.87	0.11	1.32	16.99	2.43	1.59	0.07	3.80	9.78	103
TMX122	56.49	0.55	13.27	0.05	1.77	10.75	2.00	3.72	0.07	2.36	8.78	100
TMX118	70.91	0.53	16.23	0.03	1.89	0.53	1.64	3.17	0.10	3.37	2.50	100
TMX15	65.63	0.36	13.13	0.03	1.61	6.10	1.74	2.62	0.05	1.51	7.40	100
TMX38	51.94	0.90	14.34	0.04	10.59	1.62	2.04	4.51	0.12	6.72	7.30	100
TMX34	60.28	0.50	13.87	0.05	3.22	4.42	1.23	3.66	0.06	4.39	8.23	100
TMX127	48.20	0.92	11.34	0.14	7.35	5.12	0.30	7.71	0.19	5.93	12	100
J90	40.50	0.90	11.90	0.15	11.49	5.75	1.99	1.42	0.16	10.58	15	100
J87	44.68	1.03	13.50	0.17	13.43	6.97	2.29	1.44	0.17	11.77	4.12	100
TMX19	58.23	0.35	12.99	0.06	2.39	6.70	2.67	2.10	0.06	3.33	10.	100

APPENDIX 17. WHOLE ROCK MAJOR ELEMENTS OF THE MIAHUATEPEC FORMATION. GEOGRAPHIC AND STRATIGRAPHIC LOCATION OF EACH SAMPLE IS SHOWN IN APPENDIX 18.

	Oxides percentages											
Sample	SiO2	TiO2	Al2O	MnO	MgO	CaO	Na2O	K2O	P2O5	Fe2O	LOI	Total
TMX51	47.52	0.98	14.03	0.14	7.52	3.19	4.91	0.62	0.13	10.18	11.23	100
TMX55	71.71	0.52	16.56	0.03	1.88	0.50	1.69	3.17	0.08	3.32	2.5	102
TMX162A	55.42	0.70	13.35	0.05	1.83	12.6	2.23	2.21	0.06	3.01	8.54	100
TMX164A	73.67	0.37	15.82	0.03	1.74	0.73	1.50	2.70	0.07	2.93	3.44	103
TMX68	69.68	0.55	16.30	0.03	1.34	2.84	2.42	2.68	0.07	2.62	2.47	101
TMX160	63.24	0.51	14.43	0.04	1.94	6.97	1.69	2.95	0.07	4.12	4.59	101
TMX65	71.27	0.39	15.60	0.01	1.16	1.98	2.59	2.52	0.05	1.24	3.33	100
TMX57	55.41	0.56	12.00	0.11	1.34	16.87	2.45	1.58	0.07	3.84	6.33	100
TMX170	53.71	1.01	16.73	0.07	2.02	7.77	3.19	2.80	0.11	4.09	8.68	100
TMX69	59.42	0.88	17.81	0.06	2.15	6.48	3.95	2.75	0.10	3.72	2.73	100
TMX53	73.73	0.37	15.85	0.03	1.63	0.67	1.53	2.70	0.07	2.93	2.73	102
TMX58	64.62	0.69	16.19	0.04	3.26	2.10	3.39	2.02	0.08	6.88	2.50	102
TMX67	67.90	0.58	15.90	0.03	1.64	1.34	3.12	2.36	0.07	3.88	2.53	101
M34	61.18	0.68	15.19	0.06	1.92	9.72	2.10	2.35	0.08	4.50	2.66	100
M33B	51.79	0.60	13.15	0.08	4.17	8.34	3.48	1.12	0.12	6.31	10.77	100

APPENDIX 18. GEOGRAPHIC AND STRATIGRAPHIC LOCATION OF SAMPLES.

* PETROGRAPHIC STUDY.

+ GEOCHEMICAL ANALYSIS.

Arc-related succession

Sample	Stratigraphic Position	Geographic Position
J10*+	Section Zacatlancillo	18° 25' N 99° 58' W
J11+	Section Zacatlancillo	18° 25.2' N 99° 58.2' W
J12*+	Section Zacatlancillo	18° 25.5' N 99° 58.2' W
J62*	Section Villa Ayala	18° 24.8'N 100° 01.8' W
J63*	Section Villa Ayala	18° 24.8'N 100° 01.8' W
TMX77*+	Section Alpixafia	18° 24.5'N 99° 53' W
TMX79+	Section Alpixafia	18° 24.8'N 99° 53.2' W
J68*	Section Alpixafia	18° 24.7'N 99° 54' W
J77*	Section Alpixafia	18° 24.7'N 99° 54.5' W
TMX132*+	Section Alpixafia	18° 24.8'N 99° 53' W
J71*+	Section Alpixafia	18° 24.7'N 99° 54' W
TMX127*+	Section Acatempan	18° 19' N 99° 53.6' W
TMX17*+	Section Cerro Pipilo	18° 11.6' N 99° 51.8' W
TMX118*+	Section Cerro Pipilo	18° 11.3' N 99° 51.6' W
TMX122*+	Section Cerro Pipilo	18° 11' N 99° 51.8' W
TMX15*+	Section Cerro Pipilo	18° 10.8' N 99° 51.3' W
TMX116B+	Section Cerro Pipilo	18° 10.9' N 99° 51.4' W
TMX116+	Section Cerro Pipilo	18° 10.9' N 99° 51.4' W
TMX18+	Section Cerro Pipilo	18° 12.5' N 99° 51.2' W
TMX123+	Section Cerro Pipilo	18° 12.1' N 99° 51.7' W

APPENDIX 18 (CONTINUED). GEOGRAPHIC AND STRATIGRAPHIC LOCATION OF SAMPLES.

* PETROGRAPHIC STUDY. + GEOCHEMICAL ANALYSIS.

Arc-related succession

Sample	Stratigraphic Position	Geographic Position
TMX31*+	Section Laguna Seca	18° 16' N 99° 57.9' W
J21*+	Section Laguna Seca	18° 16.3' N 99° 58.3' W
TMX33*+	Section Laguna Seca	18° 16.1' N 99° 58.4' W
J25+	Section Laguna Seca	18° 16.5' N 99° 58.5' W
J34+	Section Laguna Seca	18° 16.8' N 99° 58.8' W
TMX30+	Section Laguna Seca	18° 16' N 99° 57.9' W
TMX19+	Section Los Sauces	18° 15.3' N 99° 50.5' W
TMX38+	Section Los Sauces	18° 15.3' N 99° 50.5' W
J87+	Section Mirabales	18° 17.8' N 99° 54.1' W
J90*+	Section Mirabales	18° 17.4' N 99° 54' W
J05*	Section Mirabales	18° 17.6' N 99° 53.8' W
TMX34+	Section Mirabales	18° 17.8' N 99° 54' W
TMX136+	Section Alcholoa	18° 25.2'N 99° 54' W

APPENDIX 18 (CONTINUED). GEOGRAPHIC AND STRATIGRAPHIC LOCATION OF SAMPLES.

* PETROGRAPHIC STUDY. + GEOCHEMICAL ANALYSIS.

Mezcala Formation

Sample	Stratigraphic Position	Geographic Position
TMX03*	Section Pachivia	18° 21.3'N 99° 47' W
TMX09*	Section Pachivia	18° 23'N 99° 47' W
TMX11*	Section Pachivia	18° 20.4'N 99° 49.4' W
TMX112*	Section Pachivia	18° 20.3'N 99° 49.3' W
TMX09A*	Section Calvario	18° 17.2'N 99° 49.2' W
TMX06	Section Calvario	18° 17'N 99° 43.9' W
TMX23*	Section Tecoziapa	18° 25.5'N 99° 47.6' W
TMX143*	Section Tecoziapa	18° 25'N 99° 47.7' W
TMX147*	Section Romita	18° 30'N 99° 48'3 W
TMX148*	Section Romita	18° 30.5'N 99° 48'5 W
TMX146*	Section Romita	18° 30.6'N 99° 48'6 W
TMX46*	Section Romita	18° 29'N 99° 48'9 W
TMX47*	Section Romita	18° 29.9'N 99° 48'5 W
TMX145*	Section Pipincatla	18° 27'N 99° 48.3' W
TMX143A*	Section Pipincatla	18° 27'N 99° 48.3' W
TMX12*	Section Coaxilotla	18° 09.8'N 99° 50.8' W

APPENDIX 18 (CONTINUED). GEOGRAPHIC AND STRATIGRAPHIC LOCATION OF SAMPLES.

* PETROGRAPHIC STUDY. + GEOCHEMICAL ANALYSIS.

Miahuatepec Formation

Sample	Stratigraphic Position	Geographic Position
M34A*+	Section Cacahuananche	18° 26'N 100° 14.9' W
TMX67*+	Section Cacahuananche	18° 26'N 100° 14' W
TMX68*+	Section Cacahuananche	18° 26.2'N 100° 14.6' W
TMX69*+	Section Cacahuananche	18° 26'N 100° 14.7' W
M32B*	Section Copaltepec	18° 24.7'N 100° 16.2' W
M33B+	Section Copaltepec	18° 24.9'N 100° 16.1' W
TMX70*+	Section Copaltepec	18° 24.9'N 100° 16.3' W
TMX160*+	Section Copaltepec	18° 24.6'N 100° 16.1' W
TMX162A*+	Section Copaltepec	18° 24.5'N 100° 16.2' W
TMX164A*+	Section Copaltepec	18° 24.8'N 100° 16' W
TMX51*+	Section Miahuatepec	18° 22.9'N 100° 12.6' W
TMX52*	Section Miahuatepec	18° 22.8'N 100° 12.7' W
TMX53*+	Section Miahuatepec	18° 22.7'N 100° 14.2' W
TMX55*+	Section Miahuatepec	18° 21.9'N 100° 14.3' W
TMX58*+	Section Ceibas	18° 23.1'N 100° 14.9' W
TMX57*+	Section Ceibas	18° 22.9'N 100° 14.6' W
TMX65*+	Section El Charco	18° 26.3'N 100° 13.6' W